Investigating virus diversity in Australian domestic cats and bats

Kate Van Brussel

2023

The University of Sydney

Faculty of Science

A thesis submitted in fulfilment of the requirements for the degree of Doctor of Philosophy

Statement of Originality

This is to certify that to the best of my knowledge the contents of this thesis are my own work. This thesis has not been submitted for any other degree or other purpose.

I certify that the intellectual content of this thesis is the product of my own work and that all the assistance received in preparing this thesis and sources have been acknowledged.

PhD Candidate

Name: Kate Van Brussel

Signature:

Date: 27 January 2023

Authorship attribution statement

Chapter two of this thesis was published as: Carrai M, **Van Brussel K**, Shi M, Li CX, Chang WS, Munday JS, Voss K, McLuckie A, Taylor D, Laws A, Holmes EC, Barrs VR, Beatty JA. 2020. Identification of a novel papillomavirus associated with squamous cell carcinoma in a domestic cat. Viruses 12(1):124. *I performed the laboratory work and analysed the data. I also wrote the manuscript in conjunction with the other authors*.

Chapter three of this thesis was published as: **Van Brussel K**, Wang X, Shi M, Carrai M, Li J, Martella V, Beatty JA, Holmes EC, Barrs VR. 2021. Identification of novel astroviruses in the gastrointestinal tract of domestic cats. Viruses 12(11):1301. *I performed all the laboratory work, analysed the data in conjunction with another author, and wrote the manuscript.*

Chapter four of this thesis was published as: **Van Brussel K**, Wang X, Shi M, Carrai M, Feng S, Li J, Beatty JA, Holmes EC, Barrs VR. 2022. The enteric virome of cats with feline panleukopenia is altered in abundance and diversity compared with healthy cats. Transboundary and Emerging Diseases 69(5):2952-2966. *I performed all the laboratory work, analysed the data and wrote the manuscript.*

Chapter five of this thesis was published as: **Van Brussel K**, Holmes EC. 2022. Zoonotic disease and virome diversity in bats. Current Opinion in Virology 52:192-202. *I wrote the manuscript in conjunction with my supervisor.*

Chapter six of this thesis was published as: **Van Brussel K**, Mahar JE, Ortiz-Baez AS, Carrai M, Spielman D, Boardman WSJ, Baker ML, Beatty JA, Geoghegan JL, Barrs VR, Holmes EC. 2022. Faecal virome of the Australian grey-headed flying fox from urban/suburban environments contains novel coronaviruses, retroviruses and sapoviruses. Virology, 576**,** 42-51. *I performed all the laboratory work, analysed the data and wrote the manuscript.*

Appendix I was published as: **Van Brussel K**, Carrai M, Lin C, Kelman M, Setyo L, Aberdein D, Brailey J, Lawler M, Maher S, Plaganyi I, Lewis E, Hawkswell A, Allison AB, Meers J, Martella V, Beatty JA, Holmes EC, Decaro N, Barrs VR. 2019. Distinct Lineages of Feline Parvovirus Associated with Epizootic Outbreaks in Australia, New Zealand and the United Arab Emirates. Viruses, 11(12):1155. *I performed the laboratory work, analysed the data and helped write the manuscript in conjunction with other authors.*

Appendix II was published as: Bordicchia M, Fumian TM, **Van Brussel K**, Russo AG, Carrai M, Le SJ, Pesavento PA, Holmes EC, Martella V, White P, Beatty JA, Shi M, Barrs VR. 2021. Feline calicivirus virulent systemic disease: clinical epidemiology, analysis of viral isolates and in vitro efficacy of novel antivirals in Australian outbreaks. Viruses, 13(10):2040. *I contributed to data analysis in part and reviewed and edited the manuscript.*

Appendix III was published as: Carrai M, Decaro N, **Van Brussel K**, Dall'Ara P, Desario C, Frasasso M, Slapeta J, Colombo E, Bo S, Beatty JA, Meers J, Barrs VR. 2021. Canine parvovirus is shed infrequently by cats without diarrhoea in multi-cat environments. Veterinary Microbiology, 261:109204. *I contributed to the laboratory work.*

Appendix IV was published as: Wang X, Carrai M, **Van Brussel K**, Feng S, Beatty JA, Shi M, Holmes EC, Li J, Barrs VR. 2022. Low Intrahost and Interhost Genetic Diversity of Carnivore Protoparvovirus 1 in Domestic Cats during a Feline Panleukopenia Outbreak. Viruses, 14(7):1412. *I performed the laboratory work, analysed the data in part and reviewed and edited the manuscript.*

I declare that the authorship attribution statements made above are true. In addition to the statements above, in cases where I am not the corresponding author of a published item, permission to include the published material has been granted by the corresponding authors, my supervisors.

PhD Candidate

Name: Kate Van Brussel

Signature:

Date: 27 January 2023

As supervisor for the candidature upon which this thesis is based, I can confirm that the authorship attribution statements above are correct.

Supervisor name: Professor Edward C. Holmes

Signature:

Date: 27 January 2023

Acknowledgements

I would like to dedicate this thesis to my family; Mum, Dad, Brother, Nephew and cat who got me through this journey and continue to attend trivia with me even though we always finish last.

First, I would like to acknowledge my supervisors, Professor Edward Holmes for taking me on as an orphan student midway through my PhD and Professor Vanessa Barrs and Professor Julia Beatty for dealing with my stress and anxiety during my PhD. The support that they offered me allowed me to continue when I was really struggling through the research. The opportunity to work in both research groups let me gain confidence in both wet and dry laboratory skills that will serve me well in the future. I am also grateful for the scholarships they created for me so I could continue to complete my PhD full time and reduce my hours at my casual job. I am thankful to all the calibrators I was lucky enough to work with, especially Xiuwan Wang, Dr Karrie Ross and Mang Shi. To Xiuwan, I would like to say thank you for offering your time to help me and answering my many emails. I wish you all the best with your PhD thesis and future, I look forward to meeting you soon. To Dr Karrie Ross, thank you for including me in your fantastic research and allowing me to study a group of animals I am passionate about. I also enjoyed our late-night RNA extractions and learnt a lot from just chatting with you. Although the nights were long I would do it all again. Finally, I would like to thank Mang Shi for assisting me during the start of my PhD, I learnt a lot from you.

I would like to thank the members of the Holmes group, Wei-shan, Susana, Jon, Vince, Callum, Sabrina, Erin, Jackie, Michelle, Rebecca and Mary for including me in your group from day one and always providing support when I was stuck with my research. And to my American office mate Anna, thank you for the great chats and for answering all my medical and American questions, it has been amazing to get to know you. I'm sure we will continue to stay in touch in the future, as I'm expecting an invitation to family thanksgiving. To Susana, thank you for helping me troubleshoot all my scripts, you have been a great teacher! Thank you to Jackie who continues to book the table for trivia every week and pressuring people to attend, I look forward to it every week.

I would also like to acknowledge the friends that have supported me throughout the four and a half years of my PhD. Thank you for the endless Sunday lunch chat sessions at work. To Raani and Jacqui, one day we will finish that puzzle, I promise. I would also like to thank Jessi for all the bat related information she provided through my PhD.

Finally, I would like to thank Maura for everything she has done for me over the last four years. I knew since the first day I met you that we would be fast friends and that we would do some great research together. I enjoyed the Friday lunch outings and really appreciate the assistance and wisdom you offered me during my PhD. You are a great person and a great scientist; I wish you all the best in the future and hope we get to work together again.

Completing a PhD was something I also wanted to do, although it was a challenging few years it was worth the struggle to work with all the great people in the Holmes and Barrs/Beatty groups. Thank you everyone!

Kate Van Brussel

27 January 2023

Table of Contents

List of figures

List of tables

Abstract

The field of virus discovery has made dramatic advances since the development of metagenomic next-generation sequencing. Although this technique has been used to identify important novel viruses, to date there have been few studies using metagenomics to reveal the diversity and evolution of those viruses carried by wildlife and companion animal species in Australia. In particular, little is known about the viral diversity carried by bats of the order Chiroptera, with most current studies directed toward the screening of specific viruses. Similarly, the prevalence of enteric viruses in domestic cats is understudied in Australia compared to other countries. To reduce these major knowledge gaps, I used metagenomic next-generation sequencing to characterise the viruses present in five bat species (grey-headed, black and little red flying fox, large footed myotis and eastern-bent wing bat) and in faecal and tissue samples from healthy and diseased domestic cats. This led to the identification of 13 known viruses from the faeces of domestic cats and two from the tissue of bats. Additionally, sequence comparisons and phylogenetic analysis revealed eleven novel mammalian viruses from the families *Astroviridae*, *Caliciviridae*, *Coronaviridae*, *Picornaviridae*, *Papillomaviridae* and *Retroviridae* in domestic cat and bat faecal and tissue samples. By performing two large-scale domestic cat and grey-headed flying fox faecal virome studies, I also determined that a large diversity of viruses are shed via the faeces, including likely host, dietary, bacterial, fungal and invertebrate viruses. In addition, the studies presented in this thesis provide the first evidence of the circulation of feline kobuvirus, feline picornavirus, feline chaphamaparvovirus, bat sapovirus, bat astroviruses, bat kunsagivirus and possible exogenous bat betaretroviruses in Australia. In sum, this thesis presents an overview of the virus diversity in domestic cats and urban/suburban bat populations and highlights the power of metagenomic sequencing to detect novel virus species in diseased and health mammals.

Chapter One: General introduction

1.1 The history of virology

1.1.1 The early days of virology

Since the identification of the first virus in the late 1800s, researchers have attempted to generate better ways of identifying and characterising novel viruses in all life systems. The history of virology arguably began in 1796 when the English physician Edward Jenner developed the first smallpox vaccine by inoculating people with the milder cowpox virus. Following this, Louis Pasteur developed the first vaccine for rabies in 1885 by drying nerve tissue from rabbits in which he successfully grew the virus (although, of course, he did not know he was working on a virus).

Our modern knowledge of viruses arguably began in the late 1800s when two scientists, both using the Chamberland filter developed by Charles Chamberland in 1885, demonstrated that an organism smaller than bacteria existed. Dmitri Ivanovski was the first to propose that an infectious agent smaller than bacteria was the causative agent of Tobacco mosaic disease when he discovered that the infectious agent could pass through the Chamberland filter in 1892, although at the time believed it was due to a toxin (Ivanovski, 1892). The 1892 Ivanovski experiment was later replicated by Martinus Beijerinck in 1898 who was able to filter and grow the agent of Tobacco mosaic virus in plant cells (Beijerinck, 1899). At the same time, two German scientists, Friedrich Loeffler and Paul Frosch, passed the causative agent of foot-and-mouth disease through the Chamberland filter and showed the particle to still be infectious (Loeffler, 1898). The Chamberland filter continued to be the most popular method for studying viruses until the first visualisation of a viral particle with the introduction of the electron microscope in the 1930s. The era of the electron microscope advanced further 26 years later with the introduction of the negative-contrast electron microscope that could produce higher resolution images to accurately visualise the morphological characteristics of viruses.

1.1.2 Modern virology techniques

The introduction of the electron microscope provided the first visualisation of virus particles, although more modern virological techniques provide insight into the genomic structure and include techniques that are still widely used today. Cell culture and the polymerase chain reaction (PCR) were the main virological advancements of the late 20th century (Kumar et al.,

2017, Leland and Ginocchio, 2007). Cell culture is popular among scientists as a way to grow, isolate and study the behaviour of viruses in controlled environmental conditions, removing the need to use live animal models (Kumar et al., 2017, Leland and Ginocchio, 2007). Indeed, cell culture was utilised in the 1930s to propagate both the smallpox and yellow fever virus to produce vaccines. However, cell culture is not without its limitations given that it can be a time-consuming process that can take several days to weeks before a cytopathic effect is observed, and not all viruses successfully grow in cell culture and therefore cannot be studied *in vitro* (Leland and Ginocchio, 2007, Kumar et al., 2017). However, perhaps the main limitation of cell culture is that this technique provides no evidence on the nature of the viral genetic sequence. This gap in knowledge led to the use of modern PCR (Mullis et al., 1986), sequence independent single primer amplification or SISPA (Reyes and Kim, 1991) and Sanger sequencing (Sanger et al., 1977) techniques to amplify and sequence sections of DNA or RNA, including from viruses, for downstream visualisation of nucleotide and translated amino acid sequences. Despite their transformational impact, PCR and Sanger sequencing are not without their preconditions, including that PCR requires some prior knowledge of the genetic sequence to be targeted for the design of primer sequences for annealing, and Sanger sequencing will necessarily generate a consensus sequencing by reporting the most common nucleotide at each site in a sequence, thereby limiting variant information. This means viruses that are highly divergent from those already characterised are neglected by PCR and Sanger sequencing, greatly reducing their utility for virus discovery. To combat this problem new technologies were developed to identify divergent virus sequences unexplored by PCR and Sanger sequencing.

1.2 The current status of virus discovery – metagenomics

Metagenomic next generation sequencing (mNGS) is the newest high-throughput genomic sequencing method available to researchers. It includes the "second-generation" sequencers – Roche 454 pyrosequencing (2004), SOLiD (2006), Solexa (2006), Ion torrent (2010) and the Illumina sequencing platforms (2010) – and the "third-generation" PacBio SMRT (2011) and Oxford nanopore sequencers (2015). In essence, the second-generation sequencers produce short-read fragments while the third-generation sequencers were designed to sequence long-read fragments. Of importance, the "shotgun" sequencing approach inherent to mNGS allows the entire microbial community within a sample to be captured in a single sequencing reaction (Figure 1.2.1). This is achieved by fragmenting the DNA or RNA randomly and

ligating adapter sequences to the ends of the fragments to be sequenced single-end or paired-end on a flow cell.

A current approach to mNGS involves multiplexing - the adding of adapter sequences to the ends of fragments that are unique to each library so that multiple libraries can be pooled and simultaneously sequenced on a single flow cell. The large sample processing compacity and unbiased approach to sequencing, coupled with the cost effectiveness of sequencing large sample numbers, easy accessibility, low sample input requirements, quick sample processing (< 24 hours) and sequencing time, high sensitivity and low detection limit, means scientists around the world are moving away from Sanger sequencing to mNGS for many applications. In this thesis I will highlight its utility for virus discovery.
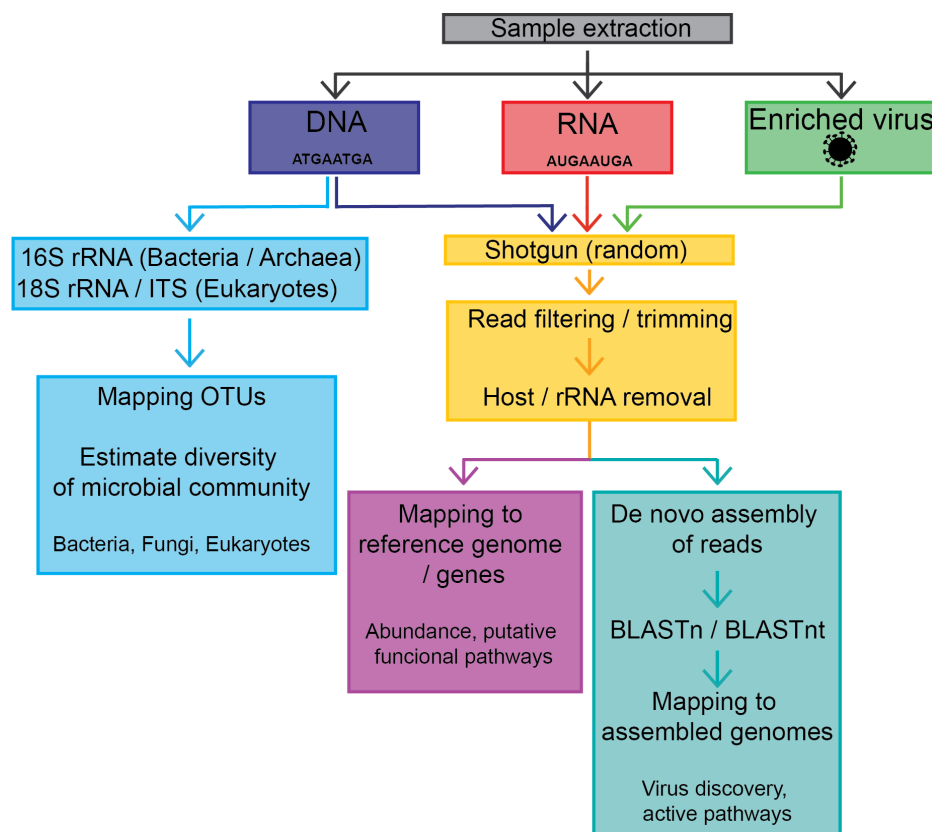
Figure 1.2.1: Overview of mNGS for targeted rRNA sequencing used to analysis data.

Despite its growing utility, it is also the case that some of the advantages of mNGS can also be disadvantages when used for virus discovery. The main issue with virus discovery mNGS is the background data (i.e., host and microbial reads) that is generated by sequencing all the nucleic acids in a sample, which can dominate the data set. In the case of total RNA sequencing (i.e., metatranscriptomics), this issue can be minimalised by the addition of a ribosomal (r) RNA depletion step before the preparation of sequencing libraries, as rRNA is

often the dominant host transcript obtained. In addition, the amount of viral nucleic acid can be enhanced compared to host and bacterial DNA by the use of virus particle enrichments methods before library preparation (Figure 1.2.1) (Conceicao-Neto et al., 2015, Daly et al., 2011, Kohl et al., 2015, Rosseel et al., 2015). Alternatively, rRNA and host DNA can be removed from the data set after sequencing and before the de novo assembly of reads (Figure 1.2.1), although this can mean that virus reads may be underrepresented or missed if at low abundance as a result of insufficient sequencing depth. Furthermore, the misassignment of reads to libraries due to multiplexing (a phenomenon known as "index-hopping"), sequencing of viruses inadvertently present in laboratory reagents (the so-called "kitome"), the production of large data sets that must be analysed bioinformatically, and the often complex association between virus and specific disease are additional challenges associated with the use of mNGS technology. However, these challenges can be minimised by using unique index combinations for library preparation, sequencing extraction kit reagents to determine the kitome, and comparing diseased and health animals to help identify viruses that are part of the natural animal virome. Despite these limitations, mNGS is still the most robust way for scientists to explore and expand the virosphere and will be used extensively in this thesis.

Table 1.2: Current methods for virus discovery.

Technology	Advantages	Disadvantages
Cell culture	• Propagate virus in desired cell lines • Observe the cytopathic effects of viruses *in vitro*	• Cannot be used for all viruses – some will not grow in culture • Can be time-consuming – incubation periods can stretch days
PCR	• Rapid protocol – can take less than ~3 hours • Allows scientists to target specific regions of a virus genome • Sensitive and specific	• Requires prior knowledge on the virus genome sequence • Cost increases with the number of target virus sequences • Low detection capacity for divergent viruses
Sanger Sequencing	• Rapid protocol • Cost effective when sequencing low numbers of samples	• Can only sequence small sections of DNA – quality degrades the longer the target sequence • Low sensitivity – sequences the consensus bases
Next generation sequencing	• High throughput • Sequence short and long reads • High sensitivity • Sequences a broad virus community in one run • Cost effective for large sample numbers • Can detect highly divergent viruses – best way to explore the virosphere	• Multiplexing approach can cause index-hopping • Large data sets that need to be computationally analysed • Background reads can overwhelm the data set – host, bacterial and rRNA • No disease association information

In 2021 alone, 906 of the 1,296 (70%) non-redundant nucleotide reference sequences deposited on the NCBI/Reference sequence database (i.e., RefSeq) listed next generation sequencing as their source, with 639 (49%) using Illumina sequence platforms (Figure 1.2.2). In comparison, in 2015, 264 of the 803 (33%) non-redundant virus nucleotide sequences deposited on NCBI/RefSeq have a next generation sequence listed as the sequencing method (Figure 1.2.2). Most virus discovery studies are now utilising mNGS as the main sequencing technique and incorporating additional downstream applications such as PCR and Sanger sequencing for result validation, to complete partial genomes and to test additional samples for newly discovered viruses. In short, mNGS has revolutionised virus discovery.

RefSeq sequences deposited in 2015
0.4% 4% 6% 31% 9% 37% 13%

RefSeq sequences deposited in 2021
1% 4% 10% 9% 6% 21% 49%

Legend:
- Illumina and other NGS platforms
- Illumina platform
- Not listed
- Other NGS platforms
- Sanger
- Sanger and Illumina platforms
- Sanger and NGS platform
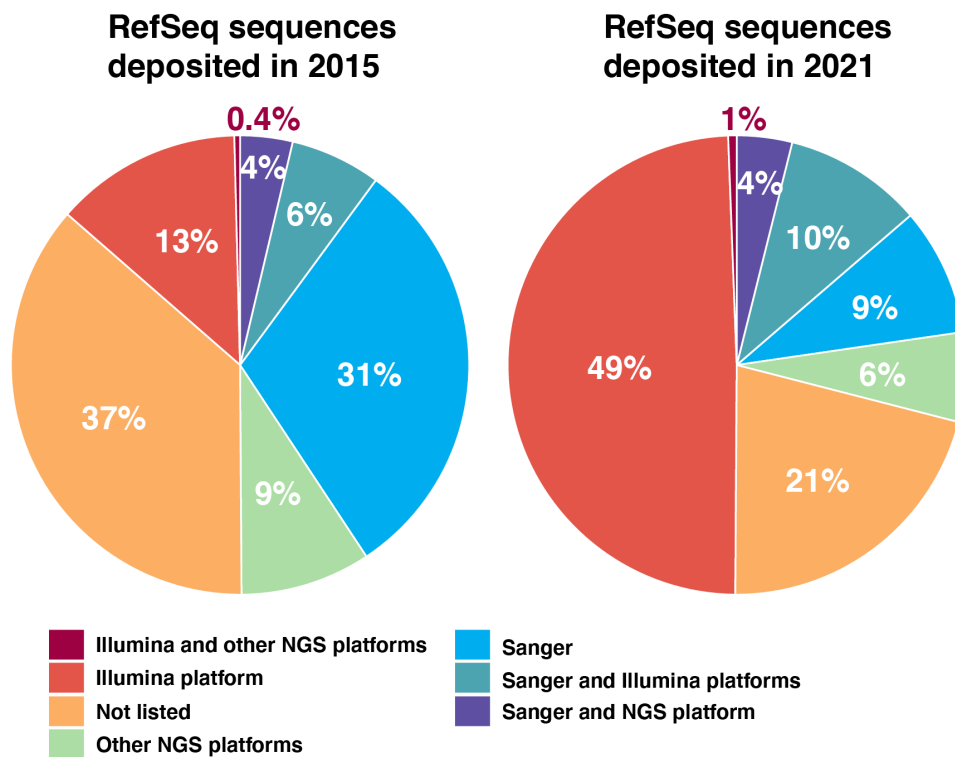
Figure 1.2.2: Graphical representation, as a percentage, of the number of non-redundant virus nucleotide sequences deposited on NCBI/RefSeq in 2015 and 2021. Numbers are separated by the sequencing technology used to generate the nucleotide sequences. Any nucleotide sequence with no sequencing method information on NCBI/GenBank is represented by "not listed".

1.3 Virus taxonomy

The Baltimore classification system, first introduced in 1971, is a commonly used classification method based on whether the viruses in question possess an RNA or DNA

genome (Baltimore, 1971). Viruses can then be further classified under the Baltimore system into those with single-stranded or double-stranded and positive-sense or negative-sense genomes (Baltimore, 1971). DNA viruses fall into two groups: group I, that possess a double-stranded genomes and group II with single-stranded genomes (Baltimore, 1971). The RNA viruses are classified into the remaining five groups: group III (double-stranded RNA), group IV (positive-sense single-stranded RNA), group V (negative-sense single-stranded RNA), group VI (positive-sense single-stranded RNA with a DNA intermediate) and group VII (double-stranded DNA with an RNA intermediate) (Baltimore, 1971). The groups VI (*Retroviridae* and *Caulimoviridae*) and VII (*Hepdnaviridae*) use reverse transcription to replicate, and in the case of the *Retroviridae* and *Caulimoviridae* integrate their DNA into that of the host genome.

Working from this system, the International Committee on Taxonomy of Viruses (ICTV) created the system of virus taxonomy that is currently utilised, in which viruses are classified into multiple levels that mimic the Linnean classification system used in eukaryotes: realm, kingdom, phylum, class, order, family, genus and species based on certain criteria specific for each level. While the ICTV has managed to produce a taxonomic system for grouping related and unrelated viruses based on key features such as sequence relatedness, phylogenetic position and genome arrangement, the introduction of mNGS has characterised a diverse collection of viruses that sometimes fall outside of the current system, especially viruses sampled from invertebrates and environmental sources, including aquatic systems (Chen et al., 2022, Li et al., 2015, Shi et al., 2016). These viruses often fall basal to known families and while they disrupt the current taxonomy scheme, they provide essential information on the evolutionary relationships between established orders and families by "filling in the gaps" in phylogenetic spaces. They also hint at the untapped diversity of RNA viruses and provide essential information on their early evolution. One newly proposed family, the *Chuviridae,* is an example of a group of recently identified viruses that form a monophyletic group that is phylogenetically positioned between segmented and non-segmented families and contains viruses that possess a segmented, bi-segmented and circular genome (Li et al., 2015). Such diversity is difficult to clearly classify. As a consequence of the rapid detection of highly divergent viruses from invertebrates and environmental sources by mNGS, a reclassification of the current taxonomy structure is becoming increasingly necessary. As a case in point, a recent study analysing the evolutionary relationships in the *Lenarviricota* - that comprises a huge array of viruses with microbial hosts - suggested reordering of this phylum based on

phylogeny and genome structure, the proposal of a new family, and the restructuring of the taxonomic orders and their member families (Figure 1.3) (Sadiq et al., 2022).
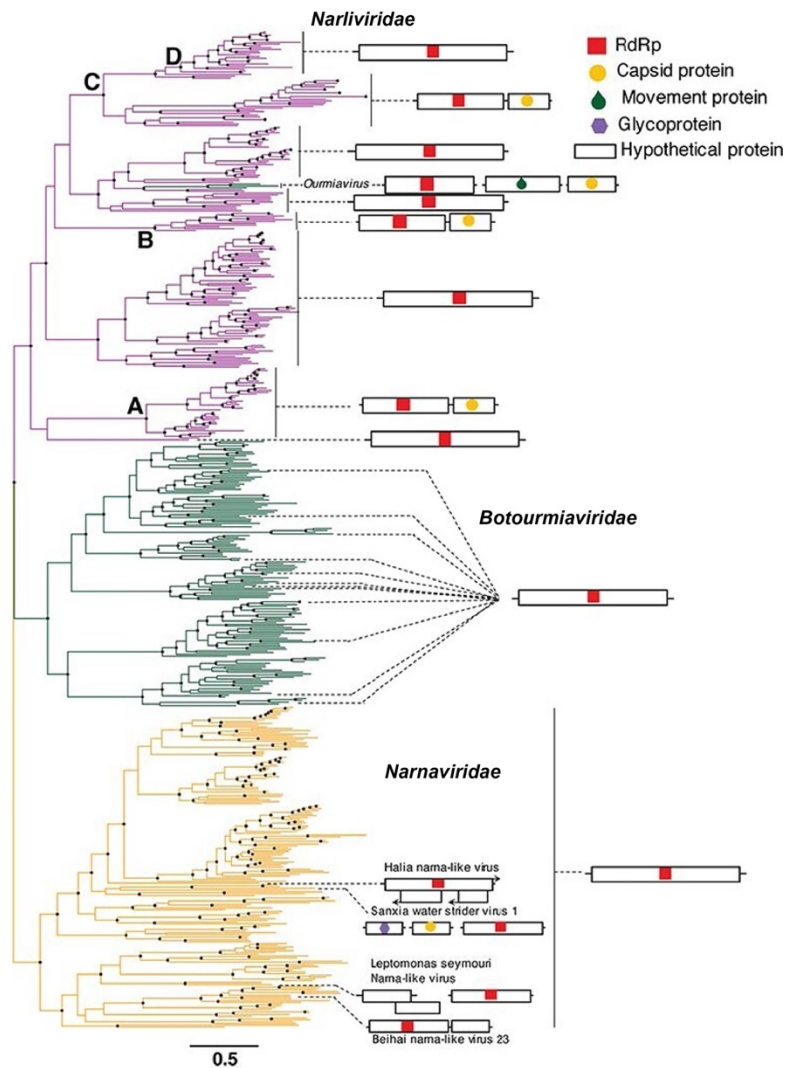
Figure 1.3: Example of the complex evolutionary relationships within the Lenarviricota. Phylogenetic representation of the class Amabiliviricetes in a midrooted tree based on the RNA-dependent RNA polymerase. The phylogenetic position of the viruses suggest a reclassifying of the existing families Narnaviridae and Botourmiaviridae and the addition of a new family the Narliviridae (Reproduced from Sadiq, S., Chen, Y.M., Zhang, Y.Z., Holmes, E.C. 2022. Resolving deep evolutionary relationships within the RNA virus phylum Lenarviricota. Virus Evolution, 8(1))

1.4 Impacts of viral outbreaks on Australian mammals

Australia is home to 8,393 animal species in which 3,682 are endemic, and 341 mammalian species of which 233 are endemic (IUCN, 2021). Australia's endemic mammalian species belong to 9 orders, the largest being the rodents (Rodentia - 53 species), bats (Chiroptera – 78 species), marsupials (Diprotodontia – 81 species) and carnivorous marsupials (Dasyuromorphia – 56) (IUCN, 2021). Currently, the International Union for Conservation of Nature's red list has eight endemic Australian mammalian species flagged as critically endangered, 12 as endangered, 37 as vulnerable and 38 as near threatened (IUCN, 2021). Australia also contains a large mammalian livestock population with 22.1 million beef cattle, 2.3 million dairy cows, 68 million sheep and lambs and 2.5 million pigs recorded over the 2020 – 2021 period (ABS, 2022). The recorded number of domestic animals owned in Australia during 2021 is much less than the number of livestock, at around 6.3 million domestic dogs, 4.9 million domestic cats and 1.5 million small mammals (Statista Search Department, 2022). With such an extensive mammalian population in Australia, many of which are endemic and in danger of extinction, it is important that screening and surveillance is undertaken to mitigate outbreaks of viral disease. For example, the zoonotic Hendra virus and Menangle virus and the threat from Australian bat lyssavirus (overview in section 1.6.1) highlight the importance of virus screening in Australian wildlife, while the presence of Pestivirus C and Equine influenza A viruses further highlight the importance of virus screening in livestock populations. Pestivirus C is a member of the *Flaviviridae* that causes classical swine fever that can present as acute, chronic or subclinical disease and death in wild and domestic pigs (Ganges et al., 2020). The virus has since been eradicated from Australia and is now listed as classical swine fever free by the World Organisation for Animal Health (OIE); however, reintroduction from countries where classical swine fever is endemic is a constant threat to Australia's porcine industry. Equine influenza A virus (*Orthomyxoviridae*) which causes equine influenza is another virus that has since been eradicated from Australia, although an outbreak in 2007 resulted in a massive financial loss to the Australian equine and racing industry (Smyth et al., 2011).

The current screening of viruses in Australian mammals is largely directed toward those species associated with the economically important agricultural industry. The genera *Bos*, *Sus* and *Equus* that contain cattle, pig and horse, respectively, have well over 100 virus sequences available on NCBI/GenBank for the families *Orthomyxoviridae*, *Herpesviridae*,

Rhabdoviridae and *Sedoreoviridae* (Figure 1.4.1). For the genus *Bos*, 80.5% of the *Sedoreoviridae* sequences represent Bluetongue virus, an endemic vector-borne virus that generally does not cause clinical disease in cattle, although is epidemiologically important as cattle can serve as reservoirs for the transmission to midges that can then infect sheep and cause serious disease. Influenza A virus, that causes swine fever in pigs and can give rise to zoonotic subtypes that can infect humans, comprise 100% of the *Orthomyxoviridae Sus* associated virus sequences characterised in Australia. A similar pattern can be seen for the *Phascolarctos*, the mammalian genus that includes the koala, in which 100% of the *Retroviridae* sequences associated with this genus represent koala retrovirus. Finally, the screening of rabbit populations to monitor the evolution, spread and inclusion of rabbit haemorrhage disease virus (RHDV) in Australia (Mahar et al., 2018b, Kovaliski et al., 2014, Mahar et al., 2018a) has led to the characterisation of 553 RHDV sequences, comprising 92.6% off all the *Caliciviridae* and 75.8% off all the *Oryctolagus* associated virus sequences.

Australia's island status means that virus introductions can be mitigated by employing strong border security to prevent viral disease outbreaks in the mammalian population. Despite this, Australia is still at constant threat from exotic viral diseases from neighbouring countries and from those in which we rely on for the livestock trade. The current foot-and-mouth disease virus outbreak in Indonesia, caused by a picornavirus that is highly infectious in cloven foot animals, as well as the constant threat of the introduction of the arbovirus African horse sickness virus, are potent examples of exotic viruses that if allowed to enter Australia would have a devastating effect on Australia's meat, dairy and equine industry.

Australia's wildlife and companion animal populations are also at risk from the introduction of exotic viruses or the establishment of virus infections in naïve populations that can lead to mortality events and major outbreaks. A mass mortality event associated with a novel nidovirus that nearly caused the extinction of the endangered Bellinger River snapping turtle was detected in 2015 (Zhang et al., 2018). In 2013, the causative agent for the mortality of numerous dolphins in South Australia was found to be likely due to cetacean morbillivirus infection (Kemper et al., 2016). Two novel marsupial viruses, bandicoot papillomatosis carcinomatosis virus type 1 and type 2, detected in western barred bandicoots and a southern brown bandicoot, respectively, have been tentatively associated with the presentation of papilloma and carcinoma lesions, impacting feeding and movement in clinical animals (Woolford et al., 2007, Bennett et al., 2008). Bellinger river virus, cetacean morbillivirus and bandicoot papillomatosis virus are all illustrative examples of the destructive effect a single

viral outbreak can have on wildlife populations, especially in species with low population numbers. A recent study highlighted the usefulness of mNGS for Australian wildlife disease surveillance, in which the metatranscriptomic analysis of archived Australian brushtail possum tissue samples afflicted by a wobbly possum-like disease was able to identify a novel arterivirus genetically distinct from the New Zealand wobbly possum disease virus, as well as co-infection with a novel hepacivirus (Chang et al., 2019). In addition, mNGS has been used for the sequencing of complete genomes from previously known viruses including Wallal virus and Warrego virus – both vector-borne viruses that have been implicated as a cause of blindness in marsupials (Coffey et al., 2014, Belaganahalli et al., 2014).
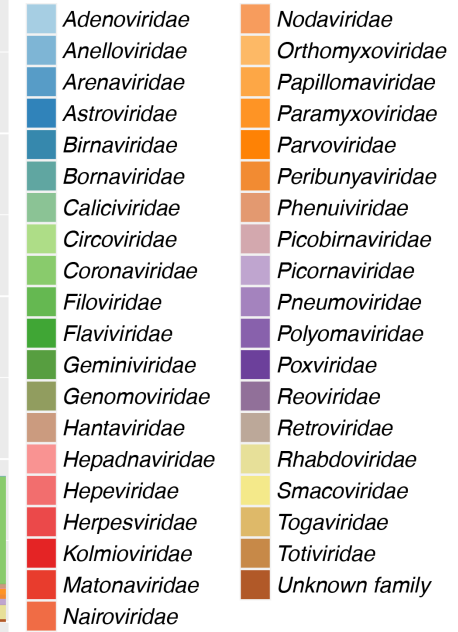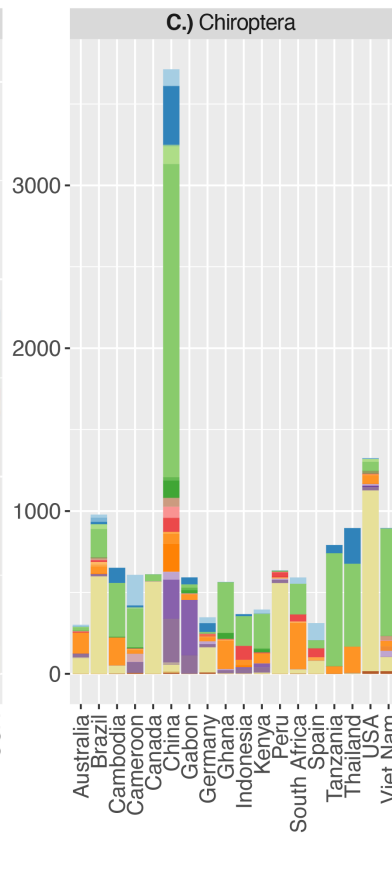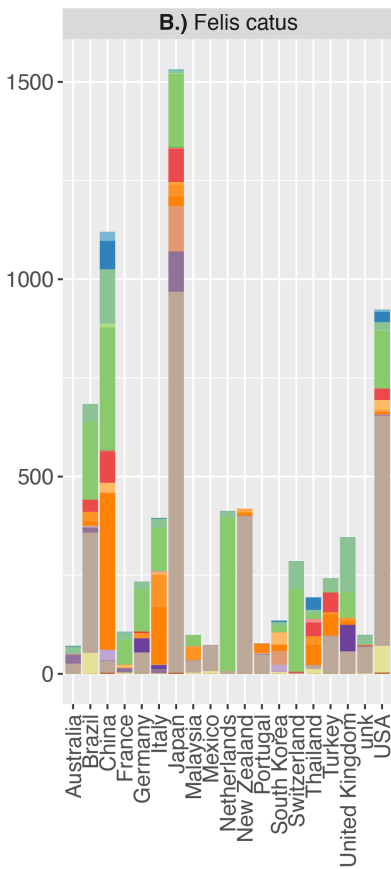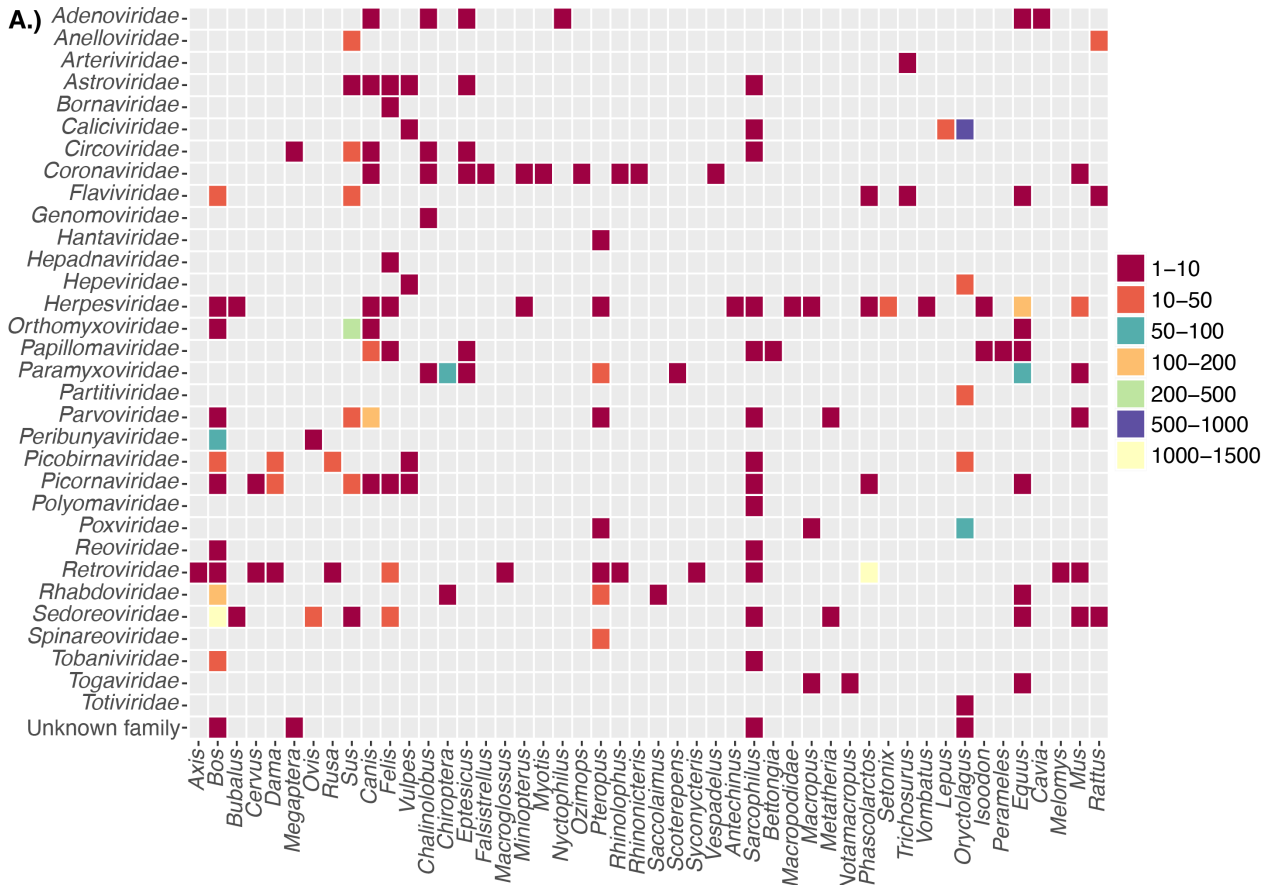
Figure 1.4.1: Graphical illustration of the number of virus sequences on NCBI/GenBank with Australian mammals listed as the host species. A.) Virus sequences separated by mammalian genus and virus family, B.) The number of Felis catus associated sequences and C.) Chiroptera associated virus sequences separated by country of origin. The graph does not contain the virus sequences associated with humans and those presented in the subsequent chapters and Appendices of this thesis. Countries with virus sequence numbers lower than the number for Australia are not displayed in B.) and C.).

Similar to Australia, countries like the USA and China are home to a large number of mammalian species, at around 470 and 573, respectively (IUCN, 2021). However, both countries have a greater number of non-redundant virus reference sequences on NCBI/RefSeq than those from Australia (Figure 1.4.2). The proportion of non-redundant sequences obtained by Illumina sequencing for Australia, USA and China is relatively similar, at 20.9%, 27.5% and 35.2%, respectively. The non-redundant reference sequences obtained by mNGS of Australian mammals belong to the families *Adenoviridae*, *Herpesviridae*, *Paramyxoviridae*, *Poxviridae* and *Rhabdoviridae*, in which two were sequenced from horses, three from bats, one from a kangaroo and three from the genus *Bos*, respectively. In Australia, the viral community of the domestic cat and the order Chiroptera (bats) is relatively under-explored.
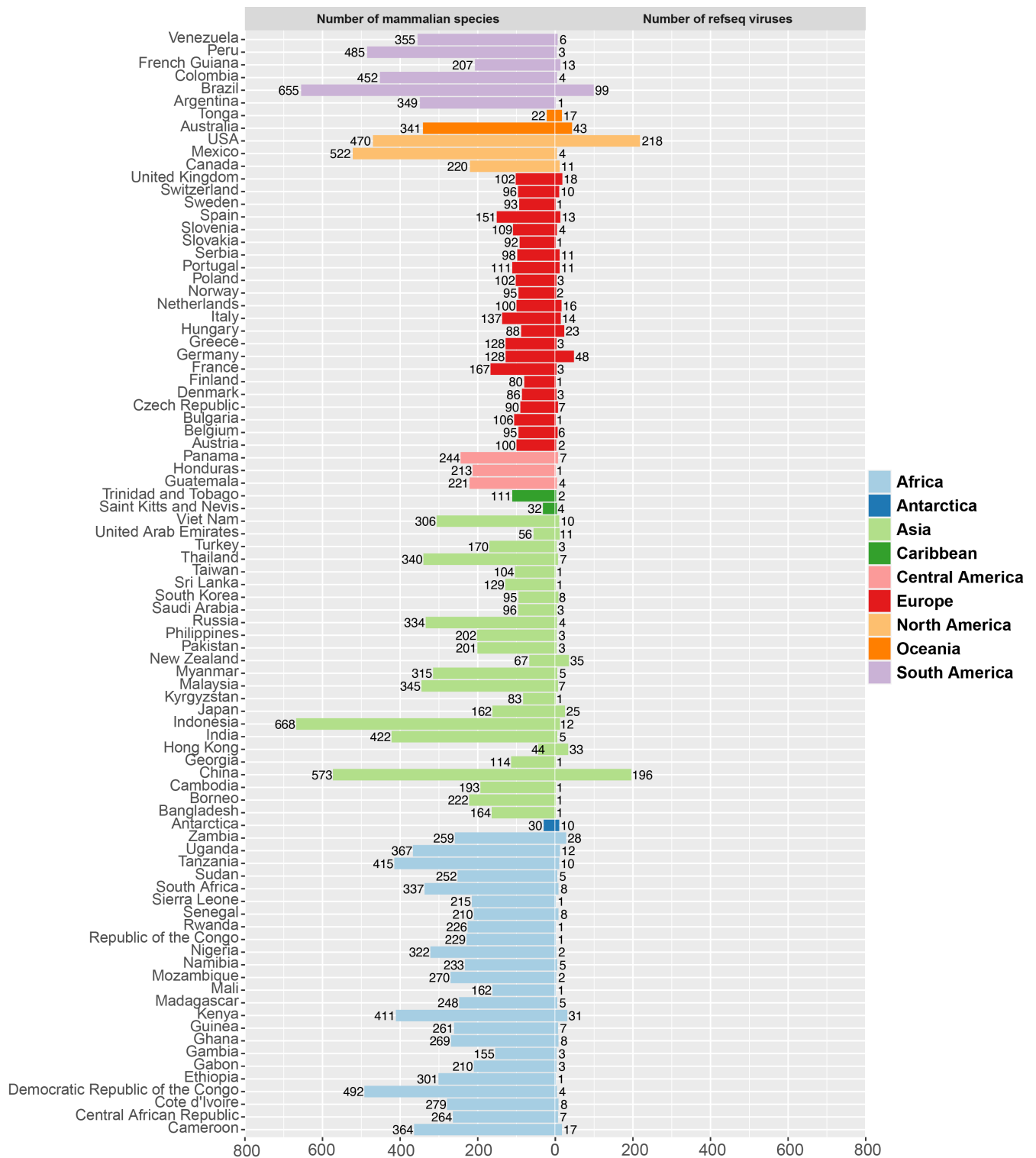
Figure 1.4.2: Graphical illustration of the number of mammalian species found in each country and the number of non-redundant virus nucleotide reference sequences currently deposited on NCBI/RefSeq. The number of mammalian species per country was retrieved from the International Union for the Conservation of Nature's Red List of Threatened Species and excludes all mammalian species that are listed as extinct. The number of RefSeq viruses

33

represents the non-redundant nucleotide reference sequences that have an associated mammalian host, excluding those assigned as Homo sapiens.

1.5 Viral diversity in the domestic cat.

1.5.1 Important viral infections in cats.

Domestic cats are susceptible to a number of viral infections and the transmission, severity of disease and prevalence are influenced by vaccination status, age, sex (in the case of feline immunodeficiency virus) and the environment, especially densely housed environments including breeding colonies and shelters. The feline viruses of major veterinary importance include those that cause gastroenteritis (feline parvovirus and feline coronavirus), respiratory illness (feline calicivirus) and immune deficiencies (feline immunodeficiency virus and feline leukemia virus) (Beatty and Hartmann, 2021).

Carnivore protoparvovirus 1, particularly the variants denoted as feline and canine parvovirus, is a DNA virus of veterinary importance worldwide. Infections in cats result in panleukopenia, dehydration, lethargy and often death. Feline parvovirus has been circulating since the 1900s and has a host range that includes all domestic and wild felids. In contrast, canine parvovirus has only been circulating in the canine population since the 1970s and infects species of Canidae (i.e. dogs) (Parrish, 1999). Notably, however, the CPV-2a, 2b and 2c variants that arose from the classical CPV-2 gained the ability to infect felines and therefore domestic cats (Figure 1.5.1) (Parrish, 1999). This host shift was due to a single mutation in the capsid gene (VP2) that allowed these canine parvovirus variants to bind to the feline transferrin receptor (Parrish, 1999). Although canine parvovirus can infect felines, infections in domestic cats are generally single occurrences and not associated with outbreaks of feline panleukopenia (Barrs, 2019). Shelter-housed and multi-cat environments are optimal for the spread of feline parvovirus as transmission can occur directly through the faecal oral route or indirectly through fomites and the environment (Figure 1.5.1) (Barrs, 2019). Feline panleukopenia outbreaks in Australia were virtually non-existent due to the introduction of an inactivated vaccine and a modified live vaccine in the 1960s (Barrs, 2019). Indeed, feline parvovirus outbreaks were not recorded in Australia for 30 years. However, the virus re-emerged to cause an outbreak of feline panleukopenia in Victoria in 2014, followed by two more subsequent outbreaks in Eastern Australia, described in Appendix I. A high seroprevalence of feline parvovirus has been detected in several countries and a high case

percentage in kittens, likely due to waning maternal antibodies and inadequate protection from vaccination (Barrs, 2019).

Similarly, Feline calicivirus is another virus of veterinary importance that commonly infects Australian owned and stray domestic cats (Nguyen et al., 2019). Feline calicivirus infections usually result in upper respiratory disease, however, in certain cases cats can become infected with a form of the virus that causes a severe virulent systemic disease, that can result in multiple organ damage and death (Pedersen et al., 2000, Schorr-Evans et al., 2003, Reynolds et al., 2009). Vaccines are used as a current prevention method, although Feline calicivirus continually mutates potentially decreasing the effectiveness of vaccines. Feline calicivirus is transmitted to susceptible animals through direct contact with saliva, respiratory secretions and indirectly through aerosol droplets (Figure 1.5.1). Studies performed on domestic cats in Europe determined that a risk factor for Feline calicivirus infection is multi-cat environments (Fernandez et al., 2017, Afonso et al., 2017). More recently, feline calicivirus was detected in faecal samples (Di Martino et al., 2020, Guo et al., 2022), raising the question of whether there are enteric strains that may cause gastroenteric disease.

Feline coronavirus is another common viral infection in felines worldwide, including Australia. Feline coronavirus is an alphacoronavirus (Alphacoronavirus 1) that usually causes asymptomatic infection and occasionally gastroenteritis (Haake et al., 2020). The most common type of feline coronavirus is feline enteric coronavirus that replicates in the gastrointestinal tract of infected felines (Haake et al., 2020). Asymptomatic persistent carriers serve as a source of continual reintroduction of feline enteric coronavirus into the cat population when the virus is shed in faeces, such that the prevalence is high in shelter-housed cats and breeding colonies (Soma et al., 2013, Herrewegh et al., 1997, Sharif et al., 2009, Sabshin et al., 2012, Andersen et al., 2018, Haake et al., 2020). In some circumstances feline enteric coronavirus can mutate into feline infectious peritonitis virus to cause feline infectious peritonitis, a fatal disease (Haake et al., 2020). The pathogenesis of feline infectious peritonitis virus is incompletely understood, although acquired mutations can allow feline enteric coronavirus to macrophages that transport the virus around the body (Kennedy, 2020, Haake et al., 2020). Feline infectious peritonitis develops when the host immune system mounts a response to the virus resulting in an intense inflammatory response (Kennedy, 2020).

Two viruses not included in the routine feline vaccine program are feline immunodeficiency virus and feline leukemia virus – both members of the *Retroviridae* (i.e. retroviruses) that cause acquired immune deficiency in infected animals. The prevalence of feline immunodeficiency virus (FIV) is high among free roaming unneutered male cats that display aggressive and territorial behaviours (Levy et al., 2006, Westman et al., 2016b), as the main transmission route is via bites. However, transmission can also occur from mother to kitten during gestation but is rare (Figure 1.5.1). The transmission of feline leukemia virus among cats is broader and virus can be transferred through direct contact with infected saliva via grooming, sharing water and fighting and from mother to kitten during gestation or by infected milk (Figure 1.5.1). In Australia, the prevalence of FIV is generally higher than that of feline leukemia virus (Norris et al., 2007, Westman et al., 2016). A recent study found the seroprevalence of FIV to be around 6-15% and feline leukemia virus to be 1-4% (Westman et al., 2016).
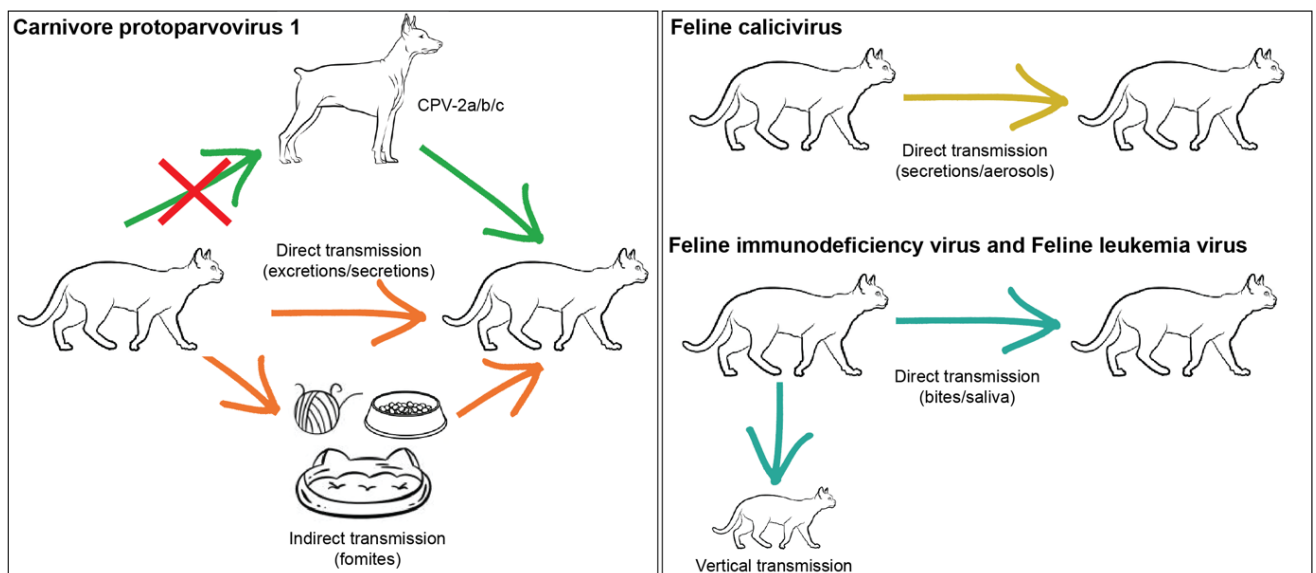
Figure 1.5.1: The different transmission routes of feline and canine parvovirus, feline calicivirus, feline immunodeficiency virus and feline leukemia virus in domestic cats. Vertical transmission depicts the transmission of the virus from mother to kitten during gestation.

1.5.2 The status of mNGS in domestic cats

There are 54 *Felis catus* associated virus sequences characterised from Australian domestic cats deposited on NCBI/Genbank (excluding those presented in this thesis and appendices). These encompass viruses from the *Bornaviridae* (genus *Orthobornavirus*), *Reoviridae* (genus *Rotavirus*), *Herpesviridae* (genus *Percavirus*), *Retroviridae* (genera *Lentivirus* and

Felispumavirus) and *Hepdnaviridae* (genus *Orthohepadnavirus*) (Figure 1.4.1). In comparison, Japan, a country with double the number of owned cats than Australia at around 9 million, has 21 times more *Felis catus* associated virus sequences on NCBI/GenBank covering 14 viral families (Figure 1.4.1). Virus sequences from the *Retroviridae* and *Coronaviridae* constitute 25% and 37%, respectively, of the total *Felis catus* virus sequences on NCBI/GenBank and for countries such as the Netherlands and New Zealand make up over 94% of sequences (Figure 1.4.1). In sum, it is clear that there are considerably lower numbers of the available virus sequences associated with domestic cats in Australia compared to other countries (Figure 1.4.1). In addition, only one of those sequences was obtained by mNGS – a novel feline hepadnavirus that constitutes the first hepadnavirus sampled from a companion animal, detected in a cat with a feline immunodeficiency virus infection (Aghazadeh et al., 2018).

Faecal virome studies on healthy shelter-housed cats using mNGS have found the presence of feline astrovirus, feline calicivirus, feline coronavirus, feline norovirus, feline parvovirus and feline picobirnavirus, together with novel bocaviruses, a feline picornavirus and a feline astrovirus (Zhang et al., 2014, Ng et al., 2014, Li et al., 2020, Li et al., 2021). Investigations of the faecal virome of shelter-housed cats has been performed in the USA, China, Hong Kong, Portugal and Canada using both RT-PCR and mNGS and showed a high prevalence of multiple viruses circulating in the population. In an outbreak study performed on shelter-house cats presenting with vomiting and diarrhoea episodes in California, USA, a novel *Parvoviridae* (denoted feline chaphamaparvovirus) was characterised using mNGS and detected in 47% of affected cats after all other enteric pathogens were excluded, and suggested a likely association with the onset of disease (Li et al., 2020). A separate outbreak investigation on shelter-housed cats in Canada suggested that feline astrovirus was potentially associated with the onset of vomiting after the virus was detected in mNGS data and shed by 91% of affected cats (Li et al., 2021). Both studies also detected the presence of other enteric viruses including feline bocaparvoviruses, feline norovirus and a novel feline dependoparvovirus, which is not uncommon when sampling faeces from cats in densely housed environment (Li et al., 2020, Li et al., 2021). A novel feline rotavirus was detected in a single cat with diarrhoea and in the absence of other enteric pathogens, giving a strong indication that this divergent rotavirus could possibly play a role in the presentation of diarrhoea, although the sample size for this study is too small to make definitive conclusions (Phan et al., 2017). Finally, Lyon-IARC polyomavirus DNA was detected in a mNGS data set

comprised of five pooled faecal samples from cats with diarrhoea (Fahsbender et al., 2019). The virus was confirmed in three of the five faecal samples and in one animal as a coinfection with feline parvovirus (Fahsbender et al., 2019).

The faecal virome of health cats has also been accessed by mNGS in two studies performed on shelter-housed cats in California, USA and one cat from Portugal (Ng et al., 2014, Zhang et al., 2014). The study performed on a single cat from Portugal successfully characterised the complete genomes of two novel feline viruses, feline sakobuvirus A and feline bocaparvovirus 2, and a further two partial sequences of a divergent rotavirus and picornavirus (Ng et al., 2014). In the healthy shelter-housed cats from California, three novel viruses were sequenced, feline astrovirus D1, feline bocaparvovirus 3 and feline cyclovirus (Zhang et al., 2014).

1.6 Viral diversity in Australian bats

1.6.1 Australian bats as reservoirs for importance zoonotic viruses

Chiroptera (bats) is a mammalian order well known for containing a large number of animal species that inhabit six of the seven continents worldwide. In Australia, bats comprise 22% of Australia's mammalian species covering nine families: the *Pteropodidae*, *Megadermatidae*, *Rhinolophidae*, *Hipposideridae*, *Rhinonycteridae*, *Emballonuridae*, *Molossidae*, *Miniopteridae* and *Vespertilionidae* (IUCN, 2021). These families are distributed over all six Australian states and two territories and even onto several Australian territories (Parish et al., 2012). Their diet can consist of fruits, nectar, pollen, insects and small invertebrates (frogs, birds, lizzards, fish, small mammals) and their habitats range from caves, forests, trees, tunnel systems to urban environments (national parks and parkland areas), depending on the bat species (Parish et al., 2012). Colony numbers also vary depending on the bat species, with members of the megabat genus *Pteropus* (i.e., flying foxes) sharing roosting camps along the east coast of Australia where populations sizes can exceed 50,000 individuals (Commonwealth Department of the Environment, 2015). The four *Pteropus* species that inhabit mainland Australia are the grey-headed flying fox (*P. poliocephalus*), little red flying fox (*P. scapulatus*), spectacled flying fox (*P. conspicillatus*) and the black flying fox (*P. alecto*) and their distribution is mainly limited to the coastal regions from the north of Australia into Queensland and New South Wales and even as far south as South Australia (Figure 1.6.1) (IUCN, 2021). The little red flying fox has the largest distribution spanning

four states and two territories, in contrast to the spectacled flying fox that is restricted to a small region of north Queensland (IUCN, 2021). The only *Pteropus* species that is distributed as far south as South Australia is the grey-headed flying fox (Figure 1.6.1) (IUCN, 2021). Bats are important drivers of a sustainable ecosystem, although they are now also infamous as reservoir hosts for important zoonotic diseases, especially the *Pteropus*.

In Australia, bats have been implicated in the spill over of two important zoonotic paramyxoviruses - Hendra virus and Menangle virus (discussed in chapter five of this thesis) (Halpin et al., 2000, Philbey et al., 1998, Philbey et al., 2008). Flying foxes are the reservoir host for Hendra virus and transmit the virus to horses which can then infect humans (Figure 1.6.1) (Field, 2016). No bat-to-human or human-to-human transmission of Hendra virus has been reported to date, and humans act as an incidental and dead-end host for the virus (Field, 2016). From 1994 to 2022, 88 cases of Hendra virus infections in horses in Queensland and New South Wales have been confirmed (Figure 1.6.1), with a further 20 cases unconfirmed but suspected to be to Hendra virus (Field, 2016, Queensland Government, 2022, Taylor et al., 2022). Outbreaks of Hendra virus have been restricted to Queensland and New South Wales, although a seroprevalence of 5.1% using antibodies that are cross-reactive to Hendra virus has been detected in *Vespertilionidae* and *Molossidae* species from Western Australia in 2016 – 2018 (Prada et al., 2019b). A Hendra virus seroprevalence of 43.2% has also been recorded in grey-headed flying fox camps in Adelaide, South Australia sampled from 2015 – 2018 (Boardman et al., 2020). In the same Adelaide grey-headed flying fox population the occurrence of two additional paramyxoviruses, Cedar virus and Tioman virus, was assessed. The bat population was seropositive for both viruses, at a remarkable 95.7% for Tioman virus, although this may result from cross reactivity with Menangle virus that is suggested to be antigenically related to Tioman virus (Boardman et al., 2020, Chua, 2001). Cedar and Tioman virus were both identified in flying foxes (*P. alecto* and *P. poliocephalus* mixed sample and *P. hypomelanus*, respectively) and are currently considered non-pathogenic. More recently, a novel Hendra virus genotype was identified in flying foxes from Victoria, South Australia and Western Australia using RT-PCR and mNGS and the prevalence of this genotype in 98 bats was 11.2% (Wang et al., 2021). Additionally, this novel Hendra virus genotype was detected in pooled and individual flying fox urine collected during 2016 to 2020 in NSW and Queensland (seroprevalence range 2.5% to 6.5%) (Peel et al., 2022).

Australian bat lyssavirus was first identified in New South Wales in 1996 during the screening of two black flying foxes for the presence of the newly emerged Hendra virus

(Fraser et al., 1996). Both animals were seronegative for Hendra virus, although were further tested due to the recording of unusual behaviour before death, including inability to fly and aggressiveness (Fraser et al., 1996). The first Australian bat lyssavirus sequence was obtained by performing RT-PCR on tissue preserved from both animals using degenerate primers targeting the lyssavirus nucleocapsid protein (Fraser et al., 1996). Prior to 1996 it was believed that Australia was lyssavirus free. However, our current knowledge is that most, if not all, Australian bat species have the capacity to be a reservoir host for Australian bat lyssavirus (Field, 2018). Active infection has been recorded in all four *Pteropus* species on mainland Australia (Gould et al., 1998, Speare et al., 1997, Barrett et al., 2020) and one microbat species, yellow-bellied sheath-tailed bat (*Saccolaimus flaviventris*) (Gould et al., 2002). Subsequently, three fatal human Australian bat lyssavirus infections have been recorded to date after all three were exposed to the virus after being bitten or scratched by infected bats (Allworth et al., 1996, Francis et al., 2014, Hanna et al., 2000, Samaratunga et al., 1998). Similar to classical rabies virus, Australian bat lyssavirus causes neurological and behavioural changes in affected bats (McColl et al., 2002, Barrett et al., 2020). Experimental infection of grey-headed flying foxes with Australian bat lyssavirus and bat associated rabies virus showed that 30% of grey-headed flying foxes infected with Australian bat lyssavirus developed clinical signs consistent with lyssavirus infection, including paralysis, trembling and muscle weakness (McColl et al., 2002). Seropositive animals have been detected as far as Western Australia in six species of *Vespertilionidae* at 2.9% (Prada et al., 2019a), although testing on grey-headed flying foxes in Adelaide, South Australia, over a three-year surveillance study found all 301 animals sampled were seronegative (Boardman et al., 2020). Additionally, Australian bat lyssavirus antigens were detected in 6.8% of bats submitted after injury, illness or death from New South Wales and Queensland and antibodies were detected in 2.7% wild caught bats (Field, 2018). A study utilising surveillance data from the period 2010 to 2016 showed that from the available data from 2281 bats, 4.5% of animals tested positive for Australian bat lyssavirus (Iglesias et al., 2021).
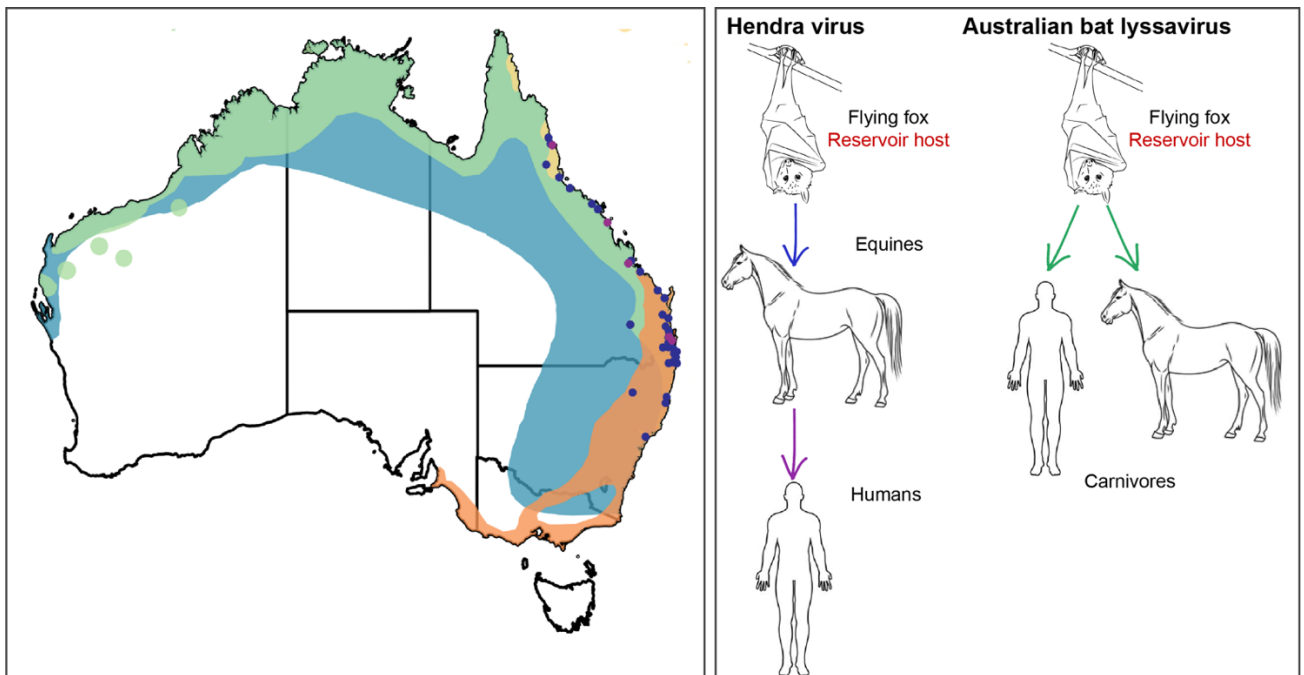
Figure 1.6.1: The left panel shows the distribution of the black flying fox (P. alecto) in green, little red flying fox (P. scapulatus) in blue, grey-headed flying fox (P. poliocephalus) in orange and spectacled flying fox (P. conspicillatus) in yellow. The green points on the map represent locations Hendra virus infections in horses have been recorded and the purple points are for infections in humans (Queensland Government, 2022). The right panel depicts the transmission route of Hendra virus and Australian bat lyssavirus (Queensland Government, 2022).

1.6.2 Current status of mNGS in endemic bat species

It is clear that in Australia there is an emphasis on conducting studies that monitor zoonotic viruses in bat populations. Indeed, it is striking that only 56 of the 302 (18.5%) bat sequences sampled from Australia deposited on NCBI/GenBank are not members of the *Rhabdoviridae*, *Coronaviridae* and *Paramyxoviridae* (Figure 1.4.1). Furthermore, all but one bat coronavirus sequence detected in Australian bats was sampled before the emergence of severe acute respiratory syndrome 1 (SARS-CoV-1) in 2002-2003. Sampling bias is also evident in other countries, mainly China and the USA where viruses of the *Coronaviridae* and *Rhadboviridae* are problematic. When comparing the NCBI/GenBank virus sequences sampled from China and the USA, 51.8% are *Coronaviridae* (53.5% betacoronaviruses and 46.5% alphacoronaviruses) and 83.7% are *Rhabdoviridae* (99% lyssaviruses), respectively (Figure 1.4.1).

To date, two notable mNGS studies have been performed on Australian bats and have characterised several novel and important viruses. Two recent mNGS studies on Australian flying foxes identified the first gammaretrovirus sequence from the brain of a black flying fox in Queensland (McMichael et al., 2019) and the first reproduction competent exogenous gammaretrovirus from the faeces of flying foxes in Queensland and New South Wales (Hayward et al., 2020), both of which are phylogenetically related to the pathogenic retroviruses koala retrovirus and gibbon ape leukemia virus (Hayward et al., 2020, McMichael et al., 2019). These studies highlighted the possible role bats play as reservoirs for retroviruses that may infect other mammalian species (Hayward et al., 2020, McMichael et al., 2019). The genome of a novel poxvirus sampled from a skin lesion from a little red flying fox was characterised using mNGS and may constitute a new genus in the *Poxviridae* (O'Dea et al., 2016).

1.7 Thesis rational

The overall aim of my thesis is to characterise existing and novel viruses in faecal and tissue samples from healthy and diseased animals in Australia. The virus diversity of domestic cats is largely unexplored in Australia. Similarly, the diversity of viruses in Australian bats is usually targeted toward those viral families deemed to be of major importance, particularly the *Rhabdoviridae*, *Paramyxoviridae* and *Coronaviridae*. The most recent feline parvovirus outbreaks in Australia and the global outbreak of SARS-CoV-2 clearly highlight why it is important to not neglect the virus diversity in domestic animals and urban wildlife populations. To help close this fundamental gap in knowledge I employed mNGS of virus DNA and RNA, in addition to PCR, to identify the virus diversity in domestic cats and bats in Australia, with a particular emphasis on the Australian grey-headed flying fox that is commonplace in urban and suburban environments in Australia, including metropolitan Sydney.

In chapter two I implemented mNGS together with virus baiting technology to sequence the tumour tissue DNA from a single cat with a squamous cell carcinoma. Notably, this method was able to capture a novel papillomavirus likely associated with the nasal squamous cell carcinoma. The mNGS yielded an almost complete novel feline papillomavirus genome that I was able to complete using PCR and Sanger sequencing.

Chapter three of this thesis describes the use of metatranscriptomic NGS of total RNA and viral particle enriched nucleic acid to detect novel viruses in the gastrointestinal tract of domestic cats. This project utilised samples collected during an outbreak of feline parvovirus in Australia and samples collected from healthy shelter-housed cats in Sydney, Australia. Two novel feline astroviruses were identified and characterised from the faecal samples collected from one cat with feline parvovirus and diarrhoea and three healthy shelter-housed cats.

Similarly, the enteric virome of several feline parvovirus infected cats sampled during several outbreaks in 2016 and 2017 and healthy shelter-housed cats were characterised using metatranscriptomic NGS and viral particle enrichment techniques and described in chapter four. This study showed that shelter-housed cats carry a large diversity of feline viruses in their gastrointestinal tract, including feline coronavirus, feline astrovirus, feline bocaparvoviruses and feline anelloviruses. Another notable finding was the identification of the first Australian feline kobuvirus strains in feline parvovirus infected cats and feline calicivirus excreted in faeces.

Chapter five is a literature review focused on the mNGS studies already performed on bat species worldwide and shows an increase in the sampling of bat populations in Asian countries post SARS-CoV-1 and SARS-CoV-2. This paper outlines the importance of understanding the viral diversity in bats and the importance of maintaining bat species worldwide for the safety of our ecosystem.

In chapter six I have used metatranscriptomics to characterise the enteric virome of the Australian grey-headed flying fox. This study sampled from three grey-headed flying fox colonies in two Australian states that are located in urban habitats close to human communities. This study highlights the usefulness of untargeted sequencing by revealing the presence of a novel betacoronavirus of the genus *Nobecovirus*, a novel sapovirus and the first in Australian bats, two novel betaretroviruses also the first detected in Australian bats and a novel birnavirus possibly associated with bats.

Finally, chapter seven presents the data I obtained from mNGS of tissue samples from diseased bats collected in Australia. This study was used to identify the aetiological agent responsible for severe disease in numerous Australian flying foxes and a single microbat. This study showed the presence of an important gammaretrovirus with a possible association

to leukemia, a novel *Picornaviridae*, novel *Astroviridae* in the skin lesion of a microbat and bat pegiviruses.

During my PhD I also contributed to an additional four publications in which I am co-author. These are presented in the Appendices to this thesis. In the first study described in Appendix I used PCR and Sanger sequencing to determine the circulating field strains of feline parvovirus responsible for outbreaks in 2014 – 2016 in Australia, in addition to strains circulating in the United Arab Emirates. Appendix II uses mNGS for the investigation of viral and clinical features of feline calicivirus strains responsible for viral systemic disease in three Australian outbreaks. The occurrence of canine parvovirus shedding in shelter-housed cats in Sydney is described in Appendix III. Finally, the study in Appendix IV describes the use of mNGS and baiting technology to identify the strains of Carnivore protoparvovirus 1 in the feline parvovirus infected cats sampled and sequenced in chapter four of this thesis by investigating the single nucleotide polymorphisms (SNPs) present in the non-structural and viral proteins.

1.8 References

Afonso, M.M., Pinchbeck, G.L., Smith, S.L., Daly, J.M., Gaskell, R.M., Dawson, S., Radford, A.D. 2017. A multi-national European cross-sectional study of feline calicivirus epidemiology, diversity and vaccine cross-reactivity. *Vaccine,* 35(20):2753-2760.

Aghazadeh, M., Shi, M., Barrs, V.R., McLuckie, A.J., Lindsay, S.A., Jameson, B., Hampson, B., Holmes, E.C., Beatty, J.A. 2018. A Novel Hepadnavirus Identified in an Immunocompromised Domestic Cat in Australia. *Viruses,* 10(5):269.

Allworth, A., Murray, K., Morgan, J. 1996. A human case of encephalitis due to a lyssavirus recently identified in fruit bats. *Communicable diseases intelligence,* 20:504-504.

Andersen, L.A., Levy, J.K., McManus, C.M., McGorray, S.P., Leutenegger, C.M., Piccione, J., Blackwelder, L.K., Tucker, S.J. 2018. Prevalence of enteropathogens in cats with and without diarrhea in four different management models for unowned cats in the southeast United States. *The Veterinary Journal,* 236:49-55.

Australian Bureau of Statistics. 2020-21. Agricultural Commodities, Australia, ABS. Viewed September 2022. https://www.abs.gov.au/statistics/industry/agriculture/agricultural-commodities-australia/latest-release.

Baltimore, D. 1971. Expression of animal virus genomes. *Bacteriological Reviews,* 35(3):235-41.

Barrett, J., Höger, A., Agnihotri, K., Oakey, J., Skerratt, L.F., Field, H.E., Meers, J., Smith, C. 2020. An unprecedented cluster of Australian bat lyssavirus in Pteropus conspicillatus indicates pre-flight flying fox pups are at risk of mass infection. *Zoonoses Public Health,* 67(4):435-442.

Barrs, V.R. 2019. Feline Panleukopenia: A Re-emergent Disease. *Veterinary Clinics of North America: Small Animal Practice,* 49(4):651-670.

Beatty, J.A., Hartmann, K. 2021. Advances in Feline Viruses and Viral Diseases. *Viruses,* 13(5):923.

Beijerinck, M. 1899. Bemerkung zu dem Aufsatz von Herrn Iwanowsky über die Mosaikkrankheit der Tabakspflanze. *Centralbl Bakteriologie, Parasitenkunde und Infektionskrankheiten II Abt,* 5:310-311.

Belaganahalli, M.N., Maan, S., Maan, N.S., Pritchard, I., Kirkland, P.D., Brownlie, J., Attoui, H., Mertens, P.P. 2014. Full genome characterization of the culicoides-borne marsupial orbiviruses: Wallal virus, Mudjinbarry virus and Warrego viruses. *PLoS One,* 9(10):e108379.

Bennett, M.D., Woolford, L., Stevens, H., Van Ranst, M., Oldfield, T., Slaven, M., O'Hara, A.J., Warren, K.S., Nicholls, P.K. 2008. Genomic characterization of a novel virus found in papillomatous lesions from a southern brown bandicoot (Isoodon obesulus) in Western Australia. *Virology,* 376(1):173-82.

Boardman, W.S.J., Baker, M.L., Boyd, V., Crameri, G., Peck, G.R., Reardon, T., Smith, I.G., Caraguel, C.G.B., Prowse, T.A.A. 2020. Seroprevalence of three paramyxoviruses; Hendra virus, Tioman virus, Cedar virus and a rhabdovirus, Australian bat lyssavirus, in a range expanding fruit bat, the Grey-headed flying fox (Pteropus poliocephalus). *PLoS One,* 15(15):e0232339.

Chang, W.S., Eden, J.S., Hartley, W.J., Shi, M., Rose, K., Holmes, E.C. 2019. Metagenomic discovery and co-infection of diverse wobbly possum disease viruses and a novel hepacivirus in Australian brushtail possums. *One Health Outlook,* 1:5.

Chen, Y.M., Sadiq, S., Tian, J.H., Chen, X., Lin, X.D., Shen, J.J., Chen, H., Hao, Z.Y., Wille, M., Zhou, Z.C., Wu, J., Li, F., Wang, H.W., Yang, W.D., Xu, Q.Y., Wang, W., Gao, W.H., Holmes, E.C., Zhang, Y.Z. 2022. RNA viromes from terrestrial sites across China expand environmental viral diversity. *Nature Microbiology,* 7(8):1312-1323.

Chua, K.B., Wang, L.F., Lam, S.K., Crameri, G., Yu, M., Wise, T. 2001. Tioman virus, a novel paramyxovirus isolated from fruit bats in Malaysia. *Virology*, 283(2):215-29.

Coffey, L.L., Page, B.L., Greninger, A.L., Herring, B.L., Russell, R.C., Doggett, S.L., Haniotis, J., Wang, C., Deng, X., Delwart, E.L. 2014. Enhanced arbovirus surveillance with deep sequencing: Identification of novel rhabdoviruses and bunyaviruses in Australian mosquitoes. *Virology,* 448:146-58.

Commonwealth Department of the Environment. 2015. Status and trends of Australia's EPBC-listed flying-foxes. Viewed September 2022. https://www.dcceew.gov.au/sites/default/files/documents/status-trends-australias-epbc-listed-flying-foxes.pdf.

Conceicao-Neto, N., Zeller, M., Lefrere, H., De Bruyn, P., Beller, L., Deboutte, W., Yinda, C.K., Lavigne, R., Maes, P., Van Ranst, M., Heylen, E., Matthijnssens, J. 2015. Modular approach to customise sample preparation procedures for viral metagenomics: a reproducible protocol for virome analysis. *Scientific Reports,* 5:16532.

Daly, G.M., Bexfield, N., Heaney, J., Stubbs, S., Mayer, A.P., Palser, A., Kellam, P., Drou, N., Caccamo, M., Tiley, L. 2011. A viral discovery methodology for clinical biopsy samples utilising massively parallel next generation sequencing. *Plos one,* 6(12):e28879.

Di Martino, B., Lanave, G., Di Profio, F., Melegari, I., Marsilio, F., Camero, M., Catella, C., Capozza, P., Bányai, K., Barrs, V.R., Buonavoglia, C., Martella, V. 2020. Identification of feline calicivirus in cats with enteritis. *Transboundary and Emerging Diseases,* 67(6):2579-2588.

Fahsbender, E., Altan, E., Estrada, M., Seguin, M.A., Young, P., Leutenegger, C.M., Delwart, E. 2019. Lyon-IARC Polyomavirus DNA in Feces of Diarrheic Cats. *Microbiology Resource Announcements,* 8(29):e00550-19.

Fernandez, M., Manzanilla, E.G., Lloret, A., León, M., Thibault, J.-C. 2017. Prevalence of feline herpesvirus-1, feline calicivirus, Chlamydophila felis and Mycoplasma felis DNA and associated risk factors in cats in Spain with upper respiratory tract disease, conjunctivitis and/or gingivostomatitis. *Journal of Feline Medicine and Surgery,* 19(4):461-469.

Field, H.E. 2016. Hendra virus ecology and transmission. *Current Opinion in Virology*, 16:120-125

Field, H.E. 2018. Evidence of Australian bat lyssavirus infection in diverse Australian bat taxa. *Zoonoses Public Health,* 65(6):742-748.

Francis, J.R., Nourse, C., Vaska, V.L., Calvert, S., Northill, J.A., McCall, B., Mattke, A.C. 2014. Australian Bat Lyssavirus in a child: the first reported case. *Pediatrics,* 133(4):1063-7.

Fraser, G.C., Hooper, P.T., Lunt, R.A., Gould, A.R., Gleeson, L.J., Hyatt, A.D., Russell, G.M., Kattenbelt, J.A. 1996. Encephalitis caused by a Lyssavirus in fruit bats in Australia. *Emerging Infectious Diseases,* 2(4):327-31.

Ganges, L., Crooke, H.R., Bohórquez, J.A., Postel, A., Sakoda, Y., Becher, P., Ruggli, N. 2020. Classical swine fever virus: the past, present and future. *Virus Research,* 289:198151.

Gould, A.R., Hyatt, A.D., Lunt, R., Kattenbelt, J.A., Hengstberger, S., Blacksell, S.D. 1998. Characterisation of a novel lyssavirus isolated from Pteropid bats in Australia. *Virus Research,* 54(2):165-87.

Gould, A.R., Kattenbelt, J.A., Gumley, S.G., Lunt, R.A. 2002. Characterisation of an Australian bat lyssavirus variant isolated from an insectivorous bat. *Virus Research,* 89(1):1-28.

Guo, J., Ding, Y., Sun, F., Zhou, H., He, P., Chen, J., Guo, J., Zeng, H., Long, J., Wei, Z., Ouyang, K., Huang, W., Chen, Y. 2022. Co-circulation and evolution of genogroups I and II of respiratory and enteric feline calicivirus isolates in cats. *Transboundary and Emerging Disease*, 69(5):2924-2937.

Haake, C., Cook, S., Pusterla, N., Murphy, B. 2020. Coronavirus Infections in Companion Animals: Virology, Epidemiology, Clinical and Pathologic Features. *Viruses,* 12(9):1023.

Halpin, K., Young, P.L., Field, H.E., Mackenzie, J.S. 2000. Isolation of Hendra virus from pteropid bats: a natural reservoir of Hendra virus. *Journal of General Virology*, 81(Pt 8):1927-1932.

Hanna, J.N., Carney, I.K., Smith, G.A., Tannenberg, A.E., Deverill, J.E., Botha, J.A., Serafin, I.L., Harrower, B.J., Fitzpatrick, P.F., Searle, J.W. 2000. Australian bat lyssavirus infection: a second human case, with a long incubation period. *Medical Journal of Australia,* 172(12):597-9.

Hayward, J.A., Tachedjian, M., Kohl, C., Johnson, A., Dearnley, M., Jesaveluk, B., Langer, C., Solymosi, P.D., Hille, G., Nitsche, A., Sánchez, C.A., Werner, A., Kontos, D., Crameri, G., Marsh, G.A., Baker, M.L., Poumbourios, P., Drummer, H.E., Holmes, E.C., Wang, L.F., Smith, I., Tachedjian, G. 2020. Infectious KoRV-related retroviruses circulating in Australian bats. *Proceedings of the National Academy of Sciences of the United States of America,* 117(17):9529-9536.

Herrewegh, A.A.P.M., Mähler, M., Hedrich, H.J., Haagmans, B.L., Egberink, H.F., Horzinek, M.C., Rottier, P.J.M., de Groot, R.J. 1997. Persistence and Evolution of Feline Coronavirus in a Closed Cat-Breeding Colony. *Virology,* 234(2):349-363.

International Union for Conservation of Nature. 2021. *The IUCN Red List of Threatened Species*. Version 2021-3. https://www.iucnredlist.org

Iglesias, R., Cox-Witton, K., Field, H., Skerratt, L.F., Barrett, J. 2021. Australian bat lyssavirus: analysis of national bat surveillance data from 2010 to 2016. *Viruses*, 13(2):189.

Ivanovski, D. 1892. Über die mosaikkrankheit der tabakspflanze. *St Petersb Acad Imp Sci Bull,* 35**,** 67-70.

Kemper, C.M., Tomo, I., Bingham, J., Bastianello, S.S., Wang, J., Gibbs, S.E., Woolford, L., Dickason, C., Kelly, D. 2016. Morbillivirus-associated unusual mortality event in South Australian bottlenose dolphins is largest reported for the Southern Hemisphere. *Royal Society Open Science,* 3(12):160838.

Kennedy, M.A. 2020. Feline Infectious Peritonitis: Update on Pathogenesis, Diagnostics, and Treatment. *Veterinary Clinics of North America: Small Animal Practice,* 50(5):1001-1011.

Kohl, C., Brinkmann, A., Dabrowski, P.W., Radonić, A., Nitsche, A., Kurth, A. 2015. Protocol for metagenomic virus detection in clinical specimens. *Emerging infectious diseases,* 21(1):48.

Kovaliski, J., Sinclair, R., Mutze, G., Peacock, D., Strive, T., Abrantes, J., Esteves, P.J., Holmes, E.C. 2014. Molecular epidemiology of Rabbit Haemorrhagic Disease Virus in Australia: when one became many. *Molecular Ecology,* 23(2):408-20.

Kumar, A., Murthy, S., Kapoor, A. 2017. Evolution of selective-sequencing approaches for virus discovery and virome analysis. *Virus Research,* 239:172-179.

Leland, D.S., Ginocchio, C.C. 2007. Role of cell culture for virus detection in the age of technology. *Clinical microbiology reviews,* 20(1):49-78.

Levy, J.K., Scott, H.M., Lachtara, J.L., Crawford, P.C. 2006. Seroprevalence of feline leukemia virus and feline immunodeficiency virus infection among cats in North America and risk factors for seropositivity. *Journal of the American Veterinary Medical Association,* 228(3):371-6.

Li, C.X., Shi, M., Tian, J.H., Lin, X.D., Kang, Y.J., Chen, L.J., Qin, X.C., Xu, J., Holmes, E.C., Zhang, Y.Z. 2015. Unprecedented genomic diversity of RNA viruses in arthropods reveals the ancestry of negative-sense RNA viruses. *Elife,* 4:e05378.

Li, Y., Gordon, E., Idle, A., Altan, E., Seguin, M.A., Estrada, M., Deng, X., Delwart, E. 2020. Virome of a Feline Outbreak of Diarrhea and Vomiting Includes Bocaviruses and a Novel Chapparvovirus. *Viruses,* 12(5):506.

Li, Y., Gordon, E., Idle, A., Hui, A., Chan, R., Seguin, M.A., Delwart, E. 2021. Astrovirus Outbreak in an Animal Shelter Associated With Feline Vomiting. *Frontiers in Veterinary Science,* 8:628082.

Loeffler, F. 1898. Berichte der Kommission zur Erforschung der Maulundklauenseuche bei dem Institut Infektionskrankheiten in Berlin. *Zentralblatt Bakteriologie, Parasitenkunde Infektiouskrankheiten, Abt. I,* 23:371-391.

Mahar, J.E., Hall, R.N., Peacock, D., Kovaliski, J., Piper, M., Mourant, R., Huang, N., Campbell, S., Gu, X., Read, A., Urakova, N., Cox, T., Holmes, E.C., Strive, T. 2018a. Rabbit Hemorrhagic Disease Virus 2 (RHDV2; GI.2) Is Replacing Endemic Strains of RHDV in the Australian Landscape within 18 Months of Its Arrival. *Journal of Virology,* 92(2):e01374-17.

Mahar, J.E., Read, A.J., Gu, X., Urakova, N., Mourant, R., Piper, M., Haboury, S., Holmes, E.C., Strive, T., Hall, R.N. 2018b. Detection and Circulation of a Novel Rabbit Hemorrhagic Disease Virus in Australia. *Emerging Infectious Disease,* 24(1):22-31.

McColl, K.A., Chamberlain, T., Lunt, R.A., Newberry, K.M., Middleton, D., Westbury, H.A. 2002. Pathogenesis studies with Australian bat lyssavirus in grey-headed flying foxes (Pteropus poliocephalus). *Australian Veterinary journal J,* 80(10):636-41.

McMichael, L., Smith, C., Gordon, A., Agnihotri, K., Meers, J., Oakey, J. 2019. A novel Australian flying-fox retrovirus shares an evolutionary ancestor with Koala, Gibbon and Melomys gamma-retroviruses. *Virus Genes,* 55:421-424.

Mullis, K., Faloona, F., Scharf, S., Saiki, R., Horn, G., Erlich, H. 1986. Specific enzymatic amplification of DNA in vitro: the polymerase chain reaction. *Cold Spring Harbor Symposia on Quantitative Biology,* 51:263-73.

Ng, T.F., Mesquita, J.R., Nascimento, M.S., Kondov, N.O., Wong, W., Reuter, G., Knowles, N.J., Vega, E., Esona, M.D., Deng, X., Vinje, J., Delwart, E. 2014. Feline fecal virome reveals novel and prevalent enteric viruses. *Veterinary Microbiology,* 171(1-2):102-11.

Nguyen, D., Barrs, V.R., Kelman, M., Ward, M.P. 2019. Feline upper respiratory tract infection and disease in Australia. *Journal of Feline Medicine and Surgery,* 21(10):973-978.

Norris, J.M., Bell, E.T., Hales, L., Toribio, J.A., White, J.D., Wigney, D.I., Baral, R.M., Malik, R. 2007. Prevalence of feline immunodeficiency virus infection in domesticated and feral cats in eastern Australia. *Journal of Feline Medicine and Surgery,* 9(4):300-8.

O'Dea, M.A., Tu, S.L., Pang, S., De Ridder, T., Jackson, B., Upton, C. 2016. Genomic characterization of a novel poxvirus from a flying fox: evidence for a new genus? *Journal of General Virology,* 97(9):2363-2375.

Parrish, C.R. 1999. Host range relationships and the evolution of canine parvovirus. *Veterinary microbiology,* 69(1-2):29-40.

Parish, S., Richards, G., Hall, L. 2012. A natural history of Australian bats: working the night shift. *CSIRO publishing, Melbourne.*

Pedersen, N.C., Elliott, J.B., Glasgow, A., Poland, A., Keel, K. 2000. An isolated epizootic of hemorrhagic-like fever in cats caused by a novel and highly virulent strain of feline calicivirus. *Veterinary microbiology,* 73(4):281-300.

Peel, A.J., Yinda, C.K., Annand, E.J., Dale, A.S., Peggy, E., Eden, J.S., Jones, D.N., Kessler, M.K., Lunn, T.J., Pearson, T., Schulz, J.E., Smith, I.L., Munster, V.J., Plowright, R.K. 2022. Novel Hendra virus variant circulating in black flying foxes and grey-headed flying foxes, Australia. *Emerging Infectious Diseases*, 28(5):1043-1047.

Phan, T.G., Leutenegger, C.M., Chan, R., Delwart, E. 2017. Rotavirus I in feces of a cat with diarrhea. *Virus Genes,* 53(3):487-490.

Philbey, A.W., Kirkland, P.D., Ross, A.D., Davis, R.J., Gleeson, A.B., Love, R.J., Daniels, P.W., Gould, A.R., Hyatt, A.D. 1998. An apparently new virus (family Paramyxoviridae) infectious for pigs, humans, and fruit bats. *Emerging Infectious Disease,* 4(2):269-71.

Philbey, A.W., Kirkland, P.D., Ross, A.D., Field, H.E., Srivastava, M., Davis, R.J., Love, R.J. 2008. Infection with Menangle virus in flying foxes (Pteropus spp.) in Australia. *Australian Veterinary Journal*, 86(2):449-54.

Prada, D., Boyd, V., Baker, M., Jackson, B., O'Dea, M. 2019a. Insights into Australian Bat Lyssavirus in Insectivorous Bats of Western Australia. *Tropical Medicine and Infectious Disease,* 4(1):46.

Prada, D., Boyd, V., Baker, M.L., O'Dea, M., Jackson, B. 2019b. Viral Diversity of Microbats within the South West Botanical Province of Western Australia. *Viruses,* 11(12):1157.

Queensland Government. 2022. Summary of Hendra virus incidicents in horses. Viewed September 2022. https://www.business.qld.gov.au/industries/service-industries-professionals/service-industries/veterinary-surgeons/guidelines-hendra/incident-summary

Reyes, G.R., Kim, J.P. 1991. Sequence-independent, single-primer amplification (SISPA) of complex DNA populations. *Molecular and Cellular Probes,* 5(6):473-81.

Reynolds, B.S., Poulet, H., Pingret, J.L., Jas, D., Brunet, S., Lemeter, C., Etievant, M., Boucraut-Baralon, C. 2009. A nosocomial outbreak of feline calicivirus associated virulent systemic disease in France. *Journal of Feline Medicine and Surgery,* 11(8):633-44.

Rosseel, T., Ozhelvaci, O., Freimanis, G., Van Borm, S. 2015. Evaluation of convenient pretreatment protocols for RNA virus metagenomics in serum and tissue samples. *Journal of virological methods,* 222:72-80.

Sabshin, S.J., Levy, J.K., Tupler, T., Tucker, S.J., Greiner, E.C., Leutenegger, C.M. 2012. Enteropathogens identified in cats entering a Florida animal shelter with normal feces or diarrhea. *Journal of the American Veterinary Medical Association,* 241(3):331-337.

Sadiq, S., Chen, Y.M., Zhang, Y.Z., Holmes, E.C. 2022. Resolving deep evolutionary relationships within the RNA virus phylum Lenarviricota. *Virus Evol,* 8(1):veac055.

Samaratunga, H., Searle, J.W., Hudson, N. 1998. Non-rabies Lyssavirus human encephalitis from fruit bats: Australian bat Lyssavirus (pteropid Lyssavirus) infection. *Neuropathology and Applied Neurobiology,* 24(24):331-5.

Sanger, F., Nicklen, S., Coulson, A.R. 1977. DNA sequencing with chain-terminating inhibitors. *Proceedings of the National Academy of Sciences,* 74(12):5463-5467.

Schorr-Evans, E.M., Poland, A., Johnson, W.E., Pedersen, N.C. 2003. An epizootic of highly virulent feline calicivirus disease in a hospital setting in New England. *Journal of Feline Medicine and Surgery,* 5(4):217-26.

Sharif, S., Arshad, S.S., Hair-Bejo, M., Omar, A.R., Zeenathul, N.A., Hafidz, M.A. 2009. Prevalence of feline coronavirus in two cat populations in Malaysia. *Journal of Feline Medicine and Surgery,* 11(12):1031-1034.

Shi, M., Lin, X.D., Tian, J.H., Chen, L.J., Chen, X., Li, C.X., Qin, X.C., Li, J., Cao, J.P., Eden, J.S., Buchmann, J., Wang, W., Xu, J., Holmes, E.C., Zhang, Y.Z. 2016. Redefining the invertebrate RNA virosphere. *Nature,* 540(7634):539-543.

Smyth, G.B., Dagley, K., Tainsh, J. 2011. Insights into the economic consequences of the 2007 equine influenza outbreak in Australia. *Australian Veterinary Journal,* 89 Suppl 1:151-8.

Soma, T., Wada, M., Taharaguchi, S., Tajima, T. 2013. Detection of Ascitic Feline Coronavirus RNA from Cats with Clinically Suspected Feline Infectious Peritonitis. *Journal of Veterinary Medical Science,* 75(10):1389-1392.

Speare, R., Skerratt, L., Foster, R., Berger, L., Hooper, P., Lunt, R., Blair, D., Hansman, D., Goulet, M., Cooper, S. 1997. Australian bat lyssavirus infection in three fruit bats from north Queensland. *Communicable Diseases Intelligence,* 21(9):117-20.

Statista Search Department. 2022. Total number of pets owned in Australia in 2019 and 2021, by type, viewed September 2022. Statista. https://www.statista.com/statistics/1239046/top-saas-countries-list/

Taylor, J., Thompson, K., Annand, E.J., Massey, P.D., Bennett, J., Eden, J.S., Horsburgh, B.A., Hodgson, E., Wood, K., Kerr, J., Kirkland, P., Finlaison, D., Peel, A.J., Eby, P., Durrheim, D.N. 2022. Novel variant Hendra virus genotype 2 infection in a horse in the greater Newcastle region, New South Wales, Australia. *One Health,*15:100423

Wang, J., Anderson, D.E., Halpin, K., Hong, X., Chen, H., Walker, S., Valdeter, S., van der Heide, B., Neave, M.J., Bingham, J., O'Brien, D., Eagles, D., Wang, L.F., Williams, D.T. 2021. A new Hendra virus genotype found in Australian flying foxes. *Virololgy Journal,* 18(1):197.

Westman, M.E., Paul, A., Malik, R., McDonagh, P., Ward, M.P., Hall, E., Norris, J.M. 2016. Seroprevalence of feline immunodeficiency virus and feline leukaemia virus in Australia: risk factors for infection and geographical influences (2011-2013). *Journal of Feline Medicine and Surgery Open Reports,* 2(1):2055116916646388.

Woolford, L., Rector, A., Van Ranst, M., Ducki, A., Bennett, M.D., Nicholls, P.K., Warren, K.S., Swan, R.A., Wilcox, G.E., O'Hara, A.J. 2007. A novel virus detected in papillomas and carcinomas of the endangered western barred bandicoot (Perameles bougainville) exhibits genomic features of both the Papillomaviridae and Polyomaviridae. *Journal of Virology,* 81(24):13280-90.

Zhang, J., Finlaison, D.S., Frost, M.J., Gestier, S., Gu, X., Hall, J., Jenkins, C., Parrish, K., Read, A.J., Srivastava, M., Rose, K., Kirkland, P.D. 2018. Identification of a novel nidovirus as a potential cause of large scale mortalities in the endangered Bellinger River snapping turtle (Myuchelys georgesi). *PLoS One,* 13(10):e0205209.

Zhang, W., Li, L., Deng, X., Kapusinszky, B., Pesavento, P.A., Delwart, E. 2014. Faecal virome of cats in an animal shelter. *Journal of General Virology,* 95(Pt 11):2553-2564.

Chapter two: Identification of a Novel Papillomavirus Associated with Squamous Cell Carcinoma in a Domestic Cat

Maura Carrai[1,*], Kate Van Brussel[1,*], Mang Shi[2,3], Ci-Xiu Li[2,3], Wei-Shan Chang[2,3], John S. Munday[4], Katja Voss[1], Alicia McLuckie[1], David Taylor[5], Andrew Laws[6], Edward C. Holmes[2,3], Vanessa R. Barrs[1,3] and Julia A. Beatty[1,3]

[1]Sydney School of Veterinary Science, Faculty of Science, University of Sydney, Sydney, NSW 2006, Australia

[2]School of Life and Environmental Sciences and School of Medical Sciences, University of Sydney, Sydney, NSW 2006, Australia

[3]Marie Bashir Institute for Infectious Diseases and Biosecurity, The University of Sydney, Sydney, NSW 2006, Australia

[4]School of Veterinary Science, Massey University, Palmerston North 4410, New Zealand

[5]Vetnostics, 60 Waterloo Rd, North Ryde, NSW 2113, Australia

[6]Wentworth Falls Animals Hospital, 1/295-297 Great Western Highway, Wentworth Falls, NSW 2782, Australia

* These authors contributed equally to this work.

2.1: Abstract

Papillomaviruses infect the skin and mucosal surfaces of diverse animal hosts with consequences ranging from asymptomatic colonization to highly malignant epithelial cancers. Increasing evidence suggests a role for papillomaviruses in the most common cutaneous malignancy of domestic cats, squamous cell carcinoma (SCC). Using total DNA sequencing we identified a novel feline papillomavirus in a nasal biopsy taken from a cat presenting with both nasal cavity lymphoma and recurrent squamous cell carcinoma affecting the nasal planum. We designate this novel virus as Felis catus papillomavirus 6 (FcaPV6). The complete FcaPV6 7453 bp genome was similar to those of other feline papillomaviruses and phylogenetic analysis revealed that it was most closely related to FcaPV3, although was distinct enough to represent a new viral type. Classification of FcaPV6 in a new genus alongside FcaPVs 3, 4 and 5 is supported. Archived excisional biopsy of the SCC, taken 20 months prior to presentation, was intensely positive on p16 immunostaining. FcaPV6, amplified using virus-specific, but not consensus, PCR, was the only papillomavirus detected in DNA extracted from the SCC. Conversely, renal lymphoma, sampled at necropsy two months after presentation, tested negative on FcaPV6-specific PCR. In sum, using metagenomics we demonstrate the presence of a novel feline papillomavirus in association with cutaneous squamous cell carcinoma.

2.2: Introduction

Papillomaviruses (PVs) are small, nonenveloped, double-stranded DNA viruses that infect the skin and mucosal surfaces of mammals and many other vertebrates in a predominantly host-specific manner. The consequences of papillomavirus infections range from clinically asymptomatic, through benign lesions, to malignant epithelial cancers. The oncogenic potential of papillomaviruses is influenced by virus genotype, host factors such as immune status, and environmental factors, including exposure to sunlight (McBride, 2017).

In domestic cats, five papillomavirus genotypes have been described to date (Munday et al., 2019). Felis catus papillomavirus (FcaPV) 1 and FcaPV2 are classified in the *Lambdapapillomavirus* and *Dyothetapapillomavirus* genera, respectively. FcaPV3 and FcaPV4 have been classified in the genus *Taupapillomavirus* although, along with FcaPV5, they have been proposed as members of a new genus, as yet unnamed, on the basis of their

L1 open reading frame (ORF) sequence, host species and biological behaviour (Munday et al., 2017).

Feline papillomaviruses are generally thought to be causal in oral papillomas (FcaPV1) (Munday and French, 2015), viral plaques and Bowenoid in situ carcinomas (BISC) (FcaPV 2, 3 and 5), all of which occur uncommonly. Of greater clinical relevance, a papillomavirus aetiology is suspected for a proportion of cutaneous squamous cell carcinomas (SCC). SCC is the most common feline cutaneous malignancy, comprising 15–48% of all skin tumours in this species (Gross et al., 2005). These neoplasms are highly invasive and can cause extensive local tissue destruction. Viral oncogene expression (E6 and E7) and downregulation of tumour suppressor genes (p53 and pRb) link FcaPV2 to a subset of cutaneous SCC, but other papillomaviruses may be contributing (Hoggard et al., 2018, Altamura et al., 2016).

Here we report a novel feline papillomavirus—denoted Felis catus papillomavirus 6 (FcaPV6)—that was discovered using metagenomic DNA sequencing of a nasal cavity biopsy from a cat presenting with two nasal cancers, high-grade lymphoma of the nasal cavity and nasal planum SCC.

2.3: Materials and methods

2.3.1: Clinical samples

A 10 year-old male, neutered, domestic, shorthair cat presented with invasive nasal planum SCC that had recurred following excisional biopsy 20 months prior (Figure 2.3.1). Concurrent nasal cavity disease was suspected from the history, physical examination and computed tomographic examination of the head. A punch biopsy from the nasal cavity lesion, obtained via a skin incision over the nasal bridge, was divided and stored as formalin-fixed paraffin-embedded (FFPE) tissue and at −80 °C for a virus discovery project with owner consent (approved by the University of Sydney Animal Ethics Committee, 2014/626). The nasal cavity lesion was diagnosed as high-grade B cell lymphoma on histopathology and immunohistochemistry. Retrovirus serology was negative for feline leukaemia virus and positive for feline immunodeficiency virus (FIV), with no prior history of FIV vaccination. Two months later, bilateral renomegaly was detected and euthanasia was requested. Tissues collected at necropsy and stored, as described above, included renal lesions that were

subsequently confirmed to be lymphoma. An archived FFPE excisional biopsy, from which the initial diagnosis of nasal planum SCC was made, was retrieved.
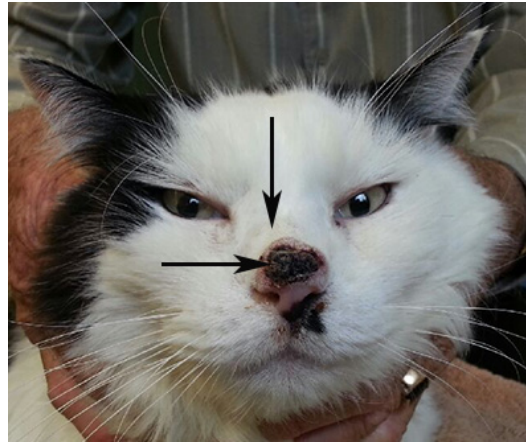
Figure 2.3.1: A recurrent invasive squamous cell carcinoma on the nasal planum (horizontal arrow) was adjacent the site of a biopsy (vertical arrow) from which high-grade lymphoma of the nasal cavity was diagnosed.

2.3.2: DNA sequencing and virus discovery

Total tumour DNA was extracted from the nasal cavity punch biopsy using the DNeasy Blood and Tissue Kit (Qiagen Pty Ltd., Chadstone, Australia). DNA libraries, constructed using the Nextera XT DNA Library Preparation kit (Illumina, San Diego, CA, USA), were enriched for herpesviruses using customized, hybridization-based target capture kits (myBaits, Arbor Biosciences, Ann Arbor, MI, USA), including a pre-treatment to deplete any remaining streptavidin, according to the manufacturer's instructions. One set of capture reactions was performed with annealing at 65 °C for 16 h. All PCR amplifications were carried out using KAPA Hi HotStart Mix (Kapa Biosystems, Cape Town, South Africa) with "reamp" primers (Meyer and Kircher, 2010), followed by purification with the GenElute PCR Clean-up kit (Sigma-Aldrich, St Louis, MO, USA). The NextSeq Illumina platform was used to sequence the enriched DNA library. The resulting 150 bp paired-end reads were de novo assembled using Megahit program version 1.1.3 and compared with the nonredundant protein database using Diamond version 0.9.25. This revealed the presence of two distinct contigs of a novel papillomavirus. PCR primers were designed based on recovered reads using Primer3web version 4.1.0 (Table 2.7.1.1) to obtain the full genome sequence. PCR reactions contained 100 ng of template DNA, 200 nM of each primer, 1x Reaction Buffer comprising 1 mM dNTPs and 3 mM MgCl2, 1.5 Unit of MyTaq™ HS Red DNA Polymerase (Bioline, Meridian Bioscience, Memphis, TN, USA) in a total volume of 25 µL. Cycling conditions

were initial denaturation at 95 °C for 1 min followed by 35 cycles of denaturation at 94 °C for 30 s, primer annealing at 58 °C for 30 s, extension at 72 °C for 30 s and a final extension step at 72 °C for 1 min. The amplicons were sequenced (Macrogen, Seoul, Korea), and Geneious 11.1.5 was used to assemble the contigs to obtain the full genome of this novel papillomavirus.

2.3.3: Phylogenetic analysis

To determine the evolutionary relationships of the novel papillomavirus identified here, we inferred a phylogenetic tree on the basis of the concatenated alignment of four protein sequences (E1, E2, L2 and L1). Accordingly, the relevant amino acid sequences of 66 papillomaviruses, representative of the full genetic diversity of these viruses in mammals (as well as six nonmammalian papillomaviruses used as outgroups to root the phylogeny), were aligned using the E-INS-I algorithm in the MAFFT v7 package (Katoh and Standley, 2013). Ambiguously aligned regions were removed using GBlocks (Talavera and Castresana, 2007). This resulted in a final sequence alignment of 850 amino acid residues. A phylogenetic tree was then estimated using the maximum likelihood method in PhyML 3.0 (Guindon and Gascuel, 2003), employing the LG+Γ model of amino acid substitution and a subtree pruning and regrafting (SPR) branch-swapping algorithm. Topological robustness was assessing using SH-like branch supports.

2.3.4: Investigation of disease association

The novel papillomavirus sequences could have originated from the SCC located on the nasal planum immediately adjacent the punch biopsy site (Figure 2.3.1), the nasal cavity lymphoma, which was the primary target of the biopsy, or other adjacent tissues. A potential association between the novel papillomavirus and the SCC or the lymphoma was therefore investigated as follows:

2.3.5: DNA extraction from FFPE SCC biopsy

DNA was extracted from scrolls of FFPE tissue cut at 8 microns using standard techniques to avoid contamination using the DNeasy Blood and Tissue Kit.

2.3.6: Papillomavirus-specific PCR

A conventional polymerase chain reaction (cPCR) assay specific for the novel papillomavirus was performed on DNA extracted from the archived FFPE SCC biopsy, and from frozen

renal lymphoma obtained at necropsy using primer sets Pap_F4 and Pap_F7 (Table 2.7.1.1). DNA extracted from the punch biopsy was used as the positive control and no-template (molecular-grade water) as the negative control in all PCR assays. Products were separated on 1.0% agarose gel containing SYBRTM Safe DNA Gel Stain (Invitrogen, Carlsbad, CA, USA) in Tris–Borate–EDTA (TBE) 1× buffer and were visualised under UV light (Bio-Rad Gel Doc XR System, Bio-Rad Laboratories Pty Ltd., Gladesville, Australia). The identity of bands migrating at the expected size was confirmed using Sanger sequencing.

2.3.7: p16 immunostaining

Sections of 5 micron thickness were cut from the archived SCC biopsy onto charged slides (Superfrost Plus, Thermoscientific, Waltham, MA, USA). Immunostaining using anti-p16CDKN2A protein (p16) antibodies (p16INK4 clone G175-405, BD Pharmingen, Franklin Lakes, NJ, USA) was performed as previously described (Munday et al., 2011).

2.3.8: Papillomavirus consensus PCR

To detect other papillomaviruses in the nasal planum SCC, DNA extracted from the FFPE biopsy was examined by PCR using consensus primers FAP59/64, MY09/11 and CP4/5, which were designed to amplify DNA from a wide range of human cutaneous and mucosal papillomavirus (Munday and French, 2015). The JMPF/R primers, which specifically amplify FcaPV2 DNA, were also used (Munday et al., 2008). DNA extracted from a BISC that contained FcaPV2 DNA was the positive control for the FAP59/64 and JMPF/R primers, while DNA extracted from a BISC that contained FcaPV3 was the positive control for the MY09/11 and CP4/5 primers.

2.4: Results and discussion

2.4.1: Identification of *Felis catus* Papillomavirus 6

Two distinctive papillomavirus contigs of lengths 2847 bp and 4184 bp were identified from metagenomic sequencing of a DNA library originally enriched for herpesvirus discovery. The sequence occupying the gaps between the two fragments was obtained by PCR to form a circular genome of 7453 bp in length and confirmed with PCR. Reads were mapped back to the full FcaPV6 genome and showed an abundance level of 153.7 RPM (reads per million) (Figure 2.4.1.1). Blast analyses based on the entire genome suggest the virus was clearly

related to those of Felis catus papillomavirus 3, 4 and 5 observed previously, with the novel papillomavirus identified here most closely related to FcaPV3. Papillomaviruses are classified based on the sequence of the highly conserved ORF L1, with PVs within the same genera sharing over 60% nucleotide similarity and PVs of the same type having over 90% similarity (Bernard et al., 2010, de Villiers et al., 2004). The ORF L1 nucleotide sequence of the novel papillomavirus was most similar to FcaPV3. However, as the two sequences were only 66.1% similar (Table 2.4.1), this is consistent with the identification of a new papillomavirus type, and a classification of FcaPV6 is proposed. The FcaPV6 L1 ORF was 60.5% similar to FcaPV4 and 59.6% similar to FcaPV5. Recently, FcaPV3, 4 and 5 were proposed to be members of a novel distinct papillomavirus genus that infects the skin of domestic cats (Munday et al., 2017). Due to the similarity of the FcaPV6 ORF L1 to these three feline papillomavirus types, it is proposed that FcaPV6 joins FcaPV3, 4 and 5 within this proposed new genus. Importantly, this pattern of relationship was strongly confirmed by the phylogenetic analysis (Figure 2.4.1.2), with FcaPV6 and FcaPV3 grouping together, and with strong support for a cat-specific cluster of papillomaviruses (i.e., FcaPV3, FcaPV4, FcaPV5 and FcaPV6). The complete genome sequence of FcaPV6 has been submitted to GenBank and assigned accession number MN857145.

Figure 2.4.1.1: Felis catus Papillomavirus 6 (FcaPV6) genome configuration using metadata. The predicted ORFs are represented by the coloured inner segments. GC content is displayed in blue, percentage nucleotide polymorphism in orange and read coverage in yellow.

DQ366842 Rousettus aegyptiacus papillomavirus 1
EU240894 Tursiops truncatus papillomavirus 1
AJ238373 Phocoena spinipinnis papillomavirus
GU220391 Bettongia penicillata papillomavirus 1
FJ379293 Erinaceus europaeus papillomavirus 1
M17463 Homo sapiens papillomavirus 5
AF486184 Bos taurus papillomavirus 3
KP757765 Rusa timorensis papillomavirus 1
DQ091200 Capra hircus papillomavirus 1
DQ217793 Bos taurus papillomavirus 7
E15111 Mesocricetus auratus papillomavirus 1
X70827 Homo sapiens papillomavirus 4
KF857586 Vulpes vulpes papillomavirus 1
AY722648 Canis familiaris papillomavirus 2
NC_021472 Felis catus papillomavirus 3
Felis catus papillomavirus 6
NC_035479 Felis catus papillomavirus 5
NC_022373 Felis catus papillomavirus 4

Taupapillomavirus

FJ796965 Ovis aries papillomavirus 3
JF304765 Saimiri sciureus papillomavirus 1
X74475 Homo sapiens papillomavirus 32
EF536349 Ursus maritimus papillomavirus 1
JQ814847 Myotis ricketti papillomavirus 1
EF395818 Sus scrofa papillomavirus 1
GU117623 Phocoena phocoena papillomavirus
HQ262535 Morelia spilota papillomavirus 1
KC858264 Eptesicus serotinus papillomavirus 2
AY609301 Trichechus manatus latirostris papilloma
K02708 Sylvilagus floridanus papillomavirus 1
V01116 Homo sapiens papillomavirus 1
KC020689 Castor canadensis papillomavirus 1
NC_004765 Felis catus papillomavirus 1
D55633 Canis familiaris papillomavirus 1
KC460986 Talpa europaea papillomavirus 1
KC858263 Eptesicus serotinus papillomavirus 1
KC858266 Rhinolophus ferrumequinum papillomavirus
X56147 Homo sapiens papillomavirus 41
AY684126 Erethizon dorsatum papillomavirus 1
JQ692938 Miniopterus schreibersii papillomavirus 2
JX123128 Eidolon helvum papillomavirus 1

Lambdapapillomavirus

U01834 Mastomys natalensis papillomavirus 1
KU963288 Equus caballus papillomavirus 8
EU796884 Felis catus papillomavirus type 2
HQ293213 Zalophus californianus papillomavirus 1
JF800657 Canis familiaris papillomavirus 10
EF584537 Canis familiaris papillomavirus 4
JF800658 Canis familiaris papillomavirus 11
DQ295066 Canis familiaris papillomavirus 3
MH625918 Equus caballus papillomavirus 2
AF498323 Equus caballus papillomavirus 1
JX035935 Equus caballus papillomavirus 7
JQ965698 Equus caballus papillomavirus 6
GU384895 Equus caballus papillomavirus 3
JQ031032 Equus caballus papillomavirus 4
JQ031033 Equus caballus papillomavirus 5
EU503122 Equus caballus papillomavirus 2
MN117918 Equus caballus papillomavirus 9
KF741371 Equus asinus papillomavirus 1
AF457465 Bos taurus papillomavirus 5
HQ912790 Camelus dromedarius papillomavirus 1
KX954132 Giraffa camelopardalis papillomavirus 1
M15953 Alces alces papillomavirus 1
KP276343 Bos taurus papillomavirus 14
X02346 Bos taurus papillomavirus 1
JQ798171 Bos taurus papillomavirus 13
M20219 Bos taurus papillomavirus 2

Dyothetapapillomavirus

0.2 subs/site

*Figure 2.4.1.2: Evolutionary relationships of FcaPV6 to other mammalian papillomaviruses, including those previously identified in cats (Felis catus). Those papillomaviruses previously identified in cats are marked with animal symbols and in red, along with their respective genera. FcaPV6 is proposed to fall as part of a proposed new genus. All virus names contain their associated GenBank accession numbers. The tree is rooted using six nonmammalian papillomaviruses that have been removed to improve clarity. All horizontal branch lengths are scaled according to the number of amino acid substitutions per site, and the * denotes nodes with SH-like branch support values >0.95.*

Table 2.4.1: Percentage pairwise nucleotide sequence identities of feline papillomaviruses in the L1 ORF.

Virus	FcaPV2	FcaPV1	FcaPV3	FcaPV6	FcaPV5	FcaPV4
FcaPV2		55.7	56.8	55.2	56.1	55.1
FcaPV1	55.7		56.4	54.2	56.5	57.4
FcaPV3	56.8	56.4		66.1	62.8	63.8
FcaPV6	55.2	54.2	66.1		59.6	60.5
FcaPV5	56.1	56.5	62.8	59.6		64.4
FcaPV4	55.1	57.4	63.8	60.5	64.4	

2.4.2: Genome characteristics

The full genome of FcaPV6 has a 48.9% GC content. Seven ORFs were predicted to encode for two late proteins, L1 and L2, and five early proteins, E1, E2, E4, E6 and E7 (Figure 2.4.1.1). The predicted ORF features are displayed in Table 2.4.2. The E2 binding site, identified by the sequence ACC-N(5-7)-GGT was predicted at twelve positions in the genome, in addition to three NF1 CGGAA and Sp1 binding sites GGCGGG and four polyadenylation sites AATAAA (Table 2.7.2; Figure 2.7.1). Zinc-binding domains CXXC-X29-CXXC were predicted in E6 (84, 157 aa), separated by 36aa, and E7 (75 aa) (Table 2.7.3; Figure 2.7.1). The ATP-binding site for the ATP-dependent helicase GPPNTGKS and cyclin RXL motif KRRLF in E1 and nuclear localisation signal in L2 RKRRR and L1 KRKR were predicted in FcaPV6 (Table 2.7.3; Figure 2.7.1).

Table 2.4.2: ORF characteristics of Felis catus Papillomavirus 6 (FcaPV6).

ORF	Start	End	Length (nt)	Length (aa)	GC%
L1	5919	7409	1491	497	46.5
L2	4261	5901	1641	547	54.4
E1	1059	2858	1800	600	44.8
E2	2836	4167	1332	444	51.2
E4	3287	3922	636	292	57.4
E6	195	785	591	197	48.2
E7	372	707	1078	124	50.0

2.4.3: Association of FcaPV6 with squamous cell carcinoma

The excisional biopsy of the nasal planum SCC showed diffuse intense p16 immunostaining (Figure 2.4.3). Overexpression of p16 is a surrogate marker for a papillomaviral aetiology in SCC in humans and cats so this result supports a papillomavirus aetiology for the SCC (Munday et al., 2011, Parry et al., 1995). DNA extracted from the same SCC biopsy tested positive for FcaPV6 on two virus-specific cPCRs, generating products of 558 bp and 191 bp, thereby confirming that this virus was associated with the nasal planum SCC at least 20 months prior to presentation. However, no additional PV types were amplified from the SCC using either consensus primers or primers specific for FcaPV2. Therefore, FcaPV6 was the only papillomavirus identified in association with the SCC. Consensus primers have been used to discover FcaPV 1 to 5 (Munday et al., 2017) but failed to detect FcaPV6 in DNA extracted from the SCC. This could have been because of sequence diversity noted at the primer binding sites. If the commonly used consensus primers do have low sensitivity for FcaPV6, this would explain why this papillomavirus type has not previously been detected in any feline cutaneous preneoplastic or neoplastic lesion. Alternatively, if FcaPV6 was present at low copy number, it is conceivable virus-specific primers would be more likely to generate a PCR product than consensus primers. Regardless, the failure of the consensus primers to detect FcaPV6 demonstrates the utility of unbiased metagenomic sequencing to discover divergent organisms. While the p16 immunostaining and detection of only FcaPV6 within the lesion supports a potential causal association between this papillomavirus and the SCC, most papillomavirus infections are asymptomatic and FcaPV6 may, like many other papillomaviruses of humans and animals, constitute part of the normal virome (Antonsson et al., 2003, Munday and Witham, 2010). Investigation of a larger number of cutaneous lesions as well as normal skin from cats is required to better understand the relationship, if any, of FcaPV6 to cutaneous neoplasia in cats.
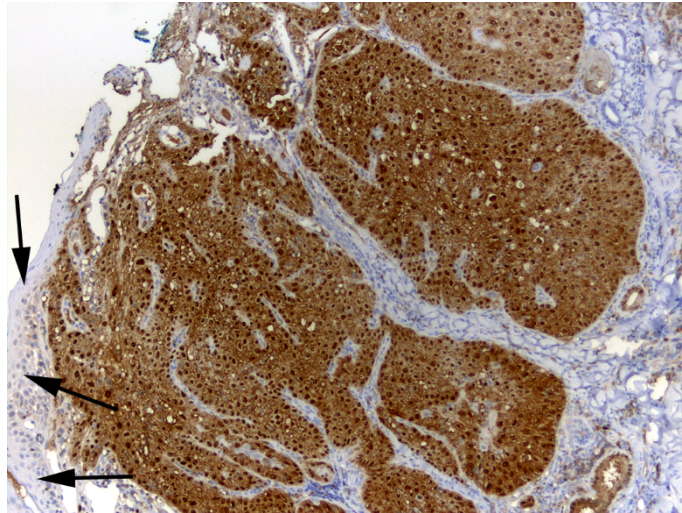
Figure 2.4.3: Photomicrograph of a nasal planum squamous cell carcinoma that contained FcaPV6 DNA. This biopsy was obtained 20 months prior to the SCC recurrence shown in Figure 3.3.1. Intense nuclear and cytoplasmic immunostaining using anti-p16CDKN2A protein (p16) antibodies is visible diffusely within the neoplastic cells. There is minimal immunostaining within adjacent non-neoplastic epidermis (arrows). Hematoxylin counterstain.

Evidence supporting an association between papillomavirus infection and a diagnosis of lymphoma is limited (Intaraphet et al., 2017). Nonetheless, given that the novel virus sequences were identified in a biopsy targeting a high-grade lymphoma, it was decided to test lymphoma tissue arising at a site distant to the nasal planum in the same patient for the presence of FcaPV6. No papillomaviral DNA was amplified from DNA extracted from a renal lymphoma lesion obtained at necropsy using FcaPV6-specific primers Pap-_4 and Pap_7.

2.5: Discussion

This study identifies a novel papillomavirus genotype, designated FcaPV6, in the presence of squamous cell carcinoma of the nasal planum in a domestic cat. The biological niche and disease associations of FcaPV6 clearly merit additional investigation. The application of unbiased virus discovery methodologies to lesions suspected to have a papillomavirus aetiology may advance pathogen discovery.

2.6: References

Altamura, G., Corteggio, A., Pacini, L., Conte, A., Pierantoni, G.M., Tommasino, M., Accardi, R., Borzacchiello, G. 2016. Transforming properties of Felis catus papillomavirus type 2 E6 and E7 putative oncogenes in vitro and their transcriptional activity in feline squamous cell carcinoma in vivo. Virology, 496:1-8.

Antonsson, A., Erfurt, C., Hazard, K., Holmgren, V., Simon, M., Kataoka, A., Hossain, S., Hakangard, C., Hansson, B.G. 2003. Prevalence and type spectrum of human papillomaviruses in healthy skin samples collected in three continents. Journal of General Virology, 84(7):1881-6.

Bernard, H.-U., Burk, R.D., Chen, Z., van Doorslaer, K., Hausen, H.z., de Villiers, E.-M. 2010. Classification of papillomaviruses (PVs) based on 189 PV types and proposal of taxonomic amendments. Virology, 401(1):70-79.

de Villiers, E.M., Fauquet, C., Broker, T.R., Bernard, H.U., zur Hausen, H. 2004. Classification of papillomaviruses. Virology, 324(1):17-27.

Gross, T.L., Ihrke, P., Walder, E.J., Affolter, V.K. 2005. Epidermal Tumors. In: GROSS, T. L., IHRKE, P., WALDER, E. J. & AFFOLTER, V. K. (eds.) Skin Diseases of the Dog and Cat.

Guindon, S., Gascuel, O. 2003. A simple, fast, and accurate algorithm to estimate large phylogenies by maximum likelihood. Systematic Biology, 52, 696-704.

Hoggard, N., Munday, J.S., Luff, J. 2018. Localization of Felis catus Papillomavirus Type 2 E6 and E7 RNA in Feline Cutaneous Squamous Cell Carcinoma. Veterinary Pathology, 55(5):409-416.

Intaraphet, S., Farkas, D.K., Johannesdottir Schmidt, S.A., Cronin-Fenton, D., Søgaard, M. 2017. Human papillomavirus infection and lymphoma incidence using cervical conization as a surrogate marker: a Danish nationwide cohort study. Hematological Oncology, 35(2):172-176.

Katoh, K., Standley, D.M. 2013. MAFFT multiple sequence alignment software version 7: improvements in performance and usability. Molecular Biology and Evolution, 30(4):772-80.

McBride, A.A. 2017. Oncogenic human papillomaviruses. Philosophical Transactions of the Royal Society B, 372(1732):20160273.

Meyer, M., Kircher, M. 2010. Illumina sequencing library preparation for highly multiplexed target capture and sequencing. Cold Spring Harbor Protocols, 2010(6).

Munday, J.S., Dittmer, K.E., Thomson, N.A., Hills, S.F., Laurie, R.E. 2017. Genomic characterisation of Felis catus papillomavirus type 5 with proposed classification within a new papillomavirus genus. Veterinary Microbiology, 207:50-55.

Munday, J.S., French, A.F. 2015. Felis catus papillomavirus types 1 and 4 are rarely present in neoplastic and inflammatory oral lesions of cats. Research in Veterinary Science, 100:220-2.

Munday, J.S., Kiupel, M., French, A.F., Howe, L. 2008. Amplification of papillomaviral DNA sequences from a high proportion of feline cutaneous in situ and invasive squamous cell carcinomas using a nested polymerase chain reaction. Veterinary Dermatology, 19(5):259-263.

Munday, J.S., Knight, C.G., French, A.F. 2011. Evaluation of feline oral squamous cell carcinomas for p16CDKN2A protein immunoreactivity and the presence of papillomaviral DNA. Research in Veterinary Science, 90(2):280-283.

Munday, J.S., Sharp, C.R., Beatty, J.A. 2019. Novel viruses: Update on the significance of papillomavirus infections in cats. Journal of Feline Medicine and Surgery, 21(5):409-418.

Munday, J.S., Witham, A.I. 2010. Frequent detection of papillomavirus DNA in clinically normal skin of cats infected and noninfected with feline immunodeficiency virus. Veterinary Dermatology, 21(3)307-310.

Parry, D., Bates, S., Mann, D.J., Peters, G. 1995. Lack of cyclin D-Cdk complexes in Rb-negative cells correlates with high levels of p16INK4/MTS1 tumour suppressor gene product. The EMBO Journal, 14(3):503-511.

Talavera, G., Castresana, J. 2007. Improvement of phylogenies after removing divergent and ambiguously aligned blocks from protein sequence alignments. Systematic Biology, 56(4):564-77.

2.7: Supplementary data

Figure S1 Felis catus Papillomavirus 6 (FcaPV6) genome configuration and nucleotide (nt) and amino acid (aa) feature location.
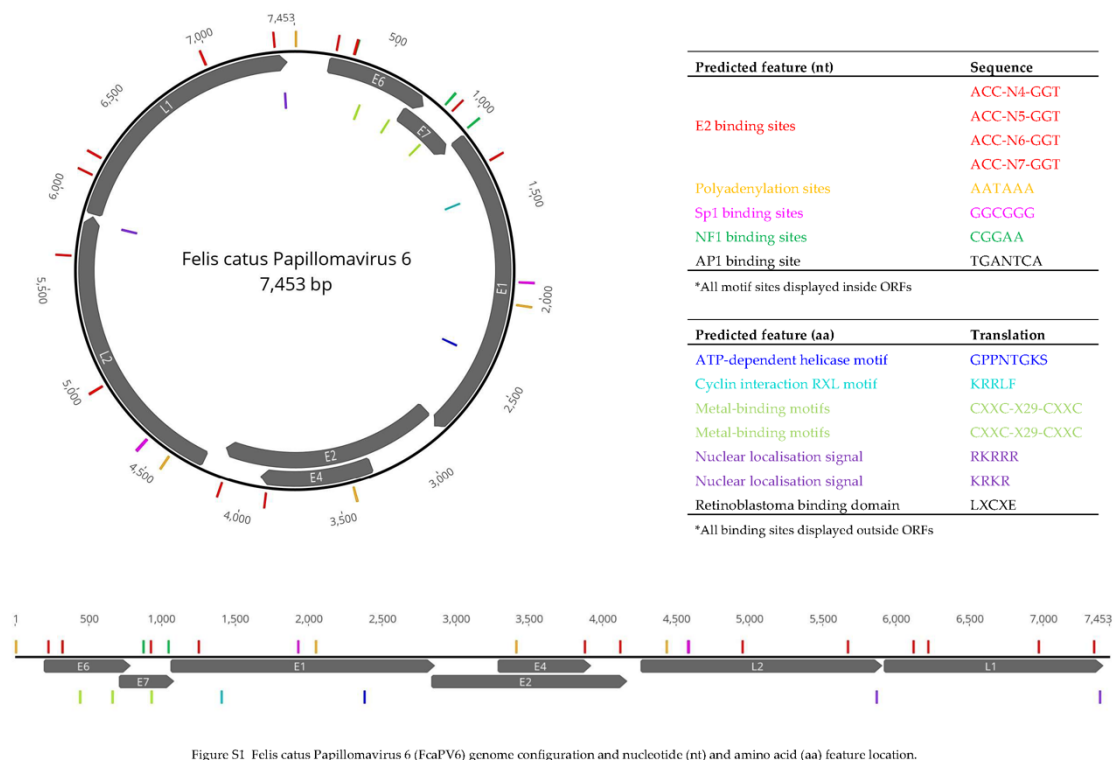
Figure 2.7.1: Felis catus Papillomavirus 6 (FcaPV6) genome configuration and nucleotide (nt) and amino acid (aa) feature location.

Table 2.7.1: Oligonucleotides used to amplify the complete genome of Felis catus papillomavirus 6 (FcaPV6).

Oligonucleotides	Sequence	Start - 5'	End - 3'	Tm (°C)	Size (bp)
Pap_F4	TCGTCCAAGTCAACCACGAG	7359	7378	60	558
Pap_R4	TAGCCCCCACAAAAGCAACA	463	444	60	558
Pap_F5	TTGGGTCAGAGGTCACAAGG	7326	7345	59	555
Pap_R5	TGAACAGGAATCCTCAGCCG	427	408	60	555
Pap_F6	TAAAAGACGCAAGCGGGACT	4359	4378	60	303
Pap_R6	ATAGTGTCCACCGGGCCTAT	4661	4642	60	303
Pap_F7	AGATTGGTAGCAGCCTCACT	4478	4497	58	191
Pap_R7	ACTGCCTATAGTGTCCACCG	4668	4649	58	191

Table 2.7.2: Predicted nucleotide features of Felis catus papillomavirus 6 (FcaPV6).

Predicted feature (nt)	Sequence	ORF	Occurrence	nt position
E2 binding sites	ACC-N4-GGT	All	3	1251, 4122, 7350
	ACC-N5-GGT		1	3881
	ACC-N6-GGT		5	226, 321, 923, 5672, 6219
	ACC-N7-GGT		3	4953, 6121, 6973
Polyadenylation sites	AATAAA	NC, E1, E2, L2	4	4, 2049, 3415, 4438
Sp1 binding sites	GGCGGG	E1, L2	3	1928, 4582, 4586
NF1 binding sites	CGGAA	E6, E7	3	323, 876, 1043
AP1 binding site	TGANTCA	-	-	-

Table 2.7.3: Predicted amino acid features of Felis catus papillomavirus 6 (FcaPV6).

Predicted feature (aa)	Translation	ORF	Occurrence	aa position
ATP-dependent helicase motif	GPPNTGKS	E1	1	441
Cyclin interaction RXL motif	KRRLF	E1	1	117
Metal-binding motifs	CXXC-X29-CXXC	E6	2	84, 157
Metal-binding motifs	CXXC-X29-CXXC	E7	1	75
Nuclear localisation signal	RKRRR	L2	1	537
Nuclear localisation signal	KRKR	L1	1	491
Retinoblastoma binding domain	LXCXE	-	-	-

Chapter three: Identification of Novel Astroviruses in the Gastrointestinal Tract of Domestic Cats

Kate Van Brussel[1,2,*], Xiuwan Wang[3,*], Mang Shi[2,4], Maura Carrai[5], Jun Li[3,6], Vito Martella[7], Julia A. Beatty[1,5], Edward C. Holmes[2] and Vanessa R. Barrs[1,5]

[1]School of Veterinary Science, Faculty of Science, University of Sydney, Sydney, NSW 2006, Australia

[2]Marie Bashir Institute for Infectious Diseases and Biosecurity, School of Life and Environmental Sciences and School of Medical Sciences, University of Sydney, Sydney, NSW 2006, Australia

[3]Department of Infectious Diseases and Public Health, Jockey Club of Veterinary Medicine and Life Sciences, City University of Hong Kong, Kowloon Tong, Hong Kong, China

[4]School of Medicine, Sun Yat-sen University, Guangzhou 510275, China

[5]Department of Veterinary Clinical Sciences, Jockey Club College of Veterinary Medicine and Life Sciences, City University of Hong Kong, Kowloon Tong, Hong Kong, China

[6]School of Data Science, City University of Hong Kong, Hong Kong, China

[7]Department of Veterinary Medicine, University of Aldo Moro of Bari, 70010 Valenzano, Italy

[*]These authors contributed equally to this article.

3.1: Abstract

Astroviruses, isolated from numerous avian and mammalian species including humans, are commonly associated with enteritis and encephalitis. Two astroviruses have previously been identified in cats, and while definitive evidence is lacking, an association with enteritis is suggested. Using metagenomic next-generation sequencing of viral nucleic acids from faecal samples, we identified two novel feline astroviruses termed Feline astrovirus 3 and 4. These viruses were isolated from healthy shelter-housed kittens (Feline astrovirus 3; 6448 bp) and from a kitten with diarrhoea that was co-infected with Feline parvovirus (Feline astrovirus 4, 6549 bp). Both novel astroviruses shared a genome arrangement of three open reading frames (ORFs) comparable to that of other astroviruses. Phylogenetic analysis of the concatenated ORFs, ORF1a, ORF1b and capsid protein revealed that both viruses were phylogenetically distinct from other feline astroviruses, although their precise evolutionary history could not be accurately determined due to a lack of resolution at key nodes. Large-scale molecular surveillance studies of healthy and diseased cats are needed to determine the pathogenicity of feline astroviruses as single virus infections or in co-infections with other enteric viruses.

3.2: Introduction

Astroviridae is a family of small (~6–7 kb), non-enveloped single-stranded RNA viruses that include two genera—*Avastrovirus* and *Mamastrovirus*. Species in the *Avastrovirus* genus infect avian hosts while those in the *Mamastrovirus* genus infect mammals including humans. As of 2019, the International Committee on Taxonomy of Viruses (ICTV) recognises 22 astrovirus species based on the capsid gene, three of which belong to *Avastrovirus* and the remainder to *Mamastrovirus* (https://talk.ictvonline.org/taxonomy/). Since then, an additional 33 and 7 candidate species have been discovered for the *Mamastrovirus* and *Avastrovirus* genera, respectively (Schultz-Cherry, 2013). The astrovirus genome comprises three open reading frames (ORFs): ORF1a and ORF1b encode the non-structural proteins involved in viral replication, including the RNA-dependent RNA polymerase (RdRp), while ORF2 encodes the capsid precursor (De Benedictis et al., 2011).

Human astroviruses are associated with acute gastroenteritis in all age groups, although they have also been reported in immunosuppressed children with encephalitis (Bosch et al., 2014, Koukou et al., 2019, Quan et al., 2010). Astroviruses are also associated with enteritis in turkeys (Mor et al., 2011), hepatitis in ducks (Gough et al., 1985, Fu et al., 2009), nephritis in

chickens (Imada et al., 2000), and encephalomyelitis in cattle (Li et al., 2013) and mink (Blomstrom et al., 2010, Gavier-Widen et al., 2004). Feline astrovirus (FAstV) was first discovered using electron microscopy in a kitten with diarrhoea in 1981 (Hoshino et al., 1981). Since then, FAstVs have been detected in both clinically healthy cats and cats with diarrhoea in multiple countries using electron microscopy, viral culture and/or molecular methods (Ng et al., 2014, Lau et al., 2013, Zhang et al., 2014, Moschidou et al., 2011, Marshall et al., 1987, Lawler et al., 2018, Yi et al., 2018). Genome sequencing has revealed at least two groups of genetically distinct FAstVs. The species Mamastrovirus 2 includes Feline astrovirus 2 and is related to classic human astroviruses (Mamastrovirus 1). In contrast, strain FAstV D1 clusters with fox, California sea lion, and mink astroviruses (Ng et al., 2014, Zhang et al., 2014), suggesting that cats may harbour a variety of astrovirus strains that have not been studied in terms of their pathobiological properties.

Herein, we used metagenomic next-generation sequencing (mNGS) of viral nucleic acids isolated from faecal samples to identify two novel FAstVs, one detected in three clinically healthy kittens and another isolated from a kitten with diarrhoea that was co-infected with feline parvovirus (FPV), a virus in the species Carnivore protoparvovirus 1.

3.3: Materials and methods

3.3.1: Ethics

The collection of faecal samples from cats in this study was approved by the University of Sydney Animal Ethics Committee (AEC approval number N00/7-2013/3/6029).

3.3.2: Sample collection

Faeces were collected from an unvaccinated 8-week-old male shelter-housed kitten with diarrhoea (cat #159) during an outbreak of feline panleukopenia (FPL) at a shelter in Sydney, New South Wales, Australia (Van Brussel et al., 2019). The kitten tested positive for FPV on a faecal antigen test and FPV infection was confirmed on Sanger sequencing of the FPV VP2 gene (Van Brussel et al., 2019). Faecal samples were also collected from three clinically healthy domestic shorthair (DSH) kittens aged 3 to 5 months (cat #AWL4, #AWL6 and #AWL8) from a second shelter in Sydney, New South Wales, Australia. All faecal samples were stored at −80 °C until processing.

3.3.3: Viral nucleic acid and total RNA isolation and sequencing

Viral nucleic acids were isolated from the faecal samples of all cats using a previously published protocol for viral particle enrichment (Conceicao-Neto et al., 2015) with minor modifications (Chong et al., 2019). The QIAamp Viral RNA Mini Kit (Qiagen, Hilden, Germany) was used to extract viral nucleic acids that were treated with DNase (Invitrogen, Thermo Fisher Scientific) to remove viral genomic DNA. The resulting viral genomic RNA was randomly amplified using the Whole Transcriptome Amplification Kit (WTA2) (Sigma-Aldrich, St. Louis, MO, USA) and 22 PCR cycles (Conceicao-Neto et al., 2015, Chong et al., 2019) to convert RNA to cDNA then purified using the GenElute PCR Clean-up Kit (Sigma-Aldrich, St. Louis, MO, USA). cDNA quantity was evaluated using the Qubit 2.0 fluorometer. The Nextera XT DNA Library Preparation Kit (Illumina, San Diego, CA, USA) was used to produce the sequencing libraries that were then sequenced on the NovaSeq6000 (Illumina, San Diego, CA, USA) platform (150 bp paired end) at the Australian Genome Research Facility (AGRF) (Melbourne, Australia). Insufficient viral genomic RNA was extracted from the faecal sample from cat #159 using the viral particle enrichment protocol such that a cDNA library could not be synthesized for sequencing. Therefore, in this case, total RNA was isolated from this sample using the RNeasy Plus Mini Kit (Qiagen, Hilden, Germany) following manufacturer instructions. Prior to total RNA isolation, the faecal sample was suspended in 600 μL lysis buffer and homogenized at 5 ms−1 for 1.5 min using the Omni Bead Ruptor (Omni international, Kennesaw, GA, USA) (Chong et al., 2019). Total RNA quality and quantity were assessed using a Bioanalyzer 2100 (Agilent, Santa Clara, CA, USA). The Zymo-Seq RiboFree Total RNA Library Kit (Zymo Research, Irvine, CA, USA) was used for rRNA depletion and library preparation and sequencing was performed on the NovaSeq6000 (Illumina, San Diego, CA, USA) platform (150 bp paired end) at the AGRF (Melbourne, Australia).

3.3.4: Genome assembly and read mapping

Raw reads were mapped to the cat genome (*Felis catus* 9.0 assembly, GenBank Assembly ID GCA_000181335.4) with BWA version 0.7.17 (Li and Durbin, 2009) and reads with over 95% mapping coverage were removed. The ribosomal RNA (rRNA) reads were filtered with SortMeRNA (Kopylova et al., 2012). Raw reads were further processed for quality control using the following procedures (Li et al., 2019, Zheng et al., 2019): (available at https://github.com/TingtZHENG/metagenomics/blob/master/scripts/fqc.pl): (i) removal of

Illumina primers/adaptors/linker sequences; (ii) removal of paired ends reads with 25 bp consecutively exact match from both ends to avoid PCR duplicates; and (iii) removal of terminal regions with continuous Phred based quality <20. After pre-processing of raw data, IDBA-UD version 1.1.2 (Peng et al., 2012) was used for de novo assembly of the cDNA libraries from cats #AWL4, #AWL6 and #AWL8. To confirm the IDBA-UD assembly accuracy de novo, assembly of the cDNA libraries was also performed using Trinity version 2.8.5 (Grabherr et al., 2011). For cat #159, Trinity (Grabherr et al., 2011) was used for the de novo assembly of the total RNA sequencing reads. Diamond version 0.9.32 was used to compare the resulting contigs to the NCBI non-redundant protein database. Viral read counts for cDNA libraries after quality control filtering and IDBA-UD assembly for cats #AWL4, #AWL6, and #AWL8 were confirmed using BWA (Li and Durbin, 2009). BWA was also used to determine the viral read count for the meta-transcriptomic library after quality control filtering and Trinity assembly for cat #159 (Li and Durbin, 2009). Astrovirus genomes were annotated and ORFs were predicted using Geneious version 2019.2.1. Transmembrane domains were predicted using TMHMM version 2.0 (http://www.cbs.dtu.dk/services/TMHMM/) and the NCBI Conserved Domain Database (CDD) was used to predict astrovirus genome motifs and domains. All astrovirus genomes described here have been deposited on GenBank under the accession numbers MW037839-41.

3.3.5: Evolutionary analysis

Phylogenetic analysis of *Mamastrovirus* genomes was performed on the individual amino acid sequence alignments of the ORF1a, ORF1b, and capsid genes, as well as on a concatenated alignment of all three ORFs. For each gene, between 39 and 48 reference sequences of mamastroviruses were included to represent the background diversity of these viruses in mammals (reference sequences were downloaded from GenBank, excluding accession numbers MN977118-9). Sequence alignments were performed in Geneious using MAFFT version 7 and the E-INS-i algorithm (Katoh and Standley, 2013), and GBlocks was used to remove ambiguously aligned regions and gaps (Castresana, 2000, Talavera and Castresana, 2007). This resulted in final amino acid alignments of 816, 230, 373, and 215 residues for the concatenated ORFs, ORF1a, ORF1b, and capsid genes, respectively. The PhyML program was used to estimate the maximum likelihood phylogenetic trees assuming the Le and Gascuel 2008 (LG) and gamma distribution (Γ) model of amino acid substitution, subtree pruning and regrafting (SPR) branch swapping, and bootstrap re-sampling (1000

replicates) to assess nodal support (Le and Gascuel, 2008, Hordijk and Gascuel, 2005, Guindon and Gascuel, 2003).

A nucleotide sequence alignment containing 39 *Mamastrovirus* reference sequences and the FAstVs identified here was created using MAFFT. The RDP, GENECOV, and Bootscan programs within the RDP4 package (Martin et al., 2015) were then used to scan this alignment for potential recombination events involving FAstV3 and FAstV4. The genomic locations of any putative recombination breakpoints were then determined using Simplot, with new (amino acid) phylogenetic trees then inferred at either side of these recombination breakpoints using the phylogenetic procedure described above.

3.4: Results

3.4.1: Genome features of novel FAstVs

Using mNGS, we identified two novel FAstVs of lengths 6448 bp (excluding the 10 bp polyA tail) and 6549 bp (in which no polyA tail was observed). The first FAstV (6448 bp), tentatively named Feline astrovirus 3 (FAstV3), was detected in three healthy cats, including whole genomes in two (#AWL4 and #AWL6) and contigs of lengths 493 bp (ORF1a) and 517 bp (ORF2) and 100% identity in the third (#AWL8). Both assemblers showed comparable results, although because Trinity added a small section of sequence to the 3′ end of FAstV3 after the polyA tail we choose the IDBA-UD assembly in this case. The second novel FAstV (6549 bp), tentatively named Feline astrovirus 4 (FAstV4), was sequenced from the sick cat (#159). The three ORFs were predicted for both FAstVs, and a polyA tail was only observed in FAstV3 (Figure 3.4.1). The GC content for FAstV3 was 50% and 45.3% for FAstV4. The ribosomal frameshift AAAAAAC motif was present in the ORF1a and ORF1b overlap in both genomes (Figure 3.4.1). TMHMM was used to predict five transmembrane domains in FAstV3 at amino acid positions 161–183, 237–256, 276–298, 302–324 and 331–353, and five in FAstV4 at positions 156–173, 243–265, 285–307, 317–335 and 342–364 in ORF1a (Figure 3.4.1). The trypsin-like peptidase domain in ORF1a, RdRp in ORF1b, and the capsid protein precursor in ORF2 were identified (Figure 3.4.1).
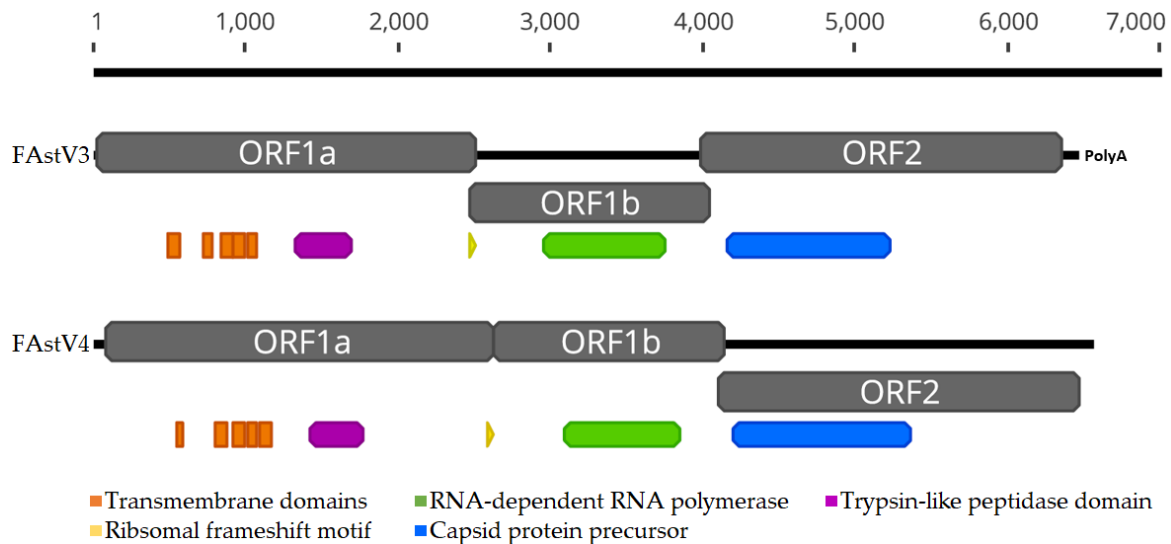
Figure 3.4.1: An overview of the genome structures of FAstV3 and FAstV4. ORFs are represented in grey, transmembrane domains in orange, trypsin-like peptidase domain in purple, RdRp in green, and capsid protein precursor in blue. The yellow triangle represents the ribosomal frameshift motif. ORF1a, ORF1b, and ORF2 are 832, 519 and 786 amino acids for FAstV3 and 848, 506 and 789 amino acids for FAstV4, respectively.

3.4.2: Abundance, sequence comparison and other viruses

The assembled FAstV3 and FAstV4 genomes were used to map sequence reads from the four filtered sequencing libraries to determine read abundance (Table 3.4.2). BlastX revealed 61% amino acid sequence similarity to Mamastrovirus 10 (GenBank accession number NC_004579) in the capsid gene for FAstV3 and 68% amino acid similarity to Canine astrovirus (GenBank accession number KX599354) in the capsid gene for FAstV4. FAstV3 and FAstV4 displayed 67% amino acid similarity to each other in the capsid gene. A complete Mamastrovirus 2 genome (6796 bp excluding polyA tail, accession number MW037841) was detected in two cDNA libraries from cats #AWL4 and #AWL6 (Table 3.4.2) and shared 92% nucleotide similarity to other Mamastrovirus 2 sequences and 97% (ORF1a and ORF1ab) and 94% (capsid gene) amino acid similarity to Mamastrovirus 2 and feline astrovirus 2, respectively.

Table 3.4.2: Summary of library and virus read counts, transcripts per million counts for each virus, and the assembler used.

Virus	Accession Number	Assembler	Library Virus was Identified	Library Read Count After Processing (Paired End)	Virus/Contig Read Count	Transcripts per Million
Feline astrovirus 3	MW037839	IDBA-UD	AWL4	7,030,294	62,663	1623
			AWL6	10,116,484	240,905	3213
			AWL8	10,578,534	222	32
					279	42
Feline astrovirus 4	MW037840	Trinity	159	77,205,956	32,003	16
Mamastrovirus 2 AUS/AWL	MW037841	IDBA-UD	AWL4	7,030,294	1636	70
					1897	114
			AWL6	10,116,484	4098	53

Feline coronavirus reads were detected in all four filtered sequencing libraries, with one complete genome observed in the total RNA library from cat #159 (29432 bp) and contigs ranging in length from 6167 bp to 457 bp in library #AWL8. Additionally, a Feline picornavirus genome (7466 bp) was detected in the #AWL8 library.

3.4.3: Phylogenetic and recombination analysis

Phylogenetic analysis of the concatenated sequences of all ORFs (Figure 3.4.3.A) shows that both FAstV3 and FAstV4 cluster in a broad group of mamastroviruses, including FAstV D1, as well as astroviruses from humans, mink, and bovines. Although FAstV4 was clearly related to FAstV D1 with 100% bootstrap support in the concatenated ORFs, ORF1a, and ORF1b trees (and relatively close to FAstV D1 in the capsid gene phylogeny; see below), the precise phylogenetic position of FAstV3 was less certain because of a lack of strong (i.e., >70%) bootstrap support and topological differences between each gene tree. In particular, in the ORF1b phylogeny (Figure 3.4.3.C), FAstV3, fell in a divergent and ambiguous

phylogenetic position, and was also relatively divergent in the ORF1a tree (Figure 3.4.3.B). Also of note was that in the phylogenetic analysis based on the capsid gene (Figure 3.4.3.D), both FAstV3 and FAstV4 clustered with Canine astrovirus, Mamastrovirus 10 (from mink), Mamastrovirus 11 (from California sea lion) and FAstV D1, although again without strong bootstrap support.

Figure 3.4.3: The phylogenetic relationships of the FAstVs described in this study to other Mamastrovirus species based on (A) concatenated ORFs, (B) ORF1a, (C) ORF1b, and (D) capsid gene sequences. All four trees are rooted at the midpoint, and bootstrap values are displayed next to the branches. GenBank accession numbers are listed for reference sequences after the organism name. The novel FAstVs and Mamastrovirus 2 in this study are marked in red. Accession numbers NC_043099, NC_0431101, NC_034975, NC_043097, KX599354, and AF056197 are missing from the concatenated ORFs, ORF1a, and ORF1b (A, B and C) trees, and accession numbers KC692365, NC_043098, and NC_043103 are missing from the concatenated ORFs and ORF1a trees due to incomplete or unavailable gene sequences on GenBank.

Because there was some evidence for topological movement in the trees, compatible with the occurrence of recombination, we performed a more detailed analysis of recombination using RDP4 (Martin et al., 2015). While this again revealed that FAstV3 and FAstV4 changed phylogenetic positions across the genome, phylogenetic trees estimated for sequence regions on either side of the putative recombination breakpoints were not significantly different (as measured by levels of bootstrap support >70%). Hence, there is no conclusive evidence for recombination in these data and any change in tree topologies may simply reflect a lack of phylogenetic resolution. Irrespective of this lack of phylogenetic resolution, FAstV3 and FAstV4 are clearly distinct from all other feline astroviruses.

3.5: Discussion

We used mNGS to detect two novel FAstVs in the gastrointestinal tract of kittens. The pathogenic potential of astroviruses in cats is not yet clearly understood. In humans, astroviruses have been shown to cause gastroenteritis and are responsible for up to 10% of non-bacterial gastroenteritis cases (Bosch et al., 2014). Similar to three previous reports, we identified one of the astroviruses (FAstV4) in a sick cat co-infected with FPV (Moschidou et al., 2011, Yi et al., 2018, Zhang et al., 2019). Since FPV causes severe gastroenteritis in cats, causality between FAstV infection and diarrhoea is difficult to ascertain. Previous evidence in support of a pathogenic role for FAstVs includes the induction of diarrhoea after experimental inoculation of SPF cats, as well as results of some molecular surveillance studies (Zhang et al., 2019, Harbour et al., 1987, Aydin and Timurkan, 2018). While one study found no significant difference in the prevalence of FAstV infection in cats with and

without diarrhoea (Cho et al., 2014), another detected FAstVs in 38/105 (36%) cats with diarrhoea and in only 8/92 (8.7%) cats without diarrhoea (Zhang et al., 2019). In the latter study, co-infections of FAstV with FPV and/or feline bocavirus (FBoV) were present in 35/105 cats with diarrhoea (33%), whereas no FAstV co-infections were detected in cats without diarrhoea.

Co-infections of some enteric viruses in humans can increase the severity of clinical signs of acute gastroenteritis caused by single virus infections (Menon et al., 2016). Whether FAstV and FPV or other enteric virus co-infections could contribute to more severe clinical disease than single virus infections warrants further investigation using large-scale NGS molecular surveillance studies of cats with and without enteric disease. All of the cats we investigated were also co-infected with feline coronavirus (FCoV), an enteric alphacoronavirus. FCoV is ubiquitous in most multicat environments and was detected in all of 37 catteries tested in Germany recently (Klein-Richers et al., 2020). FCoV most commonly exists as an avirulent pathotype that causes subclinical infection or occasionally mild enteritis but can mutate to acquire macrophage-tropism and cause the systemic inflammatory disease feline infectious peritonitis.

Phylogenetic analysis of the concatenated ORFs, ORF1a, ORF1b and capsid gene sequences revealed that despite some topological uncertainty, both FAstV3 and FAstV4 are clearly distinct from the established species Mamastrovirus *2* and FAstV2. In some of the gene trees, we observed a broad grouping of FAstV3, FAstV4, a mink astrovirus associated with diarrhoea in farmed minks (Genbank accession NC_004579) and another associated with shaking mink syndrome (GenBank accession GU985458), a FAstV from healthy shelter-housed cats (GenBank accession NC_024701), and in the case of the capsid tree a canine astrovirus detected in the faeces of a shelter-housed dog with diarrhoea (GenBank accession KX599354) and a California sea lion astrovirus (GenBank accession NC_043097). However, while FAstV4 often groups with FAstV D1 (the only exception being the capsid gene tree), the exact phylogenetic position of FAstV3 is currently unresolved. It is possible that phylogenetic uncertainty in part reflects the action of recombination that has previously been documented in mammalian astroviruses (Walter et al., 2001, Wolfaardt et al., 2011, Rivera et al., 2010, Ito et al., 2017), although we found no firm evidence for this process here.

The genetic diversity of astroviruses poses challenges for their diagnosis. For instance, there are at least five distinct *Mamastrovirus* species (1, 6, 8, 9 and the tentative species 20) in the

human host and different assays are required for their molecular diagnosis, although commercial assays are available only for classical human astroviruses (Mamastrovirus 1) (Bosch et al., 2014, Perot et al., 2017). In cats, astroviruses are not included routinely in the diagnostic algorithms of infectious diseases, thus hindering the collection of useful information in terms of epidemiological and clinical data.

In sum, these findings support that FAstVs are part of the gastrointestinal virome of domestic cats and demonstrate the extensive genetic diversity of FAstVs. Whether there are biological differences among the various FAstV strains should be considered, as astroviruses exhibit considerable biological plasticity. Accordingly, it is important to determine whether some FAstVs may act as either primary pathogens or opportunists.

3.6: References

Aydin, H., Timurkan, M. 2018. A pilot study on feline astrovirus and feline panleukopenia virus in shelter cats in Erzurum, Turkey. *Revue de Medecine Veterinaire*, 169(1):52-57.

Blomstrom, A.L., Widen, F., Hammer, A.S., Belak, S., Berg, M. 2010. Detection of a novel astrovirus in brain tissue of mink suffering from shaking mink syndrome by use of viral metagenomics. *Journal of Clinical Microbiology*, 48(12):4392-6.

Bosch, A., Pinto, R.M., Guix, S. 2014. Human astroviruses. *Clinical Microbiology Reviews*, 27(4):1048-74.

Castresana, J. 2000. Selection of conserved blocks from multiple alignments for their use in phylogenetic analysis. *Molecular Biology and Evolution*, 17(4):540-52.

Cho, Y.Y., Lim, S.I., Kim, Y.K., Song, J.Y., Lee, J.B., An, D.J. 2014. Molecular characterisation and phylogenetic analysis of feline astrovirus in Korean cats. *Journal of Feline Medicine and Surgery*, 16(8)679-83.

Chong, R., Shi, M., Grueber, C.E., Holmes, E.C., Hogg, C.J., Belov, K., Barrs, V.R. 2019. Fecal Viral Diversity of Captive and Wild Tasmanian Devils Characterized Using Virion-Enriched Metagenomics and Metatranscriptomics. *Journal of Virology*, 93(11):e00205.

Conceicao-Neto, N., Zeller, M., Lefrere, H., De Bruyn, P., Beller, L., Deboutte, W., Yinda, C.K., Lavigne, R., Maes, P., Van Ranst, M., Heylen, E., Matthijnssens, J. 2015. Modular approach to customise sample preparation procedures for viral metagenomics: a reproducible protocol for virome analysis. *Scientific Reports*, 5:16532.

De Benedictis, P., Schultz-Cherry, S., Burnham, A., Cattoli, G. 2011. Astrovirus infections in humans and animals - molecular biology, genetic diversity, and interspecies transmissions. *Infection, Genetics and Evolution*, 11(7):1529-44.

Fu, Y., Pan, M., Wang, X., Xu, Y., Xie, X., Knowles, N.J., Yang, H., Zhang, D. 2009. Complete sequence of a duck astrovirus associated with fatal hepatitis in ducklings. Journal of General Virology, 90(Pt 5):1104-1108.

Gavier-Widen, D., Brojer, C., Dietz, H.H., Englund, L., Hammer, A.S., Hedlund, K.O., Hard af Segerstad, C., Nilsson, K., Nowotny, N., Puurula, V., Thoren, P., Uhlhorn, H., Weissenbock, H., Agren, E., Klingeborn, B. 2004. Investigations into shaking mink syndrome: an encephalomyelitis of unknown cause in farmed mink (Mustela vison) kits in Scandinavia. *Journal of Veterinary Diagnostic Investigation*, 16(4):305-12.

Gough, R.E., Borland, E.D., Keymer, I.F., Stuart, J.C. 1985. An outbreak of duck hepatitis type II in commercial ducks. *Avian Pathology*, 14(2):227-36.

Grabherr, M.G., Haas, B.J., Yassour, M., Levin, J.Z., Thompson, D.A., Amit, I., Adiconis, X., Fan, L., Raychowdhury, R., Zeng, Q., Chen, Z., Mauceli, E., Hacohen, N., Gnirke, A., Rhind, N., di Palma, F., Birren, B.W., Nusbaum, C., Lindblad-Toh, K., Friedman, N., Regev, A. 2011. Full-length transcriptome assembly from RNA-Seq data without a reference genome. *Nature Biotechnology*, 29(7):644-52.

Guindon, S., Gascuel, O. 2003. A simple, fast, and accurate algorithm to estimate large phylogenies by maximum likelihood. *Systematic Biology*, 52(5):696-704.

Harbour, D.A., Ashley, C.R., Williams, P.D., Gruffydd-Jones, T.J. 1987. Natural and experimental astrovirus infection of cats. *Veterinary Records Open,* 120(23):555-7.

Hordijk, W., Gascuel, O. 2005. Improving the efficiency of SPR moves in phylogenetic tree search methods based on maximum likelihood. *Bioinformatics*, 21(24):4338-47.

Hoshino, Y., Zimmer, J.F., Moise, N.S., Scott, F.W. 1981. Detection of astroviruses in feces of a cat with diarrhea. Brief report. *Archives of Virology*, 70(4):373-6.

Imada, T., Yamaguchi, S., Mase, M., Tsukamoto, K., Kubo, M., Morooka, A. 2000. Avian nephritis virus (ANV) as a new member of the family Astroviridae and construction of infectious ANV cDNA. *Journal of Virology*, 74(18):8487-93.

Ito, M., Kuroda, M., Masuda, T., Akagami, M., Haga, K., Tsuchiaka, S., Kishimoto, M., Naoi, Y., Sano, K., Omatsu, T., Katayama, Y., Oba, M., Aoki, H., Ichimaru, T., Mukono, I., Ouchi, Y., Yamasato, H., Shirai, J., Katayama, K., Mizutani, T., Nagai, M. 2017. Whole genome analysis of porcine astroviruses detected in Japanese pigs reveals genetic diversity and possible intra-genotypic recombination. *Infection, Genetics and Evolution*, 50:38-48.

Katoh, K., Standley, D.M. 2013. MAFFT multiple sequence alignment software version 7: improvements in performance and usability. *Molecular Biology and Evolution*, 30(4):772-80.

Klein-Richers, U., Hartmann, K., Hofmann-Lehmann, R., Unterer, S., Bergmann, M., Rieger, A., Leutenegger, C., Pantchev, N., Balzer, J., Felten, S. 2020. Prevalence of Feline Coronavirus Shedding in German Catteries and Associated Risk Factors. *Viruses*, 12(9):1000.

Kopylova, E., Noe, L., Touzet, H. 2012. SortMeRNA: fast and accurate filtering of ribosomal RNAs in metatranscriptomic data. *Bioinformatics*, 28(24):3211-7.

Koukou, G., Niendorf, S., Hornei, B., Schlump, J.U., Jenke, A.C., Jacobsen, S. 2019. Human astrovirus infection associated with encephalitis in an immunocompetent child: a case report. *Journal of Medical Case Reports*, 13(1):341.

Lau, S.K., Woo, P.C., Yip, C.C., Bai, R., Wu, Y., Tse, H., Yuen, K.Y. 2013. Complete genome sequence of a novel feline astrovirus from a domestic cat in Hong Kong. *Genome Announcements*, 1(5):e00708-13.

Lawler, P.E., Cook, K.A., Williams, H.G., Archer, L.L., Schaedel, K.E., Isaza, N.M., Wellehan, J.F.X., Jr. 2018. Determination of the diversity of astroviruses in feces from cats in Florida. *Journal of Veterinary Diagnostic Investigation*, 30(2)275-279.

Le, S.Q., Gascuel, O. 2008. An improved general amino acid replacement matrix. *Molecular Biology and Evolution*, 25(7):1307-20.

Li, H., Durbin, R. 2009. Fast and accurate short read alignment with Burrows-Wheeler transform. *Bioinformatics*, 25(14):754-60.

Li, J., Rettedal, E.A., van der Helm, E., Ellabaan, M., Panagiotou, G., Sommer, M.O.A. 2019. Antibiotic Treatment Drives the Diversification of the Human Gut Resistome. *Genomics Proteomics Bioinformatics*, 17(1):39-51.

Li, L., Diab, S., McGraw, S., Barr, B., Traslavina, R., Higgins, R., Talbot, T., Blanchard, P., Rimoldi, G., Fahsbender, E., Page, B., Phan, T.G., Wang, C., Deng, X., Pesavento, P., Delwart, E. 2013. Divergent astrovirus associated with neurologic disease in cattle. *Emerging Infectious Disease*, 19(9):1385-92.

Marshall, J.A., Kennett, M.L., Rodger, S.M., Studdert, M.J., Thompson, W.L., Gust, I.D. 1987. Virus and virus-like particles in the faeces of cats with and without diarrhoea. *Australian Veterinary Journal*, 64(4):100-5.

Martin, D.P., Murrell, B., Golden, M., Khoosal, A., Muhire, B. 2015. RDP4: Detection and analysis of recombination patterns in virus genomes. *Virus Evolution*, 1(1):vev003.

Menon, V.K., George, S., Sarkar, R., Giri, S., Samuel, P., Vivek, R., Saravanabavan, A., Liakath, F.B., Ramani, S., Iturriza-Gomara, M., Gray, J.J., Brown, D.W., Estes, M.K., Kang, G. 2016. Norovirus Gastroenteritis in a Birth Cohort in Southern India. *PLoS One*, 11(6):e0157007.

Mor, S.K., Abin, M., Costa, G., Durrani, A., Jindal, N., Goyal, S.M., Patnayak, D.P. 2011. The role of type-2 turkey astrovirus in poult enteritis syndrome. *Poultry Science*, 90(12):2747-52.

Moschidou, P., Martella, V., Lorusso, E., Desario, C., Pinto, P., Losurdo, M., Catella, C., Parisi, A., Banyai, K., Buonavoglia, C. 2011. Mixed infection by Feline astrovirus and Feline panleukopenia virus in a domestic cat with gastroenteritis and panleukopenia. *Journal of Veterinary Diagnostic Investigation*, 23(3):581-4.

Ng, T.F., Mesquita, J.R., Nascimento, M.S., Kondov, N.O., Wong, W., Reuter, G., Knowles, N.J., Vega, E., Esona, M.D., Deng, X., Vinje, J., Delwart, E. 2014. Feline fecal virome reveals novel and prevalent enteric viruses. *Veterinary Microbiology*, 171(1-2):102-11.

Peng, Y., Leung, H.C., Yiu, S.M., Chin, F.Y. 2012. IDBA-UD: a de novo assembler for single-cell and metagenomic sequencing data with highly uneven depth. *Bioinformatics*, 28(11):1420-8.

Perot, P., Lecuit, M., Eloit, M. 2017. Astrovirus Diagnostics. *Viruses*, 9(1):10.

Quan, P.L., Wagner, T.A., Briese, T., Torgerson, T.R., Hornig, M., Tashmukhamedova, A., Firth, C., Palacios, G., Baisre-De-Leon, A., Paddock, C.D., Hutchison, S.K., Egholm, M., Zaki, S.R., Goldman, J.E., Ochs, H.D., Lipkin, W.I. 2010. Astrovirus encephalitis in boy with X-linked agammaglobulinemia. *Emerging Infectious Disease*, 16(6):918-25.

Rivera, R., Nollens, H.H., Venn-Watson, S., Gulland, F.M., Wellehan, J.F., Jr. 2010. Characterization of phylogenetically diverse astroviruses of marine mammals. *Journal of General Virology*, 91(Pt 1):166-73.

Schultz-Cherry, S. 2013. Astrovirus Research: Essential Ideas, Everyday Impacts, Future Directions, New York, NY, Springer-Verlag.

Talavera, G., Castresana, J. 2007. Improvement of phylogenies after removing divergent and ambiguously aligned blocks from protein sequence alignments. *Systematic Biology*, 56(4):564-77.

Van Brussel, K., Carrai, M., Lin, C., Kelman, M., Setyo, L., Aberdein, D., Brailey, J., Lawler, M., Maher, S., Plaganyi, I., Lewis, E., Hawkswell, A., Allison, A.B., Meers, J., Martella, V., Beatty, J.A., Holmes, E.C., Decaro, N., Barrs, V.R. 2019. Distinct Lineages of Feline Parvovirus Associated with Epizootic Outbreaks in Australia, New Zealand and the United Arab Emirates. *Viruses*, 11(12):1155.

Walter, J.E., Briggs, J., Guerrero, M.L., Matson, D.O., Pickering, L.K., Ruiz-Palacios, G., Berke, T., Mitchell, D.K. 2001. Molecular characterization of a novel recombinant strain of human astrovirus associated with gastroenteritis in children. *Archives of Virology*, 146(12):2357-67.

Wolfaardt, M., Kiulia, N.M., Mwenda, J.M., Taylor, M.B. 2011. Evidence of a recombinant wild-type human astrovirus strain from a Kenyan child with gastroenteritis. *Journal of Clinical Microbiology*, 49(2):728-31.

Yi, S., Niu, J., Wang, H., Dong, G., Guo, Y., Dong, H., Wang, K., Hu, G. 2018. Molecular characterization of feline astrovirus in domestic cats from Northeast China. *PLoS One*, 13(10):e0205441.

Zhang, Q., Niu, J., Yi, S., Dong, G., Yu, D., Guo, Y., Huang, H., Hu, G. 2019. Development and application of a multiplex PCR method for the simultaneous detection and differentiation of feline panleukopenia virus, feline bocavirus, and feline astrovirus. *Archives of Virology*, 164(11):2761-2768.

Zhang, W., Li, L., Deng, X., Kapusinszky, B., Pesavento, P.A., Delwart, E. 2014. Faecal virome of cats in an animal shelter. *Journal of General Virology*, 95(Pt 11):2553-2564.

Zheng, T., Li, J., Ni, Y., Kang, K., Misiakou, M.A., Imamovic, L., Chow, B.K.C., Rode, A.A., Bytzer, P., Sommer, M., Panagiotou, G. 2019. Mining, analyzing, and integrating viral signals from metagenomic data. *Microbiome*, 7(1):42.

Chapter four: The enteric virome of cats with feline panleukopenia differs in abundance and diversity from healthy cats

Kate Van Brussel[1,2], Xiuwan Wang[3], Mang Shi[2,4], Maura Carrai[3], Shuo Feng[3], Jun Li[3,5], Edward C. Holmes[2], Julia A. Beatty[1,3,6] and Vanessa R. Barrs[1,3,6]

[1]School of Veterinary Science, Faculty of Science, University of Sydney, Sydney, New South Wales, Australia

[2]Sydney Institute for Infectious Diseases, School of Life and Environmental Sciences and School of Medical Sciences, University of Sydney, Sydney, New South Wales, Australia

[3]Jockey Club College of Veterinary Medicine & Life Sciences, Centre for Animal Health and Welfare, City University of Hong Kong, Kowloon Tong, Hong Kong, China

[4]School of Medicine, Sun Yat-sen University, Guangzhou, China

[5]School of Data Science, City University of Hong Kong, Hong Kong, China

[6]Centre for Animal Health and Welfare, City University of Hong Kong, Hong Kong, China

4.1: Abstract

Feline panleukopenia (FPL) is a severe, often fatal disease caused by feline panleukopenia virus (FPV). How infection with FPV might impact the composition of the entire eukaryotic enteric virome in cats has not been characterized. We used meta-transcriptomic and viral particle enrichment metagenomic approaches to characterize the enteric viromes of 23 cats naturally infected with FPV (FPV-cases) and 36 age-matched healthy shelter cats (healthy controls). Sequencing reads from mammalian infecting viral families largely belonged to the *Coronaviridae*, *Parvoviridae* and *Astroviridae*. The most abundant viruses among the healthy control cats were feline coronavirus, Mamastrovirus 2 and Carnivore bocaparvovirus 3 (feline bocavirus), with frequent coinfections of all three. Feline chaphamaparvovirus was only detected in healthy controls (6 out of 36, 16.7%). Among the FPV-cases, in addition to FPV, the most abundant viruses were Mamastrovirus 2, feline coronavirus and Carnivore bocaparvovirus 4 (feline bocaparvovirus 2). The latter and feline bocaparvovirus 3 were detected significantly more frequently in FPV-cases than in healthy controls. Feline calicivirus was present in a higher proportion of FPV-cases (11 out of 23, 47.8%) compared to healthy controls (5 out of 36, 13.9%, p = 0.0067). Feline kobuvirus infections were also common among FPV-cases (9 out of 23, 39.1%) and were not detected in any healthy controls (p < .0001). While abundant in both groups, astroviruses were more frequently present in FPV-cases (19 out of 23, 82.6%) than in healthy controls (18 out of 36, p = .0142). The differences in eukaryotic virome composition revealed here indicate that further investigations are warranted to determine associations between enteric viral co-infections on clinical disease severity in cats with FPL.

4.2: Introduction

Feline panleukopenia virus (FPV), a small non-enveloped linear ssDNA virus with a 5.1 kb genome, is a variant of the species Carnivore Protoparvovirus 1 (family *Parvoviridae*). Feline panleukopenia virus causes an enteric and systemic disease known as feline panleukopenia (FPL) and can also infect cats subclinically (Barrs, 2019). The virus is shed in high copy numbers in all secretions of infected cats and is transmitted faeco-orally, especially via fomites. Infection by this environmentally resilient virus occurs most commonly in unvaccinated kittens that first encounter the virus, especially in animal shelters, after maternal

antibodies wane. Disease in susceptible cats is characterized by vomiting, diarrhoea, dehydration and sepsis and in severe cases can be fatal (Barrs, 2019).

Co-infections of FPV with other enteric viruses have been detected in sick and/or healthy cats including viruses from the families *Parvoviridae* (genera *Bocaparvovirus* and *Chaphamaparvovirus*), *Astroviridae* (genus *Mamastrovirus*), *Coronaviridae* (genus *Alphacoronavirus*), *Caliciviridae* (genera *Vesivirus* and *Norovirus*) and *Picornaviridae* (genus *Kobuvirus*) (Van Brussel et al., 2020, Castro et al., 2015, Di Profio et al., 2021, Ji et al., 2020, Piewbang et al., 2019).

A host can be exposed to multiple viruses with similar routes of transmission and high prevalence at the same or within a short space of time. In young children, co-infection and simultaneous detection of enteropathogens is common (Makimaa et al., 2020). Interactions among co-infecting viruses may be synergistically pathogenic and enteric virus co-infections are commonly identified for all viruses linked to acute gastroenteritis in humans (Simsek et al., 2021). Similarly, enteric co-pathogen infections may play a role in determining clinical outcomes in cats infected with FPV. Since FPV damages gastrointestinal epithelium and bone-marrow to cause local and systemic immunosuppression, viral co-infections might be more commonplace in cats with FPL than among healthy cats.

We incorporated both metatranscriptomics, the analysis of non-ribosomal RNA (rRNA) transcripts, and viral particle enrichment metagenomics to characterize the enteric virome of sick FPV-infected and clinically healthy cats. Our aim was to identify any differences in the gut virome of FPV-infected cats, particularly enteric viruses that are absent from the enteric virome of healthy control cats.

4.3: Materials and Methods

4.3.1: Ethics

The collection of faecal samples from cats in this study was approved by the University of Sydney Animal Ethics Committee (AEC approval number N00/7-2013/3/6029).

4.3.2: Faecal sample collection

From December 2016 to October 2017, faecal samples were collected from 24 domestic cats (FPV-cases) presenting to veterinary clinics in Australia with signs associated with FPL

including diarrhoea, vomiting, fever and/or unexpected death (Van Brussel et al., 2019). FPV infection was confirmed using PCR and Sanger sequencing of the VP2 protein (Van Brussel et al., 2019). The 24 FPV-cases included 20 cats from four shelters and four owned cats. Faecal samples were also collected from 36 heathy cats (healthy controls) from two of the same shelters as the FPV-cases in Sydney from April to August 2017 (Shelter 1-AWL and Shelter 2-CPS; Table 4.8.1). Healthy controls were matched for age with FPV-cases. As there were more controls, several older healthy control cats were also included (Table 4.8.2). Age, sex, breed, admission date and date of last vaccination were recorded for healthy cats (Table 4.8.2), all of which had been vaccinated at least once with a Feligen RCP live modified vaccine (Virbac, France) that contains attenuated FPV, Feline calicivirus and Felid alphaherpesvirus. Faecal samples were stored at −80°C after collection.

4.3.3: Total RNA extraction and next generation sequencing—metatranscriptome RNA

The isolation of total RNA from faecal samples, rRNA depletion, library preparation and sequencing were performed as previously described (Van Brussel et al., 2020, Chong et al., 2019). Briefly, the RNeasy plus mini kit (Qiagen, Germany) and Zymo-Seq RiboFree Total RNA Library Preparation Kit (Zymo Research, USA) were used for total RNA isolation, rRNA depletion and RNA sequencing library construction (Van Brussel et al., 2020). RNA libraries were sequenced on the Novaseq6000 platform (Illumina, USA, 150 bp paired end) at the Australian Genome Research Facility (AGRF, Melbourne, Australia) (Van Brussel et al., 2020). Faecal samples from all 24 FPV-cases and 36 healthy controls were processed and RNA libraries sequenced.

4.3.4: Virion enrichment, viral nucleic acid extraction, random amplification and NGS—metagenome cDNA and DNA

Virion enrichment from faecal samples was performed using a previously published protocol (Chong et al., 2019, Conceicao-Neto et al., 2015). Modifications were introduced to prevent DNA sequencing bias as follows: after the enrichment of virions and isolation of nucleic acids (Chong et al., 2019, Conceicao-Neto et al., 2015), nucleic acid extracts were divided into two aliquots of equal volume. One aliquot was subjected to DNase treatment (Invitrogen, Thermo Fisher Scientific, USA) to remove viral DNA, leaving viral RNA (Van Brussel et al., 2020), while the second, untreated aliquot represented the viral DNA. The viral RNA underwent random amplification using the Whole Transcriptome Amplification Kit (WTA2, Sigma-Aldrich, Merck, USA) and the maximum PCR cycle number (22 cycles) to produce

cDNA (Van Brussel et al., 2020, Chong et al., 2019, Conceicao-Neto et al., 2015). The viral DNA also underwent random amplification using the Whole Genome Amplification Kit (WGA2, Sigma-Aldrich, Merck, USA) following the manufacturer's instructions. The products from both viral RNA (cDNA) and DNA random amplification were purified using the GenElute PCR Clean-Up Kit (Sigma-Aldrich, Merck, USA). Libraries for sequencing were created and sequenced as previously described (Van Brussel et al., 2020). Briefly, cDNA and DNA libraries were produced using the Nextera XT library preparation kit (Illumina, USA) and were sequenced on the NovaSeq6000 platform (Illumina, USA, 150 bp paired end) at the AGRF (Melbourne, Australia). Four of the 24 FPV-cases faecal samples had cDNA or DNA extracts that failed quality control measurements after library preparation and were excluded from sequencing (Table 4.8.1). Additionally, five of the 24 FPV-cases cDNA libraries were of low quality and therefore sequenced on the NextSeq500 platform (Illumina, USA, 150 bp paired end) at the AGRF (Melbourne, Australia). In total 21 FPV-cases cDNA, 22 FPV-cases DNA, 36 healthy control cDNA and 36 healthy control DNA libraries were processed and sequenced.

4.3.5: Pre-processing of reads, de novo assembly and abundance mapping

Raw sequence reads were processed to remove adapters and primer sequences, PCR duplicates, ribosomal RNA (rRNA), host (*Felis catus*) reads and poor-quality terminal regions as previously described (Van Brussel et al., 2020). Briefly, rRNA reads were removed using SortMeRNA and host reads were identified and removed by mapping to the Felis catus genome (Van Brussel et al., 2020). The filtered metatranscriptomic reads (RNA) were *de novo* assembled using Trinity version 2.8.5 and the filtered metagenomic reads (cDNA and DNA) were de novo assembled using IDBA-UD version 1.1.2 (Van Brussel et al., 2020). The contigs (sequences of variable lengths obtained from *de novo* assembly of 150 bp paired end reads) were compared to the non-redundant protein database using Diamond version 2.0.4. The taxonomic classification for the filtered reads was calculated using KMA version 1.3.9a (Clausen et al., 2018) and CCMetagen version 1.2.4 (Marcelino et al., 2020) by comparing the filtered paired-end reads to the NCBI nucleotide database that contains all NCBI sequences except those of environmental eukaryotic and prokaryotic, unclassified and artificial origin. In CCMetagen read depth, specified as reads per million (RPM), was calculated and the threshold function was disabled to allow all taxonomy levels to be reported (Marcelino et al., 2020). Read abundance was further calculated by mapping filtered reads to the de novo assembled contigs observed in this dataset using Bowtie2 version 2.3.4.3.

Geneious version 2020.2.5 was used to predict ORFs and annotate genomes. The extent of index-hopping between libraries sequenced on the same lane was minimized by comparing contigs and identifying any identical sequences. The library with the highest read abundance for that sequence was then used to exclude any library that had a read abundance below 0.01% of that number.

4.3.6: Vaccine PCR and sequencing

The non-structural (NS) and VP2 genes from the FPV Feligen RCP modified live vaccine (Virbac, France) were amplified and sequenced as previously described (Pérez et al., 2014, Van Brussel et al., 2019). Amplicons were sequenced at the AGRF (Melbourne, Australia) and Geneious version 2020.2.5 was used to determine the consensus contig of the NS (accession no. ON605653) and VP2 (accession no. ON605652) based on the forward and reverse sequence.

4.3.7: Phylogenetic, recombination and statistical analysis

Nucleotide and amino acid sequences downloaded from NCBI GenBank were used for phylogenetic analysis and aligned employing the E-INS-I algorithm in MAFFT version 7 (Katoh and Standley, 2013). IQ-TREE version 1.6.7 (Nguyen et al., 2015) was used to determine the best-fit nucleotide and amino acid substitution models for each alignment using the ModelFinder program and the Akaike information criterion (AIC) (Kalyaanamoorthy et al., 2017). Phylogenetic trees were inferred using the maximum likelihood method in IQ-TREE employing the SH-like approximate likelihood ratio test (SH-aLRT) and ultrafast bootstrap with 1000 replicates to assess nodal support (Hoang et al., 2018). Branch support of > 70 SH-aLRT and > 70% UFBoot is shown as a grey circle on the branch node of all phylogenetic trees. Nucleotide alignments using MAFFT version 7 were screened for recombination events using RDP4 and possible recombination events were then confirmed using Simplot. To compare the virus composition in FPV-cases and healthy controls, a two-tailed Fisher's exact test was used and a p-value of < .05 was considered significant.

4.3.8: Excluded sequences—Contaminants, endogenous viruses and bacteriophages

Circoviridae and *Genomoviridae* contigs, as well as a complete pneumovirus genome detected in our sequencing libraries, were considered likely reagent-associated contaminants (Porter et al., 2021) and not analyzed in this study. Notably, the majority of nr hits for circovirus sequences were to viruses from an environmental source, and a phylogenetic

analysis of putative mammalian sequences revealed that all were likely reagent contaminants. Additionally, any retrovirus and bacteriophage sequences detected in this study were not analyzed. The picobirnaviruses detected here were also disregarded. Although they are commonly detected in mammalian faeces they contain a bacterial motif that is only detected in the viral genome of bacterial RNA viruses, consistent with their recent classification as bacteriophages (Krishnamurthy and Wang, 2018).

4.4: Results

4.4.1: Overview

Sequencing results from one of the 24 FPV-case samples were excluded due to poor sequencing quality in both the metatranscriptomic and metagenomic libraries. Accordingly, for FPV-cases, a total of 23 metatranscriptomic and 42 metagenomic (22 DNA and 20 cDNA) sequencing libraries were generated and analyzed (Table 4.8.1), while for the healthy control cats we obtained 36 metatranscriptomic and 72 metagenomic (36 DNA and cDNA) sequencing libraries. Overall, sequencing produced 2,316,187,631 paired end reads after filtering, including 1,174,728,799 from metatranscriptomic and 1,141,458,832 from metagenomic sequencing. De novo assembly generated 9,492,829 contigs from the metatranscriptomic sequencing libraries and 538,922 contigs from the metagenomic sequencing libraries. Viral read abundance calculated by CCMetagen and grouped by taxonomy classification is depicted in Figure 4.4.1.1. Enteric virus co-infections detected in FPV-cases and healthy control cats are summarized in Figure 4.1.1.2. GenBank accession numbers for the sequences presented in this study are listed in Table 4.8.3.
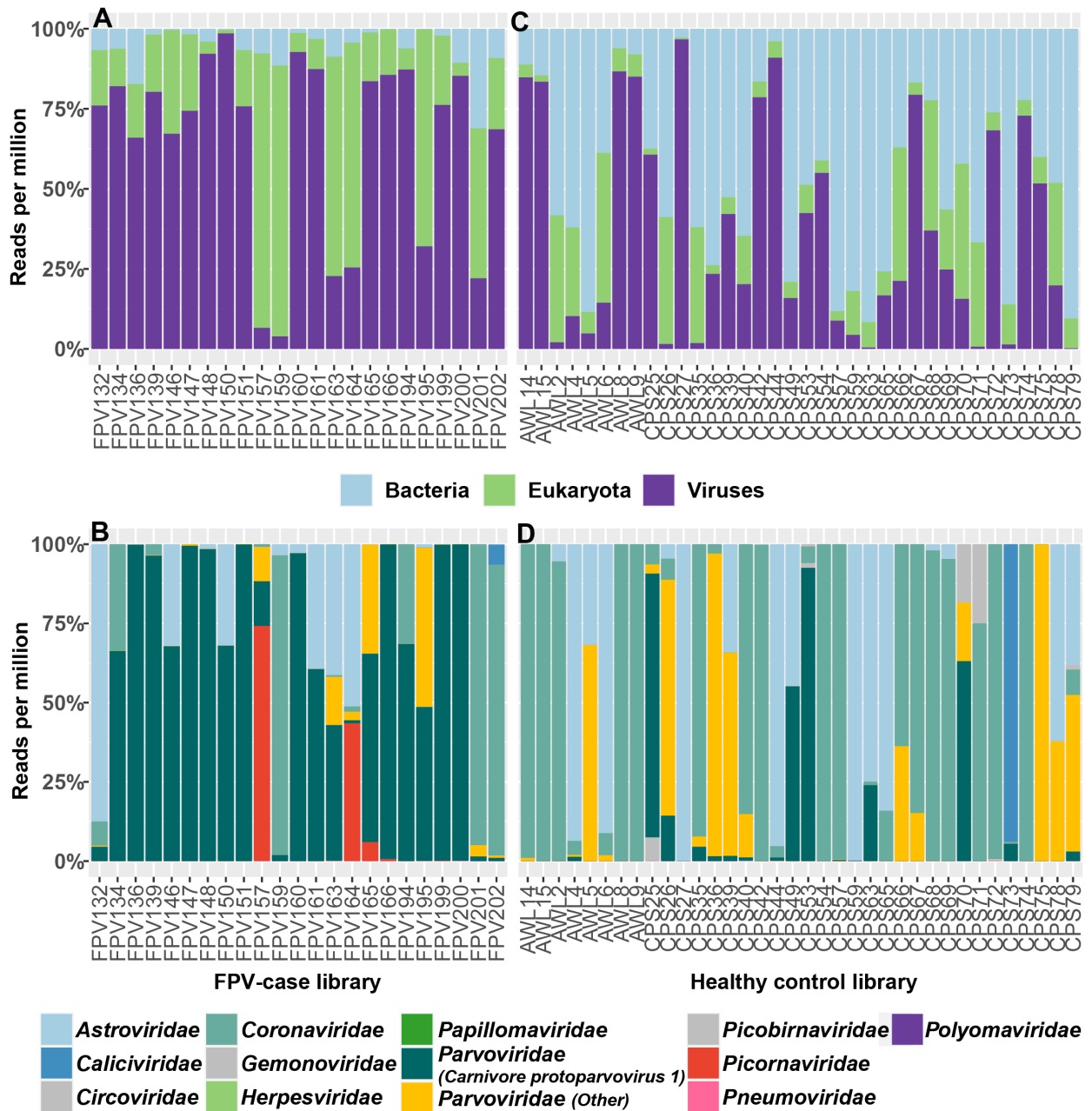
Figure 4.4.1.1: Viral read abundance calculated by CCMetagen and grouped by taxonomic classification. Abundance read count for FPV-case cat libraries by (a) Superkingdom and (b) family, and healthy control cat libraries by (c) Superkingdom and (d) family. Anelloviridae read abundance is not represented in this analysis and Picobirnaviridae, Circoviridae and Genomoviridae are coloured grey as these virus families were disregarded in this study.
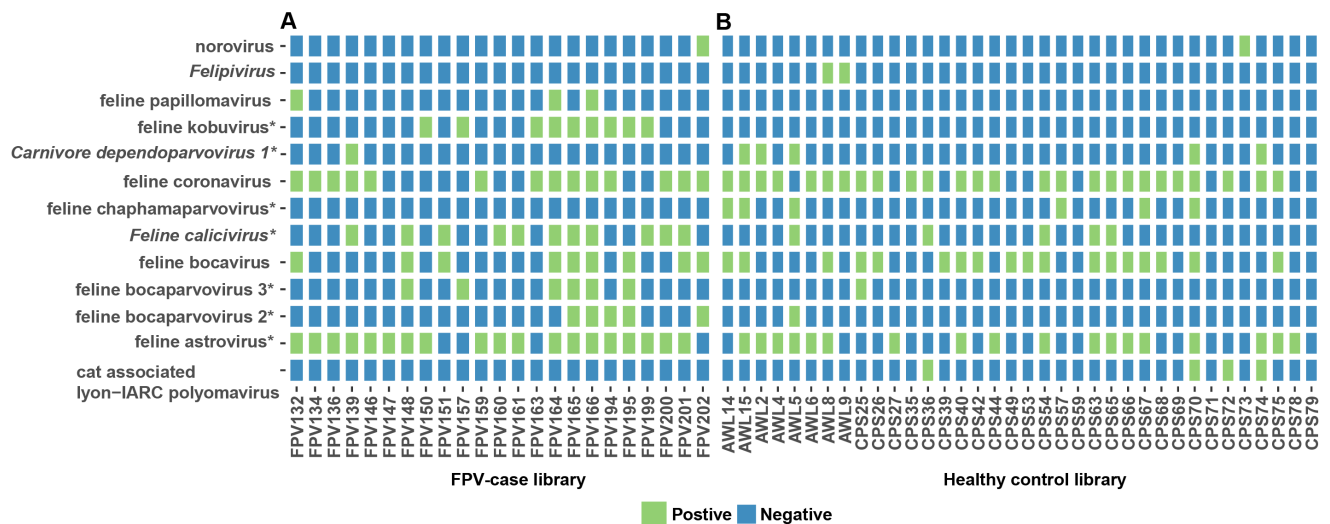
Figure 4.4.1.2: Enteric viruses detected in (a) FPV-cases and (b) healthy control cats from shelter 1 (AWL) and shelter 2 (CPS). Positive indicates detection of virus contigs in the data set, whereas viral contigs were not identified in negative samples. FPV, picobirnaviruses, circoviruses and genomoviruses have been excluded from this analysis. Asterisked viruses indicate a statistically significant difference in the number of cats that tested positive in each group (p < 0.05)

4.4.2: *Parvoviridae*

4.4.2.1: Protoparvovirus

FPV contigs were detected in all FPV-cases, in two out of eight healthy control cats from shelter 1 and in 26 out of 28 cats from shelter 2. Contigs were confirmed as FPV by identifying the presence of FPV SNPs in the VP2 or NS1 sequence. In a single healthy control cat contigs overlapping the FPV SNPs were not present, although the amino acid sequences of these contigs were 100% identical to a FPV sequence identified here and had only 98% identity to available CPV sequences. We therefore concluded that FPV was the only Carnivore protoparvovirus 1 present in our data. The FPV sequence in the two cats from shelter 1 had 100% nucleotide sequence identity to a sequence isolated from sick FPV cats in this study. This virus is circulating throughout the greater Sydney region and has only been identified in cats from New South Wales (NSW) (Van Brussel et al., 2019). At the time of collection, both shelter 1 cats were clinically healthy, consistent with a subclinical infection of FPV. For shelter 2, 25 out of 28 cats had contigs highly similar (99.9–100% for NS1 and 99.8–99.9% for VP2) to the vaccine strain, and 23 out of 25 had been vaccinated within the previous 30 days, suggesting that it likely represents the vaccine strain or a derived variant. In

total, 16 out of 28 healthy control cats had contigs that contained the VP2 region of the genome displaying the amino acid leucine at position 562, present in the FPV attenuated vaccine virus strain administered to these cats. In addition, 1 out of 28 healthy control cats from shelter 2 had an FPV VP2 sequence (1448 bp contig) that exhibited 100% identity to an FPV sequence isolated from an Australian outbreak of FPL in Mildura, Victoria in 2015 (Van Brussel et al., 2019). Read abundance for the healthy control cats was calculated by mapping to a complete FPV genome isolated from a healthy control cat (Table 4.8.4).

4.4.2.2: Bocaparvovirus

The genus *Bocaparvovirus* contains 25 recognized species that infect many mammalian species. Three species of feline bocaparvovirus have been described: Carnivore bocaparvovirus 3 (feline bocavirus), Carnivore bocaparvovirus 4 (feline bocaparvovirus 2) and Carnivore bocaparvovirus 5 (feline bocaparvovirus 3) (Lau et al., 2012, Ng et al., 2014, Zhang et al., 2014). We identified feline bocaparvovirus contigs in 11 out of 23 (47.8%) FPV-case libraries and 19 out of 36 (55.5%) healthy control libraries (Figure 4.4.1.2). Feline bocavirus contigs were detected in 18 out of 36 healthy controls (50%) and in 9 out of 23 (39%) of FPV-cases (39% 9/23) (p = .4317). Among healthy controls, feline bocavirus was the most abundant bocaparvovirus. In contrast, feline bocaparvovirus 2 was the most abundant bocaparvovirus in FPV-infected cats and was significantly more frequent in these (21.7%, 5 out of 23) than in healthy control cats (2.8%, 1/36; p = .0291). Finally, 6 out of 23 (26%) FPV-cases and 1 out of 36 (2.8%) healthy control cats had feline bocaparvovirus 3 contigs (p = .0114) (Table 4.4.2.2). Our phylogenetic analysis revealed that feline bocavirus sequences from the case and control libraries were scattered throughout the phylogeny. Feline bocaparvovirus 2 and 3 sequences were more tightly clustered, but there are insufficient numbers of sequences available within these clades to assess diversity (Figure 4.4.2.2).

Table 4.4.2.2: Enteric viral species abundance in FPV-cases and healthy control cats calculated using bowtie2.

Virus	FPV-Cases (n=23)		Healthy controls (n=36)	
	Total reads (Meta-genome and -transcriptome)	RPM	Total reads (Meta-genome and -transcriptome)	RPM
Parvoviridae				
feline panleukopenia virus (field or vaccine strains)	470,532,619	12,291,539	7,323,094	197,256
Carnivore bocaparvovirus 3	123,065	3,116	11,456,635	278,814
Carnivore bocaparvovirus 4*	12,039,049	524,515	814	26
Carnivore bocaparvovirus 5*	143,947	5,292	223,074	5,960
feline chaphamaparvovirus*	10	2	402,172	579
Carnivore dependoparvovirus 1*	110	0	16,574	15,154
Papillomaviridae				
felis catus papillomavirus 3	60	2	42	1
felis catus papillomavirus 4	199	7	377	9
Polyomaviridae				
cat associated lyon-IARC polyomavirus	12	0	2,228	42
Astroviridae				
Mamastrovirus 2*	151,373,185	3,569,170	112,953,736	3,149,338
Coronaviridae				

feline coronavirus	29,591,557	1,689,200	31,290,366	9,894,288
Caliciviridae				
Feline calicivirus*	409,597	44,710	50	20
Feline calicivirus F9 vaccine	2,889	338	6	1
norovirus GIV	767,133	21,562	1,690	1,435
Picornaviridae				
feline kobuvirus*	3,830,887	372,095	12	6
Felipivirus A	6	0	60,474	49,605

* There was a significant difference between the two groups in the numbers of cats in which this virus was detected ($p < 0.05$).
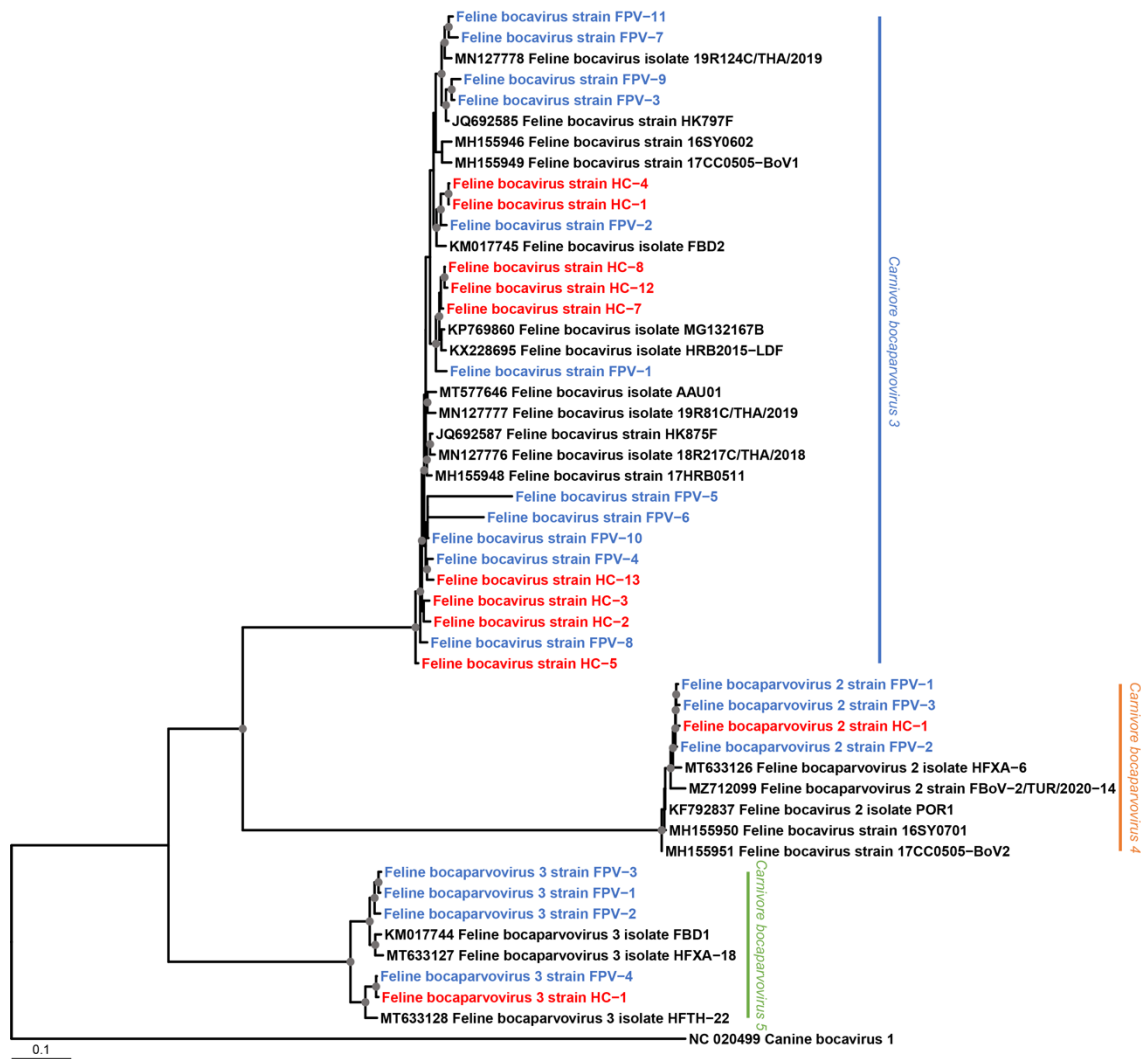
Figure 4.4.2.2: Phylogenetic analysis of the feline bocaparvovirus sequences identified in this study using the VP1 nucleotide alignment and the GTR+F+R8 nucleotide substitution model. Feline bocaparvovirus sequences from the FPV-case libraries are coloured in blue and sequences from the healthy control libraries are coloured in red. The scale bar represents the number of nucleotide substitutions per site. The tree was midpoint rooted for clarity only.

4.4.2.3: Chaphamaparvovirus and Dependoparvovirus

Chaphamaparvovirus is a genus in the *Parvoviridae*, subfamily *Hamaparvovirinae* that includes species that infect mammalian and avian hosts (Chong et al., 2019, Duarte et al., 2019, Kim et al., 2020, Li et al., 2020, Palombieri et al., 2020, Roediger et al., 2018, Souza et al., 2017, Yang et al., 2016). We did not detect feline chaphamaparvovirus contigs in any of the FPV-case libraries. However, read abundance data showed the presence of feline chaphamaparvovirus DNA in FPV-case samples at relatively low levels (maximum 25 reads in the metagenomic library). In contrast, in the healthy controls feline chaphamaparvovirus

contigs were detected in 6/36 libraries (p = .0724) (Figure 4.4.1.2). Abundance values in these six libraries ranged from 61 to 6,749 RPM for the metagenomic libraries and 87 and 4,648 RPM for the metatranscriptomic libraries. *Dependoparvovirus*, another genus in the *Parvoviridae*, includes the species Carnivore dependoparvovirus 1 (feline dependoparvovirus), previously detected in a single cat in the same shelter cat population in which feline chaphamaparvovirus was discovered (Li et al., 2020). Herein, feline dependoparvovirus DNA was detected in 1 out of 23 FPV-case libraries and 5 out of 36 healthy control libraries (p = .3886).

4.4.3: *Astroviridae*

The *Astroviridae* contain two genera *Avastrovirus* and *Mamastrovirus* that infect birds and mammals, respectively. The recognized feline astrovirus species is Mamastrovirus 2, although several novel feline astroviruses have been identified (Van Brussel et al., 2020, Zhang et al., 2014). Recently, we identified two novel feline astroviruses—feline astrovirus 3 and feline astrovirus 4—in a pilot study of four cats included here, one with FPV and diarrhoea and three healthy control cats (Van Brussel et al., 2020). Further analysis on this larger data set generated here showed the presence of astrovirus contigs at a higher frequency in FPV-cases (19/23, 82.6%) compared to healthy controls (18 out of 36, 50%; p = .0142; Figure 4.4.1.2). Two FPV-case libraries had contigs with 96–99% nucleotide similarity to feline astrovirus 4 and one contig, identified in an FPV-case library (cat #FPV166), contained the full ORF1a with 99% nucleotide similarity. The Mamastrovirus *2* sequence infecting two healthy controls is identical to the Mamastrovirus 2 sequence—AUS/AWL—described in our pilot study, with read abundance counts of 932,723 and 312,958 RPM for the two metatranscriptomic libraries and 896,065 and 862,160 RPM for the two metagenomic libraries. The capsid protein phylogeny revealed two groupings of Mamastrovirus 2 sequences (Figure 4.4.3). Interestingly, two Mamastrovirus 2 sequences—FPV-2 and FPV-8—formed a basal group to the human astroviruses in the capsid phylogeny although not in the ORF1b phylogeny (Figure 4.4.3). RDP4 and Simplot analysis detected a possible recombination event in the *Mamastrovirus* 2 sequence FPV-1 and sequence FPV-10 in the ORF1b and capsid overlap (Figure 4.8.1). However, no recombination events were detected in Mamastrovirus 2 sequence FPV-2 and FPV-8, contrary to the positioning of both sequence in the ORF1b and capsid phylogenies. It is likely that the currently limited number of complete Mamastrovirus 2 genomes available on GenBank precludes identification of recombination events.
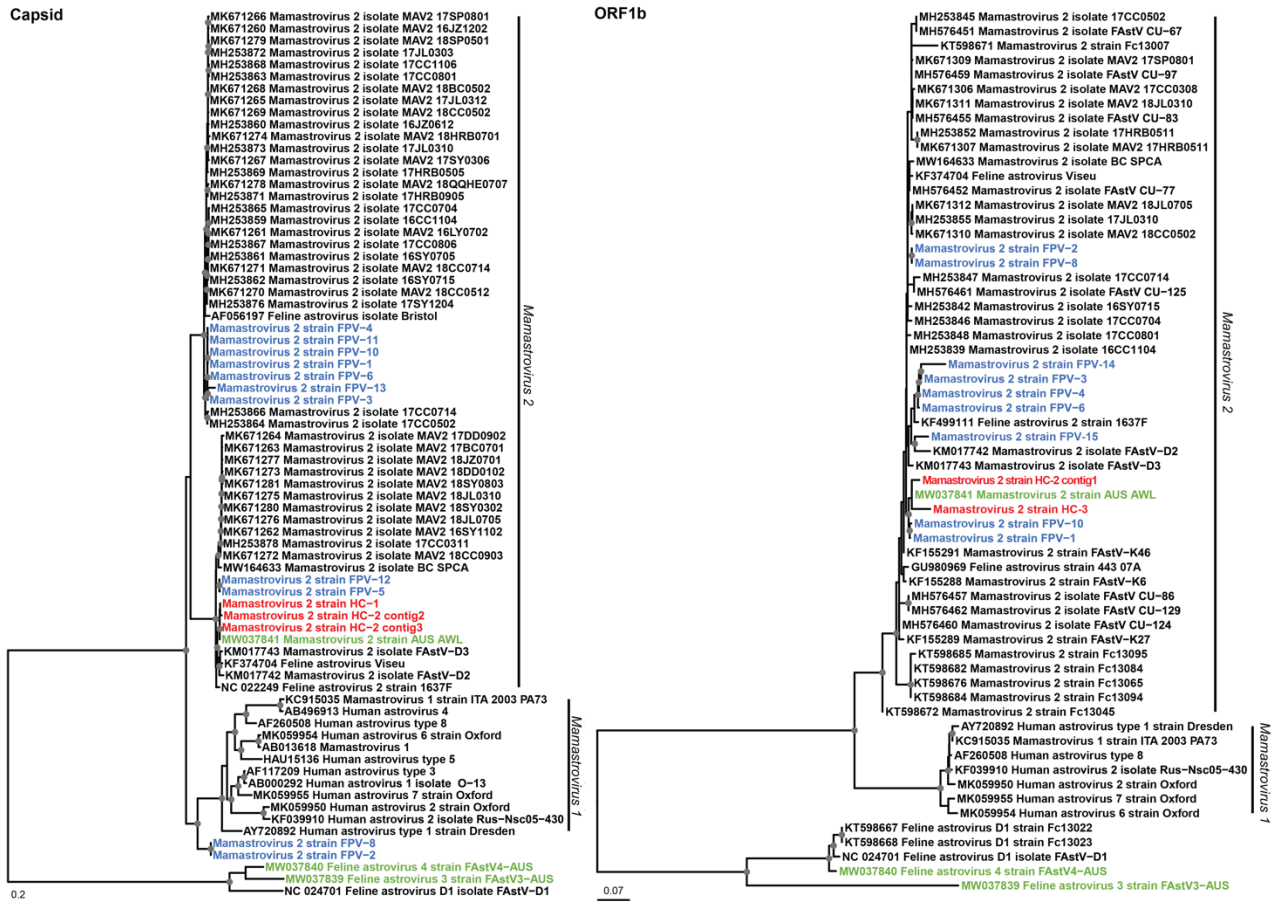
Figure 4.4.3: Phylogenetic analysis of the Mamastrovirus 2 sequences identified in FPV-cases and healthy controls using amino acid alignments of the capsid (top) and ORF1b (bottom) proteins and the LG+R3 and LG+F+R8 substitution models, respectively. The Mamastrovirus 2 sequences from the FPV-case libraries are presented in blue, the sequences from the healthy control libraries in red, and the feline astrovirus species and Mamastrovirus 2 sequence identified in the pilot study in green. The scale bar represents the number of amino acid substitutions per site. The tree was midpoint rooted for clarity only.

4.4.4: *Coronaviridae*

Alphacoronavirus 1 belongs to the family *Coronaviridae*. The read abundance and prevalence of feline coronavirus RNA was high in both the FPV-case libraries, 60.8% (14 out of 23) and in the healthy controls (80.5% 26 out of 36) (p = .4026; Figure 4.4.1.2; Table 4.4.2.2). The available spike proteins identified were screened for the amino acid mutations M1058L and S1060A, which are more commonly associated with systemic replication of feline infectious peritonitis virus (a mutant coronavirus generated de novo in vivo from Feline enteric coronavirus that causes severe multisystemic viral disease) (Chang et al., 2012). None of the spike proteins analyzed contained these spike mutations, consistent with

their isolation from faecal samples. Phylogenetic analyses of feline coronavirus sequences identified in this study using the full genome nucleotide alignment and spike protein amino acid alignment are shown in Figure 4.8.2.

4.4.5: *Caliciviridae*

4.4.5.1: Vesivirus

Feline calicivirus, genus *Vesivirus*, family *Caliciviridae*, is a highly contagious pathogen of domestic cats and other *Felidae* (Gaskell et al., 2004). Here, *Feline calicivirus* contigs were significantly more frequent in FPV-cases (47.8%, 11/23) compared to healthy controls (13.9%, 5 out of 36; p = .0067; Figure 4.4.1.2). With the exception of 2889 and six reads from the FPV-case and healthy control libraries, respectively, no Feline calicivirus contigs were identified as *Feline calicivirus* vaccine strain F9. In contrast, 409,597 reads (320 RPM) mapped to the *Feline calicivirus* contigs identified in the FPV-case libraries (Table 4.4.2.2). Feline calicivirus contigs identified in the other nine FPV-case libraries ranged from 203 to 7864 bp. In the control libraries, the longest *Feline calicivirus* contig was 815 bp. The phylogenetic analysis of the full genome and capsid protein shows the enteric sequences in this study do not group with the other identified enteric sequences in the phylogeny, instead forming a clade with other sequences from Australia (Figure 4.4.5.1).

Full genome

JX519214 Feline calicivirus isolate 1874
JX519210 Feline calicivirus isolate 5789
L40021 Feline calicivirus strain Urbana
KU373057 Feline calicivirus isolate TIG-1
KJ944377 Feline calicivirus isolate TFHLJ-8
KC835209 Feline calicivirus strain FCV-2280
AY560115 Feline calicivirus isolate UTCVM-NH3
JX519212 Feline calicivirus isolate 21223
JX519209 Feline calicivirus isolate 3786
MW194990 Feline calicivirus isolate SMU-B5-2020
JX519211 Feline calicivirus isolate 20879
AY560113 Feline calicivirus isolate UTCVM-NH1
AY560118 Feline calicivirus isolate USDA
AF479590 Feline calicivirus strain FCV2024
M86379 Feline calicivirus strain F9
AY560114 Feline calicivirus isolate UTCVM-NH2
FCU13992 Feline calicivirus CFI 68
KJ495730 Feline calicivirus isolate CH-JL3
KJ495729 Feline calicivirus isolate CH-JL2
JX519213 Feline calicivirus isolate 21749
AF109465 Feline calicivirus strain F65
AY560116 Feline calicivirus isolate UTCVM-H1
MW880762 Feline calicivirus strain U QLD10 Ging
MW880760 Feline calicivirus strain Z QLD12 Bella
MW880761 Feline calicivirus strain T QLD9 Boots
MW880765 Feline calicivirus strain Q QLD6 May
MW880771 Feline calicivirus strain S QLD8 Zee
MW880766 Feline calicivirus strain P QLD5 Merlin
MW880763 Feline calicivirus strain QLD13 KL
MW880770 Feline calicivirus strain ACT9 Smitty
MW880767 Feline calicivirus strain ACT1 Poppy
MW880768 Feline calicivirus strain ACT7 Raphael
MW880764 Feline calicivirus strain ACT3 Leo
MW880757 Feline calicivirus strain E1 V1 NSW5 Bella
MW880759 Feline calicivirus strain I V2 NSW9 SnowOwl
MW880758 Feline calicivirus strain E1 V2 NSW5 Bella
Feline calicivirus strain FPV-1
MW880769 Feline calicivirus strain ACT2 Samson
Feline calicivirus strain FPV-3
Feline calicivirus strain FPV-2
Feline calicivirus strain FPV-5
MK867378 Feline calicivirus isolate GX2019
KT206207 Feline calicivirus isolate CH-JL4
MW194991 Feline calicivirus isolate SMU-F4-2020
KT970059 Feline calicivirus strain GX01-13
KT000003 Feline calicivirus isolate SH 2014
KM016908 Feline calicivirus isolate HRB-SS
MT008250 Feline calicivirus strain FCV 160 2015 ITA
AY560117 Feline calicivirus isolate UTCVM-H2
DQ424892 Feline calicivirus strain FCV DD 2006 GE
KX371573 Feline calicivirus isolate WZ-1
KX371572 Feline calicivirus isolate XH
MT239579 Feline calicivirus isolate SH1
KP987265 Feline calicivirus SH
GU214989 Feline calicivirus strain GD
MT680938 Feline calicivirus isolate HZ-1
MT759583 Feline calicivirus isolate FCV-SX1
KT267162 Feline calicivirus isolate HB-S4
KM111557 Feline calicivirus isolate FB-NJ-13
MT759584 Feline calicivirus isolate FCV-SX2
KX815169 Feline calicivirus isolate FCV-YH 16
KJ495728 Feline calicivirus isolate CH-JL1
KJ572401 Feline calicivirus isolate 12Q087-5
KJ572400 Feline calicivirus isolate 12Q087-1

0.05

Capsid

MW194990 Feline calicivirus isolate SMU-B5-2020
FCU13992 Feline calicivirus CFI 68
JX519211 Feline calicivirus isolate 20879
KJ551381 Feline calicivirus isolate ITO 2002 JP
AY560113 Feline calicivirus isolate UTCVM-NH1
JX519212 Feline calicivirus isolate 21223
JX519209 Feline calicivirus isolate 3786
DQ910791 Feline calicivirus isolate FCV-Georgie
KJ572401 Feline calicivirus isolate 12Q087-5
KJ572400 Feline calicivirus isolate 12Q087-1
DQ910794 Feline calicivirus isolate VS-FCV-Ari
AF109467 Feline calicivirus strain LS012
KJ944377 Feline calicivirus isolate TFHLJ-8
AF109466 Feline calicivirus strain JOK63
AY996855 Feline calicivirus isolate UTCVM-NH4
DQ910789 Feline calicivirus isolate FCV-Deuce
AF479590 Feline calicivirus strain FCV2024
JX519214 Feline calicivirus isolate 1874
KU373057 Feline calicivirus isolate TIG-1
L40021 Feline calicivirus strain Urbana
JX519210 Feline calicivirus isolate 5789
KX371573 Feline calicivirus isolate WZ-1
KM016908 Feline calicivirus isolate HRB-SS
KX371572 Feline calicivirus isolate XH
KT970059 Feline calicivirus strain GX01-13
MW194991 Feline calicivirus isolate SMU-F4-2020
MN868063 Feline calicivirus isolate 354857
M86379 Feline calicivirus strain F9
AY560114 Feline calicivirus isolate UTCVM-NH2
AY996857 Feline calicivirus isolate UTCVM-NH6
JX519213 Feline calicivirus isolate 21749
DQ424892 Feline calicivirus strain FCV DD 2006 GE
X99447 Feline calicivirus strain KS20
AJ009721 Feline calicivirus isolate V66 97
MT239579 Feline calicivirus isolate SH1
MW880766 Feline calicivirus strain P QLD5 Merlin
MW880762 Feline calicivirus strain U QLD10 Ging
MW880771 Feline calicivirus strain S QLD8 Zee
MW880765 Feline calicivirus strain Q QLD6 May
MW880761 Feline calicivirus strain T QLD9 Boots
MW880760 Feline calicivirus strain Z QLD12 Bella
MW880763 Feline calicivirus strain QLD13 KL
AF031877 Feline calicivirus strain V274
AF031876 Feline calicivirus strain V83
MT008247 Feline calicivirus strain FCV 182 2015 ITA
MT008249 Feline calicivirus strain FCV 180 2015 ITA
MT008248 Feline calicivirus strain FCV 148 2015 ITA
MT008250 Feline calicivirus strain FCV 160 2015 ITA
MW880770 Feline calicivirus strain ACT9 Smitty
MW880767 Feline calicivirus strain ACT1 Poppy
MW880768 Feline calicivirus strain ACT7 Raphael
MW880764 Feline calicivirus strain ACT3 Leo
MW880758 Feline calicivirus strain E1 V2 NSW5 Bella
MW880759 Feline calicivirus strain I V2 NSW9 SnowOwl
AF031875 Feline calicivirus strain 182cvs5A
Feline calicivirus strain FPV-2
Feline calicivirus strain FPV-5
Feline calicivirus strain FPV-3
MW880769 Feline calicivirus strain ACT2 Samson
AY996858 Feline calicivirus isolate UTCVM-NH7
AY560116 Feline calicivirus isolate UTCVM-H1
EU202915 Feline calicivirus isolate 4b
MW880757 Feline calicivirus strain E1 V1 NSW5 Bella
Feline calicivirus strain FPV-1
KT000003 Feline calicivirus isolate SH 2014
DQ910793 Feline calicivirus isolate FCV-Jengo
DQ910792 Feline calicivirus isolate FCV-George Walder
DQ910795 Feline calicivirus isolate FCV-Kaos
AY560117 Feline calicivirus isolate UTCVM-H2
MT460112 Feline calicivirus isolate SH19
KT206207 Feline calicivirus isolate CH-JL4
MT008246 Feline calicivirus strain FCV 81 2014 ITA
AF109465 Feline calicivirus strain F65
AY560115 Feline calicivirus isolate UTCVM-NH3
MG214686 Feline calicivirus isolate SU
MK374292 Feline calicivirus isolate 14Q315
KJ495730 Feline calicivirus isolate CH-JL3
KJ495729 Feline calicivirus isolate CH-JL2
MK867378 Feline calicivirus isolate GX2019
KM111557 Feline calicivirus isolate FB-NJ-13
KJ495728 Feline calicivirus isolate CH-JL1
KJ551382 Feline calicivirus isolate ym3 2001 JP
KT267162 Feline calicivirus isolate HB-S4
KJ551380 Feline calicivirus isolate Gon 2003 JP
KX815169 Feline calicivirus isolate FCV-YH 16
KP987265 Feline calicivirus SH
MT759584 Feline calicivirus isolate FCV-SX2
GU214989 Feline calicivirus strain GD
MT759583 Feline calicivirus isolate FCV-SX1

0.02

Australian strain   Vaccine strain   Enteric strain

Figure 4.4.5.1: Phylogenetic analysis of the Feline calicivirus enteric sequences identified in FPV-cases and healthy controls using the full genome nucleotide alignment (left) and the GTR+F+R4 nucleotide substitution model and capsid protein amino acid alignment (right) and the LG+F+R8 amino acid substitution model, respectively. The Feline calicivirus sequences from the FPV-case libraries are coloured in blue. The scale bar represents the number of nucleotide and amino acid substitutions per site. The tree was midpoint rooted for clarity only.

4.4.5.2: Norovirus

Norwalk virus, genus *Norovirus*, is separated into 10 genogroups that are further classified into genotypes. We detected feline norovirus RNA in 1/23 FPV-cases and 1/36 healthy control cats (p = 1; Figure 4.4.1.2; Table 4.4.2.2), both in genogroup GIV (Figure 4.4.5.2). The FPV-case library (cat #FPV202) contained a complete genome. The nine feline norovirus contigs isolated from the healthy control library (cat #CPS73) were 310 to 1927 bp in length and contained sections of the polyprotein, capsid protein and VP3 regions.

Capsid

MT256407.1 Norovirus GIV isolate SMU−SC−CHN4 2019
MT256405.1 Norovirus GIV isolate SMU−SC−CHN2 2019
JF781268.1 Norovirus cat GIV.2 CU081210E USA 2010
Norovirus GIV isolate cat FPV-1
EF450827.1 Norovirus lion GGIV.2 Pistoia 387 06 ITA
LC389583.1 Norovirus GIV.2 Fe GIV.2 JP 2017 M81
MT256410.1 Norovirus GIV isolate SMU−SC−CHN10 2019
Norovirus GIV isolate cat HC-1
MT256409.1 Norovirus GIV isolate SMU−SC−CHN6 2019
MT256408.1 Norovirus GIV isolate SMU−SC−CHN5 2019
MK067288.1 Norovirus GIV isolate dog GIV.2 AN1610 USA 2017
MK067290.1 Norovirus GIV isolate dog GIV.2 AN1638 USA 2017
MK067289.1 Norovirus GIV isolate dog GIV.2 AN843 USA 2011
MN912824.1 Norovirus GIV isolate Dog GIV.2 C19 19 CH
MK726262.1 Norovirus GIV isolate G19 023
MT232232.1 Norovirus GIV isolate 549
NC 029647.1 Norovirus GIV
KT245136.1 Norovirus cat GVI.2 TE 77−13 ITA
MK067295.1 Norovirus GVI isolate dog GVI.2 AN1640 USA 2017
MN897758.1 Norovirus GVI isolate Dog GVI.2 M19 18 CH
MN897759.1 Norovirus GVI isolate Dog GVI.2 M9 18 CH
MN897757.1 Norovirus GVI isolate Dog GVI.2 W14 19 CH
KY486329.1 Norovirus GVI strain 63.15 2015 ITA
MW939576.1 Norovirus GVI isolate BUCT−K1
MW945229.1 Norovirus GVI isolate BUCT−K4
MW662289.1 Norovirus GVI isolate Dog Z7 19 CH
MK067292.1 Norovirus GVI isolate dog GVI.1 AN1632 USA 2017
KY486328.1 Norovirus GVI strain Dog 5010 2009 ITA

0.05

Figure 4.4.5.2: Phylogenetic analysis of the norovirus sequences from FPV-cases and healthy controls using the capsid protein amino acid alignment and the LG+F+R3 amino acid substitution model. The norovirus sequence from the FPV-case cat #202 is coloured in blue and from the healthy control cat #CPS73 in red. The scale bar represents the number of amino acid substitutions per site. The tree was midpoint rooted for clarity only.
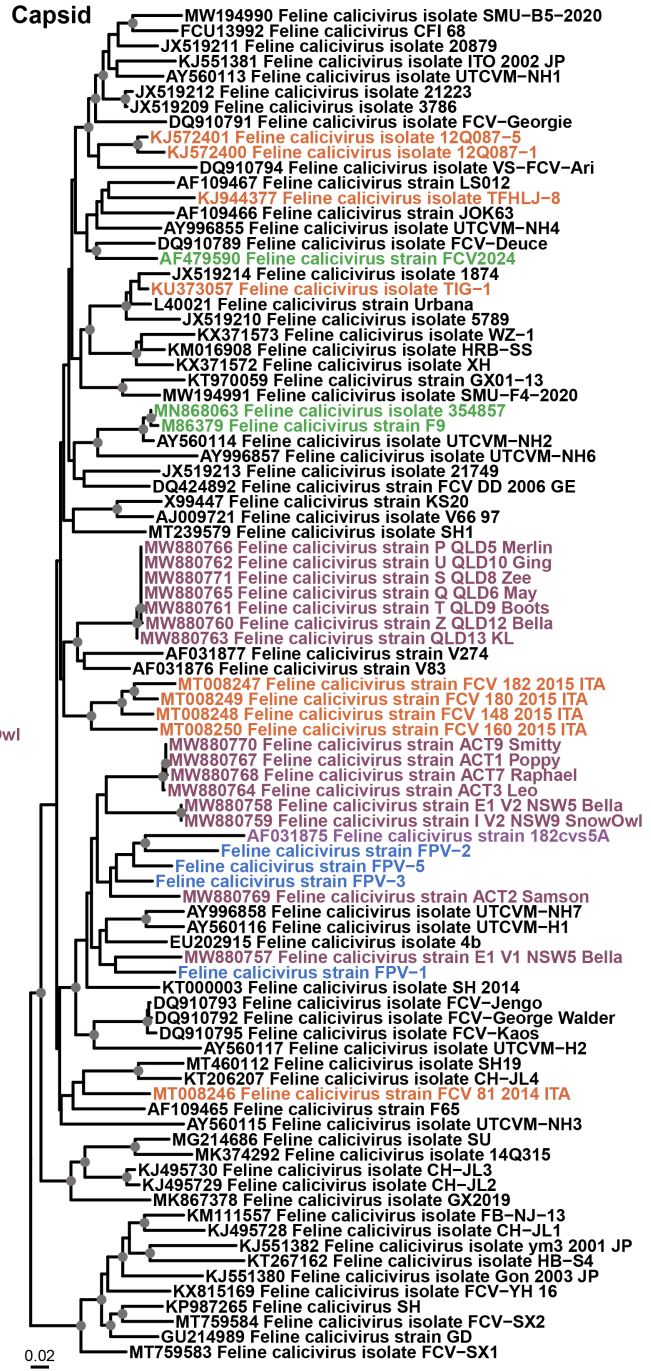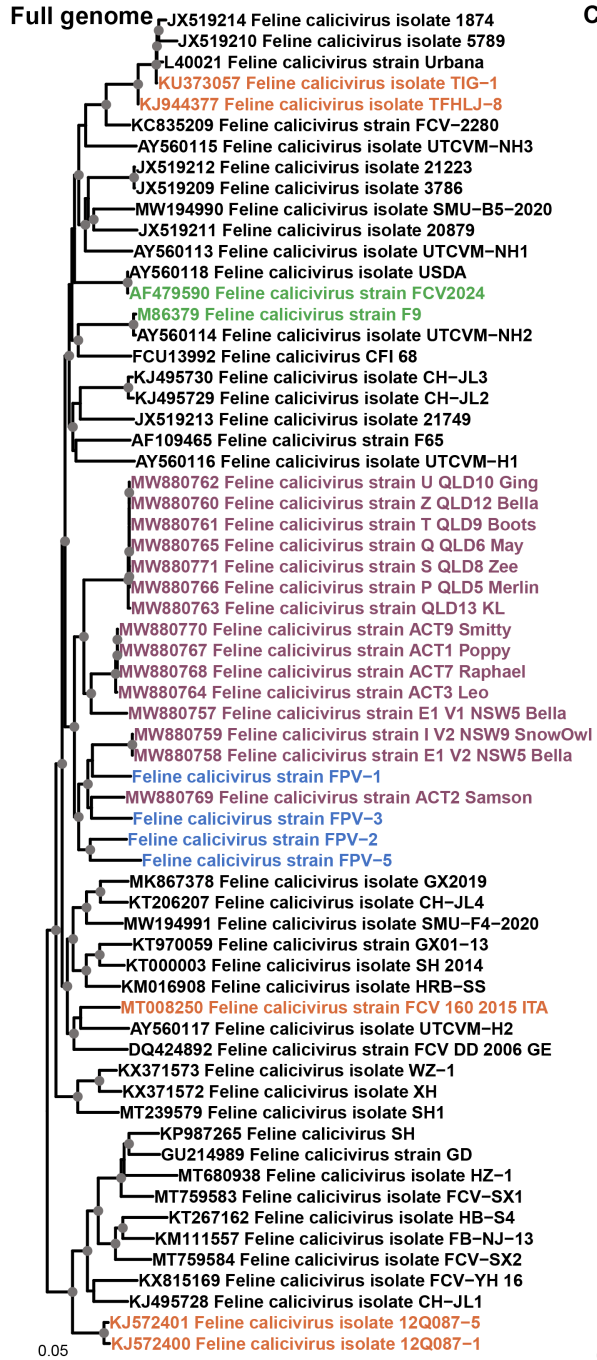
4.4.6: *Picornaviridae*

Feline kobuvirus belongs to the species Aichivirus A and was first identified in cats with diarrhoea in South Korea. Other studies have reported an association between feline kobuvirus and diarrhoea in cats (Lu et al., 2018, Niu et al., 2019). Notably, we only detected feline kobuvirus contigs in FPV-cases in 9 out of 23 libraries (39.1%; $p < .0001$; Figure 4.4.1.2). Seven of the nine kobuvirus-infected cats were kittens (6–9 weeks), two were adults (1–2 years) and four were known to have had diarrhoea. In addition, the FPV-cases from which feline kobuvirus were detected included FPV-cases from the two shelters where healthy controls were sampled, from two other shelters and owned cats (Table 4.8.1). The feline kobuvirus sequences in this study formed a clade in both the full genome and VP1 phylogenies, although feline kobuvirus sequence FPV-9 was on a different branch to the other sequences in this clade in both phylogenies (Figure 4.4.6).
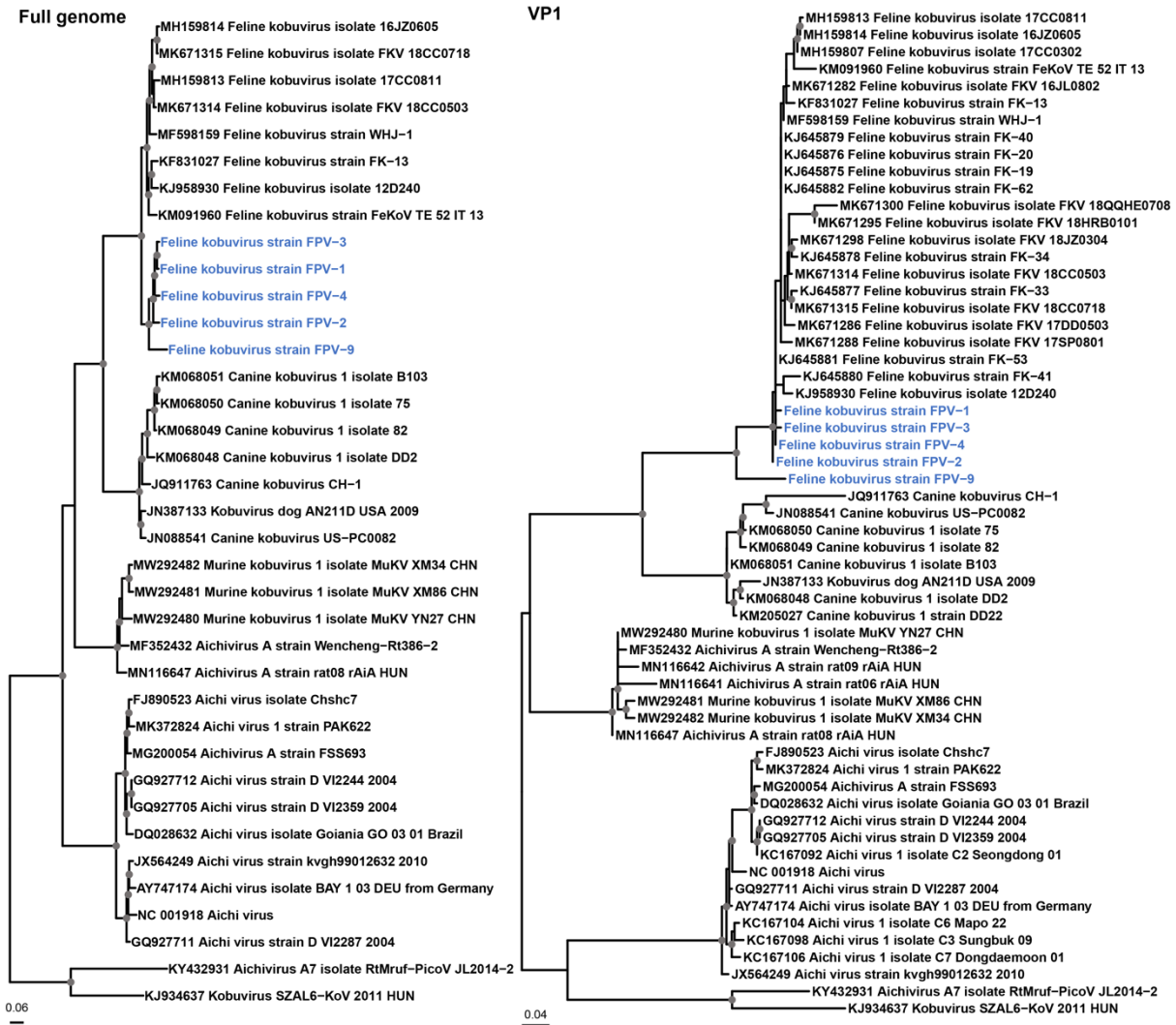
Figure 4.4.6: Phylogenetic analysis of the feline kobuvirus sequences identified FPV-cases and healthy controls. The full genome nucleotide alignment (left) and GTR+F+R4 nucleotide substitution model and VP1 amino acid alignment (right) and JTT+G4 amino acid substitution model. The feline kobuvirus sequences from this study are presented in blue. The scale bar represents the number of nucleotide and amino acid substitutions per site. The tree was midpoint rooted for clarity only.

We also identified Felipivirus A contigs in 0/23 FPV-case libraries and 2 out of 36 healthy controls (p = .5161, Figure 4.4.1.2). One healthy control library (cat #AWL8) contained a complete genome with 85.6% nucleotide and 96.1% amino acid similarity to feline picornavirus strain 073F in the complete polyprotein. Comparison of the 3D protein identified in both libraries exhibited 96.1% amino acid similarity to feline picornavirus strain 127F. The read abundance in the metatranscriptome libraries was 82 and 57 RPM and in the metagenome libraries 42,971 and 6,436 RPM for cats #AWL8 and #AWL9, respectively.

4.4.7: *Anelloviridae*

Anelloviruses are small single stranded circular DNA viruses in the *Anelloviridae* family. We observed diverse anellovirus contigs in 65.2% (15 out of 23) FPV-case and 83.3% (32 out of 36) healthy control cats (p = .1289). Contigs were relatively divergent and shared ~30–90% amino acid sequence identity. In total > 700 anellovirus contigs were detected, of which more than 400 exhibited < 50% amino acid identity to the closest virus protein hit on NCBI. Therefore, read abundance for *Anelloviridae* was not calculated, and because these sequences are so divergent, we did not perform a phylogenetic analysis.

4.4.8: *Papillomavirdae* and *Polyomaviridae*

Papillomavirus contigs were detected in 3 out of 23 (13%) FPV-cases and in 0 out of 36 the healthy controls (p = .0545; Figure 4.4.1.2). The papillomavirus contigs covered sections of the E1, E2, E6, E7, L1 and L2 genes of felis catus papillomavirus 3 and felis catus papillomavirus 4. In 0/23 FPV-cases and 4/36 (11%) healthy control cat libraries, polyomavirus contigs were detected (p = .1489). Two healthy control cats had complete polyomavirus genomes with high sequence similarity (93% nucleotide identity) to cat associated lyon-IARC polyomavirus, isolated from a cat with diarrhoea.

4.4.9: *Picobirnaviridae*

We observed a large diversity of picobirnaviruses in the faecal samples of 11/23 (47.8%) FPV-cases and 5/36 (13.8%) healthy control libraries (p = 0.0067). The complete genome sequence of both segment 1 and segment 2 was detected in one FPV-case library and four healthy control libraries.

4.5: Discussion

4.5.1: The virome of FPV-cases

We characterized the enteric eukaryotic virome of 23 FPV-cases and 36 healthy control cats using metatranscriptomic and viral particle enrichment metagenomic approaches. Metagenomic sequencing revealed a large abundance of viruses in families *Astroviridae, Parvoviridae, Coronaviridae, Caliciviridae, Picornaviridae, Anelloviridae, Polyomaviridae* and *Papillomavirdae*.

Despite the relatively small sample size, several viruses were significantly more likely to be detected in FPV-cases compared with healthy controls including feline kobuvirus, feline astroviruses, Feline calicivirus, feline bocaparvovirus 2 and feline bocaparvovirus 3. Indeed, it is notable that feline kobuvirus was only detected in FPV-cases (Figure 4.4.1.2) and the prevalence of detection (39.1%) is the highest reported to date (Chung et al., 2013, Di Martino et al., 2015, Lu et al., 2018).

In previous reports, co-infections of FPV, feline coronavirus and/or feline bocavirus were common in cats naturally infected with feline kobuvirus (Chung et al., 2013, Di Martino et al., 2015, Lu et al., 2018, Niu et al., 2019). However, in those investigations targeted conventional PCR was used to screen for a few common enteric viruses only. The use of unbiased sequencing techniques, as performed here, demonstrates that other enteric viruses including feline astroviruses, feline bocaparvovirus 2 and feline bocaparvovirus 3, as well as Feline calicivirus are also common co-infections (Figure 4.4.1.2).

The feline kobuvirus sequences detected here are the first in Australia. Their detection in sick cats from four shelters as well as owned cats, suggests active circulation among Australian cats and highlights the importance of screening for this virus in Australian cats with gastroenteritis of unknown cause. Similarly, here we documented the first Australian sequences of Felipivirus A.

Astroviruses are commonly associated with acute gastroenteritis in humans (Vu et al., 2017, Walter et al., 2001). Feline astrovirus infections have been identified in both healthy and sick cats (Van Brussel et al., 2020, Zhang et al., 2019, Zhang et al., 2014), although experimental infection of specific-pathogen kittens with feline astrovirus induces acute enteritis and viral shedding (Harbour et al., 1987). Here, although astrovirus shedding was detected in healthy controls, the prevalence of astrovirus in FPV-cases was significantly higher. Recently, feline astrovirus infection was associated with acute gastroenteritis in shelter-housed cats, where 91% of affected cats and 56% of healthy cats were found to be shedding feline astrovirus (Li et al., 2021).

We detected Feline calicivirus at a significantly higher rate in FPV-cases than in healthy cats. Although primarily a feline respiratory pathogen, evidence is mounting for an aetiological role in naturally occurring viral gastroenteritis (Castro et al., 2015, Di Martino et al., 2020). Experimental infection of cats with Feline calicivirus causes diarrhoea (Povey and Hale, 1974) and enteric strains of Feline calicivirus are resistant to low pH, trypsin and bile salts

(Di Martino et al., 2020). In a previous study, *Feline calicivirus* was not detected in healthy cat faeces but was found in 25.9% of diarrhoeic faeces and co-infections with FPV or feline coronavirus were common (Di Martino et al., 2020). In the cats shedding Feline calicivirus here, enteric co-infections, especially with feline astroviruses were common in both FPV-cases and healthy control cats (Figure 4.4.1.2).

There are conflicting reports on the prevalence of detection of bocaparvoviruses in cats with enteritis. These viruses have been detected in the faeces of cats with and without diarrhoea and in the oropharynx of healthy cats (Abayli and Can-Sahna, 2021, Li et al., 2020, Yi et al., 2018). In our study, feline bocaparvovirus 2 and feline bocaparvovirus 3 were both detected at a significantly higher prevalence in the faeces of FPV-cases compared to healthy controls. Although, evidence for an association between feline bocavirus infection and gastroenteritis in cats is accumulating, we found no significant difference in the prevalence of feline bocavirus in FPV-cases and healthy control cats. One study reported a prevalence of 24.8% in 105 cats with diarrhoea compared to 9.8% in 92 healthy cats (Yi et al., 2018). Two other reports concluded there was an association between feline bocavirus infection and severe gastroenteritis in cats, although sample numbers were small and co-infections with other pathogenic enteric viruses including FPV were common (Liu et al., 2018, Piewbang et al., 2019).

4.5.2: The virome of healthy cats

Excluding anelloviruses, read counts for feline coronavirus, Mamastrovirus 2 and Carnivore bocaparvovirus *3* were high in the healthy control cats (Table 4.4.2.2). The finding of high feline coronavirus read counts in this cohort is not surprising since this virus is endemic in shelters where the housing of multiple cats in close proximity favours virus transmission and one or more chronically infected "super-shedders" maintain cycles of infection and re-infection, since immunity is short-lived (Addie et al., 2000, Cave et al., 2004). Mamastrovirus 2 was the next most abundant virus detected in shelter-housed cats in this study, corroborating the findings of others that infection rates of astroviruses are high among clinically healthy shelter cats (Zhang et al., 2014).

We observed FPV contigs in core-vaccinated healthy control cats. Notably, 16 out of 28 healthy control cats that contained the VP2 region of the genome displayed the amino acid leucine at position 562 that is present in the FPV attenuated vaccine virus in the Feligen (Virbac, France) vaccine and in other vaccine strains Felocell (Zoetis, USA) and Purevax

(Boehringer Ingelheim, Germany). Notably, this amino acid was missing from all field strains in the 23 FPV cats in this study. FPV read counts in the cases were markedly higher than FPV vaccine virus read counts in the healthy controls, consistent with active infection. On average, FPV vaccine read counts in healthy controls were 3–6 orders of magnitude lower than the average read count for FPV-cases. Furthermore, our read abundance data suggests that the FPV vaccine virus can be shed in faeces up to four weeks after vaccination. Previous studies have demonstrated vaccine virus shedding up to 28 days after vaccination with a live modified FPV vaccine (Bergmann et al., 2019, Jacobson et al., 2022). FPV vaccine virus was detected in one control cat (#CPS35) several months after vaccination in the metagenomic library but not the metatranscriptomic library (Table 4.8.4). It is possible that the read count for this healthy control cat is a result of index-hopping during sequencing and not active shedding since a preliminary faecal PCR test was negative for FPV DNA.

Feline chaphamaparvovirus was recently discovered in the faeces of shelter-housed cats with diarrhoea (Li et al., 2020). Here, feline chaphamaparvovirus sequences were only detected in healthy control cats from both shelters sampled. Similar to other studies, co-infections with other enteric viruses were commonplace (Di Profio et al., 2021, Li et al., 2020). While feline chaphamaparvovirus has been detected in faecal or oropharyngeal samples from healthy cats elsewhere (Abayli and Can-Sahna, 2021, Di Profio et al., 2021), there is some evidence that feline chaphamaparvovirus may have pathogenic potential as a co-pathogen rather than as a single agent. Indeed, one study detected feline chaphamaparvovirus in 14/38 (36.8%) sick cats with acute gastroenteritis and 1/51 (2%) controls and all but one of the positive sick cats were co-infected with FPV, feline kobuvirus and/or feline norovirus (Di Profio et al., 2021).

4.5.3: The virome of healthy and diseased cats

We found no significant difference in the prevalence of feline norovirus between sick and healthy cats. In humans, norovirus infections by genogroups GI, GII, GIV and GVIII result in gastroenteritis in 50% of cases, whereas nearly all feline norovirus infections have been detected in cats with diarrhoea and belong to genogroups GIV and GVI (Di Martino et al., 2019, Patel et al., 2008).

Anelloviruses are the most abundant member (~70%) of the human gut eukaryotic virome, which includes over 700 viruses from 23 families, and are considered commensals with no known disease associations (Gregory et al., 2020, McElvania TeKippe et al., 2012, Ng et al., 2009, Zhang et al., 2016). Until now, feline anellovirus reads have been only identified in

sick animals (Jarošová et al., 2015, Li et al., 2020, Zhang et al., 2014). Herein, we demonstrate that diverse anelloviruses are abundant in the gut of healthy cats. Further investigations are required to characterize these viruses and to confirm their role in the feline gut virome.

4.5.4: Methodological observation

When comparing the metatranscriptomic and virion enrichment library read counts it is evident that the metagenomic libraries produced higher read depth than the metatranscriptomic libraries (Figure 4.8.3). Therefore, conducting both a metatranscriptomic and virion enrichment sequencing approach produces a broader perspective on virome diversity.

4.6: Conclusions

We revealed differences in viral abundance and diversity between FPV-cases and healthy controls, with infections with feline kobuvirus, feline astroviruses, Feline calicivirus, feline bocaparvovirus 2 and feline bocaparvovirus 3 more common in FPV-cases. Despite these differences in virome composition, whether the clinical outcome of FPV-infection is influenced by the presence of particular co-pathogen infections, or by the combined contribution of multiple co-infecting viruses, remains to be determined.

4.7: References

Abayli, H., Can-Sahna, K. 2021. First detection of feline bocaparvovirus 2 and feline chaphamaparvovirus in healthy cats in Turkey. *Veterinary Research Communications,* 46(1):127-136.

Addie, D.D., Dennis, J.M., Toth, S., Callanan, J.J., Reid, S., Jarrett, O. 2000. Long-term impact on a closed household of pet cats of natural infection with feline coronavirus, feline leukaemia virus and feline immunodeficiency virus. *Veterinary Record*, 146(15):419-24.

Barrs, V.R. 2019. Feline Panleukopenia: A Re-emergent Disease. *Veterinary Clinics of North America: Small Animal Practice,* 49(4):651-670.

Bergmann, M., Schwertler, S., Speck, S., Truyen, U., Reese, S., Hartmann, K. 2019. Faecal shedding of parvovirus deoxyribonucleic acid following modified live feline panleucopenia virus vaccination in healthy cats. *Veterinary Record*, 185(3):83.

Castro, T.X., Cubel Garcia Rde, C., Fumian, T.M., Costa, E.M., Mello, R., White, P.A., Leite, J.P. 2015. Detection and molecular characterization of caliciviruses (vesivirus and norovirus) in an outbreak of acute diarrhea in kittens from Brazil. *The Veterinary Journal*, 206(1):115-7.

Cave, T.A., Golder, M.C., Simpson, J., Addie, D.D. 2004. Risk factors for feline coronavirus seropositivity in cats relinquished to a UK rescue charity. *Journal of Feline Medicine and Surgery*, 6(2):53-8.

Chang, H.W., Egberink, H.F., Halpin, R., Spiro, D.J., Rottier, P.J. 2012. Spike protein fusion peptide and feline coronavirus virulence. *Emerging Infectious Diseases*, 18(7):1089-95.

Chong, R., Shi, M., Grueber, C.E., Holmes, E.C., Hogg, C.J., Belov, K., Barrs, V.R. 2019. Fecal Viral Diversity of Captive and Wild Tasmanian Devils Characterized Using Virion-Enriched Metagenomics and Metatranscriptomics. *Journal of Virology*, 93(11):e00205.

Chung, J.Y., Kim, S.H., Kim, Y.H., Lee, M.H., Lee, K.K., Oem, J.K. 2013. Detection and genetic characterization of feline kobuviruses. *Virus Genes*, 47(3):559-62.

Clausen, P., Aarestrup, F.M., Lund, O. 2018. Rapid and precise alignment of raw reads against redundant databases with KMA. *BMC Bioinformatics*, 19(1):307.

Conceicao-Neto, N., Zeller, M., Lefrere, H., De Bruyn, P., Beller, L., Deboutte, W., Yinda, C.K., Lavigne, R., Maes, P., Van Ranst, M., Heylen, E., Matthijnssens, J. 2015. Modular approach to customise sample preparation procedures for viral metagenomics: a reproducible protocol for virome analysis. *Scientific Reports*, 5:16532.

Di Martino, B., Di Profio, F., Melegari, I., Marsilio, F. 2019. Feline Virome-A Review of Novel Enteric Viruses Detected in Cats. *Viruses*, 11(10):908.

Di Martino, B., Di Profio, F., Melegari, I., Marsilio, F., Martella, V. 2015. Detection of feline kobuviruses in diarrhoeic cats, Italy. *Veterinary Microbiology*, 176(1-2):186-9.

Di Martino, B., Lanave, G., Di Profio, F., Melegari, I., Marsilio, F., Camero, M., Catella, C., Capozza, P., Bányai, K., Barrs, V.R., Buonavoglia, C., Martella, V. 2020. Identification of feline calicivirus in cats with enteritis. *Transboundary and Emerging Diseases*, 67(6):2579-2588.

Di Profio, F., Sarchese, V., Palombieri, A., Fruci, P., Massirio, I., Martella, V., Fulvio, M., Di Martino, B. 2021. Feline chaphamaparvovirus in cats with enteritis and upper respiratory tract disease. *Transboundary and Emerging Diseases*, 69(2):660-668.

Duarte, M.A., Silva, J.M.F., Brito, C.R., Teixeira, D.S., Melo, F.L., Ribeiro, B.M., Nagata, T., Campos, F.S. 2019. Faecal Virome Analysis of Wild Animals from Brazil. *Viruses*, 11(9):803.

Gaskell, R.M., Radford, A.D., Dawson, S. 2004. Feline Infectious Respiratory Disease. Oxford, UK: Blackwell Publishing Ltd.

Gregory, A.C., Zablocki, O., Zayed, A.A., Howell, A., Bolduc, B., Sullivan, M.B. 2020. The Gut Virome Database Reveals Age-Dependent Patterns of Virome Diversity in the Human Gut. *Cell Host Microbe*, 28(5):724-740.

Harbour, D.A., Ashley, C.R., Williams, P.D., Gruffydd-Jones, T.J. 1987. Natural and experimental astrovirus infection of cats. *Veterinary Record*, 120(23):555-7.

Hoang, D.T., Chernomor, O., von Haeseler, A., Minh, B.Q., Vinh, L.S. 2018. UFBoot2: Improving the Ultrafast Bootstrap Approximation. *Molecular Biology and Evolution*, 35(2):518-522.

Jacobson, L.S., Janke, K.J., Ha, K., Giacinti, J.A., Weese, J.S. 2022. Feline panleukopenia virus DNA shedding following modified live virus vaccination in a shelter setting. *The Veterinary Journal*, 279:105783.

Jarošová, V., Hrazdilová, K., Filipejová, Z., Schánilec, P., Celer, V. 2015. Whole genome sequencing and phylogenetic analysis of feline anelloviruses. *Infection, Genetics and Evolution*, 32:130-4.

Ji, J., Hu, W., Liu, Q., Zuo, K., Zhi, G., Xu, X., Kan, Y., Yao, L., Xie, Q. 2020. Genetic Analysis of Cachavirus-Related Parvoviruses Detected in Pet Cats: The First Report From China. *Frontiers in Veterinary Science*, 7:580836.

Kalyaanamoorthy, S., Minh, B.Q., Wong, T.K.F., von Haeseler, A., Jermiin, L.S. 2017. ModelFinder: fast model selection for accurate phylogenetic estimates. *Nature Methods*, 14(6):587-589.

Katoh, K., Standley, D.M. 2013. MAFFT multiple sequence alignment software version 7: improvements in performance and usability. *Molecular Biology and Evolution*, 30(4):772-80.

Kim, H.R., Kwon, Y.K., Jang, I., Bae, Y.C. 2020. Viral metagenomic analysis of chickens with runting-stunting syndrome in the Republic of Korea. *Virology Journal*, 17(1):53.

Krishnamurthy, S.R., Wang, D. 2018. Extensive conservation of prokaryotic ribosomal binding sites in known and novel picobirnaviruses. *Virology*, 516:108-114.

Lau, S.K.P., Woo, P.C.Y., Yeung, H.C., Teng, J.L.L., Wu, Y., Bai, R., Fan, R.Y.Y., Chan, K.H., Yuen, K.Y. 2012. Identification and characterization of bocaviruses in cats and dogs reveals a novel feline bocavirus and a novel genetic group of canine bocavirus. *Journal of General Virology*, 93(Pt 7):1573-1582.

Li, Y., Gordon, E., Idle, A., Altan, E., Seguin, M.A., Estrada, M., Deng, X., Delwart, E. 2020. Virome of a Feline Outbreak of Diarrhea and Vomiting Includes Bocaviruses and a Novel Chapparvovirus. *Viruses*, 12(5):506.

Li, Y., Gordon, E., Idle, A., Hui, A., Chan, R., Seguin, M.A., Delwart, E. 2021. Astrovirus Outbreak in an Animal Shelter Associated With Feline Vomiting. *Frontiers in Veterinary Science*, 8:628082.

Liu, C., Liu, F., Li, Z., Qu, L., Liu, D. 2018. First report of feline bocavirus associated with severe enteritis of cat in Northeast China, 2015. *Journal of Veterinary Medical Science*, 80(4):731-735.

Lu, G., Zhang, X., Luo, J., Sun, Y., Xu, H., Huang, J., Ou, J., Li, S. 2018. First report and genetic characterization of feline kobuvirus in diarrhoeic cats in China. *Transboundary and Emerging Diseases*, 65(5):1357-1363.

Makimaa, H., Ingle, H., Baldridge, M.T. 2020. Enteric Viral Co-Infections: Pathogenesis and Perspective. *Viruses*, 12(8):904.

Marcelino, V.R., Clausen, P., Buchmann, J.P., Wille, M., Iredell, J.R., Meyer, W., Lund, O., Sorrell, T.C., Holmes, E.C. 2020. CCMetagen: comprehensive and accurate identification of eukaryotes and prokaryotes in metagenomic data. *Genome Biology*, 21(1):103.

McElvania TeKippe, E., Wylie, K.M., Deych, E., Sodergren, E., Weinstock, G., Storch, G.A. 2012. Increased Prevalence of Anellovirus in Pediatric Patients with Fever. *PLOS ONE*, 7(11):e50937.

Ng, T.F., Mesquita, J.R., Nascimento, M.S., Kondov, N.O., Wong, W., Reuter, G., Knowles, N.J., Vega, E., Esona, M.D., Deng, X., Vinje, J., Delwart, E. 2014. Feline fecal virome reveals novel and prevalent enteric viruses. *Veterinary Microbiology*, 171(1-2):102-11.

Ng, T.F.F., Suedmeyer, W.K., Wheeler, E., Gulland, F., Breitbart, M. 2009. Novel anellovirus discovered from a mortality event of captive California sea lions. *Journal of General Virology*, 90(Pt 5):1256-1261.

Nguyen, L.T., Schmidt, H.A., von Haeseler, A., Minh, B.Q. 2015. IQ-TREE: a fast and effective stochastic algorithm for estimating maximum-likelihood phylogenies. *Molecular Biology and Evolution*, 32(1):268-74.

Niu, T.J., Yi, S.S., Wang, X., Wang, L.H., Guo, B.Y., Zhao, L.Y., Zhang, S., Dong, H., Wang, K., Hu, X.G. 2019. Detection and genetic characterization of kobuvirus in

cats: The first molecular evidence from Northeast China. *Infection, Genetics and Evolution,* 68:58-67.

Palombieri, A., Di Profio, F., Lanave, G., Capozza, P., Marsilio, F., Martella, V., Di Martino, B. 2020. Molecular detection and characterization of Carnivore chaphamaparvovirus 1 in dogs. *Veterinary Microbiology*, 251:108878.

Patel, M.M., Widdowson, M.A., Glass, R.I., Akazawa, K., Vinjé, J., Parashar, U.D. 2008. Systematic literature review of role of noroviruses in sporadic gastroenteritis. *Emerging Infectious Diseases*, 14(8):1224-31.

Pérez, R., Calleros, L., Marandino, A., Sarute, N., Iraola, G., Grecco, S., Blanc, H., Vignuzzi, M., Isakov, O., Shomron, N., Carrau, L., Hernández, M., Francia, L., Sosa, K., Tomás, G., Panzera, Y. 2014. Phylogenetic and genome-wide deep-sequencing analyses of canine parvovirus reveal co-infection with field variants and emergence of a recent recombinant strain. *PLoS One*, 9(11):e111779.

Piewbang, C., Kasantikul, T., Pringproa, K., Techangamsuwan, S. 2019. Feline bocavirus-1 associated with outbreaks of hemorrhagic enteritis in household cats: potential first evidence of a pathological role, viral tropism and natural genetic recombination. *Scientific Reports*, 9(1):16367.

Porter, A.F., Cobbin, J., Li, C.X., Eden, J.S., Holmes, E.C. 2021. Metagenomic Identification of Viral Sequences in Laboratory Reagents. *Viruses*, 13(11):2122.

Povey, R.C., Hale, C.J. 1974. Experimental infections with feline caliciviruses (picornaviruses) in specific-pathogen-free kittens. *Journal of Comparative Pathology*, 84(2)245-56.

Roediger, B., Lee, Q., Tikoo, S., Cobbin, J.C.A., Henderson, J.M., Jormakka, M., O'Rourke, M.B., Padula, M.P., Pinello, N., Henry, M., Wynne, M., Santagostino, S.F., Brayton, C.F., Rasmussen, L., Lisowski, L., Tay, S.S., Harris, D.C., Bertram, J.F., Dowling, J.P., Bertolino, P., Lai, J.H., Wu, W., Bachovchin, W.W., Wong, J.J., Gorrell, M.D., Shaban, B., Holmes, E.C., Jolly, C.J., Monette, S., Weninger, W. 2018. An Atypical Parvovirus Drives Chronic Tubulointerstitial Nephropathy and Kidney Fibrosis. *Cell*, 175(2):530-543.e24.

Simsek, C., Bloemen, M., Jansen, D., Beller, L., Descheemaeker, P., Reynders, M., Van Ranst, M., Matthijnssens, J. 2021. High Prevalence of Coinfecting Enteropathogens in Suspected Rotavirus Vaccine Breakthrough Cases. *Journal of Clinical Microbiology*, 59(12):e0123621.

Souza, W.M., Romeiro, M.F., Fumagalli, M.J., Modha, S., de Araujo, J., Queiroz, L.H., Durigon, E.L., Figueiredo, L.T.M., Murcia, P.R., Gifford, R.J. 2017. Chapparvoviruses occur in at least three vertebrate classes and have a broad biogeographic distribution. *Journal of General Virology*, 98(2):225-229.

Van Brussel, K., Carrai, M., Lin, C., Kelman, M., Setyo, L., Aberdein, D., Brailey, J., Lawler, M., Maher, S., Plaganyi, I., Lewis, E., Hawkswell, A., Allison, A.B., Meers, J., Martella, V., Beatty, J.A., Holmes, E.C., Decaro, N., Barrs, V.R. 2019. Distinct Lineages of Feline Parvovirus Associated with Epizootic Outbreaks in Australia, New Zealand and the United Arab Emirates. *Viruses*, 11(12):1155.

Van Brussel, K., Wang, X., Shi, M., Carrai, M., Li, J., Martella, V., Beatty, J.A., Holmes, E.C., Barrs, V.R. 2020. Identification of Novel Astroviruses in the Gastrointestinal Tract of Domestic Cats. *Viruses*, 12(11):1301.

Vu, D.L., Bosch, A., Pintó, R.M., Guix, S. 2017. Epidemiology of Classic and Novel Human Astrovirus: Gastroenteritis and Beyond. *Viruses*, 9(2):33.

Walter, J.E., Briggs, J., Guerrero, M.L., Matson, D.O., Pickering, L.K., Ruiz-Palacios, G., Berke, T., Mitchell, D.K. 2001. Molecular characterization of a novel recombinant strain of human astrovirus associated with gastroenteritis in children. *Archives of Virology*, 146(12):2357-67.

Yang, S., Liu, Z., Wang, Y., Li, W., Fu, X., Lin, Y., Shen, Q., Wang, X., Wang, H., Zhang, W. 2016. A novel rodent Chapparvovirus in feces of wild rats. *Virology Journal*, 13:133.

Yi, S., Niu, J., Wang, H., Dong, G., Zhao, Y., Dong, H., Guo, Y., Wang, K., Hu, G. 2018. Detection and genetic characterization of feline bocavirus in Northeast China. Virology Journal, 15(1):125.

Zhang, Q., Niu, J., Yi, S., Dong, G., Yu, D., Guo, Y., Huang, H., Hu, G. 2019. Development and application of a multiplex PCR method for the simultaneous detection and

differentiation of feline panleukopenia virus, feline bocavirus, and feline astrovirus. *Archives of Virology*, 164(11):2761-2768.

Zhang, W., Li, L., Deng, X., Kapusinszky, B., Pesavento, P.A., Delwart, E. 2014. Faecal virome of cats in an animal shelter. *Journal of General Virology*, 95(Pt 11):2553-2564.

Zhang, W., Wang, H., Wang, Y., Liu, Z., Li, J., Guo, L., Yang, S., Shen, Q., Zhao, X., Cui, L., Hua, X. 2016. Identification and genomic characterization of a novel species of feline anellovirus. *Virology Journal*, 13(1):146.

4.8: Supplementary data

Table 4.8.1: Feline panleukopenia case signalment and clinical signs at time of disease onset.

Cat ID#	Sex	Breed	Age	Disease presentation
FPV 132[1]	Male	Unknown	10 weeks	Signs of FPL – no specific information provided
FPV 134[*]	Female	DSH	2 years	Not eating, prolapsed anus
FPV 136[3]	Female	DSH	5 months	Underweight, depressed, hypothermic, haemorrhagic diarrhoea
FPV 139[3]	Female	DSH	2 – 6 months	Signs of FPL – no specific information provided
FPV 146[*]	Male	DSH	5 months	Signs of FPL, gastroenteritis
FPV 147[*]	Male	Unknown	6 months	Fever and flat
FPV 148[3]	Female	DSH	10 weeks	Signs of FPL – no specific information provided
FPV 150[3]	Female	DSH	6-8 weeks	Diarrhoea
FPV 151[3]	Unknown	DSH	6-8 weeks	Weight loss, diarrhoea, lethargy
FPV 157[3]	Female	DSH	9 weeks	Fever, diarrhoea, weight loss
FPV 159[3] †‡	Male	DSH	8 weeks	Diarrhoea
FPV 160[3] †	Unknown	DSH	11 weeks	Signs of FPL – no specific information provided
FPV 161[3*] †	Unknown	DSH	11 weeks	Signs of FPL – no specific information provided
FPV 163[1]	Female	DSH	1-2 years	Signs of FPL – no specific information provided
FPV 164[*]	Male	DSH	8 weeks	Signs of FPL, diarrhoea, weight loss
FPV 165[1]	Male	DSH	7 weeks	Signs of FPL – no specific information provided
FPV 166[1]	Male	DSH	8 weeks	Signs of FPL – no specific information provided

FPV 194[2]	Male	DSH	5 weeks	Signs of FPL, diarrhoea
FPV 195[2]	Male	DSH	6 weeks	Signs of FPL – no specific information provided
FPV 199[4]	Male	Unknown	1 year	Signs of FPL, diarrhoea, vomiting
FPV 200[4]	Male	Unknown	8 weeks	Signs of FPL, diarrhoea, vomiting
FPV 201[1]	Male	DSH	6 weeks	No information provided
FPV 202	Male	DMH	9 weeks	Diarrhoea and jaundice
†Metagenomic cDNA library missing due to failed library preparation				
‡ Metagenomic DNA library missing due to failed library preparation				
*owned cats				

[1] From the same shelter as healthy cats (Shelter 1 AWL, Sydney, NSW)

[2] From the same shelter as healthy cats (Shelter 2 CPS, Sydney, NSW)

[3] From a third shelter in Sydney, NSW

[4] From a fourth shelter in Sydney, NSW

Table 4.8.2: Healthy control cat signalment, vaccination, sampling and admission data.

Cat ID	Sex	Breed	Age	Vaccine type/timing prior to sampling	Faecal collection month	Date admitted to shelter
AWL2	Female	DSH	19 weeks	Feligen F3 91 days	Jun-18	Dec-17
AWL4	Female	DSH	5 months 1 week	Feligen F3 35 days	Jun-18	Feb-18
AWL5	Female	DMH	15 weeks	Feligen F3	Jun-18	May-18

				9 days		
AWL6	Female	DSH	15 weeks	Feligen F3 28 days	Jun-18	Apr-18
AWL8	Male	DMH	20 weeks	Feligen F3 9 days	Jun-18	May-18
AWL9	Female	DSH	20 weeks	Feligen F3 30 days	Jun-18	Mar-18
AWL14	Male	DSH	14 weeks	Feligen F3 21 days	Jun-18	Apr-18
AWL15	Male	DSH	15 weeks	Feligen F3 20 days	Jun-18	May-18
CPS25	Female	DSH	12 weeks	Feligen F3 9 days	May-18	Apr-18
CPS26	Male	DSH	12 weeks	Feligen F3 9 days	May-18	Apr-18
CPS27	Female	DSH	11 weeks	Feligen F3 7 days	May-18	Apr-18
CPS35	Female	Manx	1 year 6 months	Feligen F3 141 days	May-18	Nov-17
CPS36	Male	DSH	2 years	Feligen F3 11 days	May-18	Apr-18
CPS39	Female	DSH	10 weeks	Feligen F3 13 days	May-18	Apr-18

CPS40	Female	DSH	10 weeks	Feligen F3 27 days	May-18	Feb-18
CPS42	Female	DSH	10 weeks	Feligen F3 15 days	May-18	Feb-18
CPS44	Male	DSH	12 weeks	Feligen F3 15 days	May-18	Mar-18
CPS49	Male	DSH	5 months	Feligen F3 9 days	Jun-18	Jun-18
CPS53	Male	DSH	13 weeks	Feligen F3 2 days	Jun-18	May-18
CPS54	Male	DSH	10 weeks	Feligen F3 2 days	Jun-18	May-18
CPS57	Male	DSH	16 weeks	Feligen F3 8 days	Jul-18	May-18
CPS59	Male	DSH	15 weeks	Feligen F3 12 days	Jul-18	Jun-18
CPS63	Male	DSH	12 weeks	Feligen F3 7 days	Jul-18	Jun-18
CPS65	Female	DMH	6 months	Feligen F3 17 days	Aug-18	Jul-18
CPS66	Male	DSH	16 weeks	Feligen F3 9 days	Aug-18	May-18
CPS67	Female	DSH	12 weeks	Feligen F3	Aug-18	May-18

				8 days		
CPS68	Female	DSH	16 weeks	Feligen F3 9 days	Aug-18	May-18
CPS69	Male	DSH	17 weeks	Feligen F3 15 days	Aug-18	May-18
CPS70	Male	DMH	2 years 5 months	Feligen F3 13 days	Aug-18	Jun-18
CPS71	Male	DMH	3 years 5 months	Feligen F3 9 days	Aug-18	Jul-18
CPS72	Male	DSH	3 years	Feligen F3 16 days	Aug-18	Jul-18
CPS73	Male	DMH	12 years 5 months	Feligen F3 7 days	Aug-18	Jun-18
CPS74	Male	DSH	5 years	Feligen F3 9 days	Aug-18	Jul-18
CPS75	Male	DSH	10 weeks	Feligen F3 3 days	Oct-18	Sep-18
CPS78	Female	DSH	1 year	Fel-O-Vax F3 † 6 days	Oct-18	Sep-18
CPS79	Female	DSH	1 year	Feligen F3 17 days	Oct-18	Oct-18

† Inactivated vaccine

Table 4.8.3: Accession numbers for the sequences presented in this study.

Sequence name	Accession	Sequence name	Accession	Sequence name	Accession
Mamastrovirus 2 strain FPV-1	ON595824	Feline coronavirus strain FPV-4	ON595856	Feline bocaparvovirus 3 strain FPV-2	ON595886
Mamastrovirus 2 strain FPV-2	ON595825	Feline coronavirus strain FPV-5	ON595857	Feline bocaparvovirus 3 strain FPV-3	ON595887
Mamastrovirus 2 strain FPV-3	ON595826	Feline coronavirus strain FPV-6	ON595858	Feline bocaparvovirus 3 strain FPV-4	ON595888
Mamastrovirus 2 strain FPV-4	ON595827	Feline coronavirus strain FPV-7	ON595859	Feline bocaparvovirus 3 strain HC-1	ON595889
Mamastrovirus 2 strain FPV-5	ON595828	Feline coronavirus strain FPV-8	ON595860	Feline bocaparvovirus 2 strain FPV-1	ON595890
Mamastrovirus 2 strain FPV-6	ON595829	Feline coronavirus strain FPV-9	ON595861	Feline bocaparvovirus 2 strain FPV-2	ON595891
Mamastrovirus 2 strain FPV-8	ON595830	Feline coronavirus strain HC-1	ON595862	Feline bocaparvovirus 2 strain FPV-3	ON595892
Mamastrovirus 2 strain FPV-10	ON595831	Feline coronavirus strain HC-2	ON595863	Feline bocaparvovirus 2 strain HC-1	ON595893, ON595894

Mamastrovirus 2 strain FPV-11	ON595832	Feline coronavirus strain HC-3	ON595864	Feline bocavirus strain FPV-1	ON595895
Mamastrovirus 2 strain FPV-12	ON595833	Feline coronavirus strain HC-4	ON595865	Feline bocavirus strain FPV-2	ON595896
Mamastrovirus 2 strain FPV-13	ON595834	Feline coronavirus strain HC-5	ON595866	Feline bocavirus strain FPV-3	ON595897
Mamastrovirus 2 strain FPV-14	ON595835	Feline coronavirus strain HC-6	ON595867	Feline bocavirus strain FPV-4	ON595898
Mamastrovirus 2 strain FPV-15	ON595836	Feline coronavirus strain HC-7	ON595868	Feline bocavirus strain FPV-5	ON595899
Mamastrovirus 2 strain HC-1	ON595837	Feline coronavirus strain HC-8	ON595869	Feline bocavirus strain FPV-6	ON595900
Mamastrovirus 2 strain HC-2	ON595838, ON595839, ON595840	Feline coronavirus strain HC-9	ON595870	Feline bocavirus strain FPV-7	ON595901
Mamastrovirus 2 strain HC-3	ON595841	Feline coronavirus strain HC-10	ON595871	Feline bocavirus strain FPV-8	ON595902, ON595903
Feline calicivirus strain FPV-1	ON595842	Feline coronavirus strain HC-12	ON595872	Feline bocavirus strain FPV-9	ON595904

Feline calicivirus strain FPV-2	ON595843	Feline coronavirus strain HC-13	ON595873	Feline bocavirus strain FPV-10	ON595905
Feline calicivirus strain FPV-3	ON595844	Feline coronavirus strain HC-14	ON595874	Feline bocavirus strain FPV-11	ON595906
Feline calicivirus strain FPV-5	ON595845	Feline coronavirus strain HC-15	ON595875	Feline bocavirus strain HC-1	ON595907
Norovirus GIV isolate cat FPV-1	ON595846	Feline coronavirus strain HC-16	ON595876	Feline bocavirus strain HC-2	ON595908, ON595909
Norovirus GIV isolate cat HC-1	ON595847	Feline coronavirus strain HC-19	ON595877	Feline bocavirus strain HC-3	ON595910
Feline kobuvirus isolate FPV-1	ON595848	Feline coronavirus strain HC-20	ON595878	Feline bocavirus strain HC-4	ON595911
Feline kobuvirus isolate FPV-2	ON595849	Feline coronavirus strain HC-21	ON595879	Feline bocavirus strain HC-5	ON595912
Feline kobuvirus isolate FPV-3	ON595850	Feline coronavirus strain HC-22	ON595880	Feline bocavirus strain HC-7	ON595913
Feline kobuvirus isolate FPV-4	ON595851	Feline coronavirus strain HC-23	ON595881	Feline bocavirus strain HC-8	ON595914

Feline kobuvirus isolate FPV-9	ON595852	Feline coronavirus strain HC-24	ON595882	Feline bocavirus strain HC-12	ON595915, ON595916
Feline coronavirus strain FPV-1	ON595853	Feline coronavirus strain HC-25	ON595883	Feline bocavirus strain HC-13	ON595917, ON595918
Feline coronavirus strain FPV-2	ON595854	Feline coronavirus strain HC-26	ON595884	Feline bocavirus strain HC-15	ON595919, ON595920
Feline coronavirus strain FPV-3	ON595855	Feline bocaparvovirus 3 strain FPV-1	ON595885	Feline picornavirus strain HC-1	ON605651

Table 4.8.4: FPV read abundance data and vaccination information for the healthy control cat population.

Cat ID	Metagenome (DNA)		Metatranscriptome (RNA)		Days since FPV vaccination
	Abundance	RPM	Abundance	RPM	
AWL2	0	0	0	0	91
AWL4 †	126	3.2	469	42.7	35
AWL5	9	0	3	0	9
AWL6 †	11	0	1	0	28
AWL8	25	0	0	0	9
AWL9	13	0	0	0	30
AWL14	4	0	0	0	21
AWL15	33	1	0	0	20

CPS25	6,308,172	136,759	261,522	6,014	9
CPS26	11,218	249	107	4	9
CPS27	260	8	0	0	7
CPS35	1178	21	0	0	141
CPS36	14020	444	415	11	11
CPS39	1371	35	0	0	13
CPS40	1931	13.5	0	0	27
CPS42	9	0	0	0	15
CPS44	142,846	3,252	466	14	15
CPS49	538,986	13,012	21,277	541	9
CPS53	1,665	310	4	0	2
CPS54	654	49	0	0	2
CPS57	3,327	77	4	0	8
CPS59	858	99	0	0	12
CPS63	5,131	279	6	0	7
CPS65	57	0	0	0	17
CPS66	21	0	0	0	9
CPS67	5	0	0	0	8
CPS68	26	2	0	0	9
CPS69	93	2	0	0	15
CPS70	56	2	34	1	13
CPS71	4	0	0	0	9
CPS72	3,903	233	315	22	16

CPS73	2,069	335	0	0	7
CPS74 †	68	0	0	0	9
CPS75	72	2	0	0	3
CPS78 ‡	104	1	0	0	6
CPS79	141	16	5	0	17
† Healthy control cats with genomes identical to a field strain of FPV					
‡ Inactivated vaccine administered					
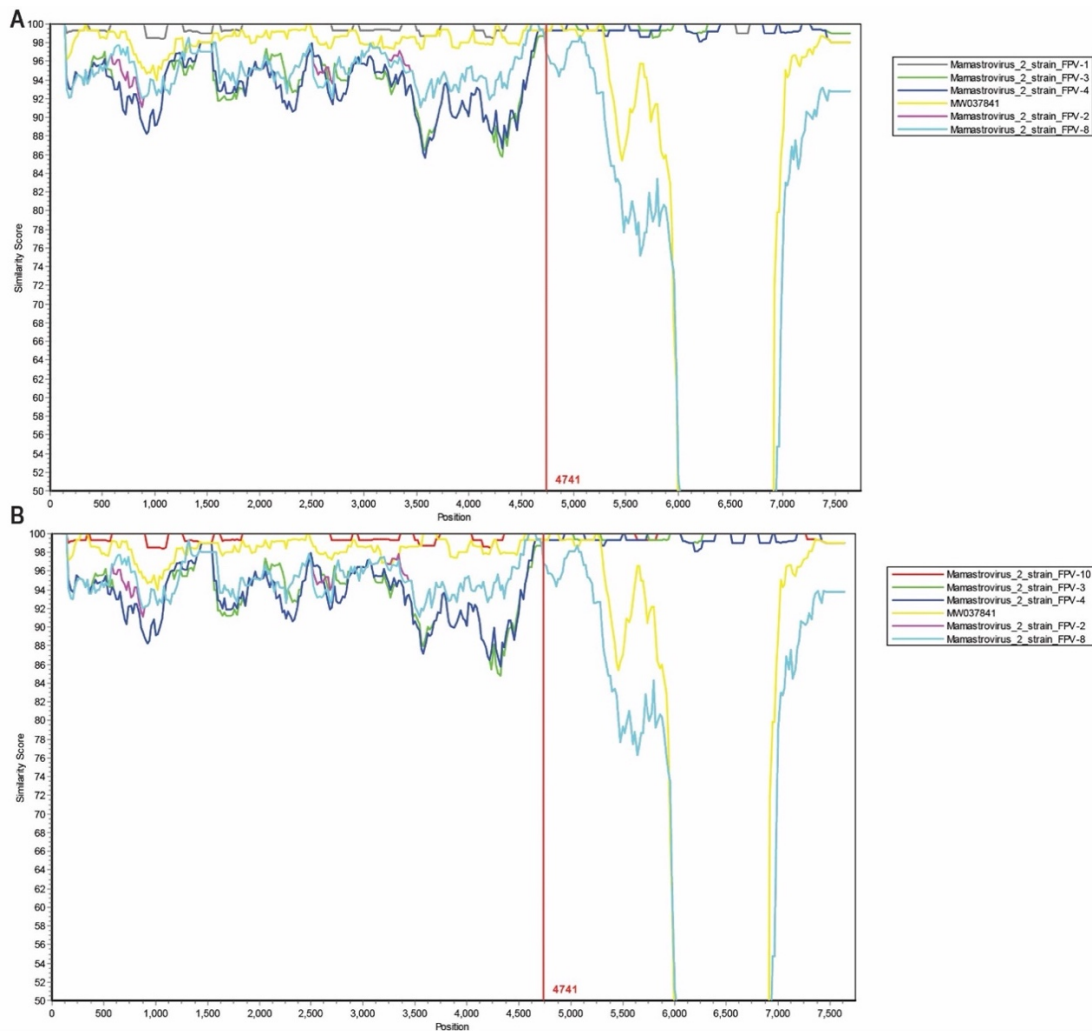
Figure 4.8.1: Simplot analysis using A Mamastrovirus 2 strain FPV-10 and Mamastrovirus 2 strain FPV-2 identified in this study as the query sequence.
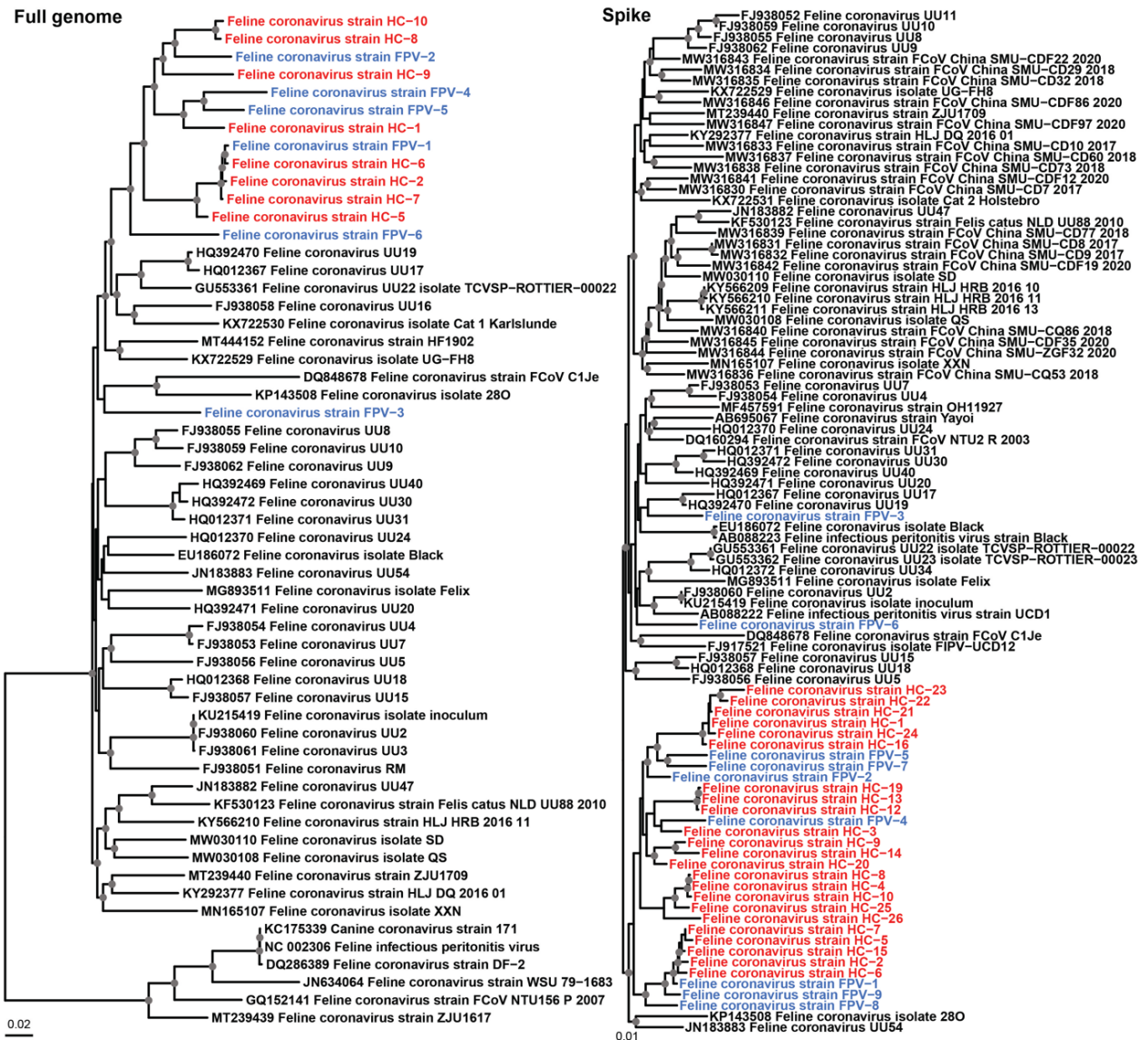
Figure 4.8.2: Phylogenetic analysis of feline coronavirus sequences identified in this study using the full genome nucleotide alignment and the GTR+F+R4 nucleotide substitution model and the spike protein amino acid alignment and FLU+F+R10 amino acid substitution model.

Figure 4.8.3: Read abundance data for the metatranscriptomic (RNA) and metagenomic (cDNA and DNA) libraries.

Chapter five: Zoonotic Disease and Virome Diversity in Bats

Kate Van Brussel[1] and Edward C. Holmes[1]

[1]Sydney Institute for Infectious Diseases, School of Life & Environmental Sciences and School of Medical Sciences, The University of Sydney, NSW, 2006, Australia.

5.1: Abstract

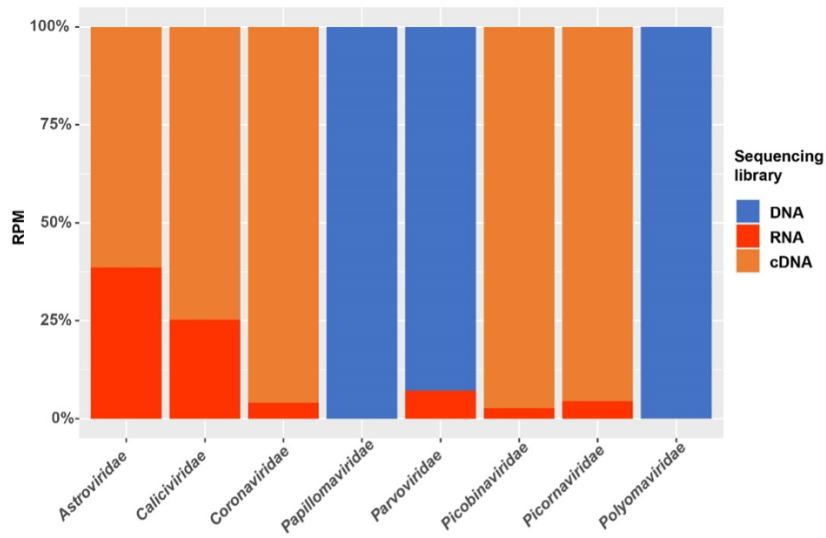The emergence of zoonotic viral diseases in humans commonly reflects exposure to mammalian wildlife. Bats (order Chiroptera) are arguably the most important mammalian reservoir for zoonotic viruses, with notable examples including Severe Acute Respiratory Syndrome coronaviruses 1 and 2, Middle East Respiratory Syndrome coronavirus, henipaviruses and lyssaviruses. Herein, we outline our current knowledge on the diversity of bat viromes, particularly through the lens of metagenomic next-generation sequencing and in the context of disease emergence. A key conclusion is that although bats harbour abundant virus diversity, the vast majority of bat viruses have not emerged to cause disease in new hosts such that bats are better regarded as critical but endangered components of global ecosystems.

5.2: Introduction

The global COVID-19 pandemic caused by Severe Acute Respiratory Syndrome coronavirus 2 (SARS-CoV-2) has intensified interest in bats as reservoirs for emerging viruses. Bats are the largest mammalian order (Chiroptera) after rodents, comprising over 1400 species from two suborders: the Yinpterochiroptera containing the *Pteropodidae* ("fruit bats") and five families of microbat, and the Yangochiroptera containing the remaining 14 microbat families (Tsagkogeorga et al., 2013). The most widespread bat families include the *Hipposideridae*, *Pteropodidae*, *Rhinolophidae*, *Molossidae*, *Emballonuridae*, *Phyllostomidae* and *Vespertilionidae* that contain up to ~190 species, while the *Craseonycteridae* and *Myzopodidae* harbour only one or two species and are geographically restricted (Puechmaille et al., 2009, Goodman et al., 2007). For dietary purposes bats can be classified as insectivores, frugivores, carnivores and nectivores, and several species use echolocation to characterise their surrounding environment and locate prey. Bats are found in every continent excluding Antarctica, in part reflecting their capacity to migrate via flight, with roosting sites that vary seasonally.

5.3: Virome diversity in bats

Metagenomic sequencing is an increasingly powerful and popular tool for virus discovery, particularly as it allows the characterisation of viruses from families that are often overlooked

in PCR-based screening that focuses on known or likely pathogens. It is therefore no surprise that much of our knowledge of bat viromes comes from the deployment of large-scale metagenomic next-generation sequencing (mNGS), particularly total RNA sequencing (metatranscriptomics). At the time of writing, ~30% of all the bat associated virus sequences deposited on NCBI/GenBank have been identified by mNGS only, an increase from 10% in 2016 (Figure 5.3.1). The recent identification of Wittenau bat nairovirus (*Nairoviridae*) and Ruhugu virus (*Matonaviridae*) serve as informative examples (Bennett et al., 2020, Kohl et al., 2021), as was the detection of deltaviruses (*Kolmioviridae*) in bats, even though these viruses were originally only associated with humans in the context of co-infection with hepatitis B virus (Bergner et al., 2021).
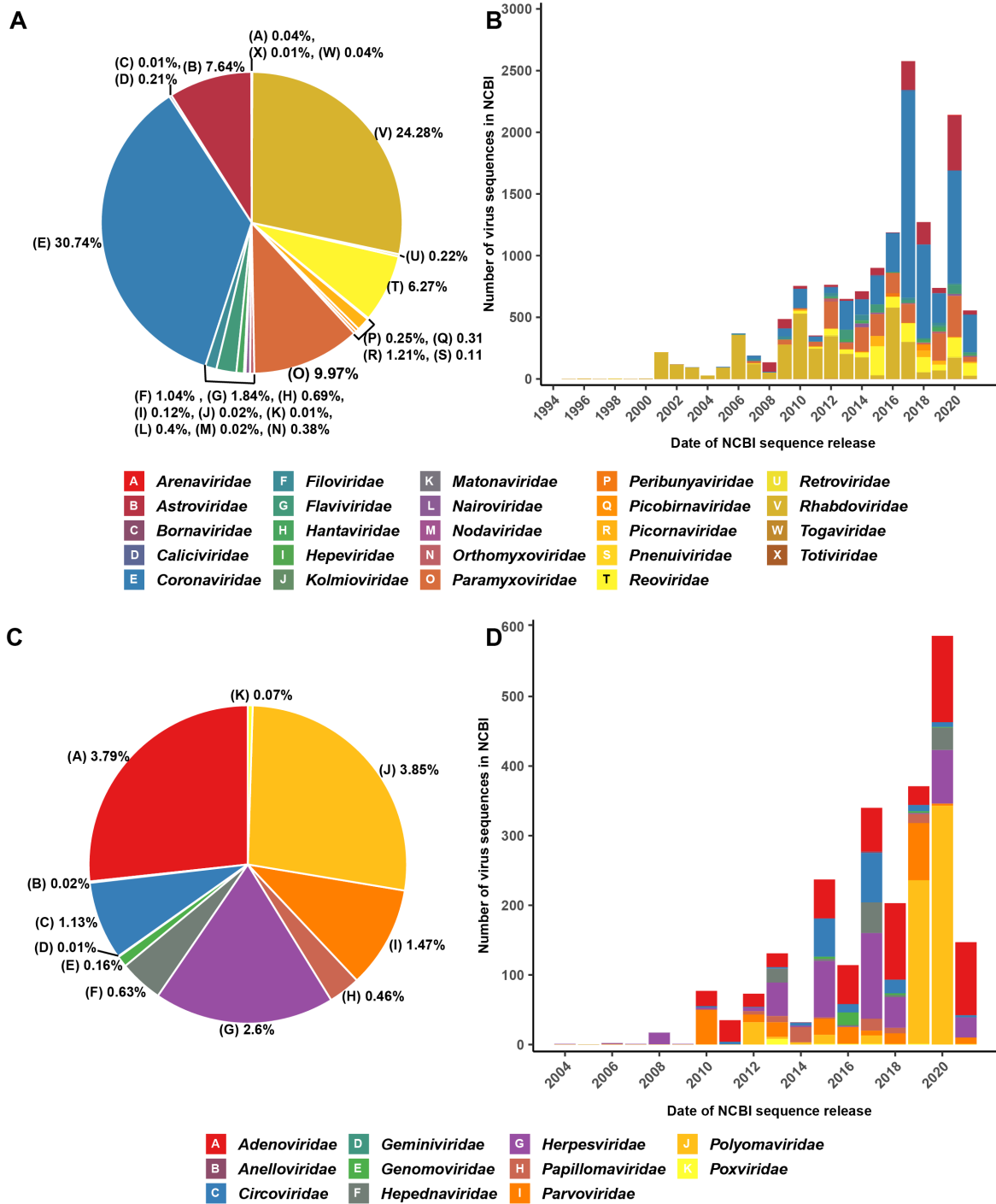
Figure 5.3.1: Taxonomic distribution of publicly available gene sequences of bat viruses. Plots show virus sequences on NCBI/GenBank in which the order Chiroptera or individual bat species are listed as hosts. (A) Percentage of bat virus sequences that belong to RNA virus families and (B) RNA virus sequences by year of NCBI release. (C) Percentage of bat virus sequences that belong to DNA virus families and (D) DNA virus sequences by year of NCBI release.

The collection of bat urine, saliva and faecal samples is commonly used in mNGS studies as this minimises the impact on bat populations. In many cases it also represents the likely route of virus transmission, although it may miss viruses associated with specific tissues. The analyses of faecal material and urine from bat species sampled on multiple continents have identified viruses from the *Adenoviridae*, *Astroviridae*, *Caliciviridae*, *Coronaviridae*, *Flaviviridae*, *Papillomaviridae*, *Paramyxoviridae*, *Parvoviridae*, *Picornaviridae*, *Polyomaviridae* and Reoviridae (Bolatti et al., 2020, Li et al., 2021b, Hardmeier et al., 2021, Yinda et al., 2018, Mendenhall et al., 2019). For example, a study of more than 4000 bat rectal and pharyngeal swabs from three common bat genera – horseshoe bats (*Rhinolophus*), mouse-eared bats (*Myotis*) and bent winged bats (*Miniopterus*) – in China identified novel virus sequences from diverse viral families, including the *Coronaviridae* and *Paramyxoviridae* (see below), as well as those from the order *Bunyavirales* of RNA viruses (Wu et al., 2016). The *Bunyavirales* currently comprises 12 families including a number associated with human disease. Five of these families have been identified in bats: the *Arenaviridae*, *Nairoviridae*, *Hantaviridae*, *Peribunyaviridae* and *Phenuiviridae* (Kohl et al., 2021, Li et al., 2021b, Geldenhuys et al., 2018, Zana et al., 2019). However, it is also important to note that rather than infecting bat themselves, many of the viruses detected in bats may be associated with aspects of the bat diet and microbiome. This is especially the case in studies utilising faecal mNGS studies (Li et al., 2010, Šimić et al., 2020, Hardmeier et al., 2021, Zheng et al., 2018, Li et al., 2021b), and care should also be taken to exclude reagent contamination (Porter et al., 2021).

A broad-scale conclusion from metagenomic studies is that bats may be particularly prone to carrying viral families that are commonly associated with zoonotic disease. Of the more than 16,600 bat associated viral sequences on NCBI/GenBank, 85% are RNA viruses, including 30% and 24% from the families *Coronaviridae* and *Rhabdoviridae*, respectively, while 10% of all bat-associated viral sequences identified to date are from the *Paramyxoviridae* (Figure 5.3.1). Indeed, those virus families that might pose a greater zoonotic risk (i.e., the *Coronaviridae*, *Paramyxoviridae* and *Rhabdoviridae*; see below) are generally associated with a narrower range of bat families compared to those viruses that may be less likely to emerge in humans (i.e., *Astroviridae*, *Reoviridae* and *Picornaviridae*) (Figure 5.3.2). As a case in point, a range of SARS-CoV-2 related coronaviruses have been characterised through mNGS of bats sampled in China and parts of south-east Asia (Zhou et al., 2021, Zhou et al., 2020, Temman et al., 2022). The viruses carried by bats also vary markedly by bat family

(Figure 5.3.2). As expected, the widespread and species rich bat families (i.e., the *Vespertilionidae*, *Rhinolophidae*, *Pteropodidae*, *Phyllostomidae* and *Hipposideridae*) harbour a greater diversity of viruses than the less speciose families (*Noctilionidae*, *Natalidae*, *Myzopodidae* and *Furipteridae*).
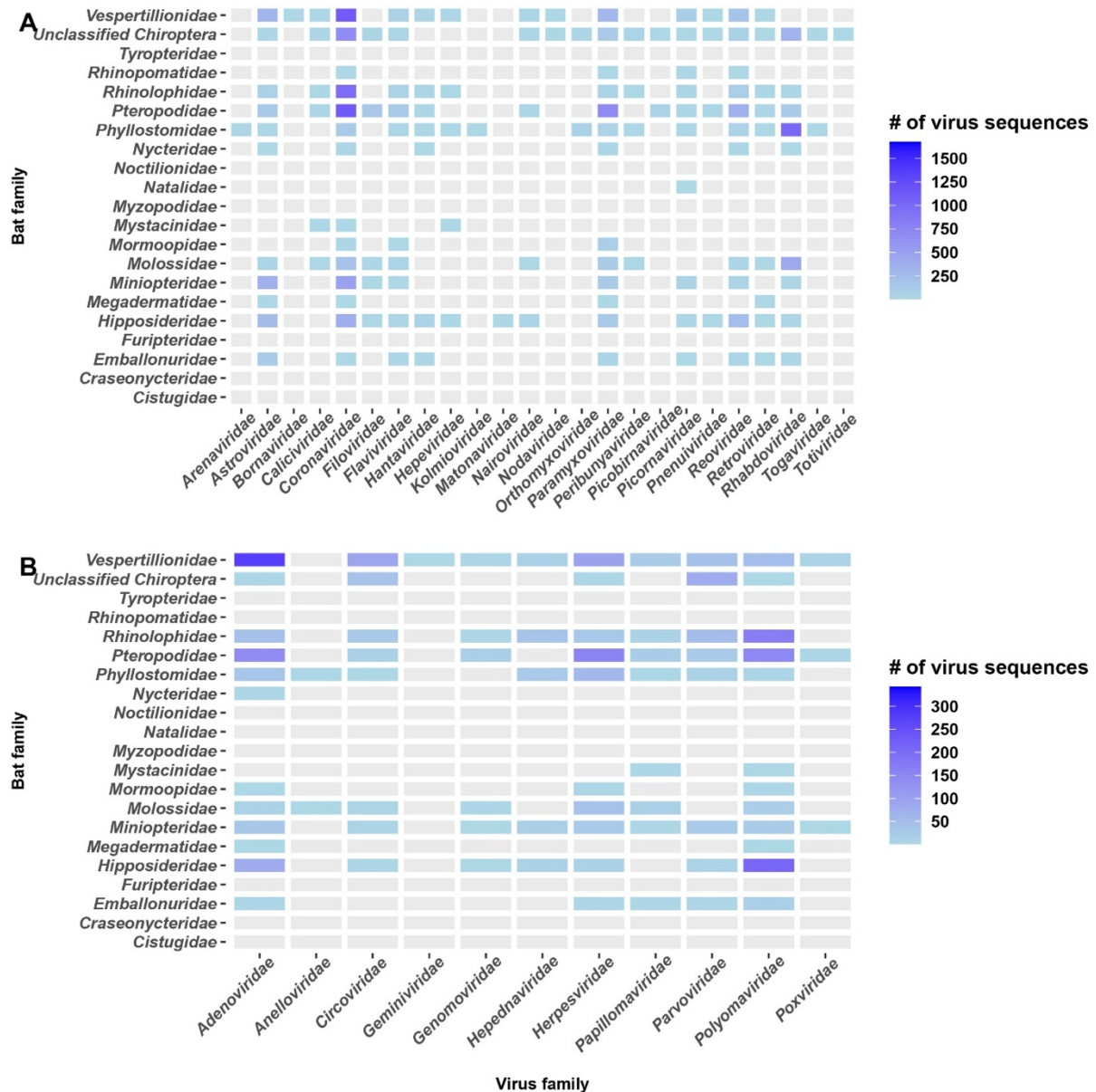
Figure 5.3.2: Number of publicly available virus gene sequences for each family of bats. The heat map shows (A) the number of RNA viruses and (B) the number of DNA viruses separated by virus family, and the corresponding bat host family as given on NCBI. Virus sequences with an unspecified bat host (i.e. host listed as Chiroptera) are represented as "unclassified Chiroptera".

5.4: Notable zoonotic outbreaks associated with bats

5.4.1: *Coronaviridae*

The current interest in bats as reservoirs for emerging viruses began with the outbreak of SARS-CoV-1 in 2002/2003 (WHO, 2015), and there has recently been intense research activity in documenting the diversity of alphacoronviruses and betacoronaviruses (Figure 5.4.1).

Figure 5.4.1: Representative phylogenetic diversity of bat coronaviruses. An amino acid alignment of the RdRp of the Coronaviridae was used to infer the maximum likelihood phylogeny using IQ-TREE (Nguyen et al., 2015). The phylogeny was estimated using viruses from the four coronavirus genera as marked by coloured lines to the right of the phylogeny. The tree was mid-point rooted and bootstrap values are represented by coloured circles. Bat viruses are shown in red font and fall into the Alphacoronavirus and Betacoronavirus genera. Animal silhouettes representing host species are displayed next to viruses that do not list a host species in the virus name.

Initial studies showed that civets (*Paguma larvata*) were the likely source of SARS-CoV-1, with emergence in humans associated with their presence in live animal markets in southern China (Tu et al., 2004). However, the subsequent sampling of bats in China provided serological evidence of infection with SARS-like coronaviruses in bats of the genus *Rhinolophus* (i.e. horseshoe bats) in Hubei and Guangxi provinces, confirmed by PCR of faecal samples (Li et al., 2005). Bats of the genus *Rhinolophus* are therefore the likely reservoir hosts for SARS-CoV-1, with onward transmission to civets and (perhaps raccoon dogs) that acted as "intermediate" hosts to seed human infection (Li et al., 2005). The presence of SARS-like coronaviruses with high sequence similarity to SARS-CoV-1 were later identified in Chinese horseshoe bats (*R. sinicus*) (Wu et al., 2016, Lau et al., 2005). Notably, a study from multiple locations in China detected the conserved RNA-dependent RNA polymerase (RdRp) domain of coronaviruses in 6.5% of bat species from the genera *Rhinolophus*, *Pipistrellus*, *Scotophilus*, *Myotis*, *Tylonycteris* and *Miniopterus*, with phylogenetic analysis showing that three of the coronaviruses detected, all from the genus *Rhinolophus*, clustered with SARS-like coronaviruses (Tang et al., 2006).

In 2012 Middle Eastern Respiratory Syndrome coronavirus (MERS-CoV) appeared in Saudi Arabia, resulting in respiratory illness and relatively high levels of mortality (Zaki et al., 2012). Studies of Dromedary camels identified multiple MERS-CoV-like lineages (as well as the alphacoronavirus HCoV-229E) reflecting several decades of circulation in these animals with multiple transmission events to humans and widespread recombination (Sabir et al., 2016). Notably, MERS-like CoVs were also identified in multiple bat species (*Pipistrellus cf. hesperdus, Nycteris cf. gambiensis, P. nathusii, P. pipistrellus, P. pygmaeus and Neoromica cf. zuluensis*) (Anthony et al., 2017, Annan et al., 2013, Ithete et al., 2013). Hence, these bat viruses likely represent the reservoir wildlife hosts for the viruses that later emerged, via

camels, as MERS-CoV. However, the bat coronaviruses most closely related to MERS-CoV also differed markedly in the spike protein and had reduced capacity to bind to the human dipeptidyl peptidase 4 cell receptor used by MERS-CoV (Yang et al., 2014, Anthony et al., 2017).

SARS-CoV-2 was first reported to cause severe pneumonia in humans in Wuhan, China in late 2019 (Wu et al., 2020). Metagenomic surveys and associated phylogenetic analyses have identified viruses closely related to SARS-CoV-2 in *Rhinolophus* bat species from several Asian countries (China, Cambodia, Thailand, Japan and Laos) (Zhou et al., 2021, Zhou et al., 2020, Li et al., 2021a, Murakami et al., 2020, Temman et al., 2022, Delaune et al., 2021). For example, five SARS-CoV-2 related coronaviruses were detected in pooled faecal samples collected from bats (*Rhinolophus pusillus, R. stheno and R. malayanus*) in two studies of a single tropical botanical garden in Yunnan province, China (Zhou et al., 2020, Zhou et al., 2021). Close relatives of the alphacoronavirus porcine epidemic disease virus were identified at the same sampling site (Zhou et al., 2021). Of most note, five SARS-CoV related coronaviruses were recently identified in three *Rhinolophus* species in Laos (*R. malayanus, R. pusillus and R. marshalli*), three of which grouped closely with human SARS-CoV-2 on phylogenetic trees and possessed a receptor binding domain with high sequence similarity to that of SARS-CoV-2 and the ability to bind to the human ACE2 receptor (Temman et al., 2022). This provides strong evidence that viruses with the capacity to infect humans exists in wildlife species and hence represent a pandemic risk. Genomic recombination has also been commonplace among viruses of the SARS-CoV-2-like lineage (i.e. the sarbecoviruses) (Temman et al., 2022, Li et al., 2021a, Zhou et al., 2021, Boni et al., 2020), greatly complicating attempts to accurately reconstruct evolutionary history and suggesting that mixed infection is commonplace in bats and perhaps other mammalian species.

Although most of the focus has necessarily been on human disease, coronaviruses of bat ancestry have resulted in disease outbreaks in species other than humans. For example, a novel alphacoronavirus - Swine Acute Diarrhoea Syndrome coronavirus (SADS-CoV) – caused the death of upwards of 24,000 pigs in China in 2016 (Zhou et al., 2018). SADS-related coronaviruses were detected in rectal swabs from horseshoe bats in Guangdong province from 2013-2016 (Zhou et al., 2018).

5.4.2: *Paramyxoviridae*

Interest in bat paramyxoviruses began with the discovery of Hendra, Nipah and Menangle viruses (see below). Since then, a large number of bat paramyxoviruses have been characterised, exhibiting considerable phylogenetic diversity (Figure 5.4.2). For example, 14 novel bat paramyxoviruses were discovered in nine species of bats in a single mNGS study from China (Wu et al., 2016), while in 2020 a novel bat paramyxovirus - Achimota Pararubulavirus 3 – was identified in a urine sample from *Eidolon helvum* (Baker et al., 2020).
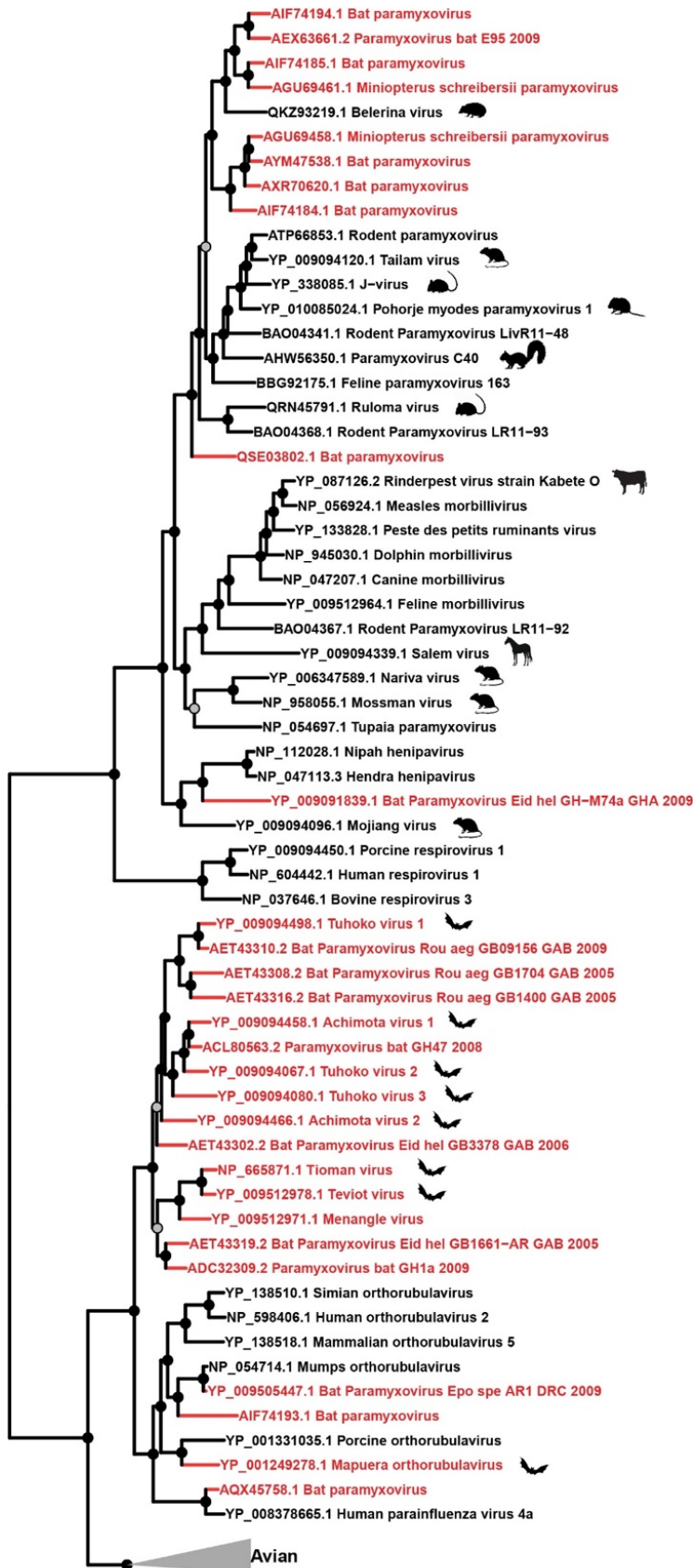
Figure 5.4.2: Representative phylogenetic diversity of bat paramyxoviruses. An amino acid alignment of the L protein that contains the RdRp of the Paramyxoviridae was used to infer a maximum likelihood tree using IQ-TREE (Nguyen et al., 2015). The tree was mid-point rooted and bootstrap values are represented by coloured circles. Bat viruses are shown in red font. Animal silhouettes representing animal host species are displayed next to viruses that do not provide a host species in the virus name. The avian paramyxovirus clade has been collapsed to enhance visualisation.

Hendra virus (genus *Henipavirus*, family *Paramyxoviridae*) was first reported to cause acute respiratory illness in horses and encephalitis in humans in Queensland, Australia in 1994, initially resulting in the death of 16 horses and two humans who had contact with sick horses (O'Sullivan et al., 1997, Rogers et al., 1996, Selvey et al., 1995, Murray et al., 1995). After 2000 horses tested serologically negative to the virus it was proposed that it likely originated from a wildlife source (Ward et al., 1996, Young et al., 1996), and the black flying fox (*Pteropus alecto*), grey headed flying fox (*P. poliocephalus*), spectacled flying fox (*P. conspicillatus*) and little red flying fox (*P. scapulatus*) were later identified as carrying neutralising antibodies to the virus (Young et al., 1996). Hendra virus was later confirmed in the birthing fluid and foetal tissue from a grey headed flying fox and the foetal tissue from a black flying fox, as well as a high prevalence in bat urine (Halpin et al., 2000, Field et al., 2015). Urine may therefore represent the likely mode of transmission to horses, with subsequent transmission through respiratory secretions to horses and humans (Young et al., 1996, Halpin et al., 2000, Field et al., 2015).

Another member of genus *Henipavirus* – Nipah virus – has similarly made the jump from bats to domestic animals. This virus was first reported in farmed pig populations in Malaysia in late 1998 before emerging in Singapore in early 1999 and again in India and Bangladesh in 2001, causing neurological and respiratory illness in pigs and encephalitis in humans (Chua et al., 1999, Paton et al., 1999). During the 1998 Malaysia outbreak 238 humans contracted the virus, 105 of whom died (Chua et al., 2000). Following the identification of Hendra virus in flying foxes (genus *Pteropus*), the large flying fox (*P. vampyrus*), small flying fox (*P. hypomelanus*), cave nectar bat (*Eonycteris spelaea*), lesser short-nosed fruit bat (*Cynopterus brachyotis*) and lesser Asiatic yellow bat (*Scotophilus kuhlii*) were identified as carrying neutralising antibodies to the virus (Yob et al., 2001). The Indian flying fox (*P. medius*,

previously *P. giganteus*) has similarly been linked to the Nipah virus outbreaks in India and Bangladesh (Yadav et al., 2012, Epstein et al., 2008).

The third zoonotic virus of the family *Paramyxoviridae* carried by bats is Menangle virus (genus *Pararubulavirus*). Menangle virus successfully established infection in a farmed pig population in 1997, presenting as reproductive complications (Philbey et al., 1998). Two humans working at separate piggeries recorded severe influenza-like symptoms during the 1997 piggery outbreak and were seropositive for Menangle virus (Chant et al., 1998). Both workers confirmed they had been exposed to fluids from pigs housed at the outbreak farm (Chant et al., 1998). Like Hendra, the grey headed flying fox, black flying fox and spectacled flying fox were later identified as carrying neutralising antibodies for Menangle virus and hence likely act as reservoir hosts (Philbey et al., 1998, Philbey et al., 2008), although no Menangle virus outbreaks have been recorded in Australia since 1997.

5.4.3: *Rhabdoviridae*

The *Rhabdoviridae* are a diverse set of negative-sense RNA viruses comprising multiple genera, one of which, the genus Lyssavirus, can cause rabies in mammals (the ecology and evolution of which has been extensively reviewed elsewhere (Fisher et al., 2018)). Bats are the likely reservoir hosts for most lyssaviruses, although classic rabies lyssavirus is mainly transmitted to humans through bites or scratches from carnivores like dogs and racoons. Lyssaviruses currently include 17 characterised species that have been detected in bat species in a range of geographic locations, including Australian bat lyssavirus (Gould et al., 1998), Irkut lyssavirus (Russia) (Botvinkin et al., 2003), Bokelon bat lyssavirus (Germany) (Freuling et al., 2011), European bat lyssavirus 1 and 2 (McElhinney et al., 2013), Aravan and Khujand virus (Asia) (Kuzmin et al., 2003) and Gannoruwa bat lyssavirus (Sri Lanka) (Gunawardena et al., 2016). Unfortunately, a lack of sampling makes it difficult to determine whether these viruses are present in other mammalian species.

For most bat species interactions with humans and other animals are limited to occasional occurrences such as through animal carers and in backyards and households. Accordingly, there is only sporadic lyssavirus transmission from bats to humans, although outcomes are often fatal. In contrast, the common vampire bat (*Desmodus rotundus*), hairy-legged vampire bat (*Diphylla ecaudata*) and white-winged vampire bat (*Diaemus youngi*) from South and Central America have a unique blood-feeding diet that provides an opportunistic route of the transmission for classic rabies lyssavirus into livestock (Benavides et al., 2017).

5.5: Why are bats good reservoir hosts?

Bats undoubtedly harbour a large and diverse array of viruses, some of which have jumped species boundaries to emerge in new hosts and occasionally cause disease outbreaks. The question that naturally arises is why bats are seemingly such important reservoir hosts for zoonotic viruses, particularly as some studies indicate that the number of viruses carried by bats is significantly greater than other mammalian orders (Olival et al., 2017). The social dynamics of bat populations, including very large roosting numbers and species co-habitation, provide the perfect setting for viral transmission, while the capacity of bats to travel to different or new geographical regions provides a mechanism for viruses to become established in naïve bat populations. It is also likely that the characteristic flight-adapted physiology of bats in part provides an explanation for their high virus burden (Letko et al., 2020, Irving et al., 2021), while the unique anti-inflammatory and proinflammatory responses in bats, as well as distinctive immunological traits such as the reduced number of interferon genes (such as in the black flying fox) and that the interferon genes are continually expressed in the absence of an initiated immune response, may in part explain why bats are often asymptomatic carriers for a myriad of viruses (Zhou et al., 2016, Kacprzyk et al., 2017, Irving et al., 2021, Letko et al., 2020). More detailed studies of the innate and adaptive immune responses in a broader range of Yinpterochiroptera and Yangochiroptera should clearly be a research priority.

Despite the mounting evidence that bats harbour a particularly large and abundant virome, it is important to acknowledge that the increasing frequency with which bat viruses are described is also impacted by major ascertainment and confirmation biases. Indeed, following the discovery of the bat reservoir for SARS-CoV there has been a marked increase in studies of bat viromes, with an emphasis on sampling from bat populations in China and other Asian countries (Ge et al., 2012, Wu et al., 2012, Wu et al., 2016, Zhou et al., 2021, Han et al., 2017), and of particular genera such as *Rhinolophus*, although the population density of these animals varies markedly in space (Zhou et al., 2021). Obviously, the more a particular group of animals is sampled then, on average, the more novel viruses will be characterised, and some studies have suggested that bats carry no more virus than expected given their species richness (Mollentze and Streicker, 2020). Perhaps more importantly, although virus species richness in bats is high, these viruses rarely establish successful human infection and most bat

viruses classed as zoonotic are not directly transmitted from bats to humans. Rather, bat-to-human transmission routinely involves an intermediate animal host (such as pigs, camels and horses). Indeed, a number of the viral families that appear regularly in virome studies have not yet spilled over into human populations (Figure 5.3.2). Indeed, the zoonotic risk posed by bat viruses needs to be qualified by the observation that many of these viruses have been associated with bats for millennia with only a small number of spill-over events. For example, the common ancestor of the sabecoviruses has been estimated to have existed ~21,000 years ago (Ghafari et al., 2021), while the origin of the orthocoronaviruses has been dated to over 150 million years ago (Hayman and Knox, 2021).

5.6: Challenges in bat viromics

The increasing use of mNGS has identified a multitude of novel and highly diverse RNA and DNA viruses in bats, greatly expanding our knowledge of the known virosphere and providing important information on the origins of specific viruses. The advantages of mNGS are manifold, including its unbiased and multiplex approach, easy application, high sensitivity and continually decreasing cost. However, the computational challenges of analysing the abundant sequence data produced by mNGS can be considerable, particularly in resource poor settings, and accurately identifying viruses that infect bats as opposed to components of their diet or microbiome can be challenging (Cobbin et al., 2021). In particular, bats consume insects and are also susceptible to arthropod parasites, both of which may commonly carry viruses (Xu et al., 2021, Bennett et al., 2019), and both insect viruses and bacteriophages are commonly detected in bat metagenomic data (Kohl et al., 2021, Li et al., 2010, Li et al., 2021b, Šimić et al., 2020). Hence, to fully exploit the growing information obtained by mNGS studies of bat viromes new bioinformatics tools need to be developed that can rapidly and accurate identify those viruses most likely to infect bats. Similarly, determining which of the myriad of bat viruses are of likely human pandemic potential may not be possible though computational analyses alone. For example, although closely related to SARS-CoV-2, *Rhinolophus affinis* virus RaTG13 is unable to bind to the human ACE2 receptor (Wrobel et al., 2020).

5.7: Conclusions - an uncertain future for bats

Bats play a central role in maintaining a sustainable ecosystem, helping to pollinate, distribute seeds and control pests for thousands of plant species (Voigt and Kingston, 2016). Since the identification of bats as reservoir hosts for many zoonotic viruses this group of animals has acquired an unjustified negative reputation, especially those species that roost in urban habitats, leading to an unsympathetic mindset among many communities. Climate change, urbanisation and industrial and agricultural advancements have greatly impacted bat populations globally (Voigt and Kingston, 2016), while encroachment onto bat habitats through urbanisation has increased the chance of viral spillover events into humans or companion and production animals. Currently, 106 bat species are listed as endangered or critically endangered on the IUCN (International Union for Conservation of Nature) red list, with 110 species threatened. Irrespective of any potential zoonotic risk, efforts to increase bat numbers should be prioritised. It is essential that we conserve this diverse group of animals, not only for the benefits to our ecosystem but also to enhance our understanding of viral biodiversity and evolution, and mammalian immunology.

5.8: References

Annan, A., Baldwin, H.J., Corman, V.M., Klose, S.M., Owusu, M., Nkrumah, E.E., Badu, E.K., Anti, P., Agbenyega, O., Meyer, B., Oppong, S., Sarkodie, Y.A., Kalko, E.K., Lina, P.H., Godlevska, E.V., Reusken, C., Seebens, A., Gloza-Rausch, F., Vallo, P., Tschapka, M., Drosten, C., Drexler, J.F. 2013. Human betacoronavirus 2c EMC/2012-related viruses in bats, Ghana and Europe. *Emerging Infectious Dissease*, 19(3):456-9.

Anthony, S.J., Gilardi, K., Menachery, V.D., Goldstein, T., Ssebide, B., Mbabazi, R., Navarrete-Macias, I., Liang, E., Wells, H., Hicks, A., Petrosov, A., Byarugaba, D.K., Debbink, K., Dinnon, K.H., Scobey, T., Randell, S.H., Yount, B.L., Cranfield, M., Johnson, C.K., Baric, R.S., Lipkin, W.I., Mazet, J.A. 2017. Further Evidence for Bats as the Evolutionary Source of Middle East Respiratory Syndrome Coronavirus. *mBio*, 8(2):e00373.

Baker, K.S., Tachedjian, M., Barr, J., Marsh, G.A., Todd, S., Crameri, G., Crameri, S., Smith, I., Holmes, C.E.G., Suu-Ire, R., Fernandez-Loras, A., Cunningham, A.A., Wood, J.L.N., Wang, L.F. 2020. Achimota Pararubulavirus 3: A New Bat-Derived Paramyxovirus of the Genus Pararubulavirus. *Viruses*, 12(11):1236.

Benavides, J.A., Rojas Paniagua, E., Hampson, K., Valderrama, W., Streicker, D.G. 2017. Quantifying the burden of vampire bat rabies in Peruvian livestock. *PLoS Neglected Tropical Disease*, 11(12):e0006105.

Bennett, A.J., Bushmaker, T., Cameron, K., Ondzie, A., Niama, F.R., Parra, H.J., Mombouli, J.V., Olson, S.H., Munster, V.J., Goldberg, T.L. 2019. Diverse RNA viruses of arthropod origin in the blood of fruit bats suggest a link between bat and arthropod viromes. *Virology*, 528:64-72.

Bennett, A.J., Paskey, A.C., Ebinger, A., Pfaff, F., Priemer, G., Höper, D., Breithaupt, A., Heuser, E., Ulrich, R.G., Kuhn, J.H., Bishop-Lilly, K.A., Beer, M., Goldberg, T.L. 2020. Relatives of rubella virus in diverse mammals. *Nature*, 586(7829):424-428.

Bergner, L.M., Orton, R.J., Broos, A., Tello, C., Becker, D.J., Carrera, J.E., Patel, A.H., Biek, R., Streicker, D.G. 2021. Diversification of mammalian deltaviruses by host

shifting. *Proceedings of the National Academy of Sciences of the United States of America,* 118(3):e2019907118.

Bolatti, E.M., Zorec, T.M., Montani, M.E., Hošnjak, L., Chouhy, D., Viarengo, G., Casal, P.E., Barquez, R.M., Poljak, M., Giri, A.A. 2020. A Preliminary Study of the Virome of the South American Free-Tailed Bats (Tadarida brasiliensis) and Identification of Two Novel Mammalian Viruses. *Viruses*, 12(4):422.

Boni, M.F., Lemey, P., Jiang, X., Lam, T.T., Perry, B.W., Castoe, T.A., Rambaut, A., Robertson, D.L. 2020. Evolutionary origins of the SARS-CoV-2 sarbecovirus lineage responsible for the COVID-19 pandemic. *Nature Microbiology*, 5(11):1408-1417.

Botvinkin, A.D., Poleschuk, E.M., Kuzmin, I.V., Borisova, T.I., Gazaryan, S.V., Yager, P., Rupprecht, C.E. 2003. Novel lyssaviruses isolated from bats in Russia. Emerging Infectious Dissease, 9(12):1623-5.

Chant, K., Chan, R., Smith, M., Dwyer, D.E., Kirkland, P. 1998. Probable human infection with a newly described virus in the family Paramyxoviridae. The NSW Expert Group. Emerging Infectious Disease, 4(2):273-5.

Chua, K.B., Bellini, W.J., Rota, P.A., Harcourt, B.H., Tamin, A., Lam, S.K., Ksiazek, T.G., Rollin, P.E., Zaki, S.R., Shieh, W., Goldsmith, C.S., Gubler, D.J., Roehrig, J.T., Eaton, B., Gould, A.R., Olson, J., Field, H., Daniels, P., Ling, A.E., Peters, C.J., Anderson, L.J., Mahy, B.W. 2000. Nipah virus: a recently emergent deadly paramyxovirus. *Science*, 288(5470):1432-5.

Chua, K.B., Goh, K.J., Wong, K.T., Kamarulzaman, A., Tan, P.S., Ksiazek, T.G., Zaki, S.R., Paul, G., Lam, S.K., Tan, C.T. 1999. Fatal encephalitis due to Nipah virus among pig-farmers in Malaysia. *Lancet*, 354(9186):1257-9.

Cobbin, J.C., Charon, J., Harvey, E., Holmes, E.C., Mahar, J.E. 2021. Current challenges to virus discovery by meta-transcriptomics. *Current Opinion in Virology*, 51:48-55.

Delaune, D., Hul, V., Karlsson, E.A., Hassanin, A., Ou, T.P., Baidaliuk, A., Gambaro, F., Prot, M., Tu, V.T., Chea, S., Keatts, L., Mazet, J., Johnson, C.K., Buchy, P., Dussart, P., Goldstein, T., Simon-Loriere, E., Duong, V. 2021. A novel SARS-CoV-2 related coronavirus in bats from Cambodia. *Nature Communication*, 12(1):6563.

Epstein, J.H., Prakash, V., Smith, C.S., Daszak, P., McLaughlin, A.B., Meehan, G., Field, H.E., Cunningham, A.A. 2008. Henipavirus infection in fruit bats (Pteropus giganteus), India. *Emerging Infectious Disease*, 14(8):1309-11.

Field, H., Jordan, D., Edson, D., Morris, S., Melville, D., Parry-Jones, K., Broos, A., Divljan, A., McMichael, L., Davis, R., Kung, N., Kirkland, P., Smith, C. 2015. Spatiotemporal Aspects of Hendra Virus Infection in Pteropid Bats (Flying-Foxes) in Eastern Australia. *PLoS One*, 10(12):e0144055.

Fisher, C.R., Streicker, D.G., Schnell, M.J. 2018. The spread and evolution of rabies virus: conquering new frontiers. *Nature Reviews Microbiology*, 16(4):241-255.

Freuling, C.M., Beer, M., Conraths, F.J., Finke, S., Hoffmann, B., Keller, B., Kliemt, J., Mettenleiter, T.C., Mühlbach, E., Teifke, J.P., Wohlsein, P., Müller, T. 2011. Novel lyssavirus in Natterer's bat, Germany. Emerging Infectious Disease, 17(8):1519-22.

Ge, X., Li, Y., Yang, X., Zhang, H., Zhou, P., Zhang, Y., Shi, Z. 2012. Metagenomic analysis of viruses from bat fecal samples reveals many novel viruses in insectivorous bats in China. *Journal of Virology*, 86(8):4620-30.

Geldenhuys, M., Mortlock, M., Weyer, J., Bezuidt, O., Seamark, E.C.J., Kearney, T., Gleasner, C., Erkkila, T.H., Cui, H., Markotter, W. 2018. A metagenomic viral discovery approach identifies potential zoonotic and novel mammalian viruses in Neoromicia bats within South Africa. *PLoS One*, 13(3):e0194527.

Ghafari, M., Simmonds, P., Pybus, O.G., Katzourakis, A. 2021. A mechanistic evolutionary model explains the time-dependent pattern of substitution rates in viruses. Current Biology, 31(21):4689-4696 e5.

Goodman, S.M., Rakotondraparany, F., Kofoky, A. 2007. The description of a new species of Myzopoda (Myzopodidae: Chiroptera) from western Madagascar. *Mammalian biology: Zeitschrift für Säugetierkunde*, 72(2):65-81.

Gould, A.R., Hyatt, A.D., Lunt, R., Kattenbelt, J.A., Hengstberger, S., Blacksell, S.D. 1998. Characterisation of a novel lyssavirus isolated from Pteropid bats in Australia. *Virus Research*, 54(2):165-87.

Gunawardena, P.S., Marston, D.A., Ellis, R.J., Wise, E.L., Karawita, A.C., Breed, A.C., McElhinney, L.M., Johnson, N., Banyard, A.C., Fooks, A.R. 2016. Lyssavirus in Indian Flying Foxes, Sri Lanka. *Emerging Infectious Disease*, 22(8):1456-9.

Halpin, K., Young, P.L., Field, H.E., Mackenzie, J.S. 2000. Isolation of Hendra virus from pteropid bats: a natural reservoir of Hendra virus. *Journal of General Virology*, 81(Pt 8):1927-1932.

Han, H.J., Wen, H.L., Zhao, L., Liu, J.W., Luo, L.M., Zhou, C.M., Qin, X.R., Zhu, Y.L., Liu, M.M., Qi, R., Li, W.Q., Yu, H., Yu, X.J. 2017. Novel coronaviruses, astroviruses, adenoviruses and circoviruses in insectivorous bats from northern China. *Zoonoses Public Health*, 64(8):636-646.

Hardmeier, I., Aeberhard, N., Qi, W., Schoenbaechler, K., Kraettli, H., Hatt, J.M., Fraefel, C., Kubacki, J. 2021. Metagenomic analysis of fecal and tissue samples from 18 endemic bat species in Switzerland revealed a diverse virus composition including potentially zoonotic viruses. *PLoS One*, 16(6):e0252534.

Hayman, D.T.S., Knox, M.A. 2021. Estimating the age of the subfamily Orthocoronavirinae using host divergence times as calibration ages at two internal nodes. *Virology*, 563:20-27.

Irving, A.T., Ahn, M., Goh, G., Anderson, D.E., Wang, L.F. 2021. Lessons from the host defences of bats, a unique viral reservoir. *Nature*, 589(7842):363-370.

Ithete, N.L., Stoffberg, S., Corman, V.M., Cottontail, V.M., Richards, L.R., Schoeman, M.C., Drosten, C., Drexler, J.F., Preiser, W. 2013. Close relative of human Middle East respiratory syndrome coronavirus in bat, South Africa. *Emerging Infectious Disease,* 19(10):1697-9.

Kacprzyk, J., Hughes, G.M., Palsson-McDermott, E.M., Quinn, S.R., Puechmaille, S.J., O'Neill, L.A.J., Teeling, E.C. 2017. A Potent Anti-Inflammatory Response in Bat Macrophages May Be Linked to Extended Longevity and Viral Tolerance. *Acta chiropterologica Journal*, 19(2):219-228.

Kohl, C., Brinkmann, A., Radonić, A., Dabrowski, P.W., Mühldorfer, K., Nitsche, A., Wibbelt, G., Kurth, A. 2021. The virome of German bats: comparing virus discovery approaches. *Science Reports*, 11(1):7430.

Kuzmin, I.V., Orciari, L.A., Arai, Y.T., Smith, J.S., Hanlon, C.A., Kameoka, Y., Rupprecht, C.E. 2003. Bat lyssaviruses (Aravan and Khujand) from Central Asia: phylogenetic relationships according to N, P and G gene sequences. *Virus Research*, 97(2):65-79.

Lau, S.K., Woo, P.C., Li, K.S., Huang, Y., Tsoi, H.W., Wong, B.H., Wong, S.S., Leung, S.Y., Chan, K.H., Yuen, K.Y. 2005. Severe acute respiratory syndrome coronavirus-like virus in Chinese horseshoe bats. *Proceedings of the National Academy of Sciences of the United States of America*, 102(39):14040-5.

Letko, M., Seifert, S.N., Olival, K.J., Plowright, R.K., Munster, V.J. 2020. Bat-borne virus diversity, spillover and emergence. *Nature Reviews Microbiology*, 18(8):461-471.

Li, L., Victoria, J.G., Wang, C., Jones, M., Fellers, G.M., Kunz, T.H., Delwart, E. 2010. Bat guano virome: predominance of dietary viruses from insects and plants plus novel mammalian viruses. *Journal of Virology*, 84(14):6955-65.

Li, L.L., Wang, J.L., Ma, X.H., Sun, X.M., Li, J.S., Yang, X.F., Shi, W.F., Duan, Z.J. 2021a. A novel SARS-CoV-2 related coronavirus with complex recombination isolated from bats in Yunnan province, China. *Emerging Microbes and Infections*, 10(1):1683-1690.

Li, W., Shi, Z., Yu, M., Ren, W., Smith, C., Epstein, J.H., Wang, H., Crameri, G., Hu, Z., Zhang, H., Zhang, J., McEachern, J., Field, H., Daszak, P., Eaton, B.T., Zhang, S., Wang, L.F. 2005. Bats are natural reservoirs of SARS-like coronaviruses. *Science*, 310(5748):676-9.

Li, Y., Altan, E., Reyes, G., Halstead, B., Deng, X., Delwart, E. 2021b. Virome of Bat Guano from Nine Northern California Roosts. *Journal of Virology*, 95(3):e01713-20.

McElhinney, L.M., Marston, D.A., Leech, S., Freuling, C.M., van der Poel, W.H., Echevarria, J., Vázquez-Moron, S., Horton, D.L., Müller, T., Fooks, A.R. 2013. Molecular epidemiology of bat lyssaviruses in Europe. *Zoonoses Public Health*, 60(1):35-45.

Mendenhall, I.H., Wen, D.L.H., Jayakumar, J., Gunalan, V., Wang, L., Mauer-Stroh, S., Su, Y.C.F., Smith, G.J.D. 2019. Diversity and Evolution of Viral Pathogen Community in Cave Nectar Bats (Eonycteris spelaea). *Viruses*, 11(3):250.

Mollentze, N., Streicker, D.G. 2020. Viral zoonotic risk is homogenous among taxonomic orders of mammalian and avian reservoir hosts. Proceedings of the National Academy of Sciences of the United States of America, 117(17):9423-9430.

Murakami, S., Kitamura, T., Suzuki, J., Sato, R., Aoi, T., Fujii, M., Matsugo, H., Kamiki, H., Ishida, H., Takenaka-Uema, A., Shimojima, M., Horimoto, T. 2020. Detection and Characterization of Bat Sarbecovirus Phylogenetically Related to SARS-CoV-2, Japan. *Emerging Infectious Disease*, 26(12):3025-3029.

Murray, K., Rogers, R., Selvey, L., Selleck, P., Hyatt, A., Gould, A., Gleeson, L., Hooper, P., Westbury, H. 1995. A novel morbillivirus pneumonia of horses and its transmission to humans. *Emerging Infectious Disease*, 1(1):31-3.

Nguyen, L.T., Schmidt, H.A., von Haeseler, A., Minh, B.Q. 2015. IQ-TREE: a fast and effective stochastic algorithm for estimating maximum-likelihood phylogenies. *Molecular Biology and Evolution*, 32(1):268-74.

O'Sullivan, J.D., Allworth, A.M., Paterson, D.L., Snow, T.M., Boots, R., Gleeson, L.J., Gould, A.R., Hyatt, A.D., Bradfield, J. 1997. Fatal encephalitis due to novel paramyxovirus transmitted from horses. *Lancet*, 349(9045):93-5.

Olival, K.J., Hosseini, P.R., Zambrana-Torrelio, C., Ross, N., Bogich, T.L., Daszak, P. 2017. Host and viral traits predict zoonotic spillover from mammals. *Nature*, 546(7660):646-650.

Paton, N.I., Leo, Y.S., Zaki, S.R., Auchus, A.P., Lee, K.E., Ling, A.E., Chew, S.K., Ang, B., Rollin, P.E., Umapathi, T., Sng, I., Lee, C.C., Lim, E., Ksiazek, T.G. 1999. Outbreak of Nipah-virus infection among abattoir workers in Singapore. *Lancet*, 354(9186):1253-6.

Philbey, A.W., Kirkland, P.D., Ross, A.D., Davis, R.J., Gleeson, A.B., Love, R.J., Daniels, P.W., Gould, A.R., Hyatt, A.D. 1998. An apparently new virus (family Paramyxoviridae) infectious for pigs, humans, and fruit bats. *Emerging Infectious Disease,* 4(2):269-71.

Philbey, A.W., Kirkland, P.D., Ross, A.D., Field, H.E., Srivastava, M., Davis, R.J., Love, R.J. 2008. Infection with Menangle virus in flying foxes (Pteropus spp.) in Australia. *Australian Veterinary Journal*, 86(2):449-54.

Porter, A.F., Cobbin, J., Li, C., Eden, J.-S., Holmes, E.C. 2021. Metagenomic identification of viral sequences in laboratory reagents. *Viruses*,13(11):2122.

Puechmaille, S.J., Soisook, P., Yokubol, M., Piyapan, P., Ar Gouilh, M., Mie Mie, K., Khin Kyaw, K., Mackie, I., Bumrungsri, S., Dejtaradol, A., Nwe, T., Hla Bu, S.S., Satasook, C., Bates, P.J., Teeling, E.C. 2009. Population size, distribution, threats and conservation status of two endangered bat species Craseonycteris thonglongyai and Hipposideros turpis. *Endangered species research*, 8:15-23.

Rogers, R.J., Douglas, I.C., Baldock, F.C., Glanville, R.J., Seppanen, K.T., Gleeson, L.J., Selleck, P.N., Dunn, K.J. 1996. Investigation of a second focus of equine morbillivirus infection in coastal Queensland. *Australian Veterinary Journal*, 74(3):243-4.

Sabir, J.S., Lam, T.T., Ahmed, M.M., Li, L., Shen, Y., Abo-Aba, S.E., Qureshi, M.I., Abu-Zeid, M., Zhang, Y., Khiyami, M.A., Alharbi, N.S., Hajrah, N.H., Sabir, M.J., Mutwakil, M.H., Kabli, S.A., Alsulaimany, F.A., Obaid, A.Y., Zhou, B., Smith, D.K., Holmes, E.C., Zhu, H., Guan, Y. 2016. Co-circulation of three camel coronavirus species and recombination of MERS-CoVs in Saudi Arabia. *Science*, 351(6268):81-4.

Selvey, L.A., Wells, R.M., McCormack, J.G., Ansford, A.J., Murray, K., Rogers, R.J., Lavercombe, P.S., Selleck, P., Sheridan, J.W. 1995. Infection of humans and horses by a newly described morbillivirus. *Medical Journal of Australia*, 162(12):642-5.

Šimić, I., Zorec, T.M., Lojkić, I., Krešić, N., Poljak, M., Cliquet, F., Picard-Meyer, E., Wasniewski, M., Zrnčić, V., Ćukušić, A., Bedeković, T. 2020. Viral Metagenomic Profiling of Croatian Bat Population Reveals Sample and Habitat Dependent Diversity. *Viruses*, 12(8):891.

Tang, X.C., Zhang, J.X., Zhang, S.Y., Wang, P., Fan, X.H., Li, L.F., Li, G., Dong, B.Q., Liu, W., Cheung, C.L., Xu, K.M., Song, W.J., Vijaykrishna, D., Poon, L.L., Peiris, J.S., Smith, G.J., Chen, H., Guan, Y. 2006. Prevalence and genetic diversity of coronaviruses in bats from China. *Journal of Virology*, 80(15):7481-90.

Temman, S., Vongphayloth, K., Baquero, E., Munier, S., Bonomi, M., Regnault, B., Douangboubpha, B., Karami, Y., Chretien, D., Sanamxay, D., Xayaphet, V., Paphaphanh, P., Lacoste, V., Somlor, S., Lakeomany, K., Phommavanh, N., Perot, P.,

Dehan, O., Amara, F., Donati, F., Bigot, T., Nilges, M., Rey, F.A., van der Werf, S., Brey, P.T., Eloit, M. 2022. Bat coronaviruses related to SARS-CoV-2 infectious for human cells. *Nature*, 604:330-336.

Tsagkogeorga, G., Parker, J., Stupka, E., Cotton, J.A., Rossiter, S.J. 2013. Phylogenomic analyses elucidate the evolutionary relationships of bats. *Current Biology*, 23(22):2262-2267.

Tu, C., Crameri, G., Kong, X., Chen, J., Sun, Y., Yu, M., Xiang, H., Xia, X., Liu, S., Ren, T., Yu, Y., Eaton, B.T., Xuan, H., Wang, L.F. 2004. Antibodies to SARS coronavirus in civets. *Emerging Infectious Disease*, 10(12):2244-8.

Voigt, C.C., Kingston, T. 2016. Bats in the Anthropocene : Conservation of Bats in a Changing World, Cham, Springer Open.

Ward, M.P., Black, P.F., Childs, A.J., Baldock, F.C., Webster, W.R., Rodwell, B.J., Brouwer, S.L. 1996. Negative findings from serological studies of equine morbillivirus in the Queensland horse population. *Australian Veterinary Journal*, 74(3):241-3.

World Health Organisation. 2015. Summary of probable SARS cases with onset of illness from 1 November 2002 to 31 July 2003. WHO. Viewed August 2021. https://www.who.int/publications/m/item/summary-of-probable-sars-cases-with-onset-of-illness-from-1-november-2002-to-31-july-2003.

Wrobel, A.G., Benton, D.J., Xu, P., Roustan, C., Martin, S.R., Rosenthal, P.B., Skehel, J.J., Gamblin, S.J. 2020. SARS-CoV-2 and bat RaTG13 spike glycoprotein structures inform on virus evolution and furin-cleavage effects. *Nature Structural and Molecular Biology*, 27(8):763-767.

Wu, F., Zhao, S., Yu, B., Chen, Y.M., Wang, W., Song, Z.G., Hu, Y., Tao, Z.W., Tian, J.H., Pei, Y.Y., Yuan, M.L., Zhang, Y.L., Dai, F.H., Liu, Y., Wang, Q.M., Zheng, J.J., Xu, L., Holmes, E.C., Zhang, Y.Z. 2020. A new coronavirus associated with human respiratory disease in China. *Nature*, 579(7798):265-269.

Wu, Z., Ren, X., Yang, L., Hu, Y., Yang, J., He, G., Zhang, J., Dong, J., Sun, L., Du, J., Liu, L., Xue, Y., Wang, J., Yang, F., Zhang, S., Jin, Q. 2012. Virome analysis for

identification of novel mammalian viruses in bat species from Chinese provinces. *Journal of Virology*, 86(20):10999-1012.

Wu, Z., Yang, L., Ren, X., He, G., Zhang, J., Yang, J., Qian, Z., Dong, J., Sun, L., Zhu, Y., Du, J., Yang, F., Zhang, S., Jin, Q. 2016. Deciphering the bat virome catalog to better understand the ecological diversity of bat viruses and the bat origin of emerging infectious diseases. *ISME Journal*, 10(3):609-20.

Xu, Z., Feng, Y., Chen, X., Shi, M., Fu, S., Yang, W., Liu, W.J., Gao, G.F., Liang, G. 2021. Virome of bat-infesting arthropods: highly divergent viruses in different vectors. *Journal of Virology*, 96(4):e0146421.

Yadav, P.D., Raut, C.G., Shete, A.M., Mishra, A.C., Towner, J.S., Nichol, S.T., Mourya, D.T. 2012. Detection of Nipah virus RNA in fruit bat (Pteropus giganteus) from India. *American Journal of Tropical Medicine and Hygiene*, 87(3):576-8.

Yang, Y., Du, L., Liu, C., Wang, L., Ma, C., Tang, J., Baric, R.S., Jiang, S., Li, F. 2014. Receptor usage and cell entry of bat coronavirus HKU4 provide insight into bat-to-human transmission of MERS coronavirus. *Proceedings of the National Academy of Sciences of the United States of America*, 11121(34):516-21.

Yinda, C.K., Ghogomu, S.M., Conceição-Neto, N., Beller, L., Deboutte, W., Vanhulle, E., Maes, P., Van Ranst, M., Matthijnssens, J. 2018. Cameroonian fruit bats harbor divergent viruses, including rotavirus H, bastroviruses, and picobirnaviruses using an alternative genetic code. *Virus Evolution*, 4(1):vey008.

Yob, J.M., Field, H., Rashdi, A.M., Morrissy, C., van der Heide, B., Rota, P., bin Adzhar, A., White, J., Daniels, P., Jamaluddin, A., Ksiazek, T. 2001. Nipah virus infection in bats (order Chiroptera) in peninsular Malaysia. *Emerging Infectious Disease*, 7(3):439-41.

Young, P.L., Halpin, K., Selleck, P.W., Field, H., Gravel, J.L., Kelly, M.A., Mackenzie, J.S. 1996. Serologic evidence for the presence in Pteropus bats of a paramyxovirus related to equine morbillivirus. *Emerging Infectious Disease*, 2(3):239-40.

Zaki, A.M., van Boheemen, S., Bestebroer, T.M., Osterhaus, A.D., Fouchier, R.A. 2012. Isolation of a novel coronavirus from a man with pneumonia in Saudi Arabia. *The New England Journal of Medicine,* 367(19):1814-20.

Zana, B., Kemenesi, G., Buzás, D., Csorba, G., Görföl, T., Khan, F.A.A., Tahir, N., Zeghbib, S., Madai, M., Papp, H., Földes, F., Urbán, P., Herczeg, R., Tóth, G.E., Jakab, F. 2019. Molecular Identification of a Novel Hantavirus in Malaysian Bronze Tube-Nosed Bats (Murina aenea). *Viruses*, 11(10):887.

Zheng, X.Y., Qiu, M., Guan, W.J., Li, J.M., Chen, S.W., Cheng, M.J., Huo, S.T., Chen, Z., Wu, Y., Jiang, L.N., Chen, Q. 2018. Viral metagenomics of six bat species in close contact with humans in southern China. *Archives of Virology*, 163(1):73-88.

Zhou, H., Chen, X., Hu, T., Li, J., Song, H., Liu, Y., Wang, P., Liu, D., Yang, J., Holmes, E.C., Hughes, A.C., Bi, Y., Shi, W. 2020. A Novel Bat Coronavirus Closely Related to SARS-CoV-2 Contains Natural Insertions at the S1/S2 Cleavage Site of the Spike Protein. *Current Biology*, 30(11):3896.

Zhou, H., Ji, J., Chen, X., Bi, Y., Li, J., Wang, Q., Hu, T., Song, H., Zhao, R., Chen, Y., Cui, M., Zhang, Y., Hughes, A.C., Holmes, E.C., Shi, W. 2021. Identification of novel bat coronaviruses sheds light on the evolutionary origins of SARS-CoV-2 and related viruses. *Cell380-4391*.

Zhou, P., Fan, H., Lan, T., Yang, X.L., Shi, W.F., Zhang, W., Zhu, Y., Zhang, Y.W., Xie, Q.M., Mani, S., Zheng, X.S., Li, B., Li, J.M., Guo, H., Pei, G.Q., An, X.P., Chen, J.W., Zhou, L., Mai, K.J., Wu, Z.X., Li, D., Anderson, D.E., Zhang, L.B., Li, S.Y., Mi, Z.Q., He, T.T., Cong, F., Guo, P.J., Huang, R., Luo, Y., Liu, X.L., Chen, J., Huang, Y., Sun, Q., Zhang, X.L., Wang, Y.Y., Xing, S.Z., Chen, Y.S., Sun, Y., Li, J., Daszak, P., Wang, L.F., Shi, Z.L., Tong, Y.G., Ma, J.Y. 2018. Fatal swine acute diarrhoea syndrome caused by an HKU2-related coronavirus of bat origin. *Nature*, 556(7700):255-258.

Zhou, P., Tachedjian, M., Wynne, J.W., Boyd, V., Cui, J., Smith, I., Cowled, C., Ng, J.H., Mok, L., Michalski, W.P., Mendenhall, I.H., Tachedjian, G., Wang, L.F., Baker, M.L. 2016. Contraction of the type I IFN locus and unusual constitutive expression of IFN-α in bats. *Proceedings of the National Academy of Sciences of the United States of America*, 113(10):2696-701.

Chapter six: Faecal virome of the Australian grey-headed flying fox from urban/suburban environments contains novel coronaviruses, retroviruses and sapoviruses

Kate Van Brussel[1], Jackie E. Mahar[1], Ayda Susana Ortiz-Baez[1], Maura Carrai[2], Derek Spielman[3], Wayne S. J. Boardman[4], Michelle L. Baker[5], Julia A. Beatty[2], Jemma L. Geoghegan[6], Vanessa R. Barrs[2,7] and Edward C. Holmes[1]

[1]Sydney Institute for Infectious Diseases, School of Life & Environmental Sciences and School of Medical Sciences, The University of Sydney, NSW, 2006, Australia.

[2]Jockey Club College of Veterinary Medicine & Life Sciences, City University of Hong Kong, Kowloon Tong, Hong Kong, SAR China.

[3]School of Veterinary Science, Faculty of Science, University of Sydney, Sydney, NSW 2006, Australia.

[4]School of Animal and Veterinary Sciences, Faculty of Science, Engineering and Technology, University of Adelaide, Adelaide, SA 5371, Australia.

[5]CSIRO Australian Centre for Disease Preparedness, Health and Biosecurity Business Unit, Geelong, VIC 3220, Australia.

[6]Department of Microbiology and Immunology, University of Otago, Dunedin 9010, New Zealand; Institute of Environmental Science and Research, Wellington 5022, New Zealand.

[7]Centre for Animal Health and Welfare, City University of Hong Kong, Kowloon Tong, Hong Kong, China.

6.1: Abstract

Bats are important reservoirs for viruses of public health and veterinary concern. Virus studies in Australian bats usually target the families *Paramyxoviridae*, *Coronaviridae* and *Rhabdoviridae*, with little known about their overall virome composition. We used metatranscriptomic sequencing to characterise the faecal virome of grey-headed flying foxes from three colonies in urban/suburban locations from two Australian states. We identified viruses from three mammalian-infecting (*Coronaviridae*, *Caliciviridae*, *Retroviridae*) and one possible mammalian-infecting (*Birnaviridae*) family. Of particular interest were a novel bat betacoronavirus (subgenus *Nobecovirus*) and a novel bat sapovirus (*Caliciviridae*), the first identified in Australian bats, as well as a potentially exogenous retrovirus. The novel betacoronavirus was detected in two sampling locations 1,375 km apart and falls in a viral lineage likely with a long association with bats. This study highlights the utility of unbiased sequencing of faecal samples for identifying novel viruses and revealing broad-scale patterns of virus ecology and evolution.

6.2: Introduction

Bats (order Chiroptera) are one of the largest mammalian orders with a unique physiology adapted for flight. The number of bat colonies in urban habitats has increased in recent decades, leading to more frequent interactions with humans, companion animals and livestock that have in turn facilitated outbreaks of zoonotic disease (Plowright et al., 2011). This process has been dramatically highlighted by the emergence of severe acute respiratory syndrome coronavirus 2 (SARS-CoV-2) and the detection of SARS-like coronaviruses in Asian bat populations (Temmam et al., 2022, Zhou et al., 2021, Zhou et al., 2020, Wacharapluesadee et al., 2021, Murakami et al., 2020). In addition, bats have been associated with the emergence of Hendra virus (Halpin et al., 2000), Nipah virus (Yob et al., 2001), lyssaviruses (Botvinkin et al., 2003, Gould et al., 1998) and SARS-CoV-1 (Li et al., 2005). In turn, these outbreaks have led to an increased sampling of bat species, and the widespread use of metagenomic sequencing has enabled more detailed exploration of the bat virome (Wu et al., 2016, Hardmeier et al., 2021, Van Brussel and Holmes, 2022).

In Australia, bat species of the *Pteropus* genus are reservoir hosts for Hendra virus and Menangle virus, zoonotic pathogens of the family *Paramyxoviridae* (Halpin et al., 2000, Philbey et al., 1998), as well as Australian bat lyssavirus, a zoonotic virus of the

Rhabdoviridae that causes rabies in mammals (Gould et al., 1998). Studies of viruses in bats in Australia have largely focused on these virus families and recently identified a new member of the *Paramyxoviridae* – Cedar virus – as well as a novel genotype of Hendra virus (Wang et al., 2021, Marsh et al., 2012). Although important, these studies lack information on overall virome composition, particularly those virus families not included in targeted PCR studies.

The grey-headed flying fox (Pteropus poliocephalus), a member of the megabat family Pteropodidae and native to Australia, is a species of importance in the context of zoonotic viruses. Grey-headed flying foxes are distributed throughout the eastern coastline of Australia (Queensland, New South Wales and Victoria) and more recently a colony was established in Adelaide (South Australia). Grey-headed flying foxes feed on fruit, pollen and nectar and roost in large colonies, sometimes sharing roosting locations with other species of Pteropus, allowing intraspecies and interspecies virus transmission (Timmiss et al., 2021). Roosting sites are commonly located alongside human communities including in densely populated urban settings (Williams et al., 2006). As numerous viruses are transmitted by faeces and other excretions, the co-habitation between bats and humans likely increases the risk of zoonotic spill-over.

Herein, we used metatranscriptomic sequencing of faecal samples to describe the community of viruses present in the gastrointestinal tract of grey-headed flying foxes from three sampling locations in two Australian states – Centennial Park and Gordon in Sydney, New South Wales, and the Botanic Park, Adelaide in South Australia. Specifically, to reveal the composition and abundance of viruses in bats residing in metropolitan areas we sampled roosting sites either located in a residential setting or in parks that are frequented by humans.

6.3: Methods

6.3.1: Sample collection

Faecal samples were collected from grey-headed flying fox roosting sites in three regions of Australia: Centennial Parklands, Centennial Park New South Wales (NSW), Gordon NSW, and Botanic Park, Adelaide parklands, Adelaide, South Australia (Table 6.3.1, Figure 6.3.1.A). Sampling was conducted over two dates in 2019 for the Centennial Park and Gordon sites, while the roosting site in the Adelaide parklands was sampled over several

months in 2019 (Table 6.3.1). A plastic sheet of approximately 3 x 5 m was placed under densely populated trees the night before collection. The following morning samples captured by the plastic sheet were placed into 2 mL tubes and immediately stored at -80°C until processing. Any faecal sample touching or submerged in urine was discarded.

Table 6.3.1: Sampling overview, including number of samples allocated to sequencing pools and sequencing metadata.

| Location	Sampling date	Pool no.	No. of samples	No. of reads	No. of contigs
Centennial Park, NSW 33. 89999ºS, 151.23592ºE	5 February 2019	01	12	24,732,494	159,527
		02	9	35,835,953	147,425
		03	9	31,960,624	107,431
	26 February 2019	04	9	19,833,973	111,196
		05	11	31,410,836	136,180
		06	9	29,318,213	105,118
		07	10	19,160,704	90,339
Gordon, NSW 33.75065ºS, 151.16242ºE	12 March 2019	01	12	52,605,108	89,247
		02	12	48,784,843	50,574
		03	9	27,396,450	118,509
	26 March 2019	04	11	36,591,148	181,524
		05	12	36,815,461	146,466
		06	12	52,934,611	97,013
		07	10	37,980,832	156,960
Adelaide, SA 34.91571ºS, 138.6068ºE	2019	01	8	25,977,712	135,969
	2019	02	9	21,113,731	113,546
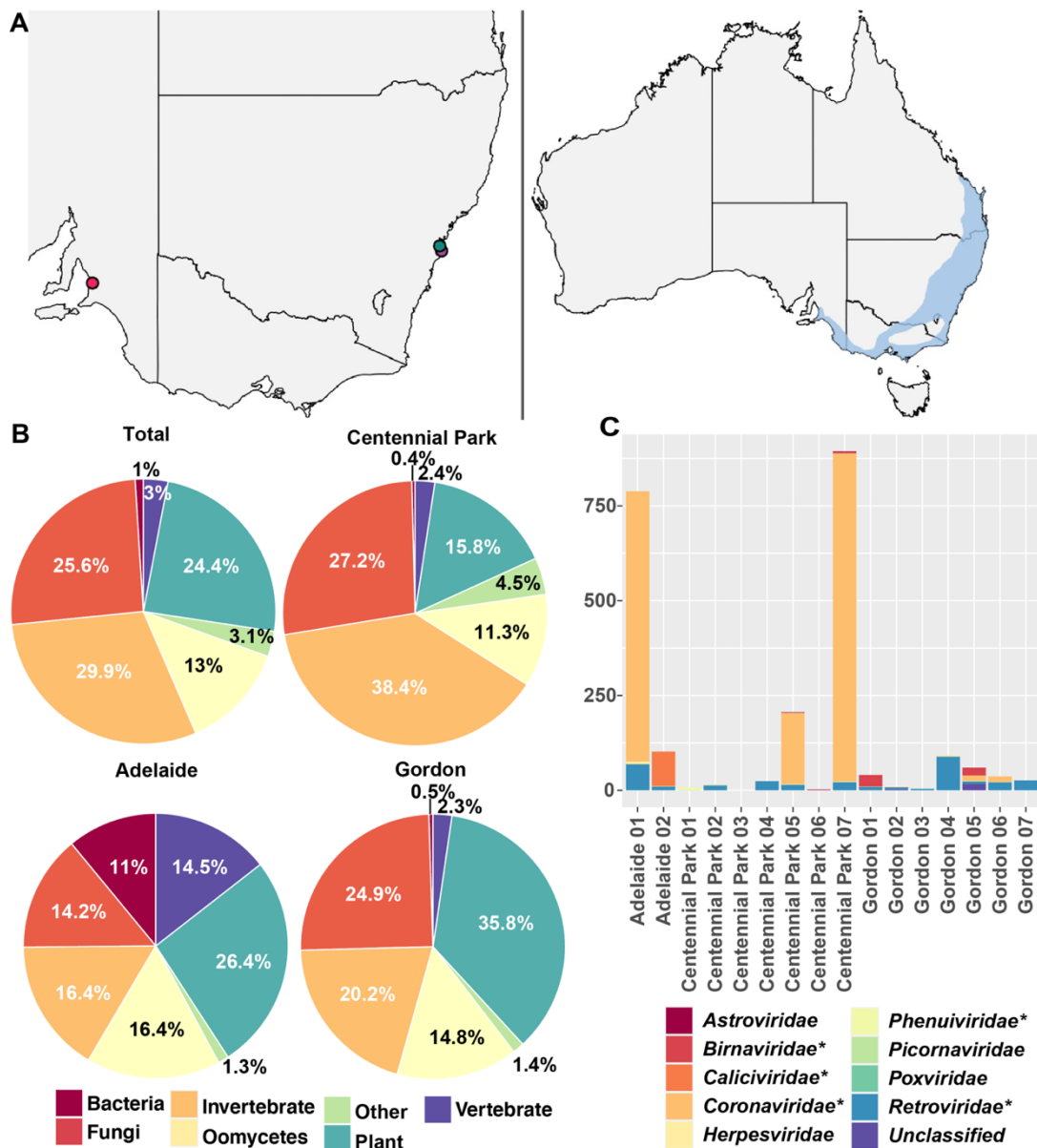
Figure 6.3.1: Overview of sampling sites and bat faecal sample composition. (A) Sampling locations in Australia (left) and distribution map of the grey-headed flying fox (right) (IUCN, 2021). (B) Likely hosts of virus contigs based on host designation of the closest relatives in the NCBI non-redundant protein database. (C) Read abundance presented as reads per million (RPM) for the vertebrate-associated virus sequences for each library and separated by virus family. The virus families discussed in this study are highlighted with an asterisk.

6.3.2: RNA extraction, sequencing and read processing

Faecal samples were homogenised at 5 ms−1 for 1.5 min using the Omni Bead Ruptor 4 with 1.44 mm ceramic beads (Omni international) in 600 μL lyse buffer. Total RNA was extracted from each sample individually using the RNeasy Plus Mini Kit (Qiagen) following the

manufacturer's protocol. RNA was pooled in equimolar ratios and separated by sampling location, date and RNA concentration (Table 6.3.1). Ribosomal RNA was depleted followed by the construction of sequencing libraries constructed using the Illumina Stranded Total RNA Prep with Ribo-Zero Plus (Illumina) preparation kit. Libraries were sequenced as 150 bp paired-end on the Illumina Novaseq 6000 platform at the Australian Genome Research Facility (AGRF). Read ends with a quality score of below 25 phred and adapter sequences were removed using cutadapt v1.8.3 (Kechin et al., 2017). Sortmerna v4.3.3 was used to remove 5 S and 5.8 S, eukaryotic 18 S and 23 S, bacterial 16 S and 23 S, and Archaea 16 S and 23 S ribosomal RNA (rRNA) reads (Kopylova et al., 2012). The filtered reads were then de novo assembled using Megahit v1.1.3 (Li et al., 2015) and the contigs were compared to the non-redundant protein database using diamond v2.0.9. The Genemark heuristic approach (Besemer and Borodovsky, 1999, Zhu et al., 2010) and information from closely related viruses were used to predict genes and annotate genomes. Intact retrovirus genomes were detected using an in-house pipeline (Chang et al., manuscript in preparation). The Geneious assembler (available in Geneious Prime version 2022.1.1) was used to reassemble megahit contigs from multiple libraries for bat faecal associated retrovirus 2 (see Results). The final sequence for bat faecal associated retrovirus 2 (see Results) was determined by mapping reads from all libraries to the reassembled genome on Geneious Prime and using a 0% (majority) threshold for the final consensus sequence. Additionally, a negative control extraction library was sequenced to help exclude viral contaminants. No viruses present in the negative control library were present in the bat faecal libraries.

6.3.3: Abundance estimation

Virus and host abundance were estimated by mapping non-rRNA reads from each library to assembled contigs, and to the COX1 gene (accession no. KF726143) from the *P. alecto* (Black flying fox) genome using the Bowtie2 v2.3.4.3 alignment method in RSEM and expected count values (Langmead and Salzberg, 2012). The impact of index-hopping was minimised by excluding the expected count for a contig in any library that was less than 0.01% of the highest read count for that assembled contig in any other library.

6.3.4: Phylogenetic analysis

Virus amino acid sequences were aligned with related sequences (i.e., representing the same virus family and/or genus) retrieved from the NCBI/GenBank database using MAFTT v7.450 (Katoh and Standley, 2013) and the E-INS-I algorithm (Katoh et al., 2005). The partial RdRp

sequence of P. alecto/Aus/SEQ/2009 was retrieved from Smith et al. (2016). The gappyout method in TrimAL v1.4.1 was used to remove ambiguous regions in the alignment (Capella-Gutiérrez et al., 2009). Maximum likelihood trees of each data set were inferred using IQ-TREE v1.6.7 (Nguyen et al., 2014), employing the best-fit amino acid substitution model determined by the ModelFinder program (Kalyaanamoorthy et al., 2017) in IQ-TREE. Nodal support was accessed using 1000 ultrafast bootstrap replicates (Hoang et al., 2017). Any virus sequence in this study with over 90% nucleotide similarity to another sequence detected here was excluded from phylogenetic analysis.

6.3.5: PCR validation of coronavirus, sapovirus and retrovirus

SuperScript IV One-Step RT-PCR (Invitrogen) was used to amplify bat faecal coronavirus CP07/aus/1 (RdRp), bat faecal sapovirus Ad02/aus/1 (RdRp), bat faecal associated retrovirus 1 G04/aus/1 (pol) and bat faecal associated retrovirus AdCPG/aus/1 (complete genome) from total RNA from all 16 sequencing library pools (Table 6.7.2).

6.4: Results

6.4.1: Virome overview

In total, 164 faecal samples allocated to 16 libraries underwent metatranscriptomic sequencing. This generated 19,160,704 to 52,934,611 reads per library (average of 33,278,293 reads) after read filtering (Table 6.3.1). Reads were de novo assembled into 50,574 to 181,524 contigs (average of 121,689 contigs) per library (Table 6.3.1). A total of 5,933 contigs were assigned as of viral origin across all the libraries. The samples collected at Centennial Park, Sydney produced the most viral contigs, with 3,216 identified from 65 virus families (Figure 6.7.1). The Gordon, NSW sample site produced 2,399 virus contigs from 66 virus families, while the Adelaide site contained 318 virus contigs from 33 virus families, although this site had only two sequencing libraries comprising 17 faecal samples, compared to seven sequencing libraries for each of the other two locations (69 faecal samples from Centennial Park, 78 from Gordon) (Table 6.3.1, Figure 6.7.1).

Analysis of read abundance of the 5,933 virus contigs identified by screening the NCBI protein database revealed that virus reads were largely associated with viruses of invertebrates (26.42% of total contigs), fungi (40.06%), plants (26.61%), representing 79 virus families (Figure 6.3.1B, Figure 6.7.1). These viruses were most likely associated with host diet and differed in frequency depending on sampling site (Figure 6.3.1B, Figure 6.7.1).

The plant, fungal, and oomycete-associated viruses, as well as those likely to be bacteriophage (including the picobirnaviruses) were not considered further. Importantly, however, we also identified sequences from viruses likely associated with mammalian infection (3% overall), including near complete genomes from members of the *Coronaviridae*, *Caliciviridae* and *Retroviridae* (Figure 6.3.1B).

6.4.2: Mammalian-associated viruses

We detected contigs from nine viral families likely to infect mammals (Figure 6.3.1C). The *Coronaviridae* and *Retroviridae* were particularly abundant and present in 10 and 16 libraries, respectively (Figure 6.3.1C). Members of the *Birnaviridae* and *Caliciviridae* were also abundant in specific libraries (Figure 6.3.1C). The remaining mammalian-associated viral families were only detected at low abundance and the contigs were not of sufficient length for further characterisation.

6.4.3: Novel betacoronavirus (*Coronaviridae*)

A novel complete betacoronavirus genome (single-strand, positive-sense RNA virus; +ssRNA) – provisionally denoted bat faecal coronavirus CP07/aus/1 – was identified in a sequencing library sampled from Centennial Park (pool no. 07) and in a sequencing library from Adelaide (pool no. 01). These two sequences exhibited 99.8% identity over the complete viral genome indicating that they represent the same species. Additionally, three sequences with 99.2-100% sequence identity to CP07/aus/1 were identified in an additional Centennial Park library (pool no. 05).

CP07/aus/1 contains ten ORFs in the arrangement ORF1a, ORF1ab, spike, NS3, envelope, matrix, nucleocapsid, NS7a, NS7b and NS7c. Transcription Regulatory Sequences (TRS) preceeded all ORFs. Additional bat coronavirus contigs ranging from 318 to 1,309 bp were detected in sequencing libraries from two Gordon sampling locations. These short contigs shared 40-95% amino acid identity to CP07/aus/1. Three of these contigs contained RdRp or spike amino acid sequences of sufficient length for phylogenetic analysis, and these were provisionally denoted bat faecal coronavirus G05/aus/1, G05/aus/2 and G05/aus/3. Based on phylogenetic analysis of the RNA-dependent RNA polymerase (RdRp) and/or spike protein, the novel betacoronaviruses detected here fell within the *Betacoronavirus* subgenus *Nobecovirus* (Figure 6.4.3) and were most closely related to P.alecto/Aus/SEQ/2009 (for which only a partial RdRp is available) sampled from a black flying fox in south east Queensland, Australia (Smith et al., 2016) and to Pteropus rufus nobecovirus sampled from a

flying fox in Madagascar (accession no. OK067319; Figure 6.4.3) (Kettenburg et al., 2022). Pairwise comparisons revealed that CP07/aus/1 had 83% amino acid identity to Pteropus rufus nobecovirus over the complete ORF1ab replicase and 97% to P.alecto/Aus/SEQ/2009 over the partial RdRp. Amino acid identity to Pteropus rufus nobecovirus over the spike and non-structural proteins was 72% and 58%, respectively. The RdRp of G05/aus/1 shared 95% amino acid identity to CP07/aus/1, while the partial spike proteins of G05/aus/2 and G05/aus/3 shared 57% and 63% amino acid identity to CP07/aus/1, respectively. It is possible that G05/aus/1 and G05/aus/2 represent transcripts from the same virus, while G05/aus/3 represents a different species to CP07/aus/1. However, this could not be confirmed as the G05/aus/3 genome was incomplete. Regardless, it is clear from the spike protein phylogeny that at least three different coronaviruses are circulating in the bats sampled here.

Figure 6.4.3: Phylogenetic relationships of the novel bat betacoronaviruses based on the amino acid sequences of the RdRp and spike protein. Amino acid alignment lengths were 832 and 1,092 residues for the RdRp and Spike protein, respectively. Representative betacoronavirus sequences from this study are coloured by sampling location (Centennial Park, Sydney – purple, Gordon – green) and the subgenera are highlighted. Bootstrap values >70% are represented by the symbol shown at the branch node. The tree is rooted at midpoint for clarity and the scale bar represents the amino acid substitutions per site.

6.4.4: Novel sapovirus (*Caliciviridae*)

A near complete genome of a novel sapovirus (*Caliciviridae*, +ssRNA virus), tentatively named bat faecal sapovirus Ad02/aus/1, was detected in a sequencing library sampled from Adelaide (pool no. 2). Nine additional bat sapovirus sequences ranging from 340 to 783 bp were detected in the same sequencing library. The nine sequences shared 66-74% nucleotide and 76-81% amino acid identity to Ad02/aus/1 over the polyprotein, suggesting the presence of additional diverse sapoviruses. The near complete Ad02/aus/1 genome is 7,254 bp and contains two ORFs encoding a polyprotein (near complete with likely 45 residues missing from the 5' end), and the VP2. Ad02/aus/1 exhibited 44.8% amino acid identity in the partial polyprotein to its closest relative – Bat sapovirus Bat-SaV/Limbe65/CAM/2014 (accession no. KX759620) – detected in the faeces of *Eidolon helvum* bats in Cameroon, Africa (Yinda et al., 2017). Phylogenetic analysis of the RdRp and VP1 revealed a clustering of bat sapoviruses in both trees that included the novel Australian bat sapoviruses found here (Figure 6.4.4). Bat sapoviruses have been assigned to the putative genogroups GXIV, GXVI, GXVII, GXVIII and GXIX based on VP1 phylogeny and amino acid sequence identities. Using the same criteria, the novel sapovirus Ad02/aus/1 identified here should be assigned to its own genogroup, putatively named GXX which would also include the partial VP1 Ad02/aus/4 sequence (Table 6.7.1, Figure 6.4.4).
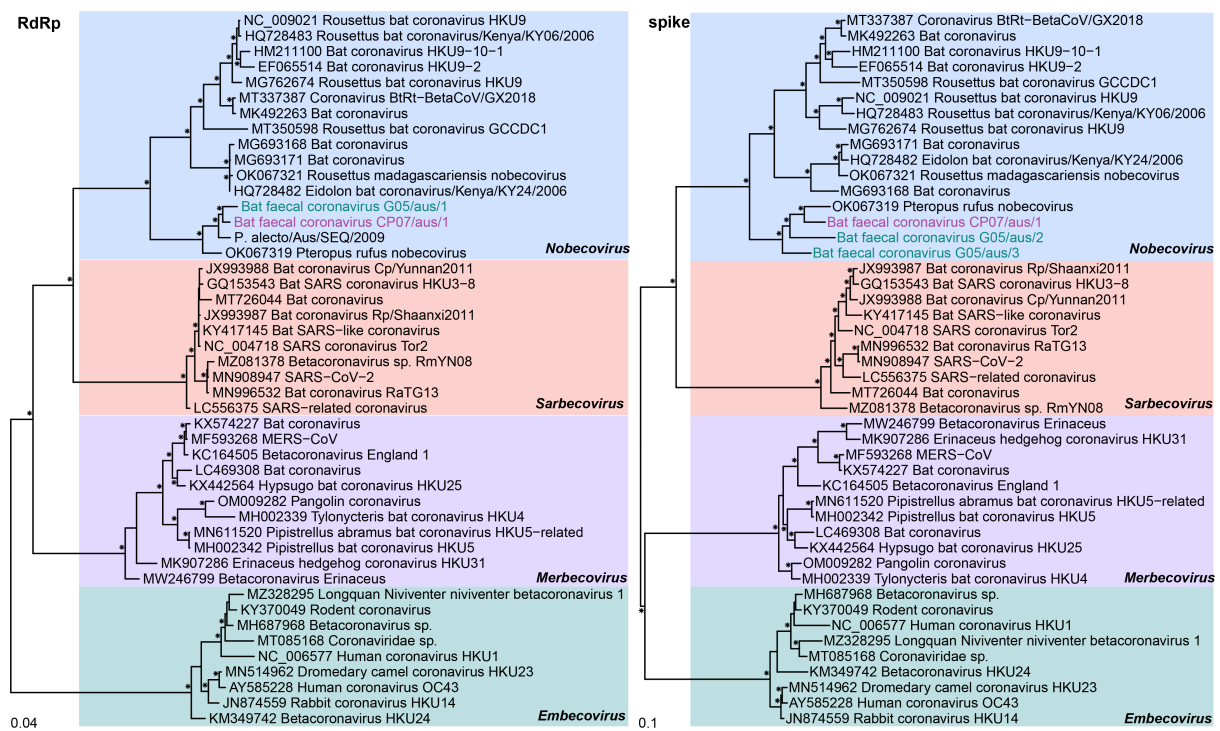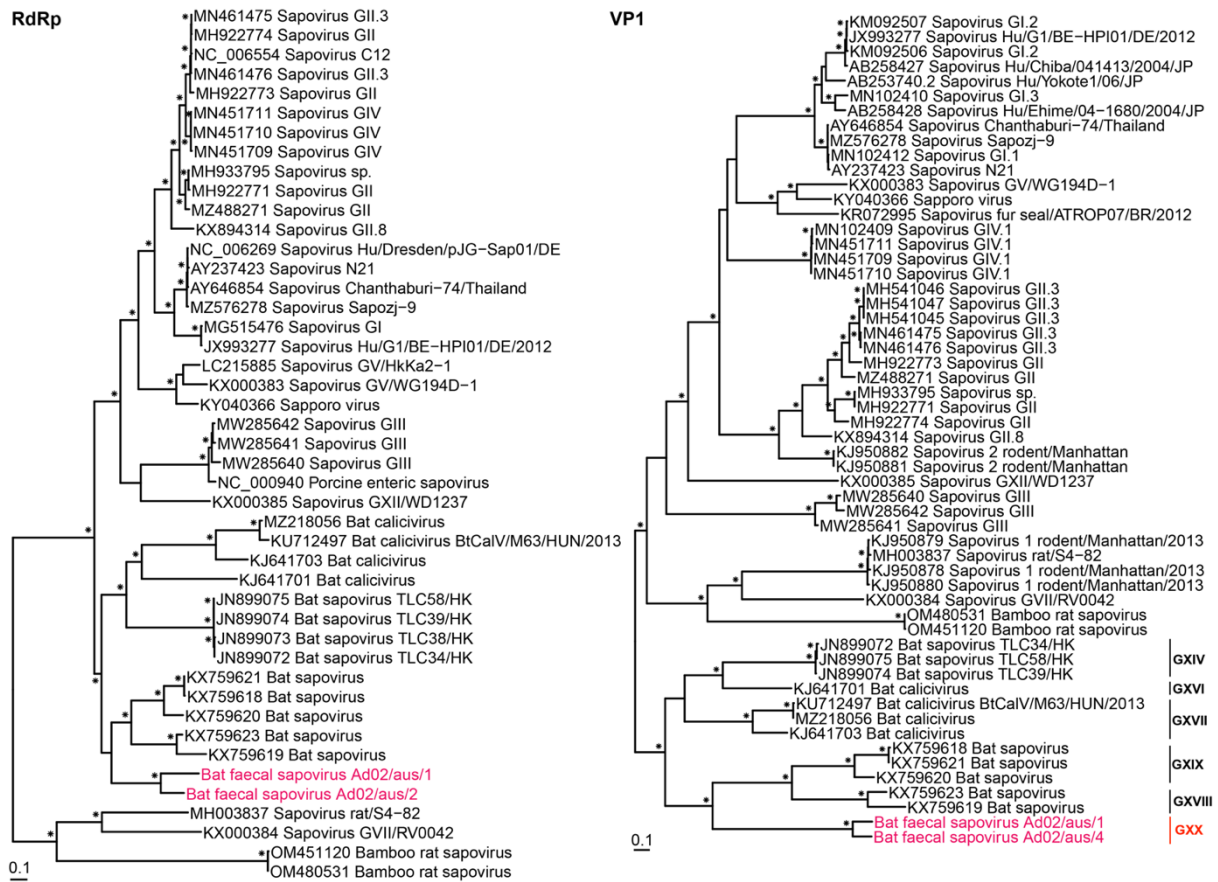
Figure 6.4.4: Phylogenetic relationships of the novel bat sapoviruses using the amino acid sequences of the RdRp and VP1. Amino acid alignment lengths were 491 and 623 residues for the RdRp and VP1, respectively. Bat sapoviruses from this study are coloured by sampling location (Adelaide – pink) and bootstrap values >70% are represented by the symbol shown at the branch node. The putative bat sapovirus genogroups are displayed to the right of the VP1 tree and our proposed putative genogroup is coloured in red. The trees are rooted at midpoint for clarity and the scale bar represents the amino acid substitutions per site.

6.4.5: Novel birna-like virus (*Birnaviridae*)

Sequences related to the *Birnaviridae* (double-stranded RNA viruses; dsRNA) were detected in one Centennial Park and two Gordon libraries. All the birna-like virus sequences identified in the Centennial Park and Gordon libraries shared >99% nucleotide identity, and the complete coding region of segment B, which encodes the RdRp, was obtained from one library (Gordon 05). The *Birnaviridae* segment A that encodes the polyprotein and a small overlapping ORF was not identified in our data. Phylogenetic analysis revealed that the birna-

like virus RdRp sequence, denoted G05/aus/1, was most closely related (50% amino acid identity) to the disease-causing virus Chicken proventricular necrosis virus (Figure 6.4.5) (Guy et al., 2011), forming a distinct clade that is distantly related to the birnaviruses that infect a wide range of hosts.
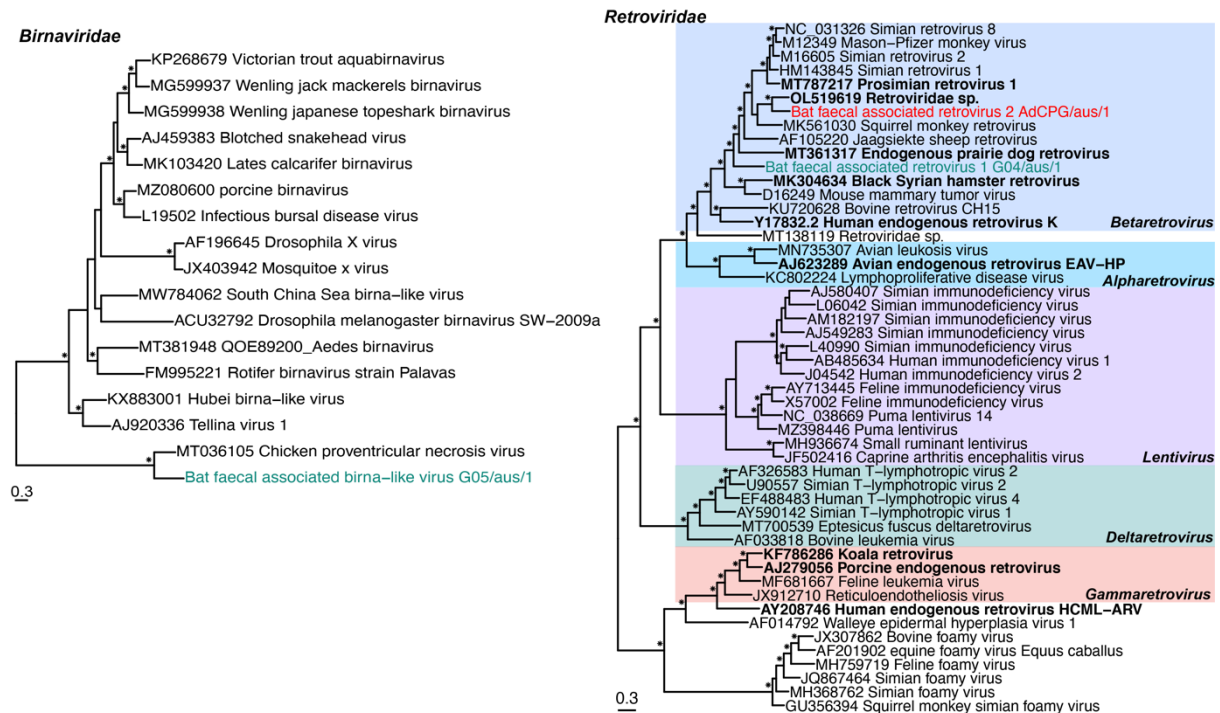

Figure 6.4.5: Phylogenetic analysis of the birna-like virus and bat retroviruses based on the RdRp and pol amino acid sequences, respectively. The Birnaviridae RdRp sequence alignment was 767 amino acid resides in length while the Retroviridae pol alignment comprised 1,356 residues. The viruses from this study are coloured by sampling location (Gordon – green) and the reassembled retrovirus sequence is in red (to indicate multiple locations). The Retroviridae genera are highlighted and bootstrap values >70% are represented by the symbol shown at the branch node. The tree is midpoint rooted for clarity, with the scale bar representing the amino acid substitutions per site.

6.4.6: Bat retrovirus (*Retroviridae*)

A near complete genome of a retrovirus was identified in Gordon library 04 and provisionally named bat faecal associated retrovirus 1 G04/aus/1. Four ORFs were observed over the 7,455 bp genome and assigned as the gag, pro, pol and env genes based on the presence of conserved domains. In the pro gene we were able to identify an active site motif DTGAD predominately observed in functional retroviruses, and a helix motif GRDVL (Turnbull and Douville, 2018). We were unable to identify complete long terminal repeat (LTR) regions in

the 7,455 bp genome, although this may be due to incomplete assembly at the 5' and/or 3' end, rather than a true absence of LTRs. Importantly, as the four ORFs contained the appropriate retrovirus conserved domains and were uninterrupted by stop codons, it is possible that G04/aus/1 is potentially exogenous and functional. A BLASTn analysis of the complete G04/aus/1 genome revealed no match to any bat reference genome on NCBI/GenBank. G04/aus/1 exhibited 56% amino acid identity in the pol protein to its closest relative, Simian retrovirus 2 (accession M16605), a presumably exogenous retrovirus (Thayer et al., 1987). The abundance for this novel retrovirus in the Gordon 04 library was 90 RPM (2,453 reads) (Figure 6.3.1C).

A further near complete retroviral genome was identified by reassembling 31 partial contig sequences from 10 libraries from all three sample locations. PCR confirmed that the entire genome was present in the G07 sequencing library pool. This Bat faecal associated retrovirus 2 AdCPG/aus/1 is 6,630 bp and contains four open reading frames encoding the gag, pro, pol and env genes. It also contains the conserved domains expected in functional retroviruses, although the terminal end of the env gene is missing (either from true truncation or incomplete assembly). AdCPG/aus/1 is most closely related to a retrovirus sampled from the lung tissue of Malayan pangolins (Ning et al., 2022). BLASTn analysis of the complete genome of AdCPG/aus/1 showed the absence of this genome in any bat reference genome on NCBI/GenBank. AdCPG/aus/1 reads were detected in 13 libraries (two Adelaide, four Centennial Park and seven Gordon) and the abundance in each library ranged from 3.7 – 68.8 RPM (127 – 1,786 reads) (Figure 6.3.1C). Phylogenetic analysis of the pol protein that contains the reverse transcriptase (RT) domain revealed that G04/aus/1 and AdCPG/aus/1 fell within the genus *Betaretrovirus*, clustering with both exogenous and endogenous retroviruses associated with various mammalian species (Figure 6.4.5).

6.4.7: PCR confirmation

PCR confirmed that bat faecal coronavirus CP07/aus/1, bat faecal sapovirus Ad02/aus/1 and bat faecal associated retrovirus 1 G04/aus/1 were present in eight, one and three library pools, respectively (Table 6.7.2). For all the library pools that were PCR positive, metagenomic read abundance was above the 0.01% index-hopping cut-off, although in the case of library pool CP06 read abundance was slightly below this cut-off. Library pools that had no sequence reads for these viruses were also negative by PCR (Table 6.7.2).

6.4.8: Invertebrate-associated viruses

We detected likely invertebrate-associated virus sequences from seven single-strand negative-sense RNA viruses (-ssRNA), three +ssRNA virus and one dsRNA virus families, in addition to the order *Bunyavirales* (-ssRNA). The virus sequences from the *Chuviridae*, *Lispiviridae*, *Artoviridae*, *Nyamiviridae*, *Xinmoviridae*, *Qinviridae*, *Disctroviridae* and *Iflaviridae* are not discussed further, although information on positive libraries is provided (Figure 6.7.1) and phylogenetic analysis was performed (Figure 6.7.2). Virus sequences from the *Orthomyxoviridae*, *Nodaviridae*, *Reoviridae* and *Bunyavirales* are considered further as these viral groups include mammalian-infecting viruses, are important vector-borne viruses, or are able to infect mammals experimentally (*Nodaviridae*, genus *Alphanodavirus*).

Orthomyxovirus (-ssRNA virus) segments were identified in five libraries from Centennial Park. Full coding regions for two polymerase segments – PB2 and PA – and the hemagglutinin segment 2 and nucleocapsid segment 5 were present in all libraries, although a full coding region for polymerase segment PB1 was only present in a single Centennial Park library. The three polymerase proteins of Centennial Park library 06 were used for phylogenetic analysis, which revealed that this sequence was most closely related to an orthomyxovirus sampled from jumping plant lice in Australia (Figure 6.4.8.1) (Käfer et al., 2019). Nodaviruses (+ssRNA virus) were detected in five Centennial Park libraries and three Gordon libraries. Both the RNA1 (RdRp) and RNA2 segments were identified, including two sequences with the complete RdRp. Nodavirus CP01/aus/1 and CP02/aus/1 were related to a nodavirus sampled from birds in China (Zhu et al., 2022) and most likely belong to the same viral species, although these fragments were only 476 and 232 amino acids, respectively. The nodavirus CP07/aus/1 RdRp segment was related to a nodavirus from arthropod hosts from China (Figure 6.4.8.1) (Shi et al., 2016). Gene segments related to the Reoviridae (dsRNA) were present in all Centennial Park, three Gordon and one Adelaide library. The reovirus VP1 Pol segments detected here were related, albeit distantly (~40% amino acid identity) to reoviruses associated with ticks (Harvey et al., 2019, Vanmechelen et al., 2021), moths (Graham et al., 2006), bat flies (Xu et al., 2022) and the Asian citrus psyllid (Nouri et al., 2015) (Figure 6.4.8.1).
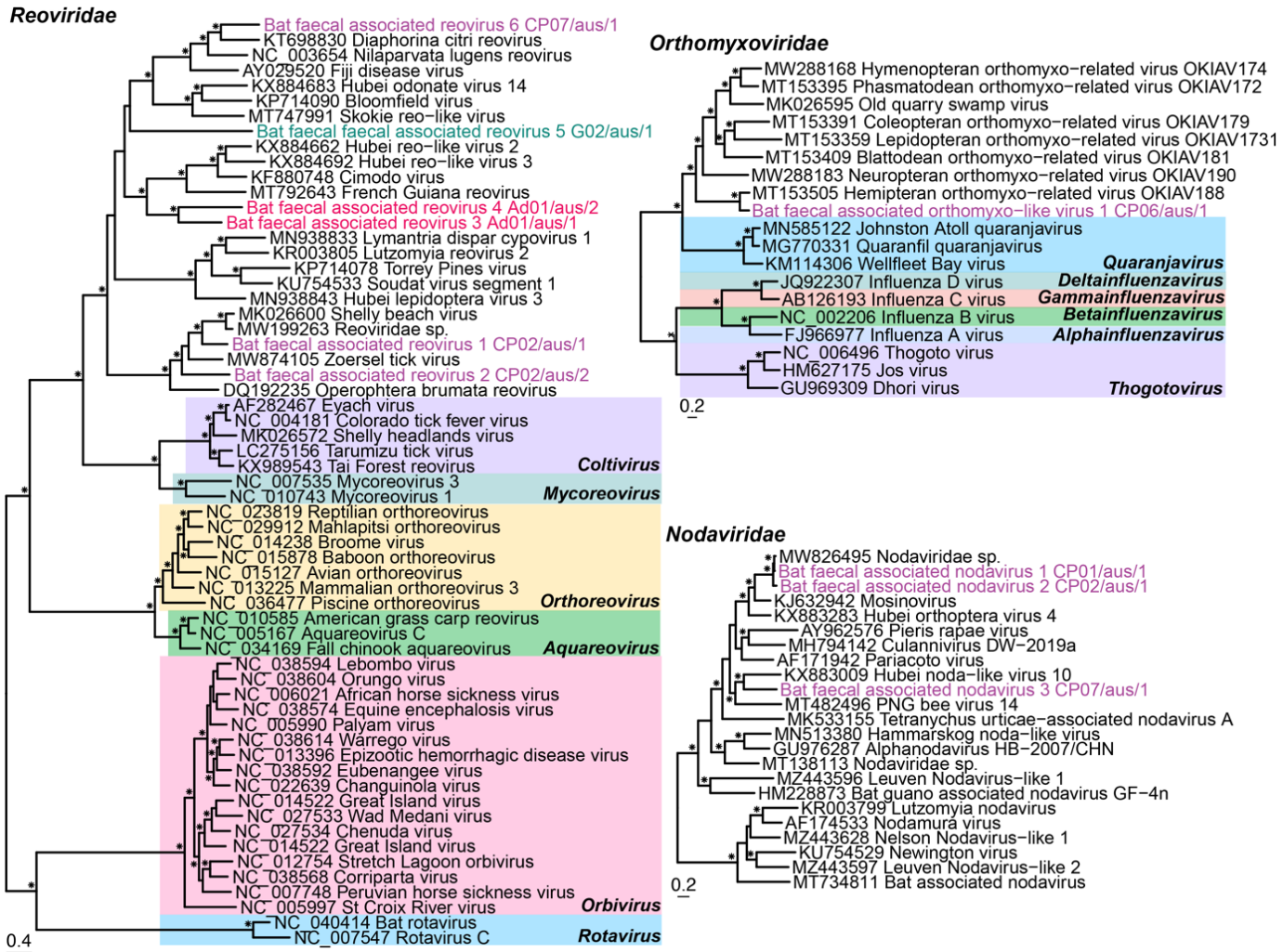
Figure 6.4.8.1: Phylogenetic analysis of the invertebrate-assocaited reoviruses, orthomyxoviruses and nodaviruses based on the VP1 Pol, concatenated PB2-PB1-PA and RdRp amino acid sequences, respectively. Amino acid alignment length were 1,020 residues for Reoviridae, 2,233 residues for the Orthomyxoviridae and 774 residues for the Nodaviridae. Viruses from this study are coloured by sampling location (Adelaide – pink, Centennial Park – purple and Gordon – green) and genera are highlighted in the Reoviridae and Orthomyxoviridae tress. Bootstrap values >70% are represented by the symbol shown at the branch node. The tree is rooted at midpoint for clarity and the scale bar represents the amino acid substitutions per site.

Finally, bunyavirus fragments were detected in all the Adelaide and Centennial Park libraries and six Gordon libraries. Eleven RdRp coding regions were used for phylogenetic analysis which revealed that two bunyavirus sequences fell into the *Phenuiviridae* and four were basal to that family, while two sequences fell into the *Phasmaviridae*, two were basal to the *Arenaviridae* and one was basal to a grouping of five families (Figure 6.4.8.2). The Adelaide

bunyavirus Ad02/aus/1 was related to the plant associated genus *Tenuivirus* and the remaining 10 were related to invertebrate hosts (Figure 6.4.8.2).
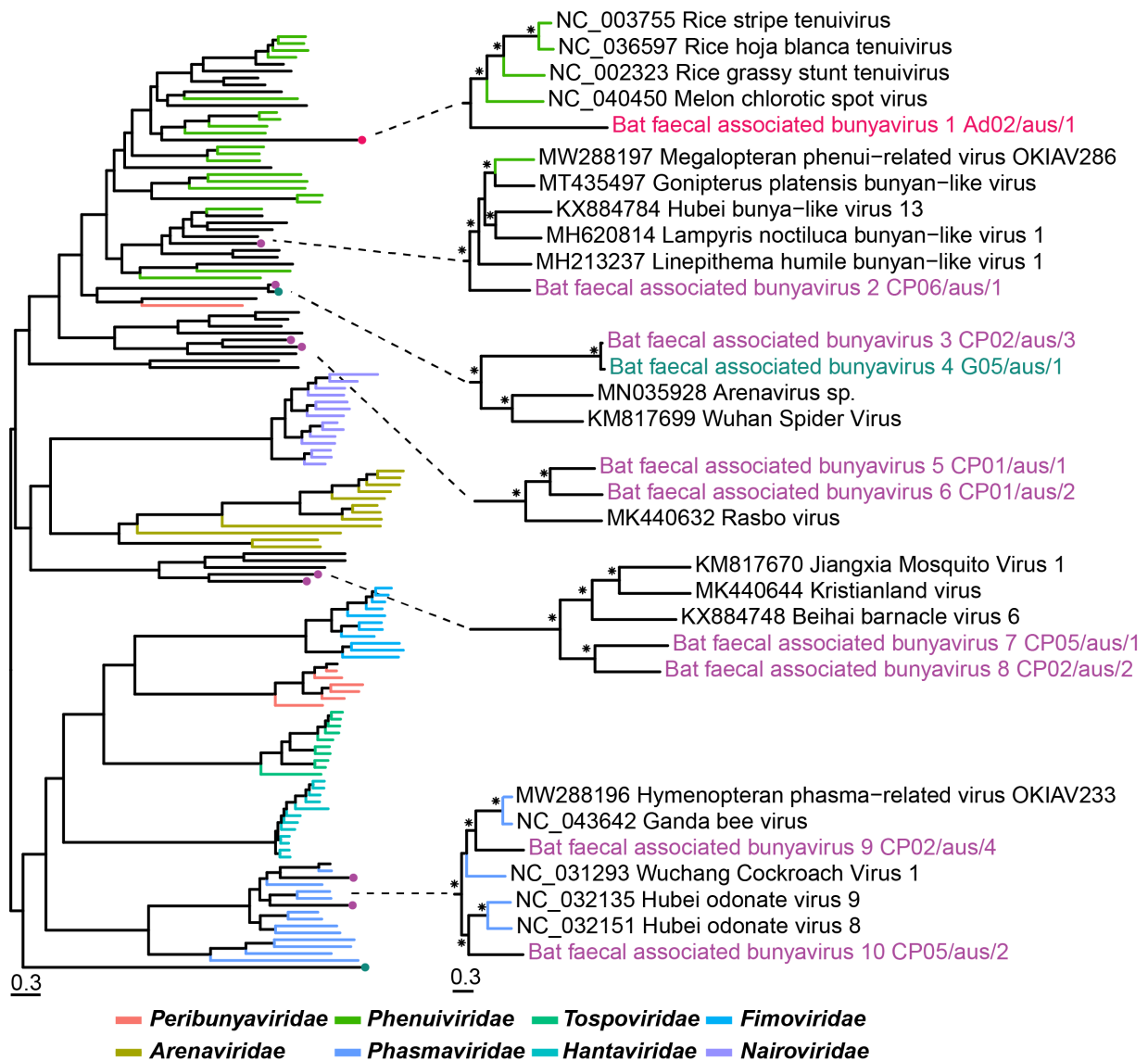
Figure 6.4.8.2: Phylogenetic analysis of viruses from the order Bunyavirales.The RdRp amino acid sequence was used to estimate phylogenetic trees and the alignment length was 1,434 amino acid residues. Viruses from this study are coloured by sampling location and bootstrap values >70% are represented by the symbol shown at the branch node. The tree is midpoint rooted for clarity and the scale bar represents the amino acid substitutions per site.

6.5: Discussion

Virological surveillance of bats in Australia has largely focused on screening for known zoonotic viruses such as Hendra virus and Australian bat lyssavirus, although the

paramyxovirus Tioman virus, for which flying foxes are the natural host, and coronaviruses are also targeted (Boardman et al., 2020, Prada et al., 2019a, Smith et al., 2016). The primary aim of these studies is to identify specific viruses using either PCR or serological data. Although such surveillance has been successful in determining the active circulation of these specific viruses, these approaches necessarily have restricted capacity to detect novel or unexpected viruses, thus providing a very limited understanding of viruses circulating in Australian bats. As bats are frequently found near human populations, they are of particular concern regarding potential zoonoses (Plowright et al., 2011, Williams et al., 2006, Halpin et al., 2000). Herein, we used metatranscriptomics to reveal the natural faecal virome of the grey-headed flying fox. Although most of the viruses identified were likely associated with bat diet, as expected from faecal sampling, we also identified viruses from three mammalian-associated families (*Coronaviridae, Caliciviridae, Retroviridae*) and one virus from the *Birnaviridae* family that may also have a mammalian association.

Both alpha- and betacoronaviruses have been identified in a variety of bat species (Smith et al., 2016, Prada et al., 2019b). Here, we characterised the complete genome of a betacoronavirus in grey-headed flying foxes that was closely related to two other betacoronaviruses sampled in flying foxes in Australia and Madagascar (Smith et al., 2016, Kettenburg et al., 2022). The current ICTV classification for coronavirus species states that less than 90% amino acid identity in the ORF1ab conserved replicase domains constitutes a new species. Although bat faecal coronavirus CP07/aus/1 shares high sequence similarity to another reported bat betacoronavirus, the P.alecto/Aus/SEQ/2009 sequence is only 146 amino acids in length, does not span the complete RdRp and is therefore difficult to classify. Accordingly, we suggest that betacoronavirus bat faecal coronavirus CP07/aus/1 represents a novel species, to which P.alecto/Aus/SEQ/2009 may also belong. The complete genome of this virus was found in both Adelaide and New South Wales (99.8% nucleotide similarity between the two genomes) and abundance counts were high in both locations (Figure 6.3.1C), indicative of virus exchange between bat populations. Flying foxes are known to travel long distances to feed, roosting sites change depending on season, and in Australia several flying fox species share roosting sites (Timmiss et al., 2021), all of which provide opportunities for viruses to infect new individuals. Importantly, while we were only able to assemble the complete genome of one novel coronavirus, we identified partial genome fragments of at least two more diverse coronaviruses (Figure 6.4.3, indicating that Australian bats carry a high diversity of coronaviruses as has been seen in other bat species.

This is the first report of a sapovirus in Australian bats. Previously, bat sapoviruses have been sampled from *Eidolon helvum* (Straw-coloured fruit bat) in Cameroon (Yinda et al., 2017) and Saudi Arabia (Mishra et al., 2019) and *Hipposideros Pomona* (Pomona leaf-nosed bat) from Hong Kong (Tse et al., 2012). Currently, the bat sapoviruses characterised have been from bats with no apparent disease (Tse et al., 2012, Yinda et al., 2017, Mishra et al., 2019). Whether this is the case here is unknown because the reliance on faecal sampling meant that there was no direct interaction with individual animals. The disease potential of bat sapoviruses should be investigated further as sapoviruses have been linked to acute gastroenteritis outbreaks in humans (Oka et al., 2015) and some animal sapoviruses are closely related to those found in humans (Mombo et al., 2014, Firth et al., 2014, Martella et al., 2008).

Until the metagenomic detection of porcine birnavirus (Yang et al., 2021) and porcupine birnavirus (He et al., 2022) it was believed the *Birnaviridae* infected fish, insects and birds exclusively (Crane et al., 2000, Da Costa et al., 2003, Chung et al., 1996, Brown and Skinner, 1996, Guy et al., 2011). We identified the segment B sequence of a novel bat faecal associated birna-like virus that was most closely related to a divergent pathogenic avian birnavirus (50% amino acid identity). Given its divergent phylogenetic position – falling basal to all other birnaviruses in a mid-point rooted tree (Figure 6.4.5) – it is currently unclear whether this virus actively infects grey-headed flying foxes or is associated with a component of their diet or microbiome. While grey-headed flying foxes are not insectivores, the ingestion of insects through the consumption of fruit and nectar seems likely given the high number of invertebrate, plant and fungi viruses sequenced here (Figure 6.3.1B, Figure 6.7.1). The moderate abundance values (81.6 and 31.3 RPM) cannot exclude either scenario as using a host reference gene such as COX1 for sequencing depth comparison may not be as reliable for faecal samples as it would be when analysing tissue. Further investigation is needed to determine the natural host of bat faecal associated birna-like virus and to determine what tissue types are affected.

Two intact, possibly exogenous retrovirus near complete genomes were also identified in this study and were most closely related to mammalian infecting retroviruses from the genus *Betaretrovirus*. Six retroviruses have been previously characterised from Australian bat brain tissue and excretions (including faeces), all from the genus *Gammaretrovirus* (Hayward et al., 2020, Cui et al., 2012) and hence highly divergent from the viruses identified here. Although the exogenous status needs to be confirmed, it is possible that bat faecal associated

retrovirus 1 G04/aus/1 and bat faecal associated retrovirus 2 AdCPG/aus/1 constitute the first exogenous and intact betaretroviruses sampled from the faeces of bats in Australia. Unfortunately, virus identification through metatranscriptomics does not provide reliable information on whether a virus is endogenous and defective, or still functional and exogenous (Hayward et al., 2013, Hayward and Tachedjian, 2021). That the retroviruses detected here have all the necessary genes to comprise a functional virus, with undisrupted ORFs, were not detected in every library, and are not present in the bat genome, at the very least suggests that they are only recently endogenized and currently unfixed in the bat population. Further work confirming the nature of the retroviruses detected here is warranted since bats are known to be major hosts for retroviruses (Cui et al., 2015) and their cross-species transmission across mammalian orders is commonplace (Hayward et al., 2013).

In addition to mammalian viruses, we detected virus sequences that are likely invertebrate-associated. Of particular interest were those from the *Orthomyxoviridae* and *Reoviridae* that span a wide variety of hosts including mammals and were at high abundance in some of the Centennial Park libraries. Notably, bat faecal associated reovirus 1 CP02/aus/1 groups with members of the *Reoviridae* associated with ticks. Tick-associated reoviruses from the genus *Coltivirus* – Colorado tick fever virus and Eyach virus (Goodpasture et al., 1978, Rehse-Küpper et al., 1976) – have been associated with human infection and disease such that their presence in urban wildlife merits attention.

Our study highlights the diversity of viruses in wildlife species from metropolitan areas. In this context it is notable that the bat coronaviruses identified fall within the subgenus *Nobecovirus* of betacoronaviruses. Currently, this subgenus is strongly associated with bats sampled on multiple continents, with the phylogenetic depth of the *Nobecovirus* lineage further suggesting that bats have harbored these viruses for millennia with no apparent infection of humans.

6.6: References

Besemer, J., Borodovsky, M. 1999. Heuristic approach to deriving models for gene finding. Nucleic Acids Research, 27(19):3911-20.

Boardman, W.S.J., Baker, M.L., Boyd, V., Crameri, G., Peck, G.R., Reardon, T., Smith, I.G., Caraguel, C.G.B., Prowse, T.A.A. 2020. Seroprevalence of three paramyxoviruses; Hendra virus, Tioman virus, Cedar virus and a rhabdovirus, Australian bat lyssavirus, in a range expanding fruit bat, the Grey-headed flying fox (Pteropus poliocephalus). *PLoS One*, 15(5):e0232339.

Botvinkin, A.D., Poleschuk, E.M., Kuzmin, I.V., Borisova, T.I., Gazaryan, S.V., Yager, P., Rupprecht, C.E. 2003. Novel lyssaviruses isolated from bats in Russia. *Emerging Infectious Disease*, 9(12):1623-5.

Brown, M.D., Skinner, M.A. 1996. Coding sequences of both genome segments of a European 'very virulent' infectious bursal disease virus. *Virus Research*, 40(1):1-15.

Capella-Gutiérrez, S., Silla-Martínez, J.M., Gabaldón, T. 2009. trimAl: a tool for automated alignment trimming in large-scale phylogenetic analyses. *Bioinformatics*, 25(15):1972-3.

Chung, H.K., Kordyban, S., Cameron, L., Dobos, P. 1996. Sequence analysis of the bicistronic Drosophila X virus genome segment A and its encoded polypeptides. *Virology*, 225(2):359-68.

Crane, M.S., Hardy-Smith, P., Williams, L.M., Hyatt, A.D., Eaton, L.M., Gould, A., Handlinger, J., Kattenbelt, J., Gudkovs, N. 2000. First isolation of an aquatic birnavirus from farmed and wild fish species in Australia. *Diseases of Aquatic Organisms*, 43(1):1-14.

Cui, J., Tachedjian, G., Wang, L.F. 2015. Bats and Rodents Shape Mammalian Retroviral Phylogeny. *Scientific Reports*, 5:16561.

Cui, J., Tachedjian, M., Wang, L., Tachedjian, G., Wang, L.F., Zhang, S. 2012. Discovery of retroviral homologs in bats: implications for the origin of mammalian gammaretroviruses. *Journal of Virology*, 86(8):4288-93.

Da Costa, B., Soignier, S., Chevalier, C., Henry, C., Thory, C., Huet, J.C., Delmas, B. 2003. Blotched snakehead virus is a new aquatic birnavirus that is slightly more related to avibirnavirus than to aquabirnavirus. *Journal of Virology*, 77(1):719-25.

Firth, C., Bhat, M., Firth, M.A., Williams, S.H., Frye, M.J., Simmonds, P., Conte, J.M., Ng, J., Garcia, J., Bhuva, N.P., Lee, B., Che, X., Quan, P.L., Lipkin, W.I. 2014. Detection of zoonotic pathogens and characterization of novel viruses carried by commensal Rattus norvegicus in New York City. *mBio*, 5(5):e01933-14.

Goodpasture, H.C., Poland, J.D., Francy, D.B., Bowen, G.S., Horn, K.A. 1978. Colorado tick fever: clinical, epidemiologic, and laboratory aspects of 228 cases in Colorado in 1973-1974. *Annals of Internal Medicine*, 88(3):303-10.

Gould, A.R., Hyatt, A.D., Lunt, R., Kattenbelt, J.A., Hengstberger, S., Blacksell, S.D. 1998. Characterisation of a novel lyssavirus isolated from Pteropid bats in Australia. *Virus Research,* 54(2):165-87.

Graham, R.I., Rao, S., Possee, R.D., Sait, S.M., Mertens, P.P., Hails, R.S. 2006. Detection and characterisation of three novel species of reovirus (Reoviridae), isolated from geographically separate populations of the winter moth Operophtera brumata (Lepidoptera: Geometridae) on Orkney. *Journal of Invertebrate Pathology*, 91(2):79-87.

Guy, J.S., West, A.M., Fuller, F.J. 2011. Physical and genomic characteristics identify chicken proventricular necrosis virus (R11/3 virus) as a novel birnavirus. *Avian Diseases*, 55(1):2-7.

Halpin, K., Young, P.L., Field, H.E., Mackenzie, J.S. 2000. Isolation of Hendra virus from pteropid bats: a natural reservoir of Hendra virus. *Journal of General Virology*, 81(Pt 8):1927-1932.

Hardmeier, I., Aeberhard, N., Qi, W., Schoenbaechler, K., Kraettli, H., Hatt, J.M., Fraefel, C., Kubacki, J. 2021. Metagenomic analysis of fecal and tissue samples from 18 endemic bat species in Switzerland revealed a diverse virus composition including potentially zoonotic viruses. *PLoS One*, 16(6):e0252534.

Harvey, E., Rose, K., Eden, J.-S., Lo, N., Abeyasuriya, T., Shi, M., Doggett, S.L., Holmes, E.C., García-Sastre, A. 2019. Extensive Diversity of RNA Viruses in Australian Ticks. *Journal of Virology*, 93(3):e01358-18.

Hayward, A., Grabherr, M., Jern, P. 2013. Broad-scale phylogenomics provides insights into retrovirus-host evolution. *Proceedings of the National Academy of Sciences of the United States of America*, 110(50):20146-51.

Hayward, J.A., Tachedjian, G. 2021. Retroviruses of Bats: a Threat Waiting in the Wings? *mBio*, 12(5):e0194121.

Hayward, J.A., Tachedjian, M., Kohl, C., Johnson, A., Dearnley, M., Jesaveluk, B., Langer, C., Solymosi, P.D., Hille, G., Nitsche, A., Sánchez, C.A., Werner, A., Kontos, D., Crameri, G., Marsh, G.A., Baker, M.L., Poumbourios, P., Drummer, H.E., Holmes, E.C., Wang, L.F., Smith, I., Tachedjian, G. 2020. Infectious KoRV-related retroviruses circulating in Australian bats. *Proceedings of the National Academy of Sciences of the United States of America*, 117(17):9529-9536.

He, W.T., Hou, X., Zhao, J., Sun, J., He, H., Si, W., Wang, J., Jiang, Z., Yan, Z., Xing, G., Lu, M., Suchard, M.A., Ji, X., Gong, W., He, B., Li, J., Lemey, P., Guo, D., Tu, C., Holmes, E.C., Shi, M., Su, S. 2022. Virome characterization of game animals in China reveals a spectrum of emerging pathogens. *Cell*, 185(7):1117-1129.e8.

Hoang, D.T., Chernomor, O., von Haeseler, A., Minh, B.Q., Vinh, L.S. 2017. UFBoot2: Improving the Ultrafast Bootstrap Approximation. *Molecular Biology and Evolution*, 35(2):518-522.

International Union for Conservation of Nature. 2021. Data from "Pteropus poliocephalus". The IUCN Red List of Threatened Species, 2021-3. https://www.iucnredlist.org/species/18751/22085511

Käfer, S., Paraskevopoulou, S., Zirkel, F., Wieseke, N., Donath, A., Petersen, M., Jones, T.C., Liu, S., Zhou, X., Middendorf, M., Junglen, S., Misof, B., Drosten, C. 2019. Re-assessing the diversity of negative strand RNA viruses in insects. *PLOS Pathogens*, 15(12):e1008224.

Kalyaanamoorthy, S., Minh, B.Q., Wong, T.K.F., von Haeseler, A., Jermiin, L.S. 2017. ModelFinder: fast model selection for accurate phylogenetic estimates. *Nature Methods*, 14(6):587-589.

Katoh, K., Kuma, K., Toh, H., Miyata, T. 2005. MAFFT version 5: improvement in accuracy of multiple sequence alignment. *Nucleic Acids Research*, 33(2):511-8.

Katoh, K., Standley, D.M. 2013. MAFFT multiple sequence alignment software version 7: improvements in performance and usability. *Molecular Biology and Evolution*, 30(4):772-80.

Kechin, A., Boyarskikh, U., Kel, A., Filipenko, M. 2017. cutPrimers: A New Tool for Accurate Cutting of Primers from Reads of Targeted Next Generation Sequencing. Journal of Computational Molecular Cell Biology, 24(11):1138-1143.

Kettenburg, G., Kistler, A., Ranaivoson, H.C., Ahyong, V., Andrianiaina, A., Andry, S., DeRisi, J.L., Gentles, A., Raharinosy, V., Randriambolamanantsoa, T.H., Ravelomanantsoa, N.A.F., Tato, C.M., Dussart, P., Heraud, J.M., Brook, C.E. 2022. Full Genome Nobecovirus Sequences From Malagasy Fruit Bats Define a Unique Evolutionary History for This Coronavirus Clade. *Frontiers in Public Health*, 10:786060.

Kopylova, E., Noé, L., Touzet, H. 2012. SortMeRNA: fast and accurate filtering of ribosomal RNAs in metatranscriptomic data. *Bioinformatics*, 28(24):3211-7.

Langmead, B., Salzberg, S.L. 2012. Fast gapped-read alignment with Bowtie 2. *Nature Methods*, 9(4):357-9.

Li, D., Liu, C.M., Luo, R., Sadakane, K., Lam, T.W. 2015. MEGAHIT: an ultra-fast single-node solution for large and complex metagenomics assembly via succinct de Bruijn graph. *Bioinformatics*, 31(10):1674-6.

Li, W., Shi, Z., Yu, M., Ren, W., Smith, C., Epstein, J.H., Wang, H., Crameri, G., Hu, Z., Zhang, H., Zhang, J., McEachern, J., Field, H., Daszak, P., Eaton, B.T., Zhang, S., Wang, L.F. 2005. Bats are natural reservoirs of SARS-like coronaviruses. *Science*, 310(5748):676-9.

Marsh, G.A., de Jong, C., Barr, J.A., Tachedjian, M., Smith, C., Middleton, D., Yu, M., Todd, S., Foord, A.J., Haring, V., Payne, J., Robinson, R., Broz, I., Crameri, G., Field,

H.E., Wang, L.F. 2012. Cedar virus: a novel Henipavirus isolated from Australian bats. *PLoS Pathogens*, 8(8):e1002836.

Martella, V., Lorusso, E., Banyai, K., Decaro, N., Corrente, M., Elia, G., Cavalli, A., Radogna, A., Costantini, V., Saif, L.J., Lavazza, A., Di Trani, L., Buonavoglia, C. 2008. Identification of a porcine calicivirus related genetically to human sapoviruses. *Journal of Clinical Microbiology*, 46(6):1907-13.

Mishra, N., Fagbo, S.F., Alagaili, A.N., Nitido, A., Williams, S.H., Ng, J., Lee, B., Durosinlorun, A., Garcia, J.A., Jain, K., Kapoor, V., Epstein, J.H., Briese, T., Memish, Z.A., Olival, K.J., Lipkin, W.I. 2019. A viral metagenomic survey identifies known and novel mammalian viruses in bats from Saudi Arabia. *PLoS One*, 14(4):e0214227.

Mombo, I.M., Berthet, N., Bouchier, C., Fair, J.N., Schneider, B.S., Renaud, F., Leroy, E.M., Rougeron, V. 2014. Characterization of a genogroup I sapovirus isolated from chimpanzees in the republic of congo. *Genome Announcements*, 2(4):e00680-14.

Murakami, S., Kitamura, T., Suzuki, J., Sato, R., Aoi, T., Fujii, M., Matsugo, H., Kamiki, H., Ishida, H., Takenaka-Uema, A., Shimojima, M., Horimoto, T. 2020. Detection and Characterization of Bat Sarbecovirus Phylogenetically Related to SARS-CoV-2, Japan. *Emerging Infectious Disease*, 26(12):3025-3029.

Nguyen, L.-T., Schmidt, H.A., von Haeseler, A., Minh, B.Q. 2014. IQ-TREE: A Fast and Effective Stochastic Algorithm for Estimating Maximum-Likelihood Phylogenies. *Molecular Biology and Evolution*, 32(1):268-274.

Ning, S., Dai, Z., Zhao, C., Feng, Z., Jin, K., Yang, S., Shen, Q., Wang, X., Sun, R., Zhang, W. 2022. Novel putative pathogenic viruses identified in pangolins by mining metagenomic data. *Journal of Medical Virology*, 94(6):2500-2509.

Nouri, S., Salem, N., Nigg, J.C., Falk, B.W. 2015. Diverse Array of New Viral Sequences Identified in Worldwide Populations of the Asian Citrus Psyllid (Diaphorina citri) Using Viral Metagenomics. *Journal of Virology*, 90(5):2434-45.

Oka, T., Wang, Q., Katayama, K., Saif, L.J. 2015. Comprehensive review of human sapoviruses. *Clinical Microbiology Reviews*, 28(1):32-53.

Philbey, A.W., Kirkland, P.D., Ross, A.D., Davis, R.J., Gleeson, A.B., Love, R.J., Daniels, P.W., Gould, A.R., Hyatt, A.D. 1998. An apparently new virus (family Paramyxoviridae) infectious for pigs, humans, and fruit bats. *Emerging Infectious Disease,* 4(2):269-71.

Plowright, R.K., Foley, P., Field, H.E., Dobson, A.P., Foley, J.E., Eby, P., Daszak, P. 2011. Urban habituation, ecological connectivity and epidemic dampening: the emergence of Hendra virus from flying foxes (Pteropus spp.). *Proceedings Biological Science*, 278(1725):3703-12.

Prada, D., Boyd, V., Baker, M., Jackson, B., O'Dea, M. 2019a. Insights into Australian Bat Lyssavirus in Insectivorous Bats of Western Australia. *Tropical Medicine and Infectious Disease*, 4(1):46.

Prada, D., Boyd, V., Baker, M.L., O'Dea, M., Jackson, B. 2019b. Viral Diversity of Microbats within the South West Botanical Province of Western Australia. *Viruses*, 11(12):1157.

Rehse-Küpper, B., Casals, J., Rehse, E., Ackermann, R. 1976. Eyach--an arthropod-borne virus related to Colorado tick fever virus in the Federal Republic of Germany. *Acta Virologica*, 20(4):339-42.

Shi, M., Lin, X.D., Tian, J.H., Chen, L.J., Chen, X., Li, C.X., Qin, X.C., Li, J., Cao, J.P., Eden, J.S., Buchmann, J., Wang, W., Xu, J., Holmes, E.C., Zhang, Y.Z. 2016. Redefining the invertebrate RNA virosphere. *Nature*, 540(7634):539-543.

Smith, C.S., de Jong, C.E., Meers, J., Henning, J., Wang, L., Field, H.E. 2016. Coronavirus Infection and Diversity in Bats in the Australasian Region. *Ecohealth*, 13(1):72-82.

Temmam, S., Vongphayloth, K., Baquero, E., Munier, S., Bonomi, M., Regnault, B., Douangboubpha, B., Karami, Y., Chrétien, D., Sanamxay, D., Xayaphet, V., Paphaphanh, P., Lacoste, V., Somlor, S., Lakeomany, K., Phommavanh, N., Pérot, P., Dehan, O., Amara, F., Donati, F., Bigot, T., Nilges, M., Rey, F.A., van der Werf, S., Brey, P.T., Eloit, M. 2022. Bat coronaviruses related to SARS-CoV-2 and infectious for human cells. *Nature*, 604:330-336.

Thayer, R.M., Power, M.D., Bryant, M.L., Gardner, M.B., Barr, P.J., Luciw, P.A. 1987. Sequence relationships of type D retroviruses which cause simian acquired immunodeficiency syndrome. *Virology*, 157(2):317-29.

Timmiss, L.A., Martin, J.M., Murray, N.J., Welbergen, J.A., Westcott, D., McKeown, A., Kingsford, R.T. 2021. Threatened but not conserved: flying-fox roosting and foraging habitat in Australia. *Australian Journal of Zoology*, 68:226-233.

Tse, H., Chan, W.M., Li, K.S., Lau, S.K., Woo, P.C., Yuen, K.Y. 2012. Discovery and genomic characterization of a novel bat sapovirus with unusual genomic features and phylogenetic position. *PLoS One*, 7(4):e34987.

Turnbull, M.G., Douville, R.N. 2018. Related Endogenous Retrovirus-K Elements Harbor Distinct Protease Active Site Motifs. *Frontiers in Microbiology*, 9:1577.

Van Brussel, K., Holmes, E.C. 2022. Zoonotic disease and virome diversity in bats. *Current Opinion in Virology*, 52:192-202.

Vanmechelen, B., Merino, M., Vergote, V., Laenen, L., Thijssen, M., Martí-Carreras, J., Claerebout, E., Maes, P. 2021. Exploration of the Ixodes ricinus virosphere unveils an extensive virus diversity including novel coltiviruses and other reoviruses. *Virus Evolution*, 7(2):veab066.

Wacharapluesadee, S., Tan, C.W., Maneeorn, P., Duengkae, P., Zhu, F., Joyjinda, Y., Kaewpom, T., Chia, W.N., Ampoot, W., Lim, B.L., Worachotsueptrakun, K., Chen, V.C., Sirichan, N., Ruchisrisarod, C., Rodpan, A., Noradechanon, K., Phaichana, T., Jantarat, N., Thongnumchaima, B., Tu, C., Crameri, G., Stokes, M.M., Hemachudha, T., Wang, L.F. 2021. Evidence for SARS-CoV-2 related coronaviruses circulating in bats and pangolins in Southeast Asia. *Nature Communications*, 12(1):972.

Wang, J., Anderson, D.E., Halpin, K., Hong, X., Chen, H., Walker, S., Valdeter, S., van der Heide, B., Neave, M.J., Bingham, J., O'Brien, D., Eagles, D., Wang, L.F., Williams, D.T. 2021. A new Hendra virus genotype found in Australian flying foxes. *Virology Journal*, 18(1):197.

Weiss, S., Dabrowski, P.W., Kurth, A., Leendertz, S.A.J., Leendertz, F.H. 2017. A novel Coltivirus-related virus isolated from free-tailed bats from Côte d'Ivoire is able to infect human cells in vitro. *Virology journal*, 14(1):181-181.

Williams, N.S.G., McDonnell, M.J., Phelan, G.K., Keim, L.D., Van Der Ree, R. 2006. Range expansion due to urbanization: Increased food resources attract Grey-headed Flying-foxes (Pteropus poliocephalus) to Melbourne. *Austral ecology*, 31(2):190-198.

Wu, Z., Yang, L., Ren, X., He, G., Zhang, J., Yang, J., Qian, Z., Dong, J., Sun, L., Zhu, Y., Du, J., Yang, F., Zhang, S., Jin, Q. 2016. Deciphering the bat virome catalog to better understand the ecological diversity of bat viruses and the bat origin of emerging infectious diseases. *Isme J*, 10(3):609-20.

Xu, Z., Feng, Y., Chen, X., Shi, M., Fu, S., Yang, W., Liu, W.J., Gao, G.F., Liang, G. 2022. Virome of Bat-Infesting Arthropods: Highly Divergent Viruses in Different Vectors. *Journal of Virology*, 96(4):e0146421.

Yang, Z., He, B., Lu, Z., Mi, S., Jiang, J., Liu, Z., Tu, C., Gong, W. 2021. Mammalian birnaviruses identified in pigs infected by classical swine fever virus. *Virus Evolution*, 7(2):veab084.

Yinda, C.K., Conceição-Neto, N., Zeller, M., Heylen, E., Maes, P., Ghogomu, S.M., Van Ranst, M., Matthijnssens, J. 2017. Novel highly divergent sapoviruses detected by metagenomics analysis in straw-colored fruit bats in Cameroon. *Emerging Microbes and Infections*, 6(5):e38.

Yob, J.M., Field, H., Rashdi, A.M., Morrissy, C., van der Heide, B., Rota, P., bin Adzhar, A., White, J., Daniels, P., Jamaluddin, A., Ksiazek, T. 2001. Nipah virus infection in bats (order Chiroptera) in peninsular Malaysia. *Emerging Infectious Disease*, 7(3):439-41.

Zhou, H., Ji, J., Chen, X., Bi, Y., Li, J., Wang, Q., Hu, T., Song, H., Zhao, R., Chen, Y., Cui, M., Zhang, Y., Hughes, A.C., Holmes, E.C., Shi, W. 2021. Identification of novel bat coronaviruses sheds light on the evolutionary origins of SARS-CoV-2 and related viruses. *Cell*, 184(17):4380-4391.e14.

Zhou, P., Yang, X.L., Wang, X.G., Hu, B., Zhang, L., Zhang, W., Si, H.R., Zhu, Y., Li, B., Huang, C.L., Chen, H.D., Chen, J., Luo, Y., Guo, H., Jiang, R.D., Liu, M.Q., Chen, Y., Shen, X.R., Wang, X., Zheng, X.S., Zhao, K., Chen, Q.J., Deng, F., Liu, L.L., Yan, B., Zhan, F.X., Wang, Y.Y., Xiao, G.F., Shi, Z.L. 2020. A pneumonia outbreak associated with a new coronavirus of probable bat origin. *Nature*, 579(7798):270-273.

Zhu, W., Lomsadze, A., Borodovsky, M. 2010. Ab initio gene identification in metagenomic sequences. *Nucleic Acids Research*, 38(12):e132.

Zhu, W., Yang, J., Lu, S., Jin, D., Pu, J., Wu, S., Luo, X.L., Liu, L., Li, Z., Xu, J. 2022. RNA Virus Diversity in Birds and Small Mammals from Qinghai-Tibet Plateau of China. *Frontiers in Microbiology*, 13:780651.

6.7: Supplementary data
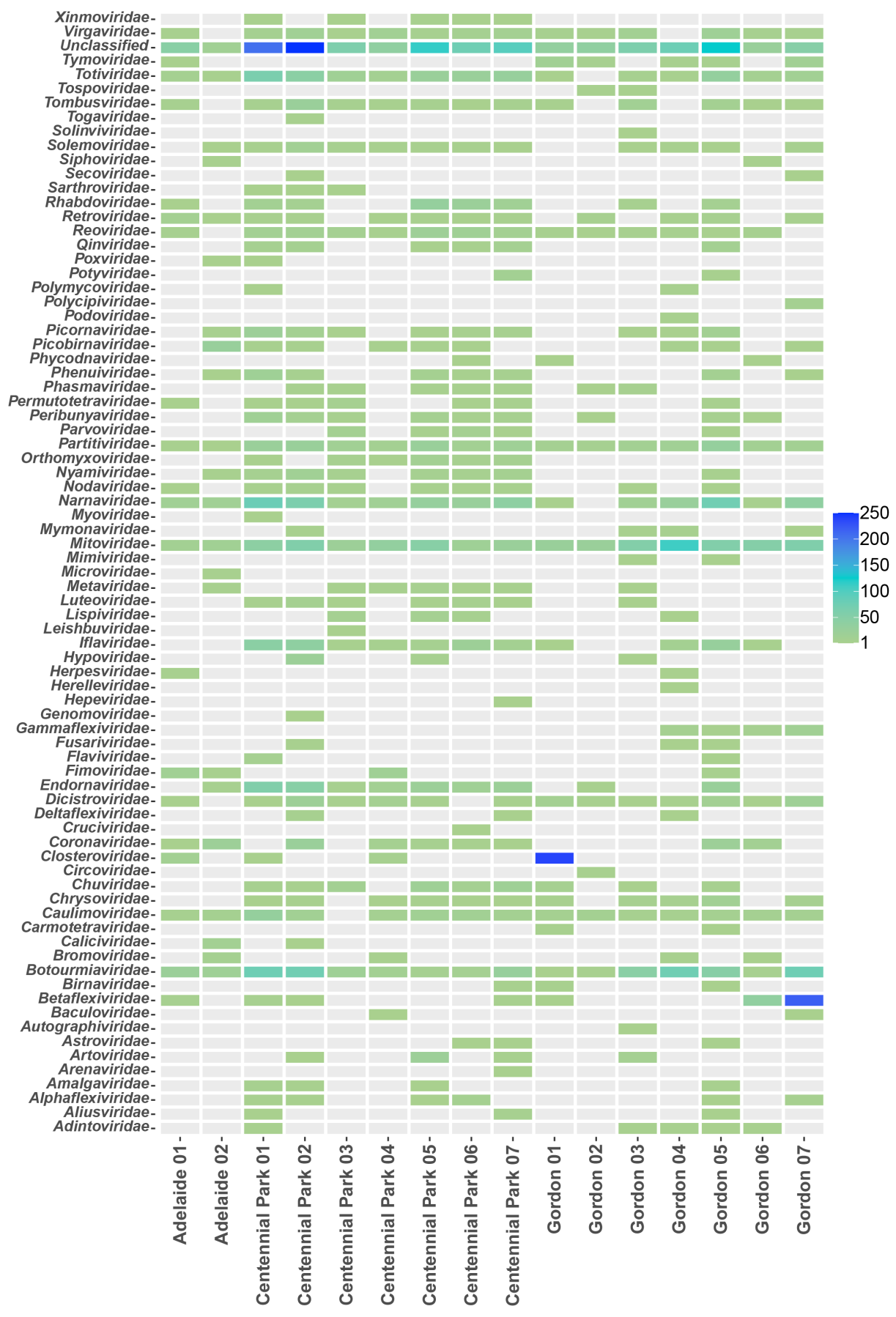
Figure 6.7.1: Overview of number of virus contigs for each sequencing library using Megahit and classified by virus family. Taxonomic classification was based on the taxonomy of the closest relatives in the NCBI non-redundant protein database.

190
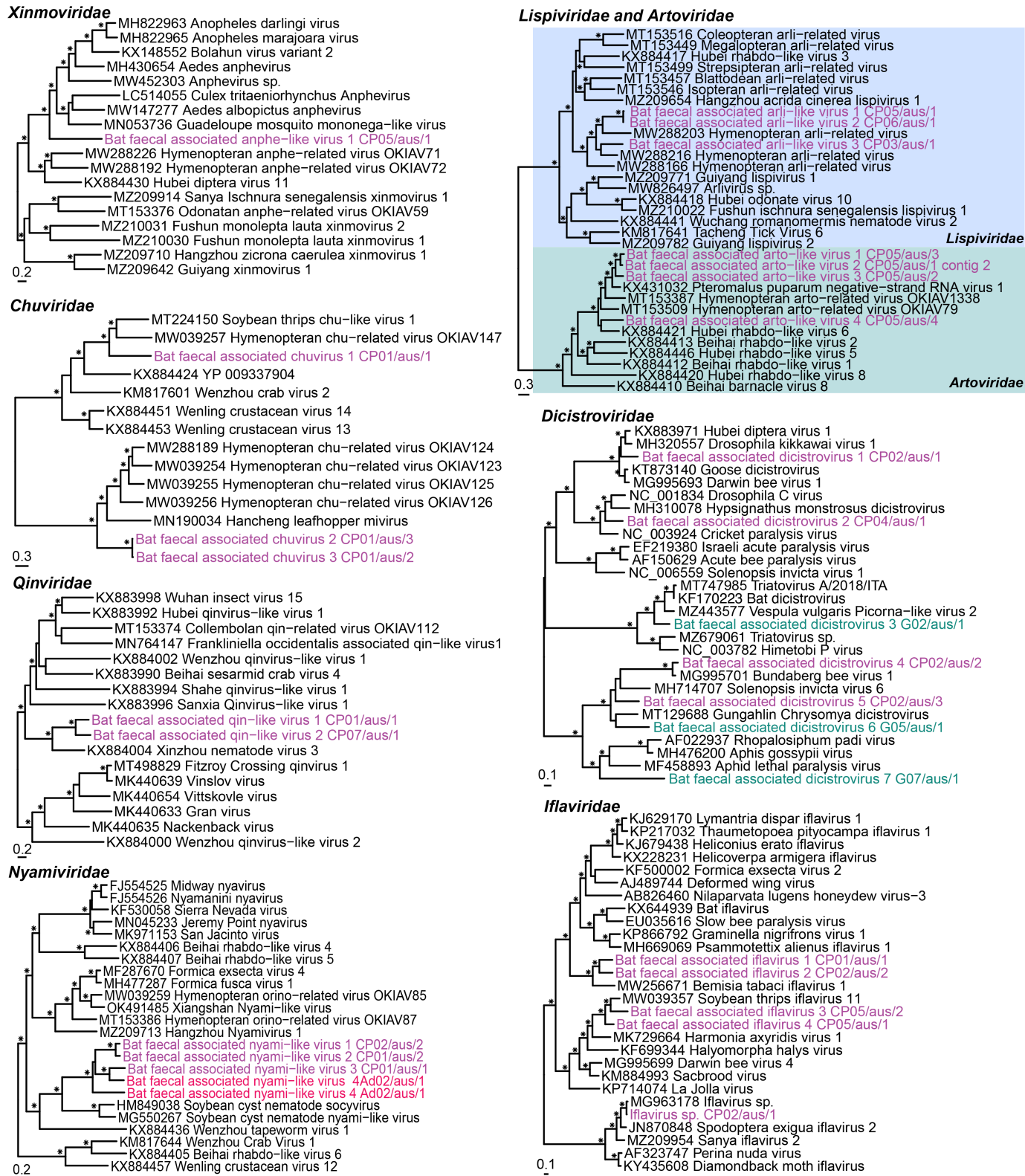
Figure 6.7.2: Phylogenetic analysis of the Lispiviridae and Artoviridae, Nyamiviridae, Chuviridae, Xinmoviridae, Qinviridae, Iflaviridae and Dicistroviridae. The RdRp amino sequence was used to estimate phylogenetic trees for all virus families (alignment lengths of 1,778, 1,575, 2,066, 1,804, 1,179, 491 and 454 amino acid residues, respectively). Viruses from this study are coloured by sampling location (Adelaide – pink, Centennial Park – purple and Gordon – green), with the Lispiviridae and Artoviridade highlighted. Bootstrap values >70% are represented by the symbol shown at the branch node and the tree is midpoint rooted for clarity and the scale bar represents the amino acid substitutions per site.
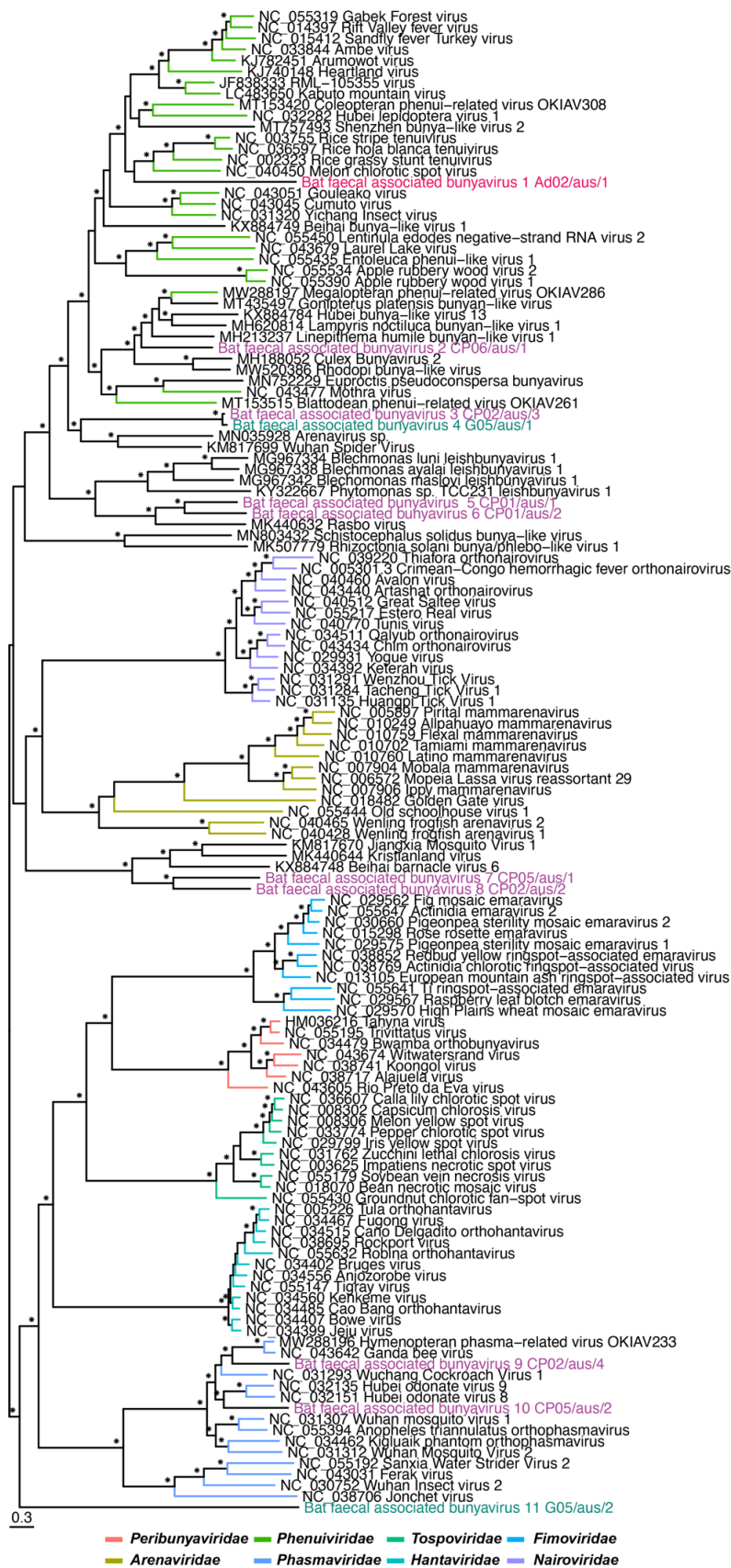
Figure 6.7.3: Complete tree presented in Figure 6 in text.

Table 6.7.1: VP1 amino acid identity of the novel sapoviruses in comparison to other bat sapoviruses.

Virus	Accession	Genogroup	Amino acid identity (%)	
			Ad02/aus/4	Ad02/aus/1
Ad02/aus/4		GXX	NA	77.7
Ad02/aus/1		GXX	77.7	NA
Bat-SaV/Limbe65/CAM/2014	KX759620	GXIX	29.6	38.8
Bat-SaV/Limbe899a/CAM/2014	KX759621	GXIX	30.7	39.9
Bat-SaV/Limbe25/CAM/2014	KX759618	GXIX	30.7	39.7
Bat-SaV/Lysoka36/CAM/2014	KX759619	GXVIII	19.8	32.1
Bat-SaV/Limbe900/CAM/2014	KX759623	GXVIII	29.8	37.5
BtMm-CalV/JX2010	KJ641703	GXVII	28.6	40.1
BtCV/OV-157/M.dau/DK/2018	MZ218056	GXVII	28.6	39.8
BtCalV/M63/HUN/2013	KU712497	GXVII	28.6	39.8
BtRs-CalV-1/GX2012	KJ641701	GXVI	25.8	36.5
TLC39/HK	JN899074	GXIV	29.1	38.8
TLC58/HK	JN899075	GXIV	29.4	38.6
TLC34/HK	JN899072	GXIV	28.7	38.5

Table 6.7.2: PCR results for coronaviruses, sapoviruses and retroviruses for each sequencing library pool.

	Bat faecal coronavirus CP07/aus/1		Bat faecal sapovirus Ad02/aus/1		Bat faecal associated retrovirus 1 G04/aus/1	
	PCR	NGS	PCR	NGS	PCR	NGS
Adelaide 01	Positive	18314.14	Negative	0	Negative	0
Adelaide 02	Positive	541	Positive	1727	Negative	0
Centennial Park 01	Negative	0	Negative	0	Negative	0
Centennial Park 02	Positive	370.79	Negative	0	Negative	0
Centennial Park 03	Negative	0	Negative	0	Negative	0
Centennial Park 04	Positive	288.68	Negative	0	Negative	0
Centennial Park 05	Positive	5787.18	Negative	0	Negative	0
Centennial Park 06	Positive	113.92	Negative	0	Negative	0
Centennial Park 07	Positive	16489	Negative	0	Positive	250.53
Gordon 01	Negative	90*	Negative	0	Negative	0
Gordon 02	Negative	0	Negative	0	Negative	0
Gordon 03	Negative	0	Negative	0	Negative	6*
Gordon 04	Negative	5*	Negative	0	Positive	2453
Gordon 05	Negative	16*	Negative	0	Negative	0
Gordon 06	Positive	615.1	Negative	0	Negative	0
Gordon 07	Negative	0	Negative	0	Positive	364

* Index-hopping

Chapter seven: Gammaretroviruses, pathogenic bacteria and novel viruses in Australian bats with neurological signs, pneumonia and skin lesions

Kate Van Brussel[1], Jackie Mahar[1], Jane Hall[2], Hannah Bender[2], Ayda Susana Ortiz-Baez[1], Wei-Shan Chang[1], Edward C. Holmes[1] and Karrie Rose[2]

[1]Sydney Institute for Infectious Diseases, School of Medical Sciences, The University of Sydney, NSW, 2006, Australia.

[2]Australian Registry of Wildlife Health, Taronga Conservation Society Australia, Mosman, New South Wales, Australia.

7.1: Abstract

More than 70 bat species are found in mainland Australia, including five megabat species from a single genus (family Pteropodidae) and more than 65 species representing six families of microbats. The conservation status of these animals varies from least concern to critically endangered. Research directed at evaluating the impact of microorganisms on bat health has been generally restricted to surveillance for specific pathogens. While most of the current bat virome studies focus on sampling apparently healthy individuals, little is known about the infectome of diseased bats. We performed traditional diagnostic techniques and metatranscriptomic sequencing on tissue samples from 43 individual bats, comprising three flying fox and two microbat species experiencing a range of disease syndromes, including mass mortality, neurological signs, pneumonia and skin lesions. We identified reads from four pathogenic bacteria and two pathogenic fungi, including *Pseudomonas aeruginosa* in lung samples from flying foxes with peracute pneumonia, and with dermatitis. Of note, we identified the recently discovered Hervey pteropid gammaretrovirus, with evidence of replication consistent with an exogenous virus, in a bat with lymphoid leukemia. In addition, one novel picornavirus, at least three novel astroviruses and bat pegiviruses were identified. We suggest that the most likely cause of peracute lung disease was *Pseudomonas aeruginosa*, while we suspect Hervey pteropid gammaretrovirus was associated with lymphoid leukemia. It is possible that any of the novel astroviruses could have contributed to the presentation of skin lesions in individual microbats. This study highlights the importance of studying the role of microorganisms in bat health and conservation.

7.2: Introduction

The order Chiroptera comprise 1456 species of bat with a near global distribution (Simmons and Cirranello, 2022). In recent years bats have gained attention for their ability to carry a large number of viruses, some of which have jumped hosts to emerge in new species (Mollentze and Streicker, 2020). As the sampling of bats has increased dramatically in the last decade, the known bat virosphere has similarly expanded, including the discovery of numerous novel viruses in addition to new variants of existing zoonotic viruses (Zhou et al., 2021, Wu et al., 2016, Wang et al., 2021, Mishra et al., 2019). Of particular importance is understanding the factors that enable bats to carry such a high diversity and abundance of viruses, likely reflecting unique immunological components in conjunction with such factors

as high body temperature during flight and large population densities (Irving et al., 2021, Banerjee et al., 2020). In turn, such research has led to a common belief that bats are able to tolerate a multitude of seemingly commensal viruses and do not experience large-scale outbreaks of infectious disease. Bats, however, are clearly susceptible to microbial infections with, for example, *Pseudogymnoascus destructans*, a fungus that causes white-nose syndrome, having a devastating effect on bats in North America (Hoyt et al., 2021, Cheng et al., 2021). In addition, infection with lyssaviruses can result in neurological and behavioural changes in bats and death (Banyard et al., 2011).

Over 70 species of bat from the families Emballonuridae, Hipposideridae, Pteropodidae, Megadermatidae, Miniopteridae, Molossidae, Rhinolophidae, Rhinonycteridae and Vespertilionidae inhabit mainland Australia (IUCN, 2021b). As of 2021, the International Union for Conservation of Nature (IUCN) Red List of Threatened Species lists nine of these as vulnerable, six as near threatened, one as endangered (the spectacled flying fox, *Pteropus conspicillatus*) and two as extinct (IUCN, 2021b). Together with the endangered spectacled flying fox, three other *Pteropus* species inhabit Australia: the grey-headed flying fox (*P. poliocephalus*), listed as vulnerable, while the little red flying fox (*P. scapulatus*) and black flying fox (*P. alecto*) are listed as of least concern. The habitat range of these flying fox species includes the north and east of Australia, with the grey-headed flying fox inhabiting as far west as Adelaide, South Australia (IUCN, 2021a). Australia is also home to several insectivorous microbat species, which, together with flying foxes (frugivores and nectivores), play an essential role in maintaining Australia's ecosystems by distributing seeds, pollinating plants and controlling insect numbers (Kolkert et al., 2020, Law and Lean, 1999, Moran et al., 2009). Consequently, any major decline in bat numbers in Australia could have a negative impact on ecosystem health (Moran et al., 2009).

While mass mortalities of adult and young flying foxes have been associated with periods of extreme heat (Mo et al., 2021, Welbergen et al., 2008), additional disease syndromes and mass mortality events have recently emerged in Australian chiropterans. Episodic mass pup abandonment has been associated with extreme heat, but also dehydration, nutritional stress, and dam death or desertion (Mo et al., 2021). Herein, we describe the emergence of several novel disease syndromes in flying foxes, including a distinctive pattern of acute to peracute vascular and inflammatory lung lesions recognised in grey-headed flying foxes and a black flying fox following exposure to stressors such as extreme heat, mass pup abandonment, or traumatic injury. Additionally, an emergent syndrome of neurological disease in flying foxes

is characterised by flaccid paralysis, severe central depression, tongue protrusion, and voice changes. Affected animals test negative for lyssavirus and often present thin, after periods of heavy rain. A dermatopathy in grey-headed flying foxes in extended rehabilitation care is characterised by depigmentation, ulceration and moist dermatitis of the wing webs. Individual cases in our study included wild flying-foxes with multisystemic lymphoma, and nodular wing web lesions associated with mite infestation.

To help identify the aetiological agents behind the presentation of severe disease in several bat species in Australia, we used traditional veterinary diagnostic techniques and a metatranscriptomic (i.e. total RNA sequencing) approach to characterise the histological change and viral and microbial diversity in tissues taken from bats displaying varying signs of disease, including neurological signs, peracute death and skin lesions (Table 7.7.1). The species of bat included in this study comprise grey-headed, black and little red flying foxes, as well as two species of microbats – eastern bent-wing bat (*Miniopterus orianae oceanensis)* and large footed myotis (*Myotis Macropus)* (Table 7.7.1).

7.3: Methods

7.3.1: Animal Ethics and sample collection

Wild bats were examined under a License to Rehabilitate Injured, Sick or Orphaned Protected Wildlife (no. MWL000100542) issued by the NSW Department of the Environment All samples were collected post-mortem from bats that were submitted for disease investigation. These samples were collected under the auspices of the Taronga Conservation Society Australia's Animal Ethics Committee (approval no. 3b1218), pursuant to NSW Office of Environment and Heritage-issued scientific license no. SL10469 and SL100104.

Samples from 38 grey-headed flying foxes, one black flying fox, one large footed myotis, one eastern bent-wing bat and two little red flying foxes were collected between November 2013 and April 2021 (Table 7.7.1). Most animals emanated from the Sydney basin and the central coast region of New South Wales. Fresh portions of brain, lung, liver, skin, heart, kidney and any lesions were collected aseptically post-mortem and frozen at –80°C. Impression smears of cut sections of lung tissue, or other lesions, were prepared from a subset of animals. The tissue was blotted onto a glass slide, air dried, fixed and stained with Quick Dip (Fronine, Thermo Fisher Scientific Aust. Pty. Ltd., Scoresby, Victoria, Australia) and examined at

1000x magnification with oil emersion microscopy. A range of tissues from each animal was fixed in 10% neutral buffered formalin, processed in ethanol, embedded with paraffin, sectioned, stained with hematoxylin and eosin, and mounted with a cover slip for examination by light microscopy.

7.3.2: Microbial culture

Microbial culture was conducted using a subset of bat tissues where there were gross or histological lesions, including 16 lung samples, and four skin samples. Culture was also conducted on four food sources used in bat rehabilitation care. Lung and lesion impression smears were stained with Gram and ZN were examined under 1000x oil immersion microscopy. Skin lesions were swabbed with a sterile applicator and the pleural surface of each lung sample was seared with a hot scalpel blade, and a sterile microbial loop was inserted into the deeper tissue to inoculate horse blood agar (HBA) and MacConkey agar (MAC) (Thermo Fisher Scientific, Scoresby, Victoria, Australia), which were incubated at 35°C in 4.5% carbon dioxide for 24–48 h. Isolates were identified with API 20 NE identification kits (bioMerieux SA, Lyon, France) using manufacturer's instructions.

7.3.3: Sample preparation, library construction and virus discovery

Tissue samples were homogenised using 2.38 mm metal beads (Qiagen) in the TissueLyser LT (Qiagen). Total RNA was extracted using the RNeasy Plus Mini Kit (Qiagen) following the manufacturer's protocol. Extracted RNA was pooled according to the syndrome, tissue type and bat species (Table S1). Sequencing libraries were constructed using the Illumina Stranded Total RNA Prep with Ribo-Zero Plus (Illumina) preparation kit. Libraries were sequenced on the Illumina NovaSeq platform as 150 bp paired end reads at the Australian Genome Research Facility (AGRF, Melbourne). Sequencing reads that contained read ends with a phred score below 25 and adapter sequences were quality trimmed using cutadapt version 1.8.3 (Kechin et al., 2017). Trimmed reads were then *de novo* assembled into contigs using Megahit version 1.1.3 (Li et al., 2015, Li et al., 2016). The resulting contigs were then compared to the non-redundant protein database using Diamond version 2.0.9 with an e-value cut-off of $1E^{-5}$. Hervey pteropid gammaretrovirus was identified using an in-house retrovirus discovery pipeline (Chang et al., manuscript in preparation). Attempts to extend virus contigs were made by using a reassembling megahit contigs using a Geneious version 2022.1.1 assembler.

RT-PCR was performed using SuperScript IV One-Step RT-PCR (Invitrogen) on total RNA to screen individual samples for Hervey pteropid gammaretrovirus, bat pegivirus GHFF04/Li/1 and Auskunsga virus. The primers used to amplify the polymerase/RdRp section of each virus are listed in Table 7.7.2.

7.3.4: Taxonomy profiling and abundance calculation

Taxonomic assignment and abundance information for bacterial, fungal and metazoan contigs was accessed using CCMetagen version 1.2.4 (Marcelino et al., 2020) and kma version 1.2.4 (Clausen et al., 2018). Taxonomic information for viral contigs was retrieved from the protein database results. Read abundance values for the virus contigs and COX1 genes (accession no. KF726143 for *Pteropus* species, MK410364 for the eastern bent wing bat and a COX1 contig identified in the large-footed myotis library) were calculated by mapping trimmed sequencing reads using the RSEM version 1.3.2 tool (Li et al., 2010a) in Trinity and Bowtie2 version 2.3.3.1 (Langmead et al., 2019, Langmead and Salzberg, 2012). The 16S rRNA genes from the *P. aeruginosa* in the bat lung libraries were obtained by mapping trimmed reads to a *P. aeruginosa* 16S rRNA gene available on NCBI GenBank (accession no. CP003149) and extracting the 0% majority consensus (i.e., least ambiguities in sequence) using Geneious version 2022.1.1.

7.3.5: Phylogenetic analysis

Amino acid and nucleotide alignments of virus genes were generated using MAFFT version 7.450 and the E-INS-I algorithm (Katoh and Standley, 2013), with ambiguously aligned regions removed using the gappyout method in TrimAL version 1.4.1 (Capella-Gutiérrez et al., 2009). The model finder program (Kalyaanamoorthy et al., 2017) in IQ-TREE version 1.6.7 (Nguyen et al., 2014) was used to determine the best-fit models of amino acid and nucleotide substitution and the same program was used to infer maximum likelihood trees. Ultrafast bootstrapping with 1000 replicates was to provide an indication of nodal support, and the nearest neighbour interchange was applied to search for optimal tree structure (Hoang et al., 2017).

7.4: Results

7.4.1: Clinical signs, gross and histological observations in bats

7.4.1.1: Peracute to actue pneumonia

Wildlife rehabilitators in the Sydney basin noted the rapid decline and demise of flying foxes following mild to moderate trauma. Affected animals refused food then became progressively weak, moribund and died within 12-48 hours. Post-mortem examination of these animals revealed a uniform pattern of voluminous lungs with multifocal petechial haemorrhages (Figure 7.4.1.1.a). Impression smears of affected lung tissue often contained fine bacilli, individually, forming palisades, or clustered within the cytoplasm of macrophages (Figure 7.4.1.1.a). Similar gross changes were noted in animals evaluated following extreme heat related mass mortalities or mass pup abandonment. On histologic examination of affected animal tissues, the lung lesions consisted of perivascular haemorrhage with interstitial oedema, fibrin deposition and necrosis (Figure 7.4.1.1.b). Lesions were often devoid of inflammatory cell infiltration (peracute), while others contained variable numbers of neutrophils and histiocytes (acute). *Pseudomonas aeruginosa* was isolated in microbial culture from nine of fifteen grey-headed flying fox lungs, and from a single black flying fox lung. Isolates were susceptible to a wide range of antimicrobial agents. Correlation between the identification of fine bacilli in lung impression smears with the isolation of *P. aeruginosa* was high. Although *P. aeruginosa* was the only isolate in six bat lung samples, *Escherichia coli*, *Klebsiella oxytoca*, *Lactococcus lactis*, *Enterobacter asburiae*, and *Streptococcus* species were also isolated in some lung tissues. *Salmonella enterica* serovar Wangata was also isolated in the lung and intestine of a young female grey-headed flying fox that died immediately after being rescued from a pup abandonment event. This animal had neutrophilic interstitial pneumonia, but also necrotising hepatitis, histiocytic colitis and evidence of septicaemia.
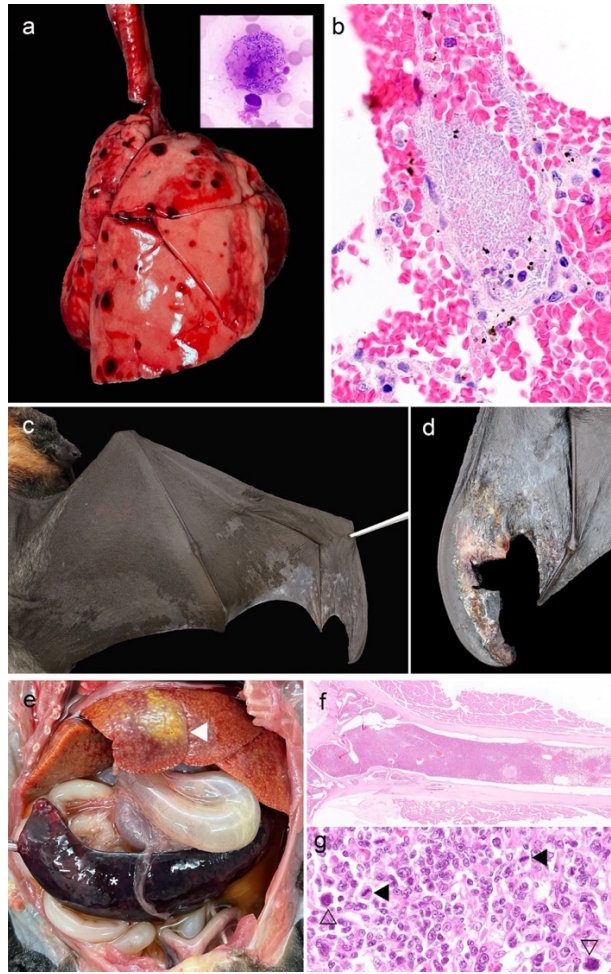
Figure 7.4.1.1: (a) Voluminous lungs with multifocal haemorrhages in a grey-headed flying fox. Inset: a pulmonary macrophage contains intracellular fine bacilli (lung impression smear, Quick Dip™ 1000x, case 14053.1). (b) Photomicrograph illustrating acute pulmonary perivascular haemorrhage associated with palisades of fine bacilli transmigrating an interstitial blood vessel wall. (c and d) Depigmentation and ulceration (d - with square excisional biopsy defect) extensively across the wing webs of grey-headed flying foxes (cases 14130.1 and 3). (e) Abdominal cavity of a grey-headed flying fox with abundant peritoneal fluid, a large liver with miliary, coalescing, raised, pale subcapsular foci (euthanasia artefact - white arrowhead) and marked splenomegaly (*). (f and g) Leukemia in a grey-headed flying fox. (f) The bone marrow is replaced with densely packed neoplastic cells (HE 20x). (g) Lymph node architecture is effaced by a confluence of medium sized round cells, some of which have bizarre nuclei (open arrowheads) or mitotic figures (black arrowheads) (case 14065.1, HE 1000x).

7.4.1.2: Flying Fox Paralysis Syndrome (Neurological)

An emergent, episodic syndrome of progressive flaccid paralysis and central nervous system depression is characterised by bats that go through stages that can include impaired mobility and swallowing, (with protruding tongues), recumbency and unusual vocalisations and breathing (FFPS Working Group, 2022). Affected bats can sometimes grasp on to wire or a branch: however, this is a passive action for the chiropteran foot, which can occur in the face of paralysis. Bats with this syndrome tend to present in clusters, or in large numbers (>150). Males can be over-represented, and their body condition is variable. In cases where body condition is poor weights 15-25% less than that expected based on the forearm measurement are observed. Events tend to occur after periods of heavy rain. No significant histological lesions have been detected in affected animals, except for a single grey-headed flying fox that had lung lesions, as described above.

7.4.1.3: Ulcerative and depigmenting dermatopathy

Ecologists and wildlife rehabilitators often report patches of depigmentation of the flying fox wing web in free-ranging animals. Flying foxes in rehabilitation care have been observed to develop extensive depigmentation of the wing web with gross and histological evidence of hyperkeratosis, dermatitis and ulceration at the tips of the wing webs. Four affected young flying foxes in wildlife rehabilitation care were euthanised and examined (Figure 7.4.1.1.c and d). *Pseudomonas aeruginosa* was isolated from swabs collected from the active lesions of each animal. Although *P. aeruginosa* was a predominant isolate from each animal, moderate growth of *Serratia marcescens* was also grown in skin swabs from three animals. Variable growth of *Pseudomonas protegens*, *Enterococcus faecalis*, alpha haemolytic *Streptococcus*, and *Fusarium* species were also detected.

7.4.1.4: Isolated cases

This study also included animals with no distinctive disease pattern. A single subadult male grey-headed flying fox with mite associated wing web lesions was euthanised after antiparasitic treatment resulted in central nervous system depression (bat no. 11501.1). A single adult female grey-headed flying fox was euthanised due to recumbency and marked abdominal distension (bat no. 14065.1). Post-mortem examination revealed marked peritoneal effusion with clear, straw-coloured fluid, and severe hepatosplenomegaly (Figure 7.4.1.1.e). The hepatic tissue contained a prominent zonal pallor, which appeared raised along the capsular surface. On histologic examination, the spleen, lymph nodes, bone marrow,

periportal hepatic parenchyma, and portions of the kidney and adrenal gland were effaced by sheets of neoplastic cells (Figure 7.4.1.1.f). An impression smear of the spleen, and histological examination of affected tissues revealed a confluent array of monomorphic medium to large lymphocytes often exhibiting karyomegaly, reniform or bizarre nuclei, and two to three mitotic figures per 1000x field (1g), characteristic of lymphoid leukemia. A single subadult male eastern-bent wing bat was euthanised after white skin lesions and underlying joint damage was observed (bat no. 13087.1). Finally, four apparently healthy animals were included in this study, a single male adult large footed myosis (bat no. 10628.1) killed in a cat attack, a single grey headed flying fox (bat no. 14048.1) that was euthanised after being electrocuted and a little red flying fox and her foetus (bat no. 14064.1 and 14064.2) found with barbed wire trauma.

7.4.2: Overview of metatranscriptomic data

In total, 32 tissue libraries were prepared for total RNA sequencing, comprising 10 from lung tissue, 10 from brain tissue, 10 from liver tissue and 2 from skin samples (Table 7.7.1). Overall, 38 grey-headed flying foxes, one black flying fox, two little red flying foxes, one eastern bent-wing bat and one large footed myotis from New South Wales (NSW) and the Australian Capital Territory (ACT) were included in this study (Table 7.7.1). Each sequencing library produced 87,000-253,000 reads and 112,000-696,000 contigs. Overall, we detected sequencing reads from 60 bacterial and 58 fungal families (Figure 7.7.1). Additionally, we identified virus sequences belonging to 15 families, including novel viruses from the *Astroviridae* and *Picornaviridae* and known viruses from the *Flaviviridae* (pegivirus) and *Retroviridae* (gammaretrovirus).

7.4.3: Overview of the bacteria and fungi present in bats

Although the bats sampled here had a diverse microbiome (Figure 7.4.3), we detected high levels of read abundance for five potentially pathogenic bacteria and fungi in nine bat libraries: *Enterococcus faecalis*, *Pseudomonas aerugosina*, *Salmonella enterica*, *Alternaria alternata* and *Fusarium oxysporum* (Figure 7.4.3).
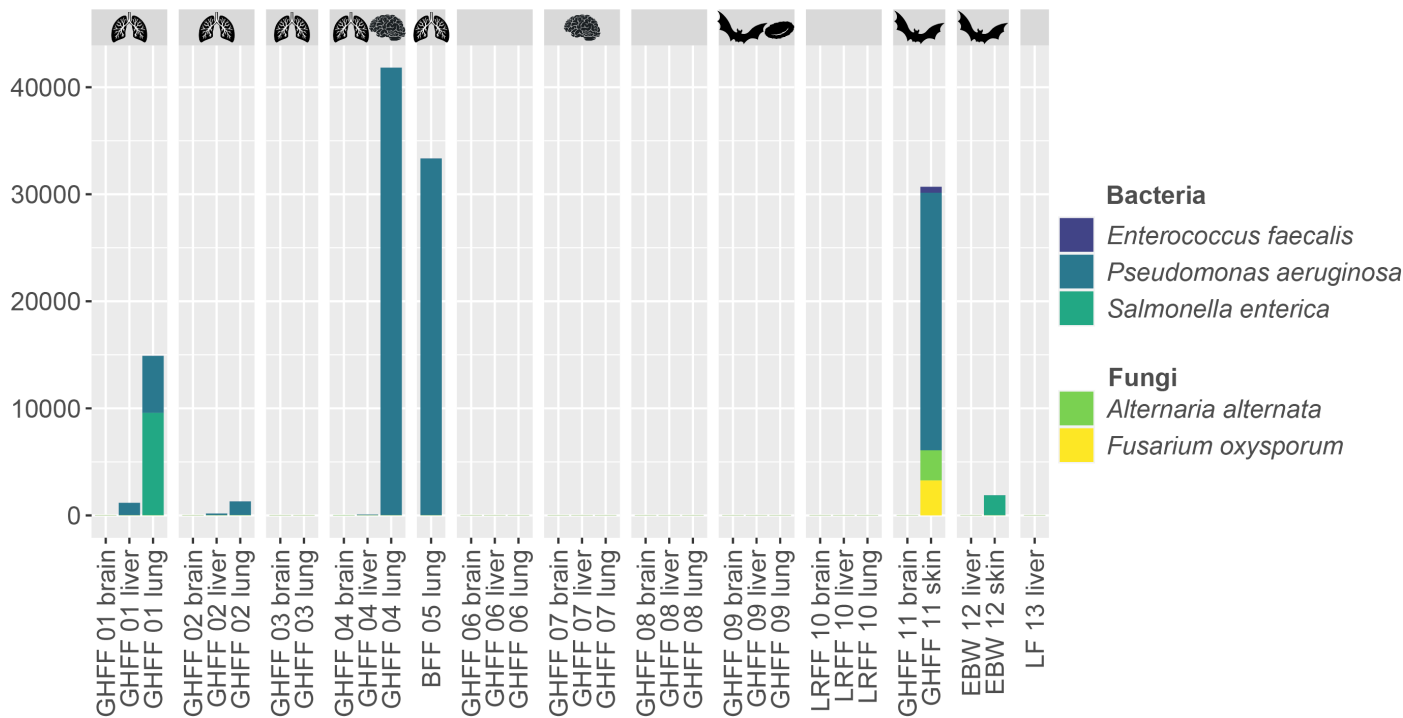
Figure 7.4.3: Read abundance displayed as reads per million (RPM) for selected bacterial and fungal families that were chosen based on pathogenic status. Libraries are separated by bat group and the lung, brain, red blood cell and bat silhouettes above the groups indicate which libraries were from bats with lung lesions, neurological signs, leukemia and skin lesions, respectively. Read abundance was calculated using CCMetagen (Marcelino et al., 2020).

P. aeruginosa (a gram-negative bacterium) had the highest read abundance and was observed in two liver, one brain, one skin and four lung libraries (Figure 7.4.3). The four lung libraries were from bats experiencing peracute decline or death with evidence of lung lesions, although we did not detect *P. aeruginosa* in an additional lung library containing bats with similar presentations and one animal with *P. aeruginosa* isolated in lung tissue (group GHFF 03). Notably, the group GHFF 11 skin library, which had comparable *P. aeruginosa* read abundance to the lung libraries from bats with pneumonia, was prepared from skin of three grey-headed flying foxes with noticeable skin lesions (Figure 7.4.1.1.c,d) where *P. aeruginosa* was isolated in culture. The 16S rRNA genes from *P. aeruginosa* from the four positive lung libraries displayed nucleotide sequence identities between 92.5 – 99.4%, with the two most abundant lung libraries, group GHFF 04 and BFF 05, having the most nucleotide sequence identity between the 16S rRNA genes (99.2%). The low sequence identities between the *P. aeruginosa* 16S rRNA genes of groups GHFF01, GHFF02 and GHFF03 should be interpreted with caution as these libraries also had low read coverage,

with some sections of the 16S rRNA gene having a coverage of only two reads. Additionally, the *P. aeruginosa* 16S rRNA gene from the skin of group GHFF 11 displayed 97.2% sequence identity to the 16S rRNA sequences from group GHFF 04 and BFF 05. *S. enterica* (gram-negative bacterium) reads were detected in one lung library (group GHFF 01) also containing *P. aeruginosa*, and a skin library from an eastern bent-wing bat (group EBW 12) (Figure 7.4.3). Finally, *E. faecalis* (a gram-positive bacterium), *A. alternata* (fungus) and *F. oxysporum* (fungus) were all observed at lower abundance than *P. aeruginosa* in the group GHFF 11 skin library with skin lesions mentioned above (Figure 7.4.3).

7.4.4: Overview of the viruses present in bats

Virus contigs matching to 14 families were identified here. Virus contigs belonging to the *Bornaviridae, Adintoviridae, Herpesviridae and Phycodnaviridae* were determined as likely to be endogenous virus elements as they contained no viral conserved domains and/or expected ORFs were interrupted by stop codons. These viral groups were therefore excluded from all analysis. Similarly, those contigs classified in the *Partitiviridae*, *Tombusviridae*, *Botourmiaviridae* and *Mitoviridae* were not analysed further as their closest relatives were viruses of plants, fungi and algae suggesting that they are dietary or environmental contaminants. Additionally, a *Picobirnaviridae* contig was disregarded as these viruses likely represent bacteriophage (Krishnamurthy and Wang, 2018). One *Parvoviridae* contig, with the closest BLASTX hit to viruses of the *Dependoparvovirus* genus, was detected in group LF 13 liver at low abundance (Figure 7.4.4), although the sequence was too short (360 bp/ 85 amino acid residues) to perform robust phylogenetic analysis. In contrast, the *Astroviridae, Flaviviridae, Picornaviridae* and *Retroviridae* contigs determined here were considered to be *bona fide* exogenous viruses of vertebrates and therefore investigated further (Figure 7.4.4).
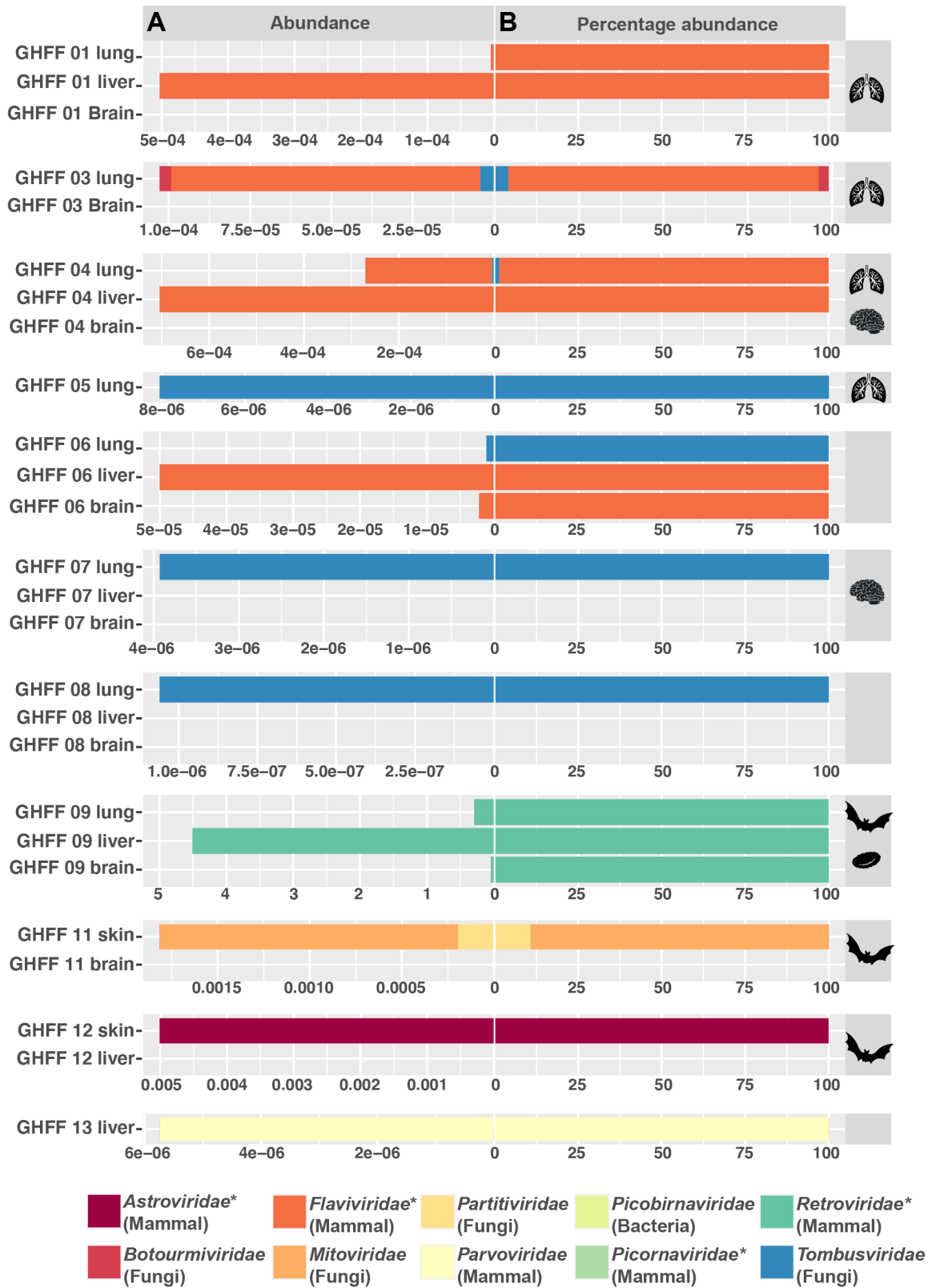
Figure 7.4.4: Read abundance of each viral family (excluding viruses determined to be endogenous), presented as (i) the expected count over the total number of trimmed sequence reads for that library multiplied by 100 to show the proportion of the library reads that are viral and (ii) the expected count as a percentage of total viral reads for that library. Virus families that are further discussed in this study are highlighted with an asterisk and the most likely host based on BLASTX for each family is in parenthesis. Groups with no virus abundance value are not shown. The lung, brain, red blood cell and bat silhouettes above the graphs denote which bat groups had bats with lung lesions, neurological signs, leukemia and skin lesions, respectively.

7.4.5: Identification of Hervey pteropid gammaretrovirus

A partial retrovirus contig of 8,105 bp was identified in the lung library from group GHFF 09. Sequence comparison over the entire contig revealed a high nucleotide identity (98%) to Hervey pteropid gammaretrovirus (GenBank accession MN413610.1) previously sampled from the faeces of a black flying fox from Queensland, Australia (Hayward et al., 2020). Amino acid sequence identities of the contig discovered here to the gag, pro-pol and env proteins were 100%, 99.2% and 99%, respectively. Such high sequence identities indicate that this represents a variant of Hervey pteropid gammaretrovirus. Complete ORFs were observed for the pro-pol and env genes, although only a partial gag protein that missed 22 bp from the 5' end, was recovered (Figure 7.4.5). The read abundance for Hervey pteropid gammaretrovirus was disproportionately high compared to the other viruses detected here (Figure 7.4.4). The liver library contained the highest read abundance (104,147 FPKM), slightly lower than observed for the host COX1 housekeeping gene (130,674 FPKM). The read abundance for the lung and brain libraries were 51,897 and 4,243 FPKM, respectively. Notably, phylogenetic analysis showed the gammaretroviruses sampled from Australian bats form a clade in the full genome phylogeny, indicative of ongoing evolution within Australia (Figure 7.4.5).
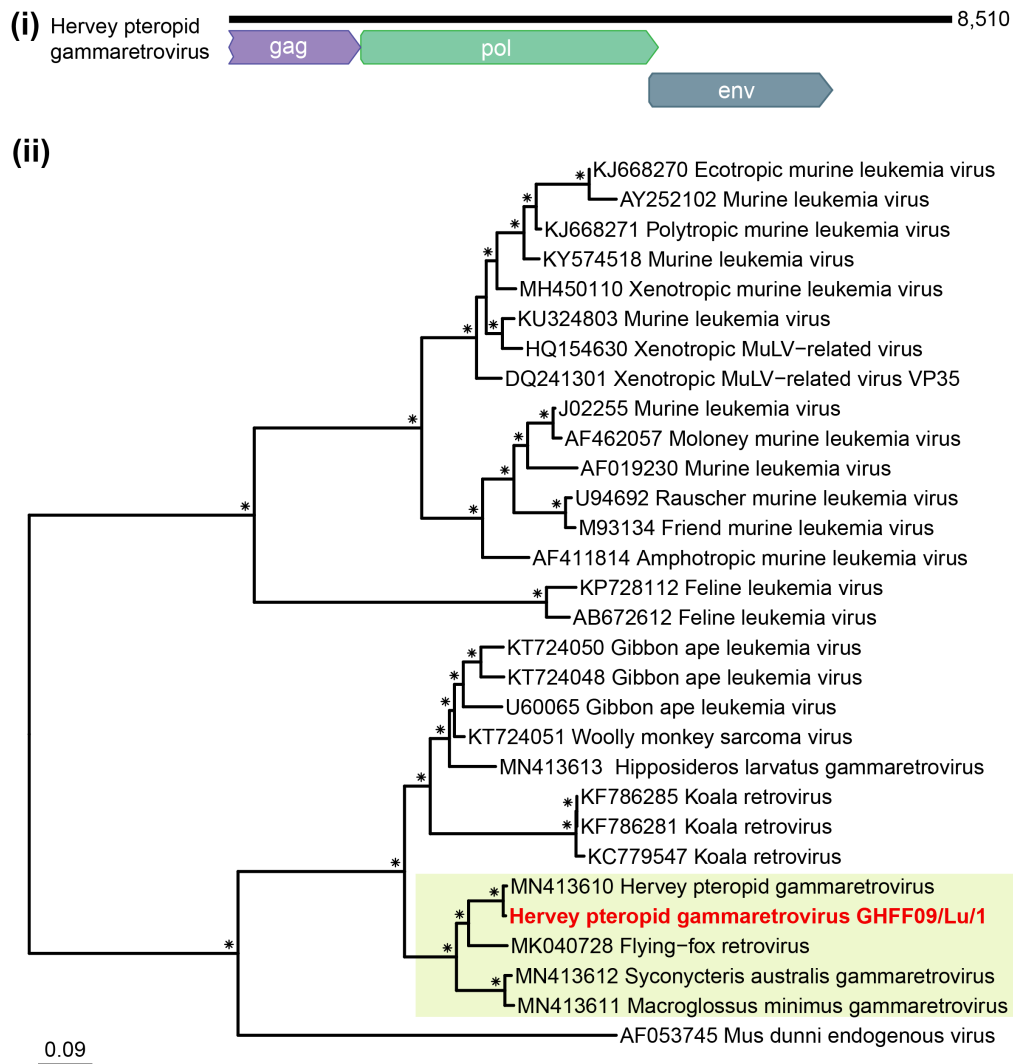
Figure 7.4.5: (i) Genome organisation of the Hervey pteropid gammaretrovirus variant detected in this study. (ii) Phylogenetic relationships of the gammaretrovirus genus determined using the full genome nucleotide sequence. The bat gammaretrovirus from this study is coloured in red and the gammaretroviruses from Australian bats are highlighted with a yellow background. Bootstrap values >70% are represented by the symbol shown at the branch node and the tree is rooted at midpoint for clarity. The scale bar represents the number of nucleotide substitutions per site.

We next performed PCR targeting the gag, pol and env genes (Table 7.4.5) on the individual lung, brain and liver RNA from the four bats included in group GHFF 09. This revealed that Hervey pteropid gammaretrovirus was present in two grey-headed flying foxes. A positive PCR result was observed in the lung, brain and liver samples from a female grey-headed flying fox found in Sydney, NSW (bat no. 14065.1; Table 7.7.1). This bat was euthanised due to ill-thrift and abdominal distension and histological changes were consistent with lymphoid

leukemia. An additional positive PCR result was seen for a liver sample from a male grey-headed flying fox with white skin lesions from Woolgoolga, NSW (bat no. 11501.1; Table 7.7.1). For this bat, RNA from other tissue types was not available for PCR.

7.4.6: Novel bat astroviruses

We identified a high abundance of astroviruses in a skin library (group EBW 12) from a single male eastern bent-wing bat with noticeable white skin lesions and underlying joint damage associated with severe mite infestation (bat no. 13087.1; Table 7.7.1). The eastern bent-wing bat was located in Yass, NSW, a town approximately 300 km from Sydney. Astroviruses possess a positive-sense single strand (+ss) RNA genome and those associated with mammals are classified in the genus *Mamastrovirus* and have been linked to gastroenteritis or neurological issues in some species (De Benedictis et al., 2011).

Near complete genomes were assembled for three distinct astroviruses, and partial genomes (with at least partial capsid or RdRp) were assembled for a further five distinct astroviruses, with contigs lengths ranging from 6,765 bp to 913 bp (Figure 7.4.6). Comparative analysis of the complete capsid protein from the three bat astroviruses with near complete genomes – provisionally denoted bat astrovirus 2 (6,765 bp; 3,377 reads), bat astrovirus 3 (6,748 bp; 3,217 reads) and bat astrovirus 4 (6,747 bp; 2,067 reads) – showed their amino acid identities to each other to be 57-67%, and only 20-55% to other characterised bat astroviruses. Hence, each likely represents a novel virus species based on the current species demarcation in ICTV.

Phylogenetic analysis of the RdRp and capsid proteins of the bat astrovirus contigs detected here with global sequences revealed a clear clustering of astroviruses collected from bats and hence a long-term virus-host association (Figure 7.4.6). The three proposed new species, bat astrovirus 2, bat astrovirus 3 and bat astrovirus 4, broadly group together in both the capsid protein and the RdRp phylogenies; although bat astrovirus 3 does not directly cluster with the other two Australian viruses in the RdRp tree due to the inclusion of additional bat astrovirus 1 sequences not present in the capsid tree. Additionally, the partial genome bat astrovirus sequences detected did not group with bat astrovirus 2, 3 and 4, suggesting that multiple lineages of bat astroviruses are evolving in Australia (Figure 7.4.6).
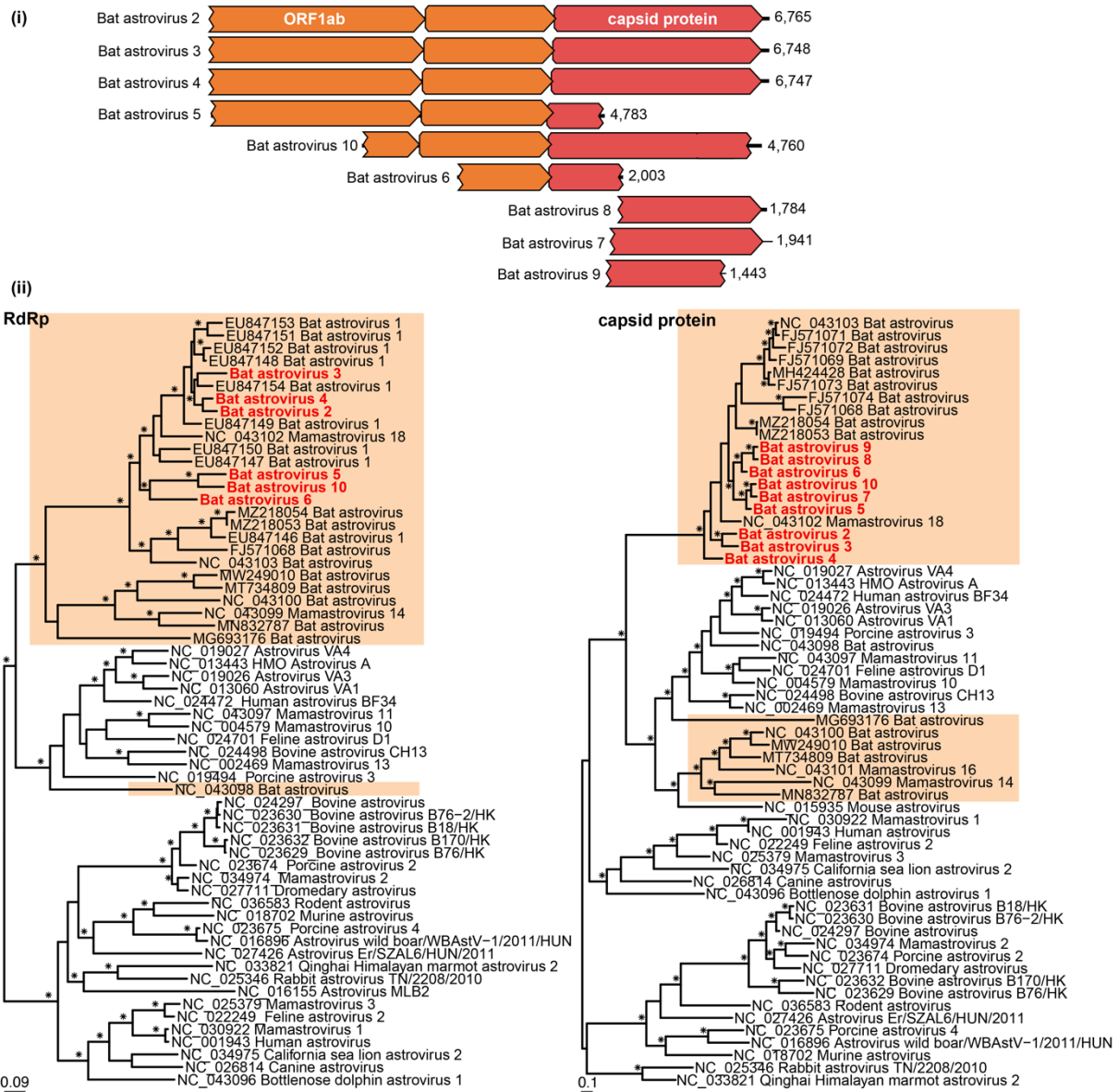
Figure 7.4.6: (i) Genomic organisation of the bat astroviruses identified in this study. (ii) Phylogenetic relationships of mamastroviruses using the RdRp and capsid protein amino acid sequence. Amino acid alignment lengths were 446 and 465 residues for the RpRp and capsid protein, respectively. Bat astroviruses are highlighted in orange and bat astroviruses from this study are coloured in red. Bootstrap values >70% are represented by the symbol shown at the branch node. The trees are rooted at midpoint for clarity and the scale bar represents the amino acid substitutions per site.

211

7.4.7: Bat pegiviruses

Pegivirus fragments were identified in four bat libraries (group GHFF 01, GHFF 03, GHFF 04 and GHFF 06) containing three, four, five and three bats, respectively (Table 7.7.1). Pegiviruses are +ssRNA viruses of the genus *Pegivirus*, family *Flaviviridae*, that are often non-pathogenic in mammalian hosts. In one liver library (group GHFF 04) a complete pegivirus genome (denoted bat pegivirus GHFF04/Li/1) of length 9,784 bp was identified with a read abundance of 1,030, and containing the expected E1, E2, NS2, NS3, NS4A, NS4B, NS5A and NS5B proteins (Figure 7.4.7). Bat pegivirus GHFF04/Li/1 contigs were also identified in the accompanying lung library from group GHFF 04, with a read abundance of 354. Using primers targeting the NS3 and NS5b region of bat pegivirus GHFF04/Li/1 (Table 7.4.5), PCR was performed on the five bats in group GHFF 04. This showed that bat pegivirus GHFF04/Li/1 was present in the lung and liver samples from an adult male grey-headed flying fox from Sydney (bat no. 14121.1; Table 7.7.1) that presented flaccid paralysis and central nervous system depression, including lack of response to stimuli. Necropsy and histopathology revealed necrotising and pyogranulomatous hepatitis, and histiocytic myocarditis. An additional eight unique bat pegivirus contigs (read abundance 221) were identified in liver library GHFF 04, with one contig containing a partial NS3 (GHFF04/Li/2) and another a partial NS5B (GHFF04/Li/3) region (Figure 7.4.7). Short pegivirus contigs distinct to the pegiviruses found in GHFF04 were assembled from the liver library from group GHFF 01 (838 reads), the liver library from group GHFF 06 (17 reads), and the lung library from group GHFF 03 (40 reads). As we were unable to extract sufficient RNA from the liver tissue of group GHFF 03, we cannot confirm whether pegivirus contigs were also present in the livers of these bats.

Phylogenetic analysis was conducted on translated contigs of sufficient length (>220 residues) encoding NS3 and NS5b (Figure 7.4.7). This demonstrated that at least four distinct pegiviruses were present in the sampled bats. The bat pegivirus contigs identified here formed a clade with bat pegiviruses previously identified from species Pegivirus B, suggesting that this species has a long association with bats (Figure 7.4.7).

Figure 7.4.7: (i) Genomic organisation of the bat pegiviruses identified in this study. (ii) Uncorrected (p) distances of the amino acid sequences the NS3 and NS5 proteins of selected bat pegivirus and GHFF04/Li/1. (iii) Phylogenetic relationships within the genus Pegivirus using the NS3 and NS5B amino acid sequence. Amino acid alignment lengths were 620 residues for the NS3 gene and 531 residues for the NS5B gene. Bat pegiviruses are highlighted in purple and the bat pegiviruses from this study are coloured in red. Bootstrap values >70% are represented by the symbol shown at the branch node. The tree was midpoint rooted for clarity and the scale bar represents the amino acid substitutions per site.

7.4.8: Novel bat kunsagivirus

A novel kunsagivirus (tentatively named Auskunsag virus for the country in which the bat was sampled, Australia) was identified in a single lung and liver library containing three grey-headed flying fox individuals from group GHFF 09. *Kunsagivirus* is a genus of the

213

Picornaviridae that have +ssRNA genomes between of 6,800 bp – 7,400 bp in length. The 7,482 bp Auskunsa virus genome comprises the P1 region containing VP0, VP1 and VP3, the P2 region containing the 2A1, 2A2, 2B and 2C and the P3 region containing the 3A, 3B, 3C and 3D (Figure 7.4.8).

PCR targeting the 3D region (Table 7.7.2) was performed on the four individual bats from group GHFF 09, confirming that Auskunsag virus was present the lung and liver sampled from a female juvenile grey-headed flying fox from Sydney with no disease presentation (bat no. 11553.1; Table 7.7.1). The read abundance values for the lung and liver libraries were 6,498 and 359, respectively. The closest related virus based on phylogenetic analysis of the P1 and 3CD regions was Kunsagivirus B1 (accession no. KX644936, Figure 7.4.8) sampled from the faeces of a straw-coloured fruit bat (*Eidolon helvum*) in Cameroon (Yinda et al., 2016). Amino acid identities between auskunsag virus and Kunsagivirus B1 over the polyprotein, P1 region and 3CD were 68%, 69% and 71%, respectively. The uncorrected (p) distances for the P1 and 3CD region was calculated to determine whether Auskunsag virus should constitute a new species in the *Kunsagivirus* genus. As Auskunsag virus exhibits nucleotide p-distances that fall below the ICTV classification which is <0.51 for P1 and <0.52 for 3CD, we propose Auskunsag virus should tentatively represent a new kunsagivirus species (Figure 7.4.8).
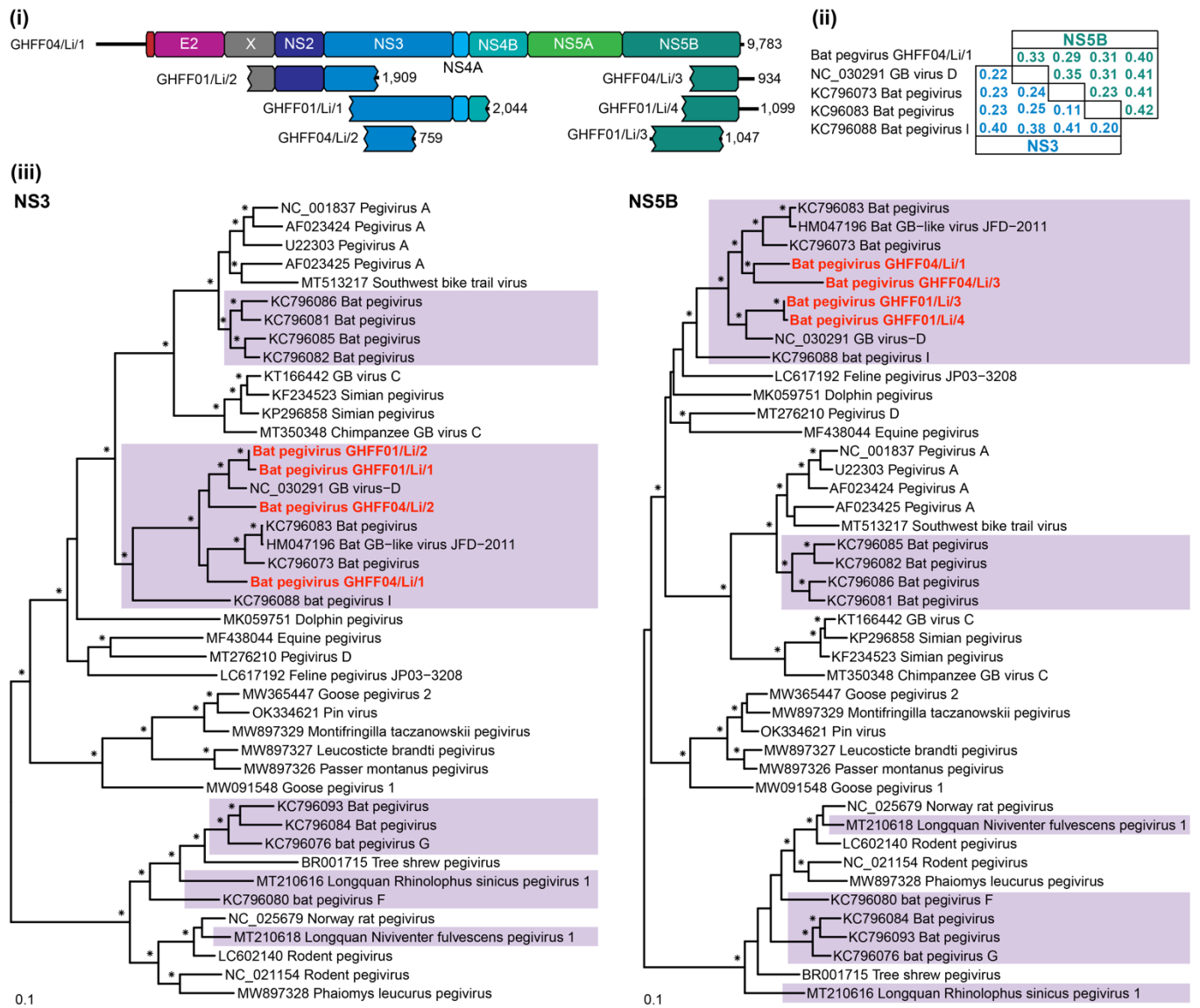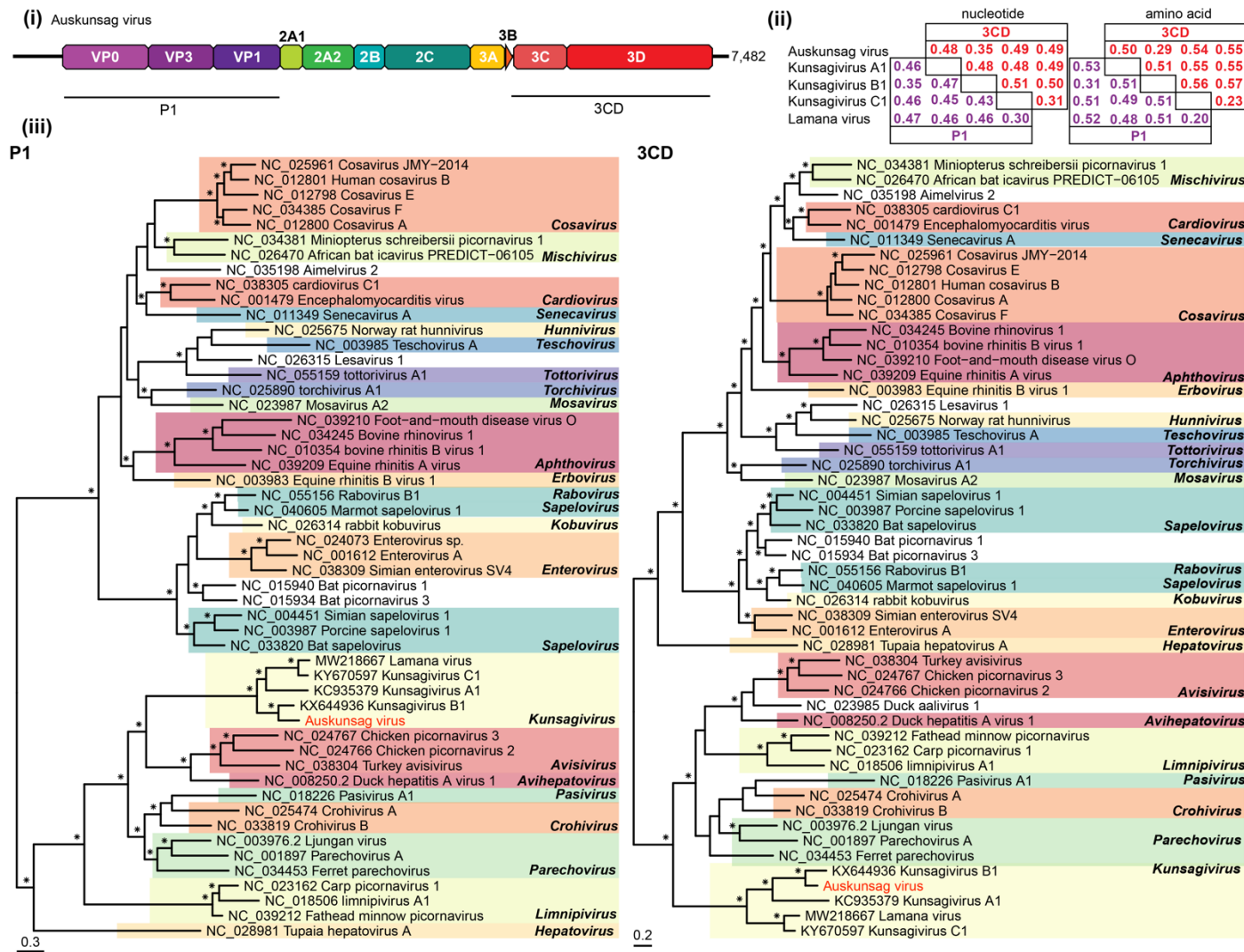
Figure 7.4.8: (i) Genomic organisation of the novel kunsagivirus identified in this study. (ii) Uncorrected (p) distances among amino acid sequences of the P1 and 3CD regions of the four members of the Kunsagivirus genus and Auskunsag virus. (iii) Phylogenetic relationships of Auskunsag virus using amino acid sequences of the P1 and 3CD genes. Amino acid alignment lengths were 737 and 653 residues for the P1 and 3CD genes, respectively. Auskunsag virus is coloured in red and the different Picornaviridae genera are highlighted in the tree. Bootstrap values >70% are represented by symbols shown at the branch node. The trees were midpoint rooted for clarity and the scale bar represents the amino acid substitutions per site.

7.5: Discussion

In Australia, numerous native bat species, including the grey-headed flying fox, have experienced population declines that have resulted in the listing of these species as vulnerable or endangered. Population declines are mainly driven by the effects of climate change and habitat loss/destruction due to urbanisation, ongoing threats that are likely to continue impacting wild populations (Welbergen et al., 2008). Any additional threat to Australian flying foxes, such as infectious disease, could lead population numbers to unrecoverable levels. Given the increasing interest in bat health and the role that bats may play as reservoirs of zoonotic microbes and viruses, we performed metatranscriptomic sequencing on tissue samples from several Australian bats with underlying health issues. From this, we were able to identify several pathogenic bacteria and fungi, an important possibly pathogenic gammaretrovirus, and RNA viruses from the vertebrate-infecting families *Astroviridae*, *Flaviviridae* and *Picornaviridae*.

A notable aspect of this study was the metatranscriptomic identification of viruses from tissue samples in bats with varied disease syndromes rather than exploring the healthy state virome. Generally, collecting faeces is the preferred method of sampling bats as it allows for the collection of data from large populations in a non-invasive manner. Although characterising the faecal virome of bats is important for identifying novel and potentially zoonotic viruses, especially from urban bat populations, the sampling of dietary invertebrate and plant viruses is common, such that viromes may differ between faecal and tissue samples (Li et al., 2010b, Cobbin et al., 2021, Hardmeier et al., 2021). Our previous study of the faecal virome of the grey-headed flying fox identified bat viruses belonging to the *Coronaviridae* and *Caliciviridae*, as well as myriad insect and plant viruses likely associated with diet (Van Brussel et al., 2022). Notably, no mammalian viruses belonging to the *Flaviviridae*, as well as only one short contig matching to *Astroviridae* and two short contigs matching to *Picornaviridae*, were identified in marked contrast to the results presented here (Van Brussel et al., 2022).

Analysis of the microbiome from Australian bat tissues identified four bacterial and two fungal species of pathogenic concern. *Salmonella enterica* serovar Wangata was isolated in culture from the lung and intestine of a young grey-headed flying fox found with histological evidence of colitis, hepatitis and interstitial pneumonia in a pattern consistent with septicaemia. This organism is an important cause of human salmonellosis in NSW (Simpson

et al., 2019). *P. aeruginosa* is an opportunistic pathogen that can cause pneumonia in immunocompromised people (Moradali et al., 2017, Reynolds and Kollef, 2021), which was identified by culture and metatranscriptomic investigation within lung tissue of ten diseased bats in this study. Affected bats had a consistent pattern of fibrin necrotising, neutrophilic or histiocytic interstitial pneumonia. In two lung libraries, both from flying foxes, *P. aeruginosa* reads were at high abundance (Figure 7.4.3). It is unclear whether the presence of *P. aeruginosa* in these bats is a primary cause of lung disease. All affected animals had a history of trauma, heat stress or involvement in a mass mortality event, suggesting that *P. aeruginosa* is acting as a secondary, opportunistic infection. Furthermore, analysis of the *P.aeruginosa* 16S rRNA gene showed sequence diversity, suggesting that the presentation of peracute pneumonia in the bats is most likely not caused by clonal expansion of a single pathogenic *P. aeruginosa* organism. The abundance of *P. aeruginosa* was also high in a single skin library (Figure 7.4.3). This library contained ulcerated and hyperkeratotic skin samples from three grey-headed flying foxes where *P. aeruginosa, Serratia marcescens*, and other bacteria were isolated in culture. It is important to note that *P. aeruginosa* is found in the environment and can be found as part of the skin microbiome (Moradali et al., 2017, Spernovasilis et al., 2021). When *P. aeruginosa* is present on the skin it can opportunistically cause skin and soft tissue infections in humans (Spernovasilis et al., 2021). The high read abundance of *P. aeruginosa* in the skin library of grey-headed flying foxes with noticeable wing skin lesions is interesting, although may constitute a harmless part of the skin microbiome at the time of sampling. In some instances, bacteria were isolated in tissue culture of bat lesions, but were not abundant within metatranscriptomic data, most likely reflecting overgrowth of highly cultivable organisms rather than true organism diversity and abundance. Alternatively, pooling samples for metatranscriptomic investigations may diminish the relative abundance of some organisms. It should also be noted that the *P. aeruginosa* could have been obtained while in care, however, this is difficult to confirm. The integration of traditional and metatranscriptomic diagnostic pipelines has the potential to more fully explore the microbial diversity of wildlife while tempering the potential biases inherent in each approach.

A notable finding was the detection of Hervey pteropid gammaretrovirus in a group of grey-headed flying foxes (group GHFF 09). This virus was previously described from the faeces of a black flying fox from Queensland, Australia, and shown to be a functional exogenous virus (Hayward et al., 2020). Investigation herein using PCR revealed that Hervey pteropid gammaretrovirus was present in two grey-headed flying foxes from the same pool of bats.

Notably, an adult female grey-headed flying fox with lymphoid leukemia in which virus was detected by PCR in lung, brain and liver samples. The second animal was a male with white skin lesions and detectable virus in the liver. RNA from other tissues was not available for this animal for PCR testing. These grey-headed flying foxes were from Sydney and Woolgoolga, NSW (Table 7.7.1), with Sydney being the furthest south this virus has been detected (Hayward et al., 2020). Hervey pteropid gammaretrovirus and three other gammaretroviruses detected in Australian bats are phylogenetically related to koala retrovirus and gibbon ape leukemia virus (Hayward et al., 2020, McMichael et al., 2019), both of which are associated with immune deficiencies and leukemia (Xu and Eiden, 2015, Kawakami et al., 1972). The presence of Hervey pteropid gammaretrovirus in a bat with lymphoid leukemia suggests a possible association with disease, although further research is needed to reveal any mechanistic role the virus plays in disease manifestation. Replication competent Hervey pteropid gammaretrovirus virions have been tested *in vitro* and confirmed to infect bat and human cell lines, although virions were synthetically constructed using the consensus sequence from RNA sequencing (Hayward et al., 2020). Isolating infectious virus from the bat with lymphoid leukemia, combined with additional *in vitro* studies, may provide better insight into transmissibility and the pathogenic potential of the virus. The FPKM counts in the liver library from group GHFF 09 (104,147) were comparable to those for the bat COX1 housekeeping gene (130,674). Such a high abundance is compatible with active virus replication at the time of sampling, although the contribution of each individual bat liver sample toward the total liver library gammaretrovirus abundance cannot be determined (Figure 7.4.5).

In the same group of bats (GHFF 09) in which we identified Hervey pteropid gammaretrovirus we detected a novel picornavirus belonging to the genus *Kunsagivirus*. This genus currently contains three recognised species sampled from the faeces of a European roller in 2011 (Boros et al., 2013) and a straw-coloured fruit bat in Cameroon (Yinda et al., 2016), respectively, and from the blood of a yellow baboon in Tanzania (Buechler et al., 2017). A fourth kunsagivirus sequence was more recently sampled from vervet monkeys from Uganda (Kuhn et al., 2020). Here, we characterised a novel kunsagivirus, tentatively named Auskunsag virus, that was identified in a liver sample from a female juvenile grey-headed flying fox from Sydney, Australia, and absent from the two bats in which Hervey pteropid gammaretrovirus was detected. Auskunsag virus is the first report of a kunsagivirus in the Asia-pacific region and of a kunsagivirus in tissue samples, indicating that this genus is

most likely mammalian-infecting and not dietary or invertebrate-associated. Viruses of the genus *Kunsagivirus* currently have no disease association, although additional research is needed for confirmation.

Multiple astroviruses were detected in a single skin library containing one eastern-bent wing bat that had noticeable skin lesions coupled with underlying joint damage. A total of 74% of the characterised bat astroviruses on NCBI GenBank were sampled exclusively from faeces. As it currently stands, no bat astroviruses have been sampled from skin, although Avian nephritis virus 3 of the genus *Avastrovirus* has been detected in the joint and tendons sampled from boiler chickens and poult turkeys with arthritis and tenosynovitis and was proposed to have a possible association with these conditions (de Wit et al., 2011). The diversity of astroviruses in Australian bats has yet to be assessed, and only one sequence of the *Astroviridae* from an Australian bat is available on GenBank. This sequence, microbat bastrovirus (accession no. MT766313), is more closely related to the diverse group of astroviruses termed bastroviruses that contain a hepe-like non-structural protein and an astro-like structural protein (Oude Munnink et al., 2016). A study of Asian and European bat species showed that astroviruses are common in apparently healthy bat populations and in some incidences were at high prevalence (Lacroix et al., 2017, Fischer et al., 2016, Kemenesi et al., 2014, Zhu et al., 2009, Fischer et al., 2017). The detection of several diverse bat astroviruses in this study suggests that numerous astroviruses may be circulating within the bat population in Australia and that further research is needed to fully understand their community structure and potential contribution to disease.

Finally, we detected bat pegivirus contigs in four grey-headed flying fox groups (GHFF 01, GHFF 03, GHFF 04 and GHFF 06), with one containing a complete genome – bat pegivirus GHFF04/Li/1. Generally, pegiviruses are non-pathogenic and associated with persistent infections in mammals, although members of the species Pegivirus D have been associated with the development of Theiler's disease in infected horses (Chandriani et al., 2013). Although we detected bat pegivirus GHFF04/Li/1 in a grey-headed flying fox with necrotising and granulomatous hepatitis and histiocytic myocarditis, we also detected bat pegiviruses in bats with no clear liver or heart disease suggesting that it is likely a commensal pathogen like most other pegiviruses.

The sustainability of micro and megabat species globally is important for the sustainably of the world's ecosystems. In countries with continual threats, such as habitat change and

destruction, land use change, agricultural practices adverse to bat health, extreme temperatures and white-nose syndrome, efforts to maintain population numbers are critical. Ongoing monitoring of bat health and disease and using traditional and metatranscriptomic diagnostic techniques is warranted to explore the diversity of microbes with pathogenic potential that might be expressed in the form of disease in populations subject to landscape-wide change. The presence of a retrovirus from a genus with members that are associated with immune deficiencies and leukemia, in a bat with lymphoid leukemia, undoubtedly warrants further investigation and broader surveillance. Additionally, the detection of numerous novel viruses with unclear disease association and reads from bacterial and fungal families that contain pathogenic species highlights the importance of virus screening in Australian bats to ensure detrimental disease outbreaks can be minimised.

7.6: References

Banerjee, A., Baker, M.L., Kulcsar, K., Misra, V., Plowright, R., Mossman, K. 2020. Novel Insights Into Immune Systems of Bats. *Frontiers in Immunology,* 11:26.

Banyard, A.C., Hayman, D., Johnson, N., McElhinney, L., Fooks, A.R. 2011. Bats and lyssaviruses. *Advances in Virus Research,* 79:239-89.

Boros, Á., Kiss, T., Kiss, O., Pankovics, P., Kapusinszky, B., Delwart, E., Reuter, G. 2013. Genetic characterization of a novel picornavirus distantly related to the marine mammal-infecting aquamaviruses in a long-distance migrant bird species, European roller (Coracias garrulus). *Journal of General Virology,* 94(Pt 9):2029-2035.

Buechler, C.R., Bailey, A.L., Lauck, M., Heffron, A., Johnson, J.C., Campos Lawson, C., Rogers, J., Kuhn, J.H., O'Connor, D.H. 2017. Genome Sequence of a Novel Kunsagivirus (Picornaviridae: Kunsagivirus) from a Wild Baboon (Papio cynocephalus). *Genome Announcements,* 5(18):e00261-17.

Capella-Gutiérrez, S., Silla-Martínez, J.M., Gabaldón, T. 2009. trimAl: a tool for automated alignment trimming in large-scale phylogenetic analyses. *Bioinformatics,* 25(15):1972-3.

Chandriani, S., Skewes-Cox, P., Zhong, W., Ganem, D.E., Divers, T.J., Van Blaricum, A.J., Tennant, B.C., Kistler, A.L. 2013. Identification of a previously undescribed divergent virus from the Flaviviridae family in an outbreak of equine serum hepatitis. *Proceedings of the National Academy of Sciences of the United States of America,* 110(15):E1407-15.

Cheng, T.L., Reichard, J.D., Coleman, J.T.H., Weller, T.J., Thogmartin, W.E., Reichert, B.E., Bennett, A.B., Broders, H.G., Campbell, J., Etchison, K., Feller, D.J., Geboy, R., Hemberger, T., Herzog, C., Hicks, A.C., Houghton, S., Humber, J., Kath, J.A., King, R.A., Loeb, S.C., Massé, A., Morris, K.M., Niederriter, H., Nordquist, G., Perry, R.W., Reynolds, R.J., Sasse, D.B., Scafini, M.R., Stark, R.C., Stihler, C.W., Thomas, S.C., Turner, G.G., Webb, S., Westrich, B.J., Frick, W.F. 2021. The scope and severity of white-nose syndrome on hibernating bats in North America. *The Journal of the Society for Conservation Biology,* 35(5):1586-1597.

Clausen, P., Aarestrup, F.M., Lund, O. 2018. Rapid and precise alignment of raw reads against redundant databases with KMA. *BMC Bioinformatics,* 19(1):307.

Cobbin, J.C., Charon, J., Harvey, E., Holmes, E.C., Mahar, J.E. 2021. Current challenges to virus discovery by meta-transcriptomics. *Current Opinion in Virology,* 51:48-55.

De Benedictis, P., Schultz-Cherry, S., Burnham, A., Cattoli, G. 2011. Astrovirus infections in humans and animals - molecular biology, genetic diversity, and interspecies transmissions. *Infect Genet Evol,* 11(7):1529-44.

de Wit, J.J., Dam, G.B., de Laar, J.M., Biermann, Y., Verstegen, I., Edens, F., Schrier, C.C. 2011. Detection and characterization of a new astrovirus in chicken and turkeys with enteric and locomotion disorders. *Avian Pathology,* 40(5):453-61.

Fischer, K., Pinho Dos Reis, V., Balkema-Buschmann, A. 2017. Bat Astroviruses: Towards Understanding the Transmission Dynamics of a Neglected Virus Family. *Viruses,* 9(2):34.

Fischer, K., Zeus, V., Kwasnitschka, L., Kerth, G., Haase, M., Groschup, M.H., Balkema-Buschmann, A. 2016. Insectivorous bats carry host specific astroviruses and coronaviruses across different regions in Germany. *Journal of Molecular Epidemiology and Evolutionary Generics in Infectious Diseases,* 37:108-16.

Flying Fox Paralysis Syndrome Working Group. 2022. Flying-fox Paralysis Syndrome (FFPS): Interim case definition, sample collection and treatment advice. Viewed January 2023. https://wildlifehealthaustralia.com.au/Portals/0/Documents/Ongoing%20Incidents/FF_Paralysis_Syndrome-case_definition_sampling_treatment.pdf

Hardmeier, I., Aeberhard, N., Qi, W., Schoenbaechler, K., Kraettli, H., Hatt, J.M., Fraefel, C., Kubacki, J. 2021. Metagenomic analysis of fecal and tissue samples from 18 endemic bat species in Switzerland revealed a diverse virus composition including potentially zoonotic viruses. *PLoS One,* 16(6):e0252534.

Hayward, J.A., Tachedjian, M., Kohl, C., Johnson, A., Dearnley, M., Jesaveluk, B., Langer, C., Solymosi, P.D., Hille, G., Nitsche, A., Sánchez, C.A., Werner, A., Kontos, D., Crameri, G., Marsh, G.A., Baker, M.L., Poumbourios, P., Drummer, H.E., Holmes, E.C., Wang, L.F., Smith, I., Tachedjian, G. 2020. Infectious KoRV-related

retroviruses circulating in Australian bats. *Proceedings of the National Academy of Sciences of the United States of America,* 117(17):9529-9536.

Hoang, D.T., Chernomor, O., von Haeseler, A., Minh, B.Q., Vinh, L.S. 2017. UFBoot2: Improving the Ultrafast Bootstrap Approximation. *Molecular Biology and Evolution,* 35(2):518-522.

Hoyt, J.R., Kilpatrick, A.M., Langwig, K.E. 2021. Ecology and impacts of white-nose syndrome on bats. *Nat Rev Microbiol,* 19**,** 196-210.

Irving, A.T., Ahn, M., Goh, G., Anderson, D.E., Wang, L.F. 2021. Lessons from the host defences of bats, a unique viral reservoir. *Nature,* 589(7842):363-370.

International Union for Conservation of Nature. 2021a. Data from "Pteropus poliocephalus". *The IUCN Red List of Threatened Species*, 2021-3. https://www.iucnredlist.org/species/18751/22085511

International Union for Conservation of Nature. 2021b. *The IUCN Red List of Threatened Species*. Version 2021-3. https://www.iucnredlist.org

Kalyaanamoorthy, S., Minh, B.Q., Wong, T.K.F., von Haeseler, A., Jermiin, L.S. 2017. ModelFinder: fast model selection for accurate phylogenetic estimates. *Nature Methods,* 14(6):587-589.

Katoh, K., Standley, D.M. 2013. MAFFT multiple sequence alignment software version 7: improvements in performance and usability. *Molecular Biology and Evolution,* 30(4):772-80.

Kawakami, T.G., Huff, S.D., Buckley, P.M., Dungworth, D.L., Synder, S.P., Gilden, R.V. 1972. C-type virus associated with gibbon lymphosarcoma. *Nature: New Biology,* 235(58):170-1.

Kechin, A., Boyarskikh, U., Kel, A., Filipenko, M. 2017. cutPrimers: A New Tool for Accurate Cutting of Primers from Reads of Targeted Next Generation Sequencing. *Journal of Computational Biology,* 24(11):1138-1143.

Kemenesi, G., Dallos, B., Görföl, T., Boldogh, S., Estók, P., Kurucz, K., Kutas, A., Földes, F., Oldal, M., Németh, V., Martella, V., Bányai, K., Jakab, F. 2014. Molecular survey of RNA viruses in Hungarian bats: discovering novel astroviruses, coronaviruses, and caliciviruses. *Vector Borne and Zoonotic Disease,* 14(12):846-55.

Kolkert, H., Andrew, R., Smith, R., Rader, R., Reid, N. 2020. Insectivorous bats selectively source moths and eat mostly pest insects on dryland and irrigated cotton farms. *Ecology and Evolution,* 10(1):371-388.

Krishnamurthy, S.R., Wang, D. 2018. Extensive conservation of prokaryotic ribosomal binding sites in known and novel picobirnaviruses. *Virology,* 516:108-114.

Kuhn, J.H., Sibley, S.D., Chapman, C.A., Knowles, N.J., Lauck, M., Johnson, J.C., Lawson, C.C., Lackemeyer, M.G., Valenta, K., Omeja, P., Jahrling, P.B., O'Connor, D.H., Goldberg, T.L. 2020. Discovery of Lanama Virus, a Distinct Member of Species Kunsagivirus C (Picornavirales: Picornaviridae), in Wild Vervet Monkeys (Chlorocebus pygerythrus). *Viruses,* 12(12):1436.

Lacroix, A., Duong, V., Hul, V., San, S., Davun, H., Omaliss, K., Chea, S., Hassanin, A., Theppangna, W., Silithammavong, S., Khammavong, K., Singhalath, S., Afelt, A., Greatorex, Z., Fine, A.E., Goldstein, T., Olson, S., Joly, D.O., Keatts, L., Dussart, P., Frutos, R., Buchy, P. 2017. Diversity of bat astroviruses in Lao PDR and Cambodia. *Journal of Molecular Evolution Genetics in Infectious Diseases,* 47:41-50.

Langmead, B., Salzberg, S.L. 2012. Fast gapped-read alignment with Bowtie 2. *Nature Methods,* 9(4):357-9.

Langmead, B., Wilks, C., Antonescu, V., Charles, R. 2019. Scaling read aligners to hundreds of threads on general-purpose processors. *Bioinformatics,* 35(3):421-432.

Law, B.S., Lean, M. 1999. Common blossom bats (Syconycteris australis) as pollinators in fragmented Australian tropical rainforest. *Biological conservation,* 91(2-3):201-212.

Li, B., Ruotti, V., Stewart, R.M., Thomson, J.A., Dewey, C.N. 2010a. RNA-Seq gene expression estimation with read mapping uncertainty. *Bioinformatics,* 26(4):493-500.

Li, D., Liu, C.M., Luo, R., Sadakane, K., Lam, T.W. 2015. MEGAHIT: an ultra-fast single-node solution for large and complex metagenomics assembly via succinct de Bruijn graph. *Bioinformatics,* 31(10):1674-6.

Li, D., Luo, R., Liu, C.M., Leung, C.M., Ting, H.F., Sadakane, K., Yamashita, H., Lam, T.W. 2016. MEGAHIT v1.0: A fast and scalable metagenome assembler driven by advanced methodologies and community practices. *Methods,* 102:3-11.

Li, L., Victoria, J.G., Wang, C., Jones, M., Fellers, G.M., Kunz, T.H., Delwart, E. 2010b. Bat guano virome: predominance of dietary viruses from insects and plants plus novel mammalian viruses. *Journal of Virology,* 84(14):6955-65.

Marcelino, V.R., Clausen, P., Buchmann, J.P., Wille, M., Iredell, J.R., Meyer, W., Lund, O., Sorrell, T.C., Holmes, E.C. 2020. CCMetagen: comprehensive and accurate identification of eukaryotes and prokaryotes in metagenomic data. *Genome Biology,* 21(1):103.

McMichael, L., Smith, C., Gordon, A., Agnihotri, K., Meers, J., Oakey, J. 2019. A novel Australian flying-fox retrovirus shares an evolutionary ancestor with Koala, Gibbon and Melomys gamma-retroviruses. *Virus Genes,* 55:421-424.

Mishra, N., Fagbo, S.F., Alagaili, A.N., Nitido, A., Williams, S.H., Ng, J., Lee, B., Durosinlorun, A., Garcia, J.A., Jain, K., Kapoor, V., Epstein, J.H., Briese, T., Memish, Z.A., Olival, K.J., Lipkin, W.I. 2019. A viral metagenomic survey identifies known and novel mammalian viruses in bats from Saudi Arabia. *PLoS One,* 14(4):e0214227.

Mo, M., Roache, M., Davies, J., Hopper, J., Pitty, H., Foster, N., Guy, S., Parry-Jones, K., Francis, G., Koosmen, A. 2021. Estimating flying-fox mortality associated with abandonments of pups and extreme heat events during the austral summer of 2019–20. *Pacific Conservation Biology,* 28:124-139.

Mollentze, N., Streicker, D.G. 2020. Viral zoonotic risk is homogenous among taxonomic orders of mammalian and avian reservoir hosts. *Proceedings of the National Academy of Sciences of the United States of America,* 117(17):9423-9430.

Moradali, M.F., Ghods, S., Rehm, B.H. 2017. Pseudomonas aeruginosa Lifestyle: A Paradigm for Adaptation, Survival, and Persistence. *Frontiers in Cellular and Infection Microbiology,* 7:39.

Moran, C., Catterall, C.P., Kanowski, J. 2009. Reduced dispersal of native plant species as a consequence of the reduced abundance of frugivore species in fragmented rainforest. *Biological conservation,* 142(3):541-552.

Nguyen, L.-T., Schmidt, H.A., von Haeseler, A., Minh, B.Q. 2014. IQ-TREE: A Fast and Effective Stochastic Algorithm for Estimating Maximum-Likelihood Phylogenies. *Molecular Biology and Evolution,* 32(1):268-274.

Oude Munnink, B.B., Cotten, M., Canuti, M., Deijs, M., Jebbink, M.F., van Hemert, F.J., Phan, M.V., Bakker, M., Jazaeri Farsani, S.M., Kellam, P., van der Hoek, L. 2016. A Novel Astrovirus-Like RNA Virus Detected in Human Stool. *Virus Evolution,* 2(1):vew005.

Reynolds, D., Kollef, M. 2021. The Epidemiology and Pathogenesis and Treatment of Pseudomonas aeruginosa Infections: An Update. *Drugs,* 81(18):2117-2131.

Simmons, N.B., Cirranello, A.L. 2022. Bat Species of the World: A taxonomic and geographic database. Accessed on January 11, 2023. https://batnames.org/.

Simpson, K.M.J., Mor, S.M., Ward, M.P., Walsh, M.G. 2019. Divergent geography of Salmonella Wangata and Salmonella Typhimurium epidemiology in New South Wales, Australia. *One Health,* 7:100092.

Spernovasilis, N., Psichogiou, M., Poulakou, G. 2021. Skin manifestations of Pseudomonas aeruginosa infections. *Current Opinion in Infectious Diseases,* 34(2):72-79.

Van Brussel, K., Mahar, J.E., Ortiz-Baez, A.S., Carrai, M., Spielman, D., Boardman, W.S.J., Baker, M.L., Beatty, J.A., Geoghegan, J.L., Barrs, V.R., Holmes, E.C. 2022. Faecal virome of the Australian grey-headed flying fox from urban/suburban environments contains novel coronaviruses, retroviruses and sapoviruses. *Virology,* 576:42-51.

Wang, J., Anderson, D.E., Halpin, K., Hong, X., Chen, H., Walker, S., Valdeter, S., van der Heide, B., Neave, M.J., Bingham, J., O'Brien, D., Eagles, D., Wang, L.F., Williams, D.T. 2021. A new Hendra virus genotype found in Australian flying foxes. *Virology Journal,* 18(1):197.

Welbergen, J.A., Klose, S.M., Markus, N., Eby, P. 2008. Climate change and the effects of temperature extremes on Australian flying-foxes. *Proceedings Biological Sciences,* 275(1633):419-25.

Wu, Z., Yang, L., Ren, X., He, G., Zhang, J., Yang, J., Qian, Z., Dong, J., Sun, L., Zhu, Y., Du, J., Yang, F., Zhang, S., Jin, Q. 2016. Deciphering the bat virome catalog to better understand the ecological diversity of bat viruses and the bat origin of emerging infectious diseases. *Isme J,* 10(3):609-20.

Xu, W., Eiden, M.V. 2015. Koala Retroviruses: Evolution and Disease Dynamics. *Annual Review of Virology,* 2(1):119-34.

Yinda, C.K., Zeller, M., Conceição-Neto, N., Maes, P., Deboutte, W., Beller, L., Heylen, E., Ghogomu, S.M., Van Ranst, M., Matthijnssens, J. 2016. Novel highly divergent reassortant bat rotaviruses in Cameroon, without evidence of zoonosis. *Science Reports,* 6:34209.

Zhou, H., Ji, J., Chen, X., Bi, Y., Li, J., Wang, Q., Hu, T., Song, H., Zhao, R., Chen, Y., Cui, M., Zhang, Y., Hughes, A.C., Holmes, E.C., Shi, W. 2021. Identification of novel bat coronaviruses sheds light on the evolutionary origins of SARS-CoV-2 and related viruses. *Cell,* 184(17):4380-4391.e14.

Zhu, H.C., Chu, D.K.W., Liu, W., Dong, B.Q., Zhang, S.Y., Zhang, J.X., Li, L.F., Vijaykrishna, D., Smith, G.J.D., Chen, H.L., Poon, L.L.M., Peiris, J.S.M., Guan, Y. 2009. Detection of diverse astroviruses from bats in China. *Journal of General Virology,* 90(Pt 11):883-887.

7.7: Supplementary information

Table 7.7.1: Overview of tissue type included in each library pool for each individual bat, species, sex, age, location of sampling and disease presentation observed.

Group	Bat no.	Species	Sex	Age	Sample location	Tissue included in library				Clinical signs and histopathology	Group findings
GHFF 01	9599.2	*P.p*		Juvenile		NA	Brain	Liver	NA	MM, NIP	Lung – *S. enterica, P. aeruginosa*, bat pegivirus
	11573.4		M	Juvenile	Centennial Park	Lung	Brain	Liver	NA	MM, NIP	
	9599.9			Juvenile		Lung	Brain	Liver	NA	MM, NIP	
	13402.1		F	Juvenile	Wyoming	Lung	Brain	NA	NA	MM, NIP	Liver – *P. aeruginosa*
GHFF 02	14054.1					NA	Brain	Liver	NA	Pneumonia	Lung – *P. aeruginosa*
	13906.1					Lung	NA	Liver	NA	NIP, HP	Liver – *P. aeruginosa*
	13940.1		F	Subadult	Centennial Park	Lung	Brain	Liver	NA	NIP	
	13977.1					Lung	Brain	Liver	NA	NIP	
	14052.1					Lung	Brain	NA	NA	NIP	
GHFF 03	14093.4					Lung	NA	NA	NA	NIP	Lung – bat pegivirus
	10124.1		M	Adult	Marsfield	Lung	NA	NA	NA	NIP	
	12126.1		M	Juvenile	Clovelly	Lung	NA	NA	NA	NIP	
	14003.1					Lung	Brain	NA	NA	NIP	
	13955.1					NA	Brain	NA	NA	NIP	
	13997.1					NA	Brain	NA	NA	NIP	
GHFF 04	14058.1					Lung	Brain	Liver	NA	HP, neurological	Lung - *P. aeruginosa*, Bat pegivirus
	14053.1					Lung	Brain	Liver	NA	NIP, neurological	
	14088.1			Adult		Lung	Brain	Liver	NA	NIP, HP,	Liver – bat pegivirus
	14093.2					NA	Brain	Liver	NA	NIP, neurological	

Group	ID	Species	Sex	Age	Location	Lung	Brain	Liver	Skin	Notes	Virus/organism
	14121.1		M	Adult	Kirribilli	NA	NA	Liver	NA	NIP, neurological, granulomatous hepatitis	
GHFF 06	11573.1		F	Juvenile	Centennial Park	Lung	Brain	Liver	NA	MM	Liver – bat pegivirus
	11573.2			Juvenile		Lung	Brain	NA	NA	MM	
	13368.1			Juvenile		NA	NA	Liver	NA	MM	
	13402.2		F	Juvenile	Wyoming	NA	NA	Liver	NA	MM, NIP	
GHFF 07	14094.4					Lung	Brain	Liver	NA	Neurological	
	14123.1		M	Adult	Lismore	Lung	Brain	Liver	NA	Neurological	
	14089.1		M	Adult	Kangaroo Valley	Lung	NA	NA	NA	Neurological	
GHFF 08	13998.1					Lung	Brain	NA	NA		
	14120.1		F	Subadult	Kingsford	Lung	Brain	Liver	NA		
	13471.1					NA	Brain	NA	NA		
	14048.1					Lung	Brain	NA	NA	Trauma	
GHFF 09	14065.1		F	Adult	Sydney	Lung	Brain	Liver	NA	Lymphoid leukemia	Lung – Hervey pteropid gammaretrovirus
	11553.1		F	Juvenile	Botanic Gardens	Lung	Brain	Liver	NA	Euthanised	Brain - Hervey pteropid gammaretrovirus
	11501.1		M	Subadult	Woolgoolga	NA	NA	Liver	NA	WSL, mites	Liver - Hervey pteropid gammaretrovirus, Auskungsa virus
	13905.1					NA	Brain	NA	NA		
GHFF 11	14130.1		F	Subadult		NA	Brain	NA	Skin	WSL	Skin –*P. aeruginosa, E. faecalis, A. alternata, F. oxysporum*
	14130.3		F	Juvenile		NA	Brain	NA	Skin	WSL	
	14130.2		F	Juvenile		NA	Brain	NA	Skin	WSL	
BFF 05	13961.1	*P.a*				Lung	NA	NA	NA	NIP, neurological	Lung – *P. aeruginosa*
LRFF 10	14064.1	*P.s*	F			Lung	Brain	Liver	NA	Trauma	
	14064.2			Foetus		NA	Brain	Liver	NA	Trauma	

| EBW 12 | 13087.1 | *M.o.o* | M | Subadult | Yass | NA | NA | Liver | Skin | WSL | Skin – *S. enterica*, Novel bat astroviruses |
| LF 13 | 10628.1 | *M.m* | M | Adult | Castle Hill | NA | NA | Liver | NA | Predation | |

    ◼ = Australian Capital Territory, ◼ = New South Wales

P.p = Pteropus policephalus, *P.a = Pteropus alecto*, *M.m = Myotis Macropus*, *M.o.o = Miniopterus orianae oceanensis*

NA = Not available/not included, Lung , Brain , Skin = Diseased tissue included in library, ◼ = Control

MM = Part of a mass mortality event of unknown origin, NIP = Neutrophilic interstitial pneumonia (lung lesions), HP = Histiocytic pneumonia (lung lesions), WSL = White skin lesions
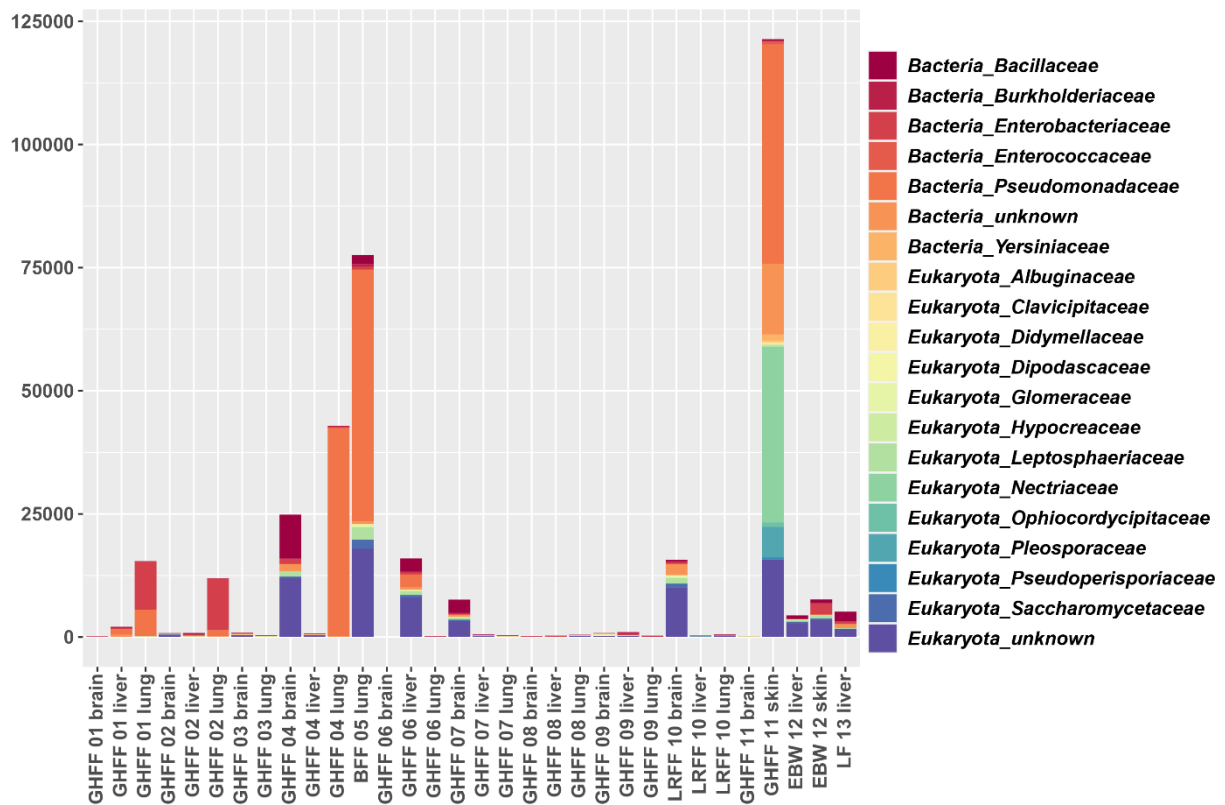
Figure 7.7: Bacteria and fungi composition within lung, brain, liver and skin samples. Columns represent the read abundance for each family presented as RPM. Only the top 20 families are displayed in the graph.

Table 7.7.2: Primers used to identify specific virus sequences in individual bats.

Name	Sequence (5'-3')	Virus target	Gene target	Fragment size (bp)
BRV_gag_F1	ACCTTCAATCTCCCTGTCAT	Hervey pteropid gammaretrovirus	gag	483
BRV_gag_R1	AAAAGGCCAATATTGTAGGG			
BRV_pol_F2	ATGTGACTGTGATTGCTTCC		pol	444
BRV_pol_R2	TATTGATGTCCTTTCCATCG			
BRV_env_F3	GCGGACCAACTATTGTGATA		env	421
BRV_env_R3	CAGAGATGTTGGTGGGTAGA			
Bat_pegi_F1	TGTACACCACATTTCACTCC	bat pegivirus GHFF04/Li/1	NS3	571
Bat_pegi_R1	GTGAGCTTCTTCATGTACGG			
Bat_pegi_F2	GTTGGTTGAGGCATGTGTTG		NS5B	211
Bat_pegi_R2	GTAGGCGGGTCCCATAATTT			
Kunsagi_F1	CTTCCGTATGCAGTTCTTGGA	Auskunsag virus	3D	397
Kunsagi_R1	TGCGTCTGGATTACACTTGAG			

Chapter Eight: General discussion

Virological studies in Australia are usually directed toward economically important animal species and those wildlife populations that may pose a threat to humans. The preference for sequencing these species, while understandable, also leads to knowledge gaps that can negatively impact animal populations and lead to mass mortality events in wildlife. This is evident when observing the mortality events in the Bellinger River snapping turtles caused by a novel nidovirus infection (Zhang et al., 2018), in cetaceans by a morbillivirus (Kemper et al., 2016), in Brushtail possums by an arterivirus (Chang et al., 2019) and in Tammar wallaby sudden death syndrome by an orbivirus (Rose et al., 2012). The most comprehensive method to characterise divergent viruses in a myriad of invertebrate, vertebrate and environmental samples is to employ an unbiased, high throughput metagenomic sequencing method. It has been demonstrated that in invertebrate and environmental samples viruses can sometimes exhibit extremely low amino acid sequence identity to known viral proteins, making them difficult to place in the current virus classification scheme and as a result would go undetected if it were not for mNGS (Shi et al., 2016, Chen et al., 2022). By using a high throughput sequencing method this thesis aims to provide an overview of the virome of the domestic cat and several bat species in Australia, in an attempt to reduce this important data gap. In particular, I used both RNA and DNA mNGS techniques to characterise the gastrointestinal and tissue viromes of stray and shelter-housed cats and several species of flying foxes and microbats.

8.1: Metagenomic sequencing

A key element of this thesis was to utilise non-invasive faecal sampling to characterise the viruses that are shed in the gastrointestinal tract of Australian mammals. The sampling of faeces provides an overview of the diversity of viruses that are shed and transmitted by the gastrointestinal tract, and chapters four and six of this thesis support that a large diversity of viruses are shed in the faeces of both domestic cats and native Australian bats. However, faecal sampling can also generate data overwhelmed by host, dietary and bacterial reads, which are all more abundant in faecal samples than viruses and does not necessarily depict the viruses present in other tissues and those associated with disease (which usually impacts other tissues). To overcome this limitation in part, in chapters three and four I employed the universal total RNA sequencing protocol (metatranscriptomics) alongside a viral particle enrichment protocol developed in 2015 (Conceicao-Neto et al., 2015) to remove all the over

abundant reads from the domestic cat faecal samples before library preparation to ensure that we captured as many viral reads as possible. The viral particle enrichment protocol includes homogenisation of faecal samples, removal of bacteria by filtration and centrifugation, removal of non-viral nucleic acids not protected in a viral particle by nuclease treatment, viral nucleic acid extraction, random amplification followed by library preparation (Conceicao-Neto et al., 2015). Using the results from a previous study on the faecal virome of Tasmanian devils in which the viral particle enrichment protocol was used and found to be more efficient in the detection of DNA rather than RNA virus reads, we introduced a modification in an attempt to reduce or eliminate this bias (Chong et al., 2019). This modification involved separating the DNA and RNA after viral nucleic acid extraction and before random amplification by using a DNase treatment and specific DNA and RNA random amplification kits. The sequencing read outputs of both the viral particle enrichment libraries and the total RNA libraries in chapter four showed that the proportion of viral reads, particularly for DNA viruses, sequenced was higher for the modified viral particle enrichment protocol than total RNA sequencing libraries, similar to the results seen in the Tasmanian devil virome study (Chong et al., 2019). However, this is not unusual as total RNA metatranscriptomic sequencing only includes a depletion step in which rRNA is removed before library preparation, so the host and bacterial mRNA are still present in the libraries and sequenced alongside viral reads. However, metatranscriptomics is still the most efficient way to capture the diversity of RNA viruses in a sample and can also identify actively replicating DNA viruses, demonstrated previously (Porter et al., 2019) and in chapter four of this thesis.

8.2: The feline faecal virome

In chapter four I identified a number of viruses in the gastrointestinal tract of domestic cats that had previously not been identified in Australian domestic cats. The presence of feline chaphamaparvovirus, a recently identified parvovirus detected in domestic cats in California after vomiting and diarrhoea episodes (Li et al., 2020) and subsequently sequenced from domestic cats in Italy with enteritis (Di Profio et al., 2021), suggest an association with the presentation of disease. While the prevalence of feline chaphamaparvovirus was high (16.9%) in cats sampled from Italy, coinfection with feline parvovirus, feline enteric coronavirus, feline kobuvirus and feline norovirus, all viruses that have been linked to gastroenteritis, was observed for all but one diarrhoeic cat (Di Profio et al., 2021). Furthermore, an additional single feline chaphamaparvovirus infection was detected in a healthy control cat (Di Profio et al., 2021). The identification of feline chaphamaparvovirus

in only healthy control shelter-housed cats in chapter four of this thesis suggests this virus may cause asymptomatic disease that may present as gastroenteritis in certain cases of infection, similar to what occurs with feline enteric coronavirus infection. Additionally, feline kobuvirus infection was detected in chapter four of this thesis and constitutes the first identification of this virus in Australian domestic cats. An association with gastroenteritis has been proposed based on evidence that the prevalence of feline kobuvirus in cats with diarrhoea is higher than in asymptomatic cats (Chung et al., 2013, Di Martino et al., 2015, Lu et al., 2018, Niu et al., 2019). An Italian study detected feline kobuvirus at a prevalence of 100% in cats with enteritis and 0% in healthy cats (Di Martino et al., 2015).

It is also commonly observed that feline kobuvirus is detected in conjunction with other enteric pathogens including feline parvovirus (Lu et al., 2018, Niu et al., 2019). The co-infection of feline kobuvirus and feline parvovirus was similarly observed in chapter four of this thesis, in which 39.1% of cats had both feline kobuvirus and feline parvovirus. Additionally, a feline kobuvirus prevalence of 0% was also observed for healthy control cats. Currently, eight pathogens are screened in the feline INDEXX Diarrhea RealPCR panel including four eukaryotic parasites (*Giardia* spp., *Tritrichomonas foetus*, *Cryptosporidium* spp. and *Toxoplasma gondii*), two bacteria (*Salmonella* spp. and *Clostridium perfringens*) and two viruses (feline enteric coronavirus and feline parvovirus). Now that feline kobuvirus has been confirmed to be circulating in the Australian domestic cat population we should consider screening cases of gastroenteritis for feline kobuvirus, especially cases in which pathogens included in the RealPCR panel are not identified as a causative agent. Moreover, as multi-cat environments including shelters facilitate the circulation of the virus in the cat population, investigating the prevalence of feline kobuvirus in Australia is warranted.

Finally, it should be noted that a positive feline coronavirus and feline parvovirus RealPCR result does not signify these viruses are causing diarrhoea in all cases. In most cases of infection feline enteric coronavirus causes an asymptomatic infection and some cats never show signs of diarrhoea. For feline parvovirus, PCR cannot determine between vaccine and field strains; therefore, a cat that has been previously vaccinated will show a positive result on PCR, and as the vaccine and field strains only differ at a few nucleotide sites, Sanger sequencing is needed to confirm positive PCR results in the absence of panleukopenia. Feline astroviruses, feline calicivirus and feline bocaparvoviruses are additional feline enteric viruses that warrant further investigation, owing to their detection in cats with gastroenteritis (Zhang et al., 2019, Guo et al., 2022, Di Martino et al., 2020, Piewbang et al., 2019, Liu et

al., 2018). A large diversity of feline astroviruses were detected in the feline parvovirus positive cats, enteric strains of feline calicivirus were detected in feline parvovirus infected cats, and a large diversity of Carnivore bocaparvovirus 4 was detected in both feline parvovirus infected and health control cats in chapter four.

8.3: The bat virome

There is a greatly increased interest in sampling bat populations globally, in large part reflecting the attention afforded to this diverse order following the SARS-CoV-1 outbreak and the current SARS-CoV-2 pandemic. In chapter five of this these we offer an overview of the current state of mNGS studies in bat populations globally. By comparing the virus sequences deposited on NCBI/GenBank we established that, in 2021, a substantial number (30%) of virus sequences were detected using mNGS alone and that this number was higher than that recorded in 2016 (10%). Additionally, we outline that sampling bias towards bats is occurring, that the detection of bat coronaviruses increased dramatically after the SARS-CoV-1 outbreaks, and that the sequencing of bat populations in Asian countries is more prominent.

While bat coronaviruses were not a major concern in Australia before SARS-CoV-1, the emergence of zoonotic paramyxoviruses and a zoonotic rhabdovirus was a cause for concern. Consequently, there is a marked sequencing bias towards these zoonotic viruses in Australia and as a result the diversity and prevalence of other important virus families such as *Astroviridae, Caliciviridae, Parvoviridae*, *Filoviridae*, *Orthomyxoviridae* and members of the *Bunyavirales*; *Arenaviridae*, *Peribunyaviridae*, *Hantaviridae*, *Nairoviridae* and *Phenuiviridae,* are mostly unexplored. In chapter six of this thesis, we used a metatranscriptomics approach to characterise the diversity of RNA viruses in faecal samples from Australian grey-headed flying foxes in an effort to minimise this sequencing imbalance. As flying foxes consume mainly plant material and fruits in their diet, we did not include the viral particle enrichment protocol used in chapter three and four of this thesis as faecal samples were difficult to homogenise and hence not compatible with the viral particle enrichment protocol. In total, we detected virus sequences associated with 79 virus families, although a majority of the virus reads were associated with the diet, bacteria and invertebrates, which created difficulty in sorting through the assembled data and determining mammalian viruses in families that contain both vertebrate and invertebrate members. However, we did characterise four novel mammalian viruses, a betacoronavirus

(*Coronaviridae*), sapovirus (*Caliciviridae*) and two potentially exogenous betaretroviruses (*Retroviridae*), as well as a possible mammalian-infected birnavirus (*Birnaviridae*). Interestingly, we detected the full-length novel coronavirus genome in two sample populations from two different states, suggesting virus exchange is common among different flying fox colonies. An important aspect of this study was the sampling of flying foxes from urban and suburban environments, and although we detected a novel betacoronavirus, this virus was phylogenetically positioned in a subgenus with a likely long association with bats (*Nobecovirus*) that have never jumped species barriers and established infection in humans.

Similarly, only a small number of studies of viruses that may pose a risk to bats have been undertake in Australia, and as a consequence of this neglect potentially pathogenic viruses may have the ability to spread unchecked among the bat population. Australian bats are under constant threat from land clearing for agriculture, disturbance of roosting site by humans, urbanisation, predation (especially microbats), bushfires, drought, flooding, pollution and reduction in food sources. A major driver of mass mortality events in Australian flying foxes is extreme heat events, where temperatures upwards for 40°C cause heat stress and hyperthermia that subsequently results in death. Australia has experienced a number of extreme summer temperature events which as a result has killed thousands of flying foxes and highlighted the consequences of climate change on vulnerable bat species. Two separate studies on flying fox mortalities during extreme summer events in 1994 – 2002 and 2019 – 2020 estimated that upwards of 30,000 and 72,000 flying foxes died from hyperthermia, respectively (Welbergen et al., 2008, Mo et al., 2021), a majority of which were grey-headed flying foxes. As nine of the Australian mainland bat species are listed as vulnerable (including the grey-headed flying fox), six as near threatened and one as endangered (spectacled flying fox), the establishment of a pathogen into the bat population could be devastating for these species. This concern is addressed in chapter seven of this thesis in which we used mNGS and veterinary diagnostic methods to describe the "infectiome" (microbes and viruses) of tissue samples from bats that were part of a mortality event and isolated cases of disease in New South Wales and Australian Capital Territory, Australia. From these data we were able to identify four mammalian infecting families, *Astroviridae* (genus *Mamastrovirus*), *Flaviviridae* (genus *Pegivirus*), *Picornaviridae* (genus *Kunsagivirus*) and *Retroviridae* (genus *Gammaretrovirus*) and bacteria and fungi pathogenic species of concern, including *Pseudomonas aeruginosa* in bats with lung lesions and peracute pneumonia. Notably, the identification of Hervey pteropid gammaretrovirus in our data set

builds on the previous study that first identified the gammaretrovirus in the faeces of flying foxes from Queensland and New South Wales, Australia, that theorised that bats potentially play a key role in the transmission of gammaretroviruses into other mammalian species (Hayward et al., 2020). Here, we showed that Hervey pteropid gammaretrovirus may actually be pathogenic in bats such that we should further monitor this virus in the Australian bat population to determine whether the virus becomes fixed in the bat population and hence leads to similar issues to those observed with koala retrovirus and feline immunodeficiency virus.

8.4: Virus discovery

The identification of numerous novel mammalian viruses from the faeces and tissue of domestic cats and bats was a theme throughout this thesis (chapters two, three, six and seven). Overall, eleven complete or near complete novel viruses from six families were documented, three sampled from domestic cats and eight from bats. All the novel viruses were detected using mNGS, although one novel virus, termed Felis catus papillomavirus 6 (chapter two), was detected using a combination of mNGS and a capture-based technique. This capture-based technique incorporates user developed oligonucleotides knows as baits to target DNA or RNA sequences in a sequencing library. In the case of chapter two of this thesis we designed baits to target a novel herpesvirus from a nasal tumour sample from a feline immunodeficiency virus infected cat. While the capture of the novel herpesvirus was unsuccessful, we were able to sequence two contigs from the novel papillomavirus for which we completed the genome using PCR. I was also involved in a study that used this capture-based technique (Appendix IV) to target Carnivore protoparvovirus 1. This study successfully captured the Carnivore protoparvovirus 1 reads from DNA sequencing libraries and determined that all Carnivore protoparvovirus 1 reads in 19 domestic cats from Australia with feline panleukopenia were feline parvovirus, hence confirming the absence of canine parvovirus. The success with this capture-based technique described in Appendix IV, and the unsuccessful attempt in chapter two, suggests that this technique is more useful for the capture of highly similar viruses and less so with novel viruses. For the latter, I propose that standard DNA or RNA mNGS is a more efficient method for identifying novel viruses. However, there are advantages of combining multiple methods in the context of virus discovery, for example utilising RNA or DNA mNGS as a starting point to discern the viral community of a subset of individuals that can then be used to screen a larger set of samples using PCR methods, as was demonstrated in this thesis.

8.5: Sample cohorts

Finally, the importance of including both healthy and diseased animals is highlighted in chapters three, four, six and seven of this thesis. By investigating the virome of healthy domestic cats and feline panleukopenia cats (chapters three and four), healthy and diseased bats (chapter six and seven) I was able to make tentative conclusions on the potential disease association of numerous virus species, including observing outcomes that challenge those documented in other studies. It is clear, however, that more research is needed to draw solid conclusions on the disease association of the viruses detected in this thesis. While mNGS is extremely useful for the discovery of novel viruses, this technique is not a "one-size-fits-all" approach, evident when discussing its use for the identification of disease-causing viruses. The misassignment of a novel *Circoviridae*-like and *Parvoviridae*-like as potentially disease causing after its detection in Chinese patients with seronegative hepatitis (Xu et al., 2013) is a relevant example of the challenges of assigning disease association with only the use of mNGS. In this case it was determined that this virus (Parvovirus NIH-CQV) and its closely related virus (parvovirus-like hybrid virus) originated from silica spin column contamination (Naccache et al., 2013, Xu et al., 2013). mNGS can be used as a starting point, however, more traditional laboratory (virus cultures) and diagnostic (histopathology) approaches should be incorporated to better understand the disease association of novel viruses.

8.6: Conclusions

Virus surveillance of mammalian species from economically beneficial industries, such as the livestock and equine industry, is essential for the prevention of harmful viral outbreaks in Australia. However, the screening of wildlife populations is arguably as important for the prevention of mass mortality events due to infectious diseases. In the case of domestic cats, the establishment of previous absent pathogenic viruses in Australia (i.e., feline parvovirus and feline kobuvirus) poses a threat to both owned cats and the considerable stray cat population. In this thesis I aimed to enhance our understanding of virus diversity in an understudied domestic species (*Felis catus*) and order (Chiroptera, bats) in Australia. I used mNGS to characterise the faecal and tissue virome of health and diseased individuals and using this approach I was able to identify mammalian viruses from the families *Astroviridae*, *Caliciviridae*, *Coronaviridae*, *Flaviviridae*, *Papillomaviridae*, *Parvoviridae*, *Picornaviridae*, *Polyomaviridae* and *Retroviridae*. Through mNGS, researchers can simultaneously sequence recognised and novel viruses together with the accompanying microbiome (bacteria and

fungi) for a complete overview of the "infectiome". The reduction in cost, increase in availability and the substantial discovery power of mNGS means that more studies are employing this technique for the identification of viruses from numerous hosts that will further improve our knowledge of the virosphere, as well as the prevalence and emergence of pathogenic viruses in wildlife and domestic species.

8.7: References

Chang, W.S., Eden, J.S., Hartley, W.J., Shi, M., Rose, K., Holmes, E.C. 2019. Metagenomic discovery and co-infection of diverse wobbly possum disease viruses and a novel hepacivirus in Australian brushtail possums. *One Health Outlook,* 1:5.

Chen, Y.M., Sadiq, S., Tian, J.H., Chen, X., Lin, X.D., Shen, J.J., Chen, H., Hao, Z.Y., Wille, M., Zhou, Z.C., Wu, J., Li, F., Wang, H.W., Yang, W.D., Xu, Q.Y., Wang, W., Gao, W.H., Holmes, E.C., Zhang, Y.Z. 2022. RNA viromes from terrestrial sites across China expand environmental viral diversity. *Nature Microbiology,* 7(8):1312-1323.

Chong, R., Shi, M., Grueber, C.E., Holmes, E.C., Hogg, C.J., Belov, K., Barrs, V.R. 2019a. Fecal Viral Diversity of Captive and Wild Tasmanian Devils Characterized Using Virion-Enriched Metagenomics and Metatranscriptomics. *Journal of Virology,* 93(11):e00205-19.

Chung, J.Y., Kim, S.H., Kim, Y.H., Lee, M.H., Lee, K.K., Oem, J.K. 2013. Detection and genetic characterization of feline kobuviruses. *Virus Genes,* 47(3):559-62.

Conceicao-Neto, N., Zeller, M., Lefrere, H., De Bruyn, P., Beller, L., Deboutte, W., Yinda, C.K., Lavigne, R., Maes, P., Van Ranst, M., Heylen, E., Matthijnssens, J. 2015. Modular approach to customise sample preparation procedures for viral metagenomics: a reproducible protocol for virome analysis. *Scientific Reports,* 5:16532.

Di Martino, B., Di Profio, F., Melegari, I., Marsilio, F., Martella, V. 2015. Detection of feline kobuviruses in diarrhoeic cats, Italy. *Veterinary Microbiology,* 176(10):186-9.

Di Martino, B., Lanave, G., Di Profio, F., Melegari, I., Marsilio, F., Camero, M., Catella, C., Capozza, P., Bányai, K., Barrs, V.R., Buonavoglia, C., Martella, V. 2020. Identification of feline calicivirus in cats with enteritis. *Transboundary and Emerging Diseases,* 67(6):2579-2588.

Di Profio, F., Sarchese, V., Palombieri, A., Fruci, P., Massirio, I., Martella, V., Fulvio, M., Di Martino, B. 2021. Feline chaphamaparvovirus in cats with enteritis and upper respiratory tract disease. *Transboundary and Emerging Diseases*, 69(2):660-668.

Guo, J., Ding, Y., Sun, F., Zhou, H., He, P., Chen, J., Guo, J., Zeng, H., Long, J., Wei, Z., Ouyang, K., Huang, W., Chen, Y. 2022. Co-circulation and evolution of genogroups I

and II of respiratory and enteric feline calicivirus isolates in cats. *Transboundary and Emerging Diseases*,69(5):2924-2937 .

Hayward, J.A., Tachedjian, M., Kohl, C., Johnson, A., Dearnley, M., Jesaveluk, B., Langer, C., Solymosi, P.D., Hille, G., Nitsche, A., Sánchez, C.A., Werner, A., Kontos, D., Crameri, G., Marsh, G.A., Baker, M.L., Poumbourios, P., Drummer, H.E., Holmes, E.C., Wang, L.F., Smith, I., Tachedjian, G. 2020. Infectious KoRV-related retroviruses circulating in Australian bats. *roceedings of the National Academy of Sciences of the United States of America,* 117(17):9529–9536.

Kemper, C.M., Tomo, I., Bingham, J., Bastianello, S.S., Wang, J., Gibbs, S.E., Woolford, L., Dickason, C., Kelly, D. 2016. Morbillivirus-associated unusual mortality event in South Australian bottlenose dolphins is largest reported for the Southern Hemisphere. *Royal Society Open Science,* 3(12):160838.

Li, Y., Gordon, E., Idle, A., Altan, E., Seguin, M.A., Estrada, M., Deng, X., Delwart, E. 2020. Virome of a Feline Outbreak of Diarrhea and Vomiting Includes Bocaviruses and a Novel Chapparvovirus. *Viruses,* 12(5):506.

Liu, C., Liu, F., Li, Z., Qu, L., Liu, D. 2018. First report of feline bocavirus associated with severe enteritis of cat in Northeast China, 2015. *Journal of Veterinary Medical Science,* 80(4):731-735.

Lu, G., Zhang, X., Luo, J., Sun, Y., Xu, H., Huang, J., Ou, J., Li, S. 2018. First report and genetic characterization of feline kobuvirus in diarrhoeic cats in China. *Transboundary and Emerging Diseases,* 65(5):1357-1363.

Mo, M., Roache, M., Davies, J., Hopper, J., Pitty, H., Foster, N., Guy, S., Parry-Jones, K., Francis, G., Koosmen, A. 2021. Estimating flying-fox mortality associated with abandonments of pups and extreme heat events during the austral summer of 2019–20. *Pacific Conservation Biology,* 28:124-139.

Naccache, S.N., Greninger, A.L., Lee, D., Coffey, L.L., Phan, T., Rein-Weston, A., Aronsohn, A., Hackett, J.Jr., Delwart, E.L., Chiu, C.Y. 2013. The perils of pathogen discovery: origin of a novel parvovirus-like hybrid genome traced to nucleic acid extraction spin columns. *Journal of virology*, 87(22):11966–11977.

Niu, T.J., Yi, S.S., Wang, X., Wang, L.H., Guo, B.Y., Zhao, L.Y., Zhang, S., Dong, H., Wang, K., Hu, X.G. 2019. Detection and genetic characterization of kobuvirus in cats: The first molecular evidence from Northeast China. *Infection, Genetics and Evolution,* 68:58-67.

Piewbang, C., Kasantikul, T., Pringproa, K., Techangamsuwan, S. 2019. Feline bocavirus-1 associated with outbreaks of hemorrhagic enteritis in household cats: potential first evidence of a pathological role, viral tropism and natural genetic recombination. *Scientific Reports,* 9(1):16367.

Porter, A.F., Shi, M., Eden, J.S., Zhang, Y.Z., Holmes, E.C. 2019. Diversity and Evolution of Novel Invertebrate DNA Viruses Revealed by Meta-Transcriptomics. *Viruses,* 11(12):1092.

Rose, K.A., Kirkland, P.D., Davis, R.J., Cooper, D.W., Blumstein, D., Pritchard, L.I., Newberry, K.M., Lunt, R.A. 2012. Epizootics of sudden death in tammar wallabies (Macropus eugenii) associated with an orbivirus infection. *Australian Veterinary Journal,* 90(12):505-9.

Shi, M., Lin, X.D., Tian, J.H., Chen, L.J., Chen, X., Li, C.X., Qin, X.C., Li, J., Cao, J.P., Eden, J.S., Buchmann, J., Wang, W., Xu, J., Holmes, E.C., Zhang, Y.Z. 2016. Redefining the invertebrate RNA virosphere. *Nature,* 540(7634):539-543.

Welbergen, J.A., Klose, S.M., Markus, N., Eby, P. 2008. Climate change and the effects of temperature extremes on Australian flying-foxes. *Proceedings of the Royal Society B,* 275(1633):419-25.

Xu, B., Zhi, N., Hu, G., Wan, Z., Zheng, X., Liu, X., Wong, S., Kajigaya, S., Zhao, K., Mao, Q., Young, N.S. 2013. Hybrid DNA virus in Chinese patients with seronegative hepatitis discovered by deep sequencing. *Proceedings of the National Academy of Sciences of the United States of America*, 110(25):10264–10269.

Zhang, J., Finlaison, D.S., Frost, M.J., Gestier, S., Gu, X., Hall, J., Jenkins, C., Parrish, K., Read, A.J., Srivastava, M., Rose, K., Kirkland, P.D. 2018. Identification of a novel nidovirus as a potential cause of large scale mortalities in the endangered Bellinger River snapping turtle (Myuchelys georgesi). *PLoS One,* 13(10):e0205209.

Zhang, Q., Niu, J., Yi, S., Dong, G., Yu, D., Guo, Y., Huang, H., Hu, G. 2019. Development and application of a multiplex PCR method for the simultaneous detection and differentiation of feline panleukopenia virus, feline bocavirus, and feline astrovirus. *Archives of Virology,* 164(11):2761-2768.

Appendix I

viruses

MDPI

Article

Distinct Lineages of Feline Parvovirus Associated with Epizootic Outbreaks in Australia, New Zealand and the United Arab Emirates

Kate Van Brussel [1], Maura Carrai [1], Carrie Lin [1], Mark Kelman [1], Laura Setyo [1],
Danielle Aberdein [2], Juliana Brailey [1], Michelle Lawler [3], Simone Maher [1], Ildiko Plaganyi [4],
Emily Lewis [5], Adele Hawkswell [5], Andrew B. Allison [6], Joanne Meers [7], Vito Martella [8],
Julia A. Beatty [1,9], Edward C. Holmes [9], Nicola Decaro [8] and Vanessa R. Barrs [1,8,9,*]

[1] Sydney School of Veterinary Science, Faculty of Science, University of Sydney, Camperdown, NSW 2050, Australia; kate.vanbrussel@sydney.edu.au (K.V.B.); maura.carrai@sydney.edu.au (M.C.); clin5923@uni.sydney.edu.au (C.L.); kelmanscientific@gmail.com (M.K.); laura.setyo@sydney.edu.au (L.S.); jbra0176@uni.sydney.edu.au (J.B.); simone.maher@sydney.edu.au (S.M.); julia.beatty@sydney.edu.au (J.A.B.)

[2] School of Veterinary Science, Massey University, Palmerston North 4410, New Zealand; D.aberdein@massey.ac.nz

[3] RSPCA NSW, Yagoona, NSW 2199, Australia; mlawler@rspcansw.org.au

[4] Lort Smith Animal Hospital, North Melbourne, Victoria 3051, Australia; iplaganyi@lortsmith.com

[5] SPCA Wellington, Wellington 6021, New Zealand; ylimesiwel@gmail.com (E.L.); adele.hawkswell@spca.nz (A.H.)

[6] Department of Comparative, Diagnostic, and Population Medicine, College of Veterinary Medicine, University of Florida, Gainesville, FL 32610, USA; aallison1@ufl.edu

[7] School of Veterinary Science, The University of Queensland, Gatton, QLD 4343, Australia; j.meers@uq.edu.au

[8] Department of Veterinary Medicine, University of Bari, Valenzano, 70121 Bari, Italy; vito.martella@uniba.it (V.M.); nicola.decaro@uniba.it (N.D.)

[9] Marie Bashir Institute for Infectious Diseases and Biosecurity, Charles Perkins Centre, School of Life & Environmental Sciences and Sydney Medical School, The University of Sydney, Sydney, NSW 2006, Australia; edward.holmes@sydney.edu.au

* Correspondence: vanessa.barrs@sydney.edu.au; Tel.: +61-439-944-605

check for updates

Abstract: Feline panleukopenia (FPL), a frequently fatal disease of cats, is caused by feline parvovirus (FPV) or canine parvovirus (CPV). We investigated simultaneous outbreaks of FPL between 2014 and 2018 in Australia, New Zealand and the United Arab Emirates (UAE) where FPL outbreaks had not been reported for several decades. Case data from 989 cats and clinical samples from additional 113 cats were obtained to determine the cause of the outbreaks and epidemiological factors involved. Most cats with FPL were shelter-housed, 9 to 10 weeks old at diagnosis, unvaccinated, had not completed a primary vaccination series or had received vaccinations noncompliant with current guidelines. Analysis of parvoviral VP2 sequence data confirmed that all FPL cases were caused by FPV and not CPV. Phylogenetic analysis revealed that each of these outbreaks was caused by a distinct FPV, with two virus lineages present in eastern Australia and virus movement between different geographical locations. Viruses from the UAE outbreak formed a lineage of unknown origin. FPV vaccine virus was detected in the New Zealand cases, highlighting the difficulty of distinguishing the co-incidental shedding of vaccine virus in vaccinated cats. Inadequate vaccination coverage in shelter-housed cats was a common factor in all outbreaks, likely precipitating the multiple re-emergence of infection events.

Keywords: carnivore protoparvovirus; feline panleukopenia; canine parvovirus; outbreaks; infectious enteritis

1. Introduction

Feline panleukopenia (FPL) is a highly contagious and often fatal disease characterised by acute severe enteritis, severe dehydration and sepsis due to lymphoid depletion and pancytopenia [1]. FPL is usually associated with infection by feline parvovirus (FPV), a member of the genus *Protoparvovirus* (formerly *Feline panleukopenia virus*). *Protoparovirus* is one of eight genera of vertebrate viruses within the subfamily *Parvovirinae* of the family *Parvoviridae.* Collectively, FPV and canine parvovirus (CPV), along with associated variants found in various carnivore species such as mink and raccoons, constitute the species *Carnivore protoparvovirus 1* [2].

Until the 1980s, FPV was the only reported viral cause of FPL in cats. FPV is able to infect cats by first binding to the feline transferrin receptor (fTfR) expressed on the surface of cells, followed by clathrin-mediated endocytosis to initiate infection [3]. Canine parvovirus CPV-2 emerged in the late 1970s and was initially unable to infect cats, as it could not bind to the fTfR [3]. However, infectivity for feline cells was acquired soon after by the genetic variant CPV-2a, which emerged in 1979 and replaced CPV-2 [4]. The ability to infect cats has also been retained by subsequent antigenic variants of CPV-2a, termed CPV-2b and CPV-2c, which only differ from CPV-2a at a single amino acid position (VP2 426). These and other antigenic variants of CPV can cause FPL in both naturally acquired and experimental infections of cats [5–8].

In contrast to parvoviral enteritis in dogs, estimated to cause 20,000 cases per year in Australia, clinical cases of FPL have rarely been diagnosed in Australia since the mid-1970s, and there have been no reports of FPL outbreaks for over 40 years [9]. In 2014, FPL re-emerged in eastern Australia, and subsequent outbreaks occurred between 2015 and 2018 in several locations in this region. Similarly, outbreaks of FPL occurred in New Zealand (NZ) between 2016 and 2018, as well as in the United Arab Emirates (UAE) in 2017, with no outbreaks of FPL reported in either country in recent decades, likely due to the widespread use of FPL vaccines.

The contemporaneous re-emergence of FPL in geographically distinct settings long considered FPL-free has raised questions as to whether virus-related or other unknown risk factors played a role in the observed FPL outbreaks. Herein, case data and clinical samples from 989 and 113 cats, respectively, were analysed to identify the lineages of *Carnivore protoparvovirus 1* responsible for the outbreaks of FPL in Australia (2014 to 2018), the UAE (2017) and NZ (2017–2018) and evaluate epidemiological factors associated with these outbreaks, including vaccination status.

2. Materials and Methods

2.1. Retrospective Case Data Analysis

Inclusion criteria for cases of FPL were (i) clinical signs typical of FPL (lethargy, fever, hypothermia, anorexia, vomiting, diarrhoea and/or sudden death) and a positive confirmatory test (faecal CPV antigen test or PCR) or (ii) clinical signs typical of FPL in a cat from a shelter with a confirmed contemporaneous outbreak of FPL.

Australian case data were extracted from a national online companion animal disease surveillance-reporting database launched in January 2010 [10] and from the medical records of animal shelters and/or veterinary hospitals in outbreak regions for the period 1 January 2014 to 31 August 2018. Data recorded included case occurrence date, shelter location, shelter post code, age at diagnosis, sex, post code of owner residence or where found as a stray before entry into shelter, clinical signs at presentation, date of last vaccination, vaccination type (inactivated or modified live virus (MLV) vaccine), time interval between last vaccination and onset of clinical signs (days), method of diagnosis and outcome. Data obtained were searched to identify cases for which serial monitoring of faecal shedding of FPV or CPV using qPCR testing had been performed. Information about animal movements, biosecurity and vaccination protocols was obtained from shelter veterinarians and/or managers.

New Zealand case data were obtained from one shelter, comprising summary data of case diagnoses for two FPL outbreaks occurring between 2016 and 2018 as well as individual data for 9 cases in which clinical samples were available for PCR and sequencing. Individual case data for UAE cases were available during the period of the outbreak in 2017.

Data were analysed using Microsoft Excel® for Mac Version 16.16.15 and Statistix® version 10.0 (Analytical Software, Tallahassee, FL, USA). Descriptive statistics were generated for FPL case numbers, age at disease diagnosis, interval between vaccination and disease and interval between admission and disease. Frequency distributions were created for age at disease diagnosis. Mapping and geospatial analysis was performed with ArcGIS® version 10.2 (Ersi, Redlands, CA, USA).

2.2. Prospective Sample Collection

Residual diagnostic faecal samples or tissue (intestine or mesenteric lymph node) obtained post-mortem were collected prospectively in Australia from 7 April 2015 until 30 August 2018 and from the UAE and New Zealand during suspected outbreaks of FPL in 2017. In addition, a stored faecal sample from a cat diagnosed with FPL in the first outbreak in Australia in 2014 was obtained for study.

2.3. DNA Extraction and PCR

DNA was extracted for sequencing of the *Carnivore protoparvovirus* 1 VP2 gene from tissue using the Qiagen DNeasy Blood and Tissue Kit (Qiagen, Hilden, Germany) or from faecal samples using the QIAamp Fast DNA Stool Mini Kit (Qiagen, Germany) or by homogenisation, boiling and centrifugation, as previously described [11]. The extracted DNA was amplified by conventional PCR using 5 u/µL of My Taq HS Red DNA polymerase (Bioline, USA), 1–90 ng of DNA, 1 x MyTaq Red reaction buffer and a final primer concentration of 0.2 µM in a final reaction volume of 25 µL. Three sets of overlapping primers were used to amplify the entire VP2 region (1931 bp) as described previously, with minor modifications (Table 1) [12]. An initial denaturation step at 94 °C for 1 min, followed by 35–40 cycles of denaturation at 94 °C for 30 s, annealing at 50 or 55 °C for 30 s and extension at 72 °C for 30 s, ending with a final extension at 72 °C for 1 min, was used for DNA amplification. The PCR products were separated by electrophoresis on a 1% agarose gel (Bio-Rad Laboratories, Hercules, CA, USA) in 1× tris-acetate EDTA and visualized using SYBR Safe DNA (Invitrogen, Carlsbad, CA, USA). Sanger sequencing of positive PCR products was performed commercially (Macrogen, Seoul, Korea).

Table 1. Primer sequence and amplicon length for amplification of the VP2 region [12].

Primer	Sequence 5′–3′	Fragment Size (bp)
CPV2679-F	CCAGATCATCCATCAACATCA	853
CPV3511-R	TGAACATCATCTGGATCTGTACC	
CPV3381-F	CCATGGAAACCAACCATACC	736
CPV4116-R	AGTTAATTCCTGTTTTACCTCCAA	
555-F	CAGGAAGATATCCAGAAGGA	583
555-R	GGTGCTAGTTGATATGTAATAAACA	

2.4. Sequence Analysis

VP2 sequences were edited, assembled and aligned using the ClustalW algorithm in Geneious Prime (Biomatters Ltd., Auckland, New Zealand) (although alignment was uncontroversial with no gaps needed). Sequences were translated in MegaX, and amino acid substitutions compared to the ICTV reference FPV sequence (FVP-3 Genbank accession no. EU659111) were identified. To determine the evolutionary history of the outbreak sequences from Australia, New Zealand and Dubai, we performed a phylogenetic analysis including these sequences and representative VP2 sequences of FPV and CPV taken from GenBank. In addition, we included an FPV VP2 sequence obtained from tissues of a healthy feral cat from Tasmania, Australia, sampled in 2010 (Genbank accession no. MN603976), for comparison. This resulted in a total data set of 205 sequences, 1774 nt in length. Phylogenetic

analysis of these was performed using the PhyML program [13] and employing the GTR+I+Γ model of nucleotide substitution and a combination of Nearest-Neighbor Interchange (NNI) and Sub-tree Pruning & Re-grafting (SPR) branch swapping. Nodal support was assessed using SH-like branch support. Finally, the five CPV sequences included were used as an outgroup clade to root the tree.

2.5. FPV Viral Load Determination by qPCR and Multiplex PCR for Faecal Co-Pathogens

An FPV strain identical to that used in a commercially available MLV FPV vaccine was detected in faecal samples from New Zealand cases. Subsequently, qPCR was performed to determine FPV viral loads in DNA extracts of mesenteric lymph nodes and tissues from these cases using a TaqMan qPCR assay as described previously [14]. Faecal samples containing vaccine virus were also submitted to a commercial laboratory for batch testing on a multiplex qPCR panel to detect potential faecal co-pathogens including Feline coronavirus, *Tritrichomonas foetus*, *Clostridium perfringens*, *Giardia* spp, *Salmonella* spp, *Campylobacter jejuni*, *Campylobacter coli* and *Toxoplasma gondii* (Idexx Pty Ltd.).

2.6. Samples for Histological Examination

Tissues (duodenum, jejunum, colon, liver, spleen, kidney, mesenteric lymph node, heart, lung, pancreas, brain and/or bone marrow) from 11 representative Australian FPL cases that had died or been euthanised, ranging in age from 8 weeks to 12 months, including one from Melbourne in 2014 and 10 from Sydney in 2017 and 2018, were available for histological examination. Tissues (intestine, +/− mesenteric lymph node) from six suspected cases of FPL from New Zealand were also examined. All tissues were collected post-mortem and animals were not euthanised for the purposes of this study.

3. Results

3.1. Australian Cases

3.1.1. Australian Cases—Outbreak Sites, Case Numbers and Distribution

Data were received from 610 cases of FPL diagnosed in Australia between January 2014 and September 2018 from 11 animal shelters, 2 rescue societies and 11 veterinary hospitals. Of the 610 cases, 87% were shelter-housed, 12% were privately owned cats presenting to veterinary hospitals, and 1% were from foster carers working with rescue societies without premises. The distribution of Australian cases by geographic region and year is shown in Table 2 and Figure 1.

Table 2. Number of Australian cases of feline panleukopenia (FPL) by year and region.

Year	NSW [1]	QLD [2]	VIC [3]	WA [4]	Total
2014	0	0	40	0	40
2015	3	0	188	1	192
2016	38	0	21	0	59
2017	211	1	66	0	278
2018	3	0	38	0	41
Total	255	1	353	1	610

[1] NSW: New South Wales; [2] VIC: Victoria; [3] QLD: Queensland; [4] WA: Western Australia.
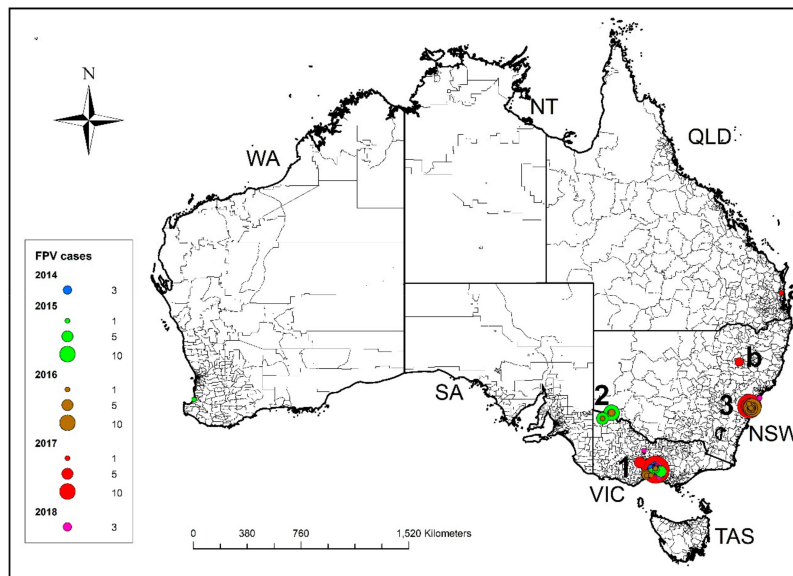
Figure 1. Distribution of cases of FPL reported in Australia between 1 January 2014 and 31 August 2018 by region and year of diagnosis. The first two outbreaks in Victoria occurred in 2014 in Melbourne (1) and in 2015 in Mildura (2). The third outbreak occurred in Sydney in December 2016 (3). Isolated cases were detected as far north as Nambour in Queensland (a) and in north western NSW in Gunnedah (b).

The first outbreak occurred in Melbourne, Victoria, between January and April 2014. A second outbreak occurred in Mildura, Victoria, some 560 km northwest of Melbourne, from February to April 2015, and a third outbreak occurred in Sydney, New South Wales (NSW), 1000 km northeast of Mildura and 900 km northeast of Melbourne from December 2016 to May 2017 (Figure 1). After the first recorded outbreak in each of these locations, between one and four recurrent seasonal outbreaks were documented, as well as isolated cases outside of the major outbreak regions, including in northwest NSW (Gunnedah) and southeast Queensland (Nambour) (Figure 1). The geographic area involved in recurrent annual seasonal outbreaks centred around Outbreak 1 from 2014 to 2018 expanded southwest in 2016, west in 2017 and northwest in 2018 (Figure 2). Similarly, there was expansion of the area involved in recurrent seasonal outbreaks centred around Sydney from 2016 to 2018, to involve the Central Coast region of NSW (Tuggerah and Wyong), 100 km north of Sydney (Supplementary Materials Figure S1).

The distribution of cases varied with month of presentation and is shown in Figure 3. Frequent transfer of cats in Victoria between shelters in Mildura (Outbreak 2 site) and Melbourne (Outbreak 1 site) suggested direct spread of the infection between these regions. Cats from two private shelters in Mildura were transported for rehoming to a shelter in Melbourne in 2014 and 2015.
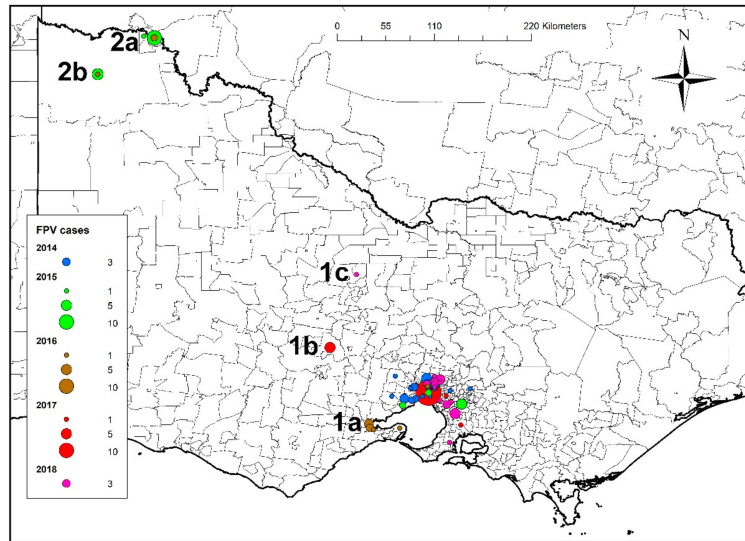
Figure 2. Distribution of cases in Outbreaks 1 and 2 from Victoria, Australia, showing expansion of the geographic area of FPL outbreaks originating in Melbourne from 2014 to 2018, including to Geelong in 2016 (1a), Bendigo in 2017 (1b) and Daylesford in 2018 (1c). Cases from the Mildura region outbreak were centred around the townships of Mildura (2a) and Benetook 2(b).
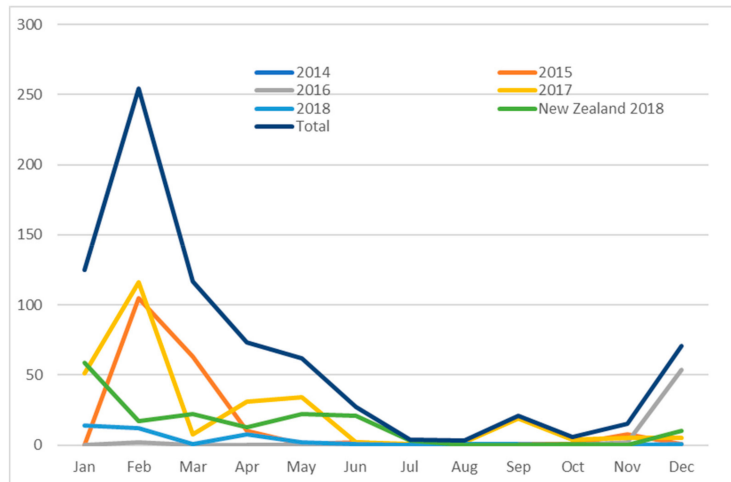

Figure 3. Seasonal distribution of Australian cases identified from 2014 to 2018 and of cases diagnosed in New Zealand in 2018.

3.1.2. Australian Cases—Vaccination Protocols and Coverage

Two of five shelters in NSW did not vaccinate cats while under their care. The other three shelters vaccinated healthy cats on admission using an inactivated FPV vaccine, whereas sick cats with suspected viral respiratory tract infections were not vaccinated until their clinical signs resolved.

None of the three shelters in Mildura vaccinated cats. Of the three shelters in Melbourne, one did not vaccinate cats, while two vaccinated cats on admission, one using an inactivated vaccine and the other an MLV vaccine. All shelters that used vaccinations gave a primary course to kittens starting at a minimum age of 6 weeks, then every 3 to 4 weeks, finishing at 12 to 14 weeks of age, while adult cats were given two vaccinations one month apart. Both rescue societies, one in NSW and one in Victoria, accepted unvaccinated cats and kittens for adoption from municipal pounds (shelters), that were fostered until adoption. For 177 shelter-housed cats, the median time from admission to diagnosis of FPL was 9 days (IQR 0–17; range 0–61 days).

Of the 610 cats diagnosed with FPL, 528 (87%) had never been vaccinated or had an unknown vaccination history. Sixty-five of the 82 (79%) cats that had received at least one vaccination were <16 weeks of age at the time of their last vaccination. For 17 cats ≥16 weeks of age at the time of last vaccination, the vaccination-to-disease interval was >10 days for 4/5 cats vaccinated with ≥2 inactivated vaccines and >7 days for 7/11 cats vaccinated with at least one MLV vaccine; vaccine type was unknown for one cat. For all vaccinated cats, the median time from last vaccination to diagnosis was 7.5 days (IQR 2–11; range 1–109 days).

Age, sex and breed data were available for 399 FPL cases. The median age at diagnosis was 10 weeks (IQR 7–20 weeks; range 3 weeks–96 months). The frequency distribution of age at diagnosis is shown in Table 3 Males (49%) and females (51%) were equally represented among FPL cases. Most cats (98%) were domestic crossbred (domestic shorthair or domestic longhair). Data on specific clinical signs were available for 153 cats. The most common clinical signs were diarrhoea (54%), lethargy (48%), vomiting (36%), anorexia (27%), weight loss or failure to gain weight (14%) and sudden death (10%). Diarrhoea was reported to be haemorrhagic in 13 of 83 cats (16%) with diarrhoea. Overall mortality for all 610 cats was 95%, noting that cases diagnosed in shelters were routinely euthanised at diagnosis to contain the infection.

Table 3. Frequency distribution of age at diagnosis for 399 cases of FPL.

Age	Frequency	Percent	Cumulative Frequency	Cumulative Percent
0–5 weeks	51	13	51	13
6–10 weeks	155	39	206	52
11–14 weeks	39	10	245	61
15–18 weeks	47	12	292	73
19–24 weeks	22	6	314	79
6–12 months	22	6	336	84
1–2 years	46	12	382	96
>2 years	17	4	399	100

3.2. Case data—New Zealand Cases

Two FPL outbreaks occurred in Wellington, New Zealand, in December 2016 and January 2018. The seasonal distribution of cases in the second outbreak is shown in Figure 3. In total, 365 cases of FPL were diagnosed, including 167 in the first outbreak and 198 in the second. During both outbreaks, 8% of feline admissions to the shelter were diagnosed with FPL. The median age at diagnosis was 9 weeks (IQR 6–14 weeks, range 2–105 weeks). At diagnosis of FPL, 32% of cats were unvaccinated, 58% had received one vaccine, 8% had been vaccinated twice, and 2% had been vaccinated three times. The median time since the last vaccination was 7 days (IQR 4–11.5 days, range 1–36 days). The median time from shelter admission to diagnosis was 7 days (IQR 0–14 days, range 0–28 days).

Of the nine cases for which clinical samples were available for PCR and sequencing, all cats had a positive faecal CPV antigen test result (FASTest Parvo Strip, Megacor Hoerbranz, Austria) and were euthanised at diagnosis. All cats had been vaccinated on admission using an MLV FPV vaccine (Felocell 3 or Felocell 4, Zoetis Pty. Ltd.). Clinical data are presented in Table 3.

3.3. Case Data—UAE Cases

Fourteen cases of FPL from Dubai, UAE, were diagnosed in domestic crossbreds with positive faecal CPV antigen test results. All cats were strays or strays that had been recently adopted, and all were unvaccinated, except an 18-month-old cat that had received a primary course of kitten vaccinations and a booster vaccination at 12 months. Clinical signs included vomiting, diarrhoea and lethargy, and the median age at diagnosis was 4 months (range 1–18 months). All cats were treated, and outcomes were known in 12 cases, of which 8 died or were euthanised, and 4 survived.

3.4. Histopathological Findings

3.4.1. Histopathological Findings—Australian Cases

In sections of duodenum and jejunum from the 11 representative cases, there was a mild to severe necrotizing lymphoplasmacytic-to-suppurative enteritis, characterized by variable blunting, fusion and loss of villi, collapse of the lamina propria, loss of crypts and replacement by abundant coccobacilli and necrotic debris. The remaining crypts were often ectatic, with variable numbers of crypt abscesses (Figure 4). Evidence of multifocal crypt regeneration was also variably present. The submucosa and tunica muscularis were variably expanded by congestion, fibrin, oedema, haemorrhage, perivascular lymphocytes and plasma cells, macrophages exhibiting erythrophagocytosis, occasional neutrophils and rare eosinophils.
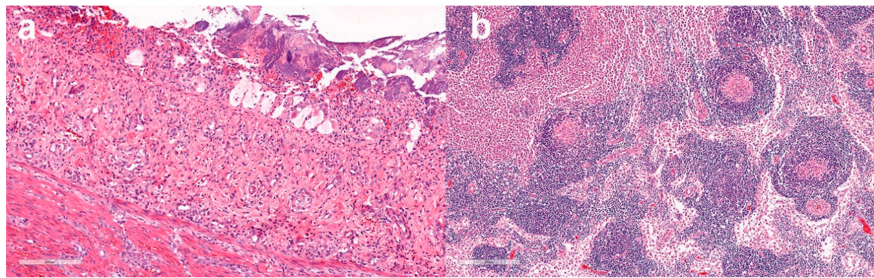

Figure 4. Case 111, 16-week old shelter-housed cat from Sydney, Australia, with diarrhoea, vomiting and fever, diagnosed with FPL. (**a**) Intestine—loss of villi and intestinal crypts of Lieberkuhn and collapse of proprial stroma with associated bacterial colonies on the luminal surface. Haematoxylin and eosin (HE) staining, scale bar 200 μm. (**b**) Mesenteric lymph node—lymphoid depletion is accompanied by accentuation of reticuloendothelial architecture with amorphous eosinophilic material within the centres of depleted follicles. HE. Scale bar 300 μm.

In sections of mesenteric lymph nodes, the most common finding was multifocal follicular and paracortical lymphoid depletion with accentuation of the reticuloendothelial architecture (Figure 4). Depleted lymphoid follicles were small, poorly populated and contained central accumulations of hyalinized eosinophilic material (follicular hyalinosis) with variable numbers of tangible body macrophages. The subcapsular and medullary sinuses were expanded by erythrocytes, oedema fluid and moderate to markedly increased numbers of macrophages, some exhibiting erythrophagocytosis.

Mild-to-moderate multifocal lymphoid depletion was also apparent in splenic sections. Extramedullary haematopoiesis characterized by the presence of myeloid and erythroid precursors was variably present within spleen and lymph nodes.

Sections of bone marrow examined were either hypocellular, characterised by increased numbers of, predominantly, adipocytes and extravasated erythrocytes interspersed with very low numbers of erythroid and myeloid precursors and megakaryocytes, or hypercellular, with increased numbers of myeloid and erythroid precursors. Some sections of the liver demonstrated hepatocellular atrophy

and congestion, with minimal periportal mononuclear infiltrates. Among the sections of myocardium examined, there were no significant lesions.

3.4.2. Histopathological findings—New Zealand cases

Histopathology of the small intestine was performed in six cases, including five in which samples were collected for PCR and sequencing (Table 4). In four of these, lesions of mild enteritis (*n* = 3) or fibrosis of the lamina propria (*n* = 1) were present. In one case (221, Table 3), histological lesions were typical of FPL (Figure 5), with multiple sections of jejunum and ileum showing mild multifocal loss and replacement of crypts by karyorrhectic and cellular debris (necrosis) and low-to-moderate numbers of neutrophils within the lamina propria. Low numbers of the remaining crypts were variably lined by degenerate or necrotic epithelium with intraluminal degenerate neutrophils, debris and sloughed necrotic epithelial cells (crypt abscesses). Neutrophils frequently invaded the remaining crypt epithelium. Rare epithelial cells contained 4–6 μm-diameter polygonal-to-ovoid, eosinophilic-to-amphophilic intranuclear inclusion bodies that occasionally marginated the chromatin. There was moderate multifocal crypt regeneration, and crypts were frequently lined by large epithelial cells with vesicular nuclei that were piled up or in mitosis. Intestinal lymphoid tissue appeared mildly depleted. The morphological diagnosis was moderate diffuse acute neutrophilic enteritis with crypt necrosis, epithelial regeneration and rare intranuclear viral inclusions. These findings were consistent with FPV/CPV infection. (Table 4). Of the cases where sections of mesenteric lymph nodes (*n* = 3) or thymus (*n* = 1) were available, lesions of mild follicular lymphoid depletion were present in one case, which was the same animal with small intestinal lesions consistent with FPV (case 221). Affected cortical follicles were small and poorly populated.

Histopathology was also performed on intestine and mesenteric lymph nodes from one unvaccinated cat with clinical signs of FPL, but for which samples were not collected for PCR and sequencing. Changes in the duodenum were similar to but more severe than those described above in case 221, including crypt necrosis and abscessation, neutrophilic infiltration of the lamina propria and the presence within epithelial cells of intranuclear inclusion bodies which variably marginated the chromatin. There was moderate lymphoid depletion in mesenteric lymph node tissue. These findings were also consistent with FPV/CPV infection.

Table 4. Summary of data obtained from New Zealand cases that had positive CPV faecal antigen test results and FPV VP2 sequence amplification using conventional PCR and/or histological findings consistent with FPL.

Case	Age (Weeks)	N [1]	D [2]	Clinical Signs	FPV Viral Copies/mg of Lymph Node	FPV Viral Copies/mg of Faeces	Faecal Co-Pathogens Detected on Multiplex PCR/Giardia Faecal Antigen Tests	Histological Findings—Small Intestine
216	10.5	2	15	Weight loss, diarrhoea	2.48×10^8	4.12×10^3	Feline coronavirus	NT
217	11	2	15	Diarrhoea	9.63×10^6	6.79×10^3	NT	NT
218	10.5	1	14	Dehydration, diarrhoea	2.87×10^7	4.12×10^3	*Giardia* spp.	Enteritis, acute, neutrophlic, mild
219	9.5	1	11	Diarrhoea	1.77×10^3	3.4×10^3	Feline coronavirus	NT, CBC WNL
220	13	1	7	Diarrhoea	8.22×10^9	6.48×10^4	Feline coronavirus	Mild diffuse fibrosis of lamina propria, CBC: mild lymphopenia
221	7	1	7	Conjunctivitis, weight loss	1.08×10^{10}	1.27×10^8	*Clostridium perfringens*	Multifocal crypt necrosis, crypt abscesses, lymphoid depletion, viral inclusion bodies
222	10	1	6	Diarrhoea	1.17×10^{10}	1.32×10^6	None	Enteritis, neutrophilic and eosinophilic, mild, acute
223	10	1	6	Diarrhoea	1.32×10^{10}	NT	NT	Enteritis, plasmacytic, mild
224	18	2	8	Diarrhoea, sneezing	1.79×10^8	8.02	Feline coronavirus	NT
88153	6	U	-	Vomiting, dehydration	NT	NT	*Giardia* spp.	Similar but more severe lesions, to case 221

[1] N: Number of vaccinations received; [2] D: Days since last vaccination; CBC: complete blood count; NT: not tested; U: unvaccinated; WNL: within normal limits
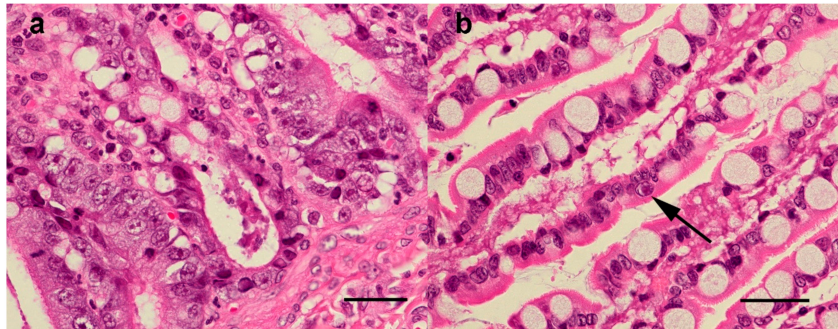
Figure 5. Small intestine, case 221, HE staining, scale bar 50 μm. (**a**) 600× Crypt epithelial cells are degenerating or necrotic and often sloughed into crypt lumens, (**b**) 1000× a villous epithelial cell contains an amphophilic intranuclear inclusion body which marginates the chromatin (arrow).

3.5. VP2 Sequencing and Phylogenetic Analysis

The entire VP2 region of *Carnivore protoparvovirus 1* was amplified from 113 suspected cases of FPL, comprising 93 from Australia, 11 from Dubai and 9 from New Zealand. Amino acid substitutions compared to the FPV reference strain are listed in Table 5. All VP2 sequences in this study were identified as FPV, with no cases attributed to CPV. Phylogenetic analysis of these VP2 sequences in comparison to a background global data set of FPV sequences revealed the presence of four distinct clades of Australian viruses (Figure 6). The first, denoted clade A, comprises 19 viruses (17 of which were identical) sampled from a wide geographic area (Melbourne, Geelong and Mildura) between 2014 and 2017. In contrast, Australia clade B comprised just two identical sequences sampled in NSW in 2015. These viruses were detected in the faeces collected from two cats in the same shelter in Sydney, NSW, in November 2015. Both cats had severe diarrhoea and tested positive for *Salmonella* spp. and *Carnivore protoparvovirus 1* on a multiplex faecal qPCR panel (Idexx Pty Ltd.). The largest Australian clade (C) comprised 66 viruses from NSW and one from Queensland, collected between December 2016 and February 2018. Viruses collected from cats in North Western NSW (Gunnedah) and South Eastern Queensland (Nambour) in 2017 were identical to those sampled from cats from four shelters and from privately owned cats in Sydney. Viruses from cats from the NSW Central Coast also fell into this clade. Finally, one sequence isolated from a cat from Melbourne in 2018 (FPV_251) was identical to viruses in clade C, with the exception of a mutation at position 694 (A694G) that resulted in an amino acid substitution I to V. This mutation was also present in viruses in Clade A.
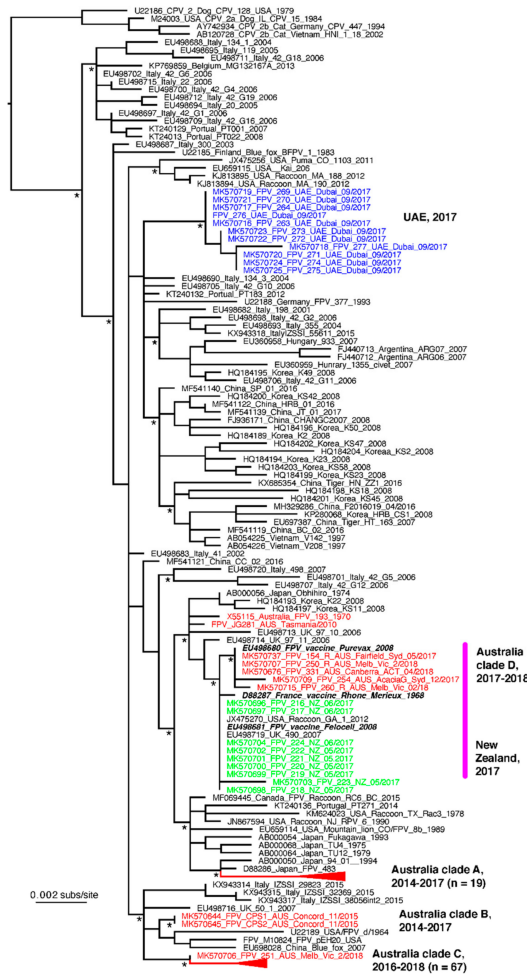
Table 5. Amino acid strain substitutions in the VP2 region of strains of feline parvovirus (FPV) isolated from cats in Australia, New Zealand and the United Arab Emirates compared to the reference FPV strain nominated by the International Committee on Taxonomy of Viruses (ICTV) (FVP-3, EU659111).

Accession No.	Variant	Year	Amino Acid VP2 Location																					
			5	80	87	93	101	103	145	204	232	297	300	305	323	373	375	426	445	462	555	562	564	568
EU659111 [1]	FPV ref	1967	A	K	M	K	T	V	I	I	V	S	A	D	D	D	D	N	T	P	V	V	N	A
MK570663	This study	2016–2018	•	•	•	•	•	•	•	•	•	•	•	•	•	•	•	•	•	•	•	•	•	•
EU498681 [2]	Felocell *	2008	•	•	•	•	•	•	•	•	I	•	•	•	•	•	•	•	•	•	•	L	•	•
EU498680 [3]	Purevax *	2008	•	•	•	•	•	•	•	•	I	•	•	•	•	•	•	•	•	•	•	L	•	•
MK570709	This study *	2017	•	•	•	•	M	•	L	•	I	•	•	•	•	•	•	•	•	•	•	L	•	•
MK570715	This study *	2018	•	•	•	•	V	•	•	•	I	•	•	•	•	•	•	•	•	•	•	L	•	•
MK570637 [4]	This study	2015–2016	T	•	•	•	•	•	•	•	•	•	•	•	•	•	•	•	•	•	•	•	•	•
MK570646	This study	2015	T	•	•	•	•	•	•	•	•	•	•	•	•	•	•	I	•	•	•	•	•	•
MK570644 [5]	This study	2015	•	•	•	•	I	•	•	•	I	•	•	•	•	•	•	•	•	•	L	•	•	•
MK570720 [6]	This study	2017	•	•	•	•	•	•	•	V	•	•	•	•	•	•	•	•	•	•	•	•	•	•
MK570654 [7]	This study	2017–2018	•	•	•	•	•	•	•	•	•	•	•	•	•	•	•	•	•	•	•	•	•	•
MK570710	This study	2017	•	•	•	•	•	•	•	•	I	•	•	•	•	N	•	•	•	•	•	•	•	•

* vaccine strain; • Amino acid identical to FPV reference EU659111; [1] MK570664, MK570667–MK570669, MK570677–MK570679, MK570684–MK570691, MK570693–MK570695, MK570707, MK570711–MK570713, MK570716, MK570717, MK570719, MK570721–MK570723, MK570726, MK570731, MK570732, MK570734–MK570736, MK570741–MK570744 and MK570746–MK570748 have identical amino acid sequences; 2 MK570696–MK570704 have identical amino acid sequences; 3 MK570707, MK570714, MK570737 and MK570676 have identical amino acid sequence; 4 MK570638–MK570643, MK570647–MK570653 and MK570749 have identical amino acid sequences; 5 MK570645 has an identical amino acid sequence; 6 MK570724, MK570725, MK570718 and MK570675 have identical amino acid sequences; 7 MK570655–MK570662, MK570665 and MK570666, MK570670–MK570674, MK570680–MK570683, MK570692, MK570705 and MK570706, MK570708, MK570727–MK570730, MK570733, MK570738–MK570740 and MK570745 have identical amino acid sequences.

Figure 6. Phylogenetic relationships of FPV associated with outbreaks in Australia (red), New Zealand (green) and the UAE (blue). The virus sequences from the largest outbreak clades (A and C) have been collapsed for clarity, with the number of sequences in these clades shown in parentheses. FPV vaccine strains are shown in bold italic in the clades adjacent to the bold pink line. The tree is rooted on a small clade of canine parvovirus (CPV) sequences; * denotes SH-like branch support values of 1.0. Branch lengths are scaled to the number of nucleotide substitutions per site.

3.6. FPV Viral Load and Concurrent Faecal Pathogens

A fourth (although not strictly monophyletic) clade (D) of viral sequences from Australian cats contained three VP2 sequences identical to that of an FPV vaccine strain (Purevax; Genbank accession no. EU498680) and two sequences that are very closely related to the vaccine strain. In one of these, from a 6-week-old kitten with acute vomiting and failure to gain weight, the vaccine strain was unlikely to be the cause of the cat's clinical signs. FPL was suspected because a multiplex qPCR faecal panel was positive for *Giardia* spp. and *Canine protoparvovirus 1*. However, the cat, from Canberra in the Australian Capital Territory, had been vaccinated 16 days before with the same MLV vaccine strain.

No littermates were affected, the cat recovered, and no other cases of suspected FPL were encountered in this region. Another sequence in this clade was from a 14-week-old stray kitten with vomiting, diarrhoea and failure to gain weight. The kitten, from a shelter in Melbourne, had been vaccinated 16 days before with the same MLV vaccine. It also tested positive on a multiplex qPCR faecal panel for *Giardia* spp. and *Canine protoparvovirus 1*. The third sequence was from an owned 8-week-old kitten in Sydney with acute onset vomiting and diarrhoea, vaccinated 3 days before (vaccine type unknown). Of the two closely related VP2 sequences, one (FPV_260) was from a 10-week-old kitten vaccinated 4 days before with the same vaccine strain, which presented for diarrhoea, vomiting and lethargy. It also tested positive for *Giardia* spp. on a faecal antigen test. The other (FPV_254) was from an unvaccinated stray 8-month-old cat that presented with vomiting, diarrhoea and anorexia and tested positive on a faecal CPV antigen test. Finally, two other Australian sequences—FPV 193/170 and Tasmania/2010—did not fall into a distinct clade but were relatively closely related to each other and to the vaccine cluster (clade D).

All 11 VP2 sequences from cats from Dubai fell into a single clade containing four unique sequence types and which was not clearly related to any other of the FPV sequences. In contrast, those viruses sampled from New Zealand in 2017 were either identical (eight of nine animals) or clearly very closely related to a vaccine strain (Felocell, Zoetis Pty Ltd.) and taken from cats with a history of recent vaccination. The single sequence that was not identical to that of the vaccine strain exhibited just two nucleotide substitutions, one of which was non-synonymous (E155K) (Table 4).

The results of the qPCR analyses to quantify FPV viral load in faeces of NZ cats and to detect faecal co-pathogens are presented in Table 4. Medical records were obtained from two unvaccinated kittens with FPL from Australia, where serial monitoring of FPV faecal shedding using qPCR was performed on pooled faecal samples after diagnosis. Testing was done at a single commercial laboratory, and results were reported as positive or negative (Table 6).

Table 6. Results of serial monitoring of faecal shedding of FPV in faecal samples from two cats diagnosed with FPL.

	CPV Faecal Antigen Test [1]	Parvovirus Detection by Faecal qPCR [2]			
	21.11.2016	07.01.2017	04.02.2017	07.03.2017	11.04.2017
Result	positive	positive	positive	positive	negative

[1] Individual samples from both cats tested positive; [2] Faecal samples from both cats were pooled for testing at all time points.

4. Discussion

An understanding of the drivers of the re-emergence of FPL, the oldest known viral disease of cats, is essential to contain this fatal infection. We provide strong evidence of multiple outbreaks of FPL in three countries. There are no previous published reports of FPL outbreaks in any of these regions for comparison, although there is anecdotal first-hand experience of FPL among veterinarians practicing in Australia from the late 1960s to the mid-1970s, before commercial vaccines were used routinely [1]. Despite the widespread circulation of CPV in Australia, this virus was not detected in any samples tested in these FPL outbreaks. Canine parvovirus causes approximately 5% of FPL cases globally, but these have been confined to sporadic individual cases, and there are no reports of FPL outbreaks caused by CPV in multi-cat environments [8,15,16]. Whether this is due to viral or to host factors is currently unknown and warrants further investigation.

A single FPV lineage (clade A) was responsible for disease in both outbreak regions in Victoria, Australia, even though these are geographically distant (550 km) from each other. Phylogenetic analysis revealed the closest related virus was taken from a domestic cat in Japan in 1994 (GenBank accession no. AB000050), although it is likely that a closer ancestral virus exists but has not been sampled here. The 100% sequence identity of VP2 sequences from cases in Mildura and Melbourne is consistent

with the epidemiological investigation, which found evidence supporting direct viral spread through transport of unvaccinated cats for adoption in 2014 and 2015. The nonenveloped virions of FPV, shed in high titres in all excretions of infected animals, are environmentally resilient and remain viable in infected premises such as shelters for over a year [17,18]. Indirect transmission by fomites is a major mechanism of parvovirus transmission among cats and dogs and was likely a crucial contributing factor to the canine global CPV pandemic in the late 1970s [19].

Unexpectedly, the FPL outbreak in Sydney, NSW, was not caused by spread of the Victorian strain, but rather by a separate clade (C) comprising a relatively distinct virus [20,21]. This finding, together with the detection of additional Australian FPVs (Clades B and D), is consistent with multiple independent virus entries into Australia, including the virus from an unvaccinated cat (clade D), which was seemingly derived from an FPV vaccine strain. Three recently vaccinated cats, in which the same vaccine virus was detected (clade D), likely did not have FPL, including two with *Giardia* co-infections initially diagnosed with FPL from a positive commercial faecal qPCR assay. MLV vaccine virus shed in faeces can be detected in qPCR assays and CPV faecal antigen tests [22,23]. Quantifying viral loads can assist in the discrimination of vaccine and field strains. However, quantification data were not provided by the commercial laboratory for these two cases. CPV vaccine viral loads in recently vaccinated dogs are 4- to 5-fold lower than those of dogs infected with field strains [24]. Similarly, a recent report found several recently vaccinated cats had low FPV viral loads ($<1.38 \times 10^2$ copies/mg of faeces) over a 28-day period of surveillance [23].

Before this investigation, only one FPV VP2 sequence from Australia had been deposited in the GenBank database (FPV 193/70, GenBank accession no. X55115). The evolutionary relationships with FPV 193/70 cannot be inferred reliably, since the isolate, obtained from a 3-month-old cat in Melbourne with peracute fatal FPL, had been serially passaged in vitro before sequencing in 1990. Interestingly, FPV 193/70 falls notably close to a clade of vaccine viruses in our analysis. In addition, we generated the VP2 sequence of an FPV strain detected in a healthy feral cat from Tasmania in 2010, which was genetically distinct from outbreak strains in this study and also fell into clade D, suggesting a vaccine-related origin. These findings, together with a report of FPV detection in the bone marrow of a healthy feral cat from Melbourne in 2012 [25], provide evidence that FPV has been circulating widely in Australia, at least since the 1970s, although the viruses are phylogenetically unrelated to the 2015–2018 outbreaks.

One possible explanation for the multiple independent FPV introductions described here is that FPV viruses circulating in the feral cat population may occasionally spill over into domestic cats. In comparison to the owned cat population, estimated at 3.8 million [26], some 2.1 to 6.3 million feral cats (free-roaming, unowned, unsocialised cats) inhabit Australia [27]. An FPV seroprevalence of 79% among feral cats in Victoria and NSW, documented in 1981, provides evidence of widespread FPV exposure [28]. Viral introductions could also have been anthropogenic, for example through fomite spread during international travel.

We were also able to analyse sequence data from a contemporaneous FPL outbreak in the UAE in 2018. This is the first study to characterise full-length VP2 sequences from the Middle East. Viruses most closely related to the UAE viruses, which formed a phylogenetically distinct lineage, were from a range of locations in Europe, Asia and the Americas, but the long lineage leading to the UAE viruses suggests that we have not yet sampled their ultimate ancestor.

The VP2 sequence data from cases analysed from a third country with contemporaneous FPL outbreaks showed that the NZ FPV strains segregated with FPV vaccine viruses. The virological findings from these cases yet again highlight the difficulty of diagnosing FPL in cats that have recently received MLV vaccines, as well as raising important questions about the potential capacity of reversion to virulence of MLV vaccines. The diagnosis of FPL in cases from NZ was initially based on consistent clinical signs and a positive faecal antigen test. Point-of-care immunochromatographic assays designed to detect CPV faecal antigen also detect FPV, so are used in practice for the diagnostic investigation of cats with clinical signs consistent with FPL [22]. However, faecal antigen tests detect both field and

vaccine strains of FPV and CPV. In one study evaluating three commercial CPV faecal antigen kits, 20% of cats vaccinated against FPV in the preceding 14 days returned positive test results [29].

The sensitivity of faecal antigen tests for the detection of parvoviruses is influenced by viral load in faeces, as well as by the presence of gut antibodies that can sequestrate viral particles and prevent binding to the test antibody [30]. CPV vaccine viral loads in recently vaccinated dogs are usually below the limit of detection of antigen tests, ranging from 1.48×10^0 to 2.5×10^4 copies/mg of faeces in one study [24] and from $\approx 10^0$ to 7.50×10^5 copies/mg of faeces in another [31]. The lower limit of detection of faecal antigen tests for CPV in dogs is 10^5 to 10^6 viral DNA copies per mg of faeces [32]. Low titres of gut FPV antibodies in the New Zealand cats could explain the positive faecal antigen test results in those cats with low faecal viral loads.

All but one of the VP2 sequences obtained from the New Zealand cases were identical to the FPV vaccine strain that the cats had been inoculated with. Co-infection with other pathogens including Feline coronavirus or *Giardia* spp. could account for the clinical signs in five of these cases, which, although consistent with FPL, were non-specific. However, in one cat, high loads of vaccine strain virus were detected concurrently in lymph node and faeces (FPV_221, Table 3), which is more consistent with loads attained by pathogenic virus strains than with those attained by vaccine virus strains. Further, unequivocal support of the diagnosis of FPL in this case was obtained from histological examination of the intestine, where lesions pathognomonic for FPL were identified (Figure 5). An FPV-vaccine strain was detected in this cat, and the sequencing chromatogram showed no evidence of a coinfecting FPV or CPV. However, deep sequencing of the sample with examination of the metatranscriptome or metagenome would be required to rule out co-infection with other pathogenic viruses not included in the qPCR test panel. An alternative explanation is that there was reversion to virulence of the vaccine strain, although this has not been described previously in cats.

Molecular analysis of faeces from dogs displaying signs of acute gastroenteritis shortly after CPV vaccination ruled out reversion to virulence of CPV MLV, since co-infection with field strains of CPV or other pathogens including Canine coronavirus, Canine distemper virus and *Isospora canis* was detected [33]. In three pups in which only the vaccine virus was detected, CPV vaccine loads were lower than those associated with enteritis from CPV field strains, ranging from 1.03×10^3 to 1.78×10^5 DNA copies/mg of faeces [33].

The re-emergence of FPL in two Australian states in relatively quick succession over a three-year period, caused by two distinct FPV lineages, raises the question as to why this disease is re-emerging now, after decades of apparent quiescence. Animal shelters are conducive environments for pathogen emergence or re-emergence because of a large number of susceptible hosts living in a confined area. This is exacerbated by factors including young age, immunological naivety or immunosuppression, close contact and co-morbidities such as heavy parasite burdens. Similarly, suboptimal biosecurity protocols favour pathogen persistence and fomite transmission [34].

Failure to vaccinate or inadequate or inappropriate vaccination in shelter-housed cats were major contributors to the re-emergence of FPL in Australia. Before these outbreaks, over half of the shelters from which cases were derived did not administer FPV vaccinations. In general, FPV vaccines are a highly effective tool in parvovirus control. For example, protective FPV antibody titres were measured in 95% of vaccinated cats in a field study of adult cats after MLV vaccination, of which 64% had pre-existing protective titres [35]. In addition, viral challenge studies of FPV-vaccinated cats usually show vaccine efficacy >90% [36]. Although state legislation mandates vaccination of owned cats in commercial boarding facilities in NSW and Victoria, vaccination is not enforced for cats admitted to private or municipal animal shelters, until they are sold for rehoming. Most shelters that did vaccinate, completed the primary course of vaccinations in kittens by 12 to 14 weeks of age and used inactivated vaccines, in contravention of the current guidelines. The World Small Animal Veterinary Association (WSAVA) Vaccination Guidelines recommend the use of MLV vaccines in shelter-housed cats for rapid induction of long-lasting humoral immunity [22,37]. A minimum age of 16 weeks for the final vaccination in the primary course is recommended, based on the failure of 45% of kittens to seroconvert

after vaccinations at 8 and 12 weeks of age with the commercial FPV MLV vaccination [37,38]. This immunity gap relates to persistent maternally derived antibodies (MDA) in kittens, which decline below protective titres yet effectively neutralize the vaccine virus and thereby prevent seroconversion [38]. Persistent MDA would explain the presence of vaccination non-responders in our study that were <16 weeks of age at the time of diagnosis of FPL, highlighting that vaccination alone cannot prevent disease in environments where susceptible kittens are exposed to FPV.

Among the 21% of vaccination non-responders that were older than 16 weeks, some were likely exposed to FPV prior to seroconversion, either before or after admission to the shelter, as indicated by the median vaccination-to-diagnosis interval of 7.5 days. The incubation period for FPL is between 2 and 10 days [17]. Other reasons for apparent vaccine failure include persistence of MDA for >16 weeks in kittens born to queens with high anti-FPV antibody titres or failure to mount an immune response to vaccination because of immunodeficiency (acquired or genetic), incorrect vaccine administration or storage errors [35,38].

The median time from shelter admission to diagnosis of FPL was 9 days. The minimum holding time for unidentified cats in municipal shelters in the states of Victoria and NSW is 7 days, after which cats can be euthanised or rehomed (Domestic Animals Act 1994, Companion Animals Act 1998). Changes in euthanasia practices resulting in longer length of stay (LOS) may have contributed to a cumulative increase in selection pressure for FPL re-emergence, especially in shelters where vaccination was not practiced. The likelihood of exposure to infectious diseases increases within a shelter environment with increasing LOS [39]. National data from Royal Society of Prevention to Cruelty (RSPCA) shelters show a progressive decline in euthanasia rates from 74% in 1995 to 27% in 2018 [40,41]. Similar declines in euthanasia have occurred in shelters in other countries such as Canada [42].

A seasonal pattern of FPL was identified in Australia and New Zealand, with an annual peak in case numbers from December to May. This pattern may reflect waning maternal immunity lagging two to three months behind the peak kitten births. Similar seasonality of FPL outbreaks was reported in the Northern Hemisphere, where seasons are inverted; case numbers peaked from July to December and were correlated with an influx of kittens born annually in spring and waning of maternal immunity over the subsequent two to three months [43].

The duration of faecal shedding of FPV, which is relevant to infection control, has been inadequately studied. This study demonstrates that virus can be shed in faeces for an extended period of up to 14 weeks from diagnosis. Faecal shedding of vaccine virus was detected by qPCR post vaccination for the duration of one four-week study [23]. Shedding of field CPV strains in dogs has been detected by qPCR for 45–50 days [44,45], while CPV vaccine virus was shed for 19–22 days on average [31,46]. Further studies are warranted in cats to further define the duration of faecal shedding of both field and vaccine strains of FPV detectable by qPCR.

5. Conclusions

Inadequate vaccination coverage was identified in the FPL outbreaks described here and was a major contributor to the re-emergence of this disease. These outbreaks highlight the importance of adherence to vaccination guidelines for shelters, recommended by professional bodies such as the WSAVA. Further research is needed to identify the duration of FPV shedding in naturally infected cats, as well as the potential for reversion to virulence of MLV vaccines.

References

1. Barrs, V.R. Feline Panleukopenia: A Re-emergent Disease. *Vet. Clin. North. Am. Small Anim. Pract.* **2019**, *49*, 651–670. [CrossRef] [PubMed]

2. Cotmore, S.F.; Agbandje-McKenna, M.; Chiorini, J.A.; Mukha, D.V.; Pintel, D.J.; Qiu, J.; Soderlund-Venermo, M.; Tattersall, P.; Tijssen, P.; Gatherer, D.; et al. The family Parvoviridae. *Arch. Virol.* **2014**, *159*, 1239–1247. [CrossRef] [PubMed]

3. Hueffer, K.; Govindasamy, L.; Agbandje-McKenna, M.; Parrish, C.R. Combinations of two capsid regions controlling canine host range determine canine transferrin receptor binding by canine and feline parvoviruses. *J. Virol.* **2003**, *77*, 10099–10105. [CrossRef] [PubMed]

4. Goodman, L.B.; Lyi, S.M.; Johnson, N.C.; Cifuente, J.O.; Hafenstein, S.L.; Parrish, C.R. Binding site on the transferrin receptor for the parvovirus capsid and effects of altered affinity on cell uptake and infection. *J. Virol.* **2010**, *84*, 4969–4978. [CrossRef]

5. Mochizuki, M.; Horiuchi, M.; Hiragi, H.; San Gabriel, M.C.; Yasuda, N.; Uno, T. Isolation of canine parvovirus from a cat manifesting clinical signs of feline panleukopenia. *J. Clin. Microbiol.* **1996**, *34*, 2101–2105.

6. Ikeda, Y.; Nakamura, K.; Miyazawa, T.; Takahashi, E.; Mochizuki, M. Feline host range of canine parvovirus: Recent emergence of new antigenic types in cats. *Emerg. Infect. Dis.* **2002**, *8*, 341–346. [CrossRef]

7. Gamoh, K.; Shimazaki, Y.; Makie, H.; Senda, M.; Itoh, O.; Inoue, Y. The pathogenicity of canine parvovirus type-2b, FP84 strain isolated from a domestic cat, in domestic cats. *J. Vet. Med. Sci.* **2003**, *65*, 1027–1029. [CrossRef]

8. Decaro, N.; Desario, C.; Amorisco, F.; Losurdo, M.; Colaianni, M.L.; Greco, M.F.; Buonavoglia, C. Canine parvovirus type 2c infection in a kitten associated with intracranial abscess and convulsions. *J. Feline Med. Surg.* **2011**, *13*, 231–236. [CrossRef]

9. Kelman, M.; Ward, M.P.; Barrs, V.R.; Norris, J.M. The geographic distribution and financial impact of canine parvovirus in Australia. *Transbound. Emerg. Dis.* **2019**, *66*, 299–311. [CrossRef]

10. Ward, M.P.; Kelman, M. Companion animal disease surveillance: A new solution to an old problem? *Spat. Spatio-Temporal Epidemiol.* **2011**, *2*, 147–157. [CrossRef]

11. Decaro, N.; Elia, G.; Desario, C.; Roperto, S.; Martella, V.; Campolo, M.; Lorusso, A.; Cavalli, A.; Buonavoglia, C. A minor groove binder probe real-time PCR assay for discrimination between type 2-based vaccines and field strains of canine parvovirus. *J. Virol. Methods* **2006**, *136*, 65–70. [CrossRef] [PubMed]

12. Decaro, N.; Desario, C.; Miccolupo, A.; Campolo, M.; Parisi, A.; Martella, V.; Amorisco, F.; Lucente, M.S.; Lavazza, A.; Buonavoglia, C. Genetic analysis of feline panleukopenia viruses from cats with gastroenteritis. *J. Gen. Virol.* **2008**, *89*, 2290–2298. [CrossRef] [PubMed]

13. Guindon, S.; Dufayard, J.F.; Lefort, V.; Anisimova, M.; Hordijk, W.; Gascuel, O. New algorithms and methods to estimate maximum-likelihood phylogenies: Assessing the performance of PhyML 3.0. *Syst. Biol.* **2010**, *59*, 307–321. [CrossRef] [PubMed]

14. Decaro, N.; Elia, G.; Martella, V.; Desario, C.; Campolo, M.; Trani, L.D.; Tarsitano, E.; Tempesta, M.; Buonavoglia, C. A real-time PCR assay for rapid detection and quantitation of canine parvovirus type 2 in the feces of dogs. *Vet. Microbiol.* **2005**, *105*, 19–28. [CrossRef]

15. Decaro, N.; Buonavoglia, D.; Desario, C.; Amorisco, F.; Colaianni, M.L.; Parisi, A.; Terio, V.; Elia, G.; Lucente, M.S.; Cavalli, A.; et al. Characterisation of canine parvovirus strains isolated from cats with feline panleukopenia. *Res. Vet. Sci.* **2010**, *89*, 275–278. [CrossRef]

16. Miranda, C.; Parrish, C.R.; Thompson, G. Canine parvovirus 2c infection in a cat with severe clinical disease. *J. Vet. Diagn. Investig.* **2014**, *26*, 462–464. [CrossRef]

17. Csiza, C.K.; Scott, F.W.; de Lahunta, A.; Gillespie, J.H. Pathogenesis of feline panleukopenia virus in susceptible newborn kittens I. Clinical signs, hematology, serology, and virology. *Infect. Immun.* **1971**, *3*, 833–837.

18. Johnson, R.H. Feline panleucopaenia virus. III. Some properties compared to a feline herpes virus. *Res. Vet. Sci.* **1966**, *7*, 112. [CrossRef]

19. Parrish, C.R. Host range relationships and the evolution of canine parvovirus. *Vet. Microbiol.* **1999**, *69*, 29–40. [CrossRef]

20. Studdert, M.J.; Peterson, J.E. Some properties of feline panleukopenia virus. *Arch. Fur Die Gesamte Virusforsch.* **1973**, *42*, 346–354. [CrossRef]

21. Martyn, J.C.; Davidson, B.E.; Studdert, M.J. Nucleotide sequence of feline panleukopenia virus: Comparison with canine parvovirus identifies host-specific differences. *J. Gen. Virol.* **1990**, *71*, 2747–2753. [CrossRef] [PubMed]

22. Patterson, E.V.; Reese, M.J.; Tucker, S.J.; Dubovi, E.J.; Crawford, P.C.; Levy, J.K. Effect of vaccination on parvovirus antigen testing in kittens. *J. Am. Vet. Med. Assoc.* **2007**, *230*, 359–363. [CrossRef] [PubMed]

23. Bergmann, M.; Schwertler, S.; Speck, S.; Truyen, U.; Reese, S.; Hartmann, K. Faecal shedding of parvovirus deoxyribonucleic acid following modified live feline panleucopenia virus vaccination in healthy cats. *Vet. Rec.* **2019**, *185*, 83. [CrossRef] [PubMed]

24. Freisl, M.; Speck, S.; Truyen, U.; Reese, S.; Proksch, A.L.; Hartmann, K. Faecal shedding of canine parvovirus after modified-live vaccination in healthy adult dogs. *Vet. J.* **2017**, *219*, 15–21. [CrossRef] [PubMed]

25. Haynes, S.M.; Holloway, S.A. Identification of parvovirus in the bone marrow of eight cats. *Aust. Vet. J.* **2012**, *90*, 136–139. [CrossRef]

26. Pets in Australia: A Survey of Pets and People. Available online: https://animalmedicinesaustralia.org.au/resources-media/ (accessed on 17 November 2019).

27. Legge, S.; Murphy, B.G.; McGregor, H.; Woinarski, J.C.Z.; Augusteyn, J.; Ballard, G.; Baseler, M.; Buckmaster, T.; Dickman, C.R.; Doherty, T.; et al. Enumerating a continental-scale threat: How many feral cats are in Australia? *Biol. Conserv.* **2017**, *206*, 293–303. [CrossRef]

28. Coman, B.J.; Jones, E.H.; Westbury, H.A. Protozoan and viral infections of feral cats. *Aust. Vet. J.* **1981**, *57*, 319–323. [CrossRef]

29. Meason-Smith, C.; Diesel, A.; Patterson, A.P.; Older, C.E.; Johnson, T.J.; Mansell, J.M.; Suchodolski, J.S.; Rodrigues Hoffmann, A. Characterization of the cutaneous mycobiota in healthy and allergic cats using next generation sequencing. *Vet. Dermatol.* **2017**, *28*, 71-e17. [CrossRef]

30. Decaro, N.; Buonavoglia, C. Canine parvovirus—A review of epidemiological and diagnostic aspects, with emphasis on type 2c. *Vet. Microbiol.* **2012**, *155*, 1–12. [CrossRef]

31. Decaro, N.; Crescenzo, G.; Desario, C.; Cavalli, A.; Losurdo, M.; Colaianni, M.L.; Ventrella, G.; Rizzi, S.; Aulicino, S.; Lucente, M.S.; et al. Long-term viremia and fecal shedding in pups after modified-live canine parvovirus vaccination. *Vaccine* **2014**, *32*, 3850–3853. [CrossRef]

32. Decaro, N.; Desario, C.; Billi, M.; Lorusso, E.; Colaianni, M.L.; Colao, V.; Elia, G.; Ventrella, G.; Kusi, I.; Bo, S.; et al. Evaluation of an in-clinic assay for the diagnosis of canine parvovirus. *Vet. J.* **2013**, *198*, 504–507. [CrossRef]

33. Decaro, N.; Desario, C.; Elia, G.; Campolo, M.; Lorusso, A.; Mari, V.; Martella, V.; Buonavoglia, C. Occurrence of severe gastroenteritis in pups after canine parvovirus vaccine administration: A clinical and laboratory diagnostic dilemma. *Vaccine* **2007**, *25*, 1161–1166. [CrossRef]

34. Pesavento, P.A.; Murphy, B.G. Common and emerging infectious diseases in the animal shelter. *Vet. Pathol.* **2014**, *51*, 478–491. [CrossRef]

35. Bergmann, M.; Schwertler, S.; Reese, S.; Speck, S.; Truyen, U.; Hartmann, K. Antibody response to feline panleukopenia virus vaccination in healthy adult cats. *J. Feline Med. Surg.* **2017**. [CrossRef]

36. Lappin, M.R.; Andrews, J.; Simpson, D.; Jensen, W.A. Use of serologic tests to predict resistance to feline herpesvirus 1, feline calicivirus, and feline parvovirus infection in cats. *J. Am. Vet. Med. Assoc.* **2002**, *220*, 38–42. [CrossRef]

37. Day, M.J.; Horzinek, M.C.; Schultz, R.D.; Squires, R.A. WSAVA Guidelines for the vaccination of dogs and cats. *J. Small Anim. Pract.* **2016**, *57*, E1-e45. [CrossRef]

38. Jakel, V.; Cussler, K.; Hanschmann, K.M.; Truyen, U.; Konig, M.; Kamphuis, E.; Duchow, K. Vaccination against Feline Panleukopenia: Implications from a field study in kittens. *BMC Vet. Res.* **2012**, *8*, 62. [CrossRef]

39. Dinnage, J.D.; Scarlett, J.M.; Richards, J.R. Descriptive epidemiology of feline upper respiratory tract disease in an animal shelter. *J. Feline Med. Surg.* **2009**, *11*, 816–825. [CrossRef]

40. RSPCA Australia National Statistics 1999–2000. Available online: https://www.rspca.org.au/sites/default/files/website/The-facts/Statistics/RSPCA%20Australia%20National%20Statistics1999-2000.pdf (accessed on 29 October 19).

41. RSPCA Australia National Statistics 2017–2018. Available online: https://www.rspca.org.au/sites/default/files/RSPCA%20Australia%20Annual%20Statistics%202017-2018.pdf (accessed on 29 October 2019).

42. Janke, N.; Berke, O.; Flockhart, T.; Bateman, S.; Coe, J.B. Risk factors affecting length of stay of cats in an animal shelter: A case study at the Guelph Humane Society, 2011–2016. *Prev. Vet. Med.* **2017**, *148*, 44–48. [CrossRef]

43. Reif, J.S. Seasonality, natality and herd immunity in feline panleukopenia. *Am. J. Epidemiol.* **1976**, *103*, 81–87. [CrossRef]

44. Decaro, N.; Desario, C.; Campolo, M.; Elia, G.; Martella, V.; Ricci, D.; Lorusso, E.; Buonavoglia, C. Clinical and virological findings in pups naturally infected by canine parvovirus type 2 Glu-426 mutant. *J. Vet. Diagn. Investig.* **2005**, *17*, 133–138. [CrossRef]

45. Decaro, N.; Campolo, M.; Desario, C.; Elia, G.; Martella, V.; Lorusso, E.; Buonavoglia, C. Maternally-derived antibodies in pups and protection from canine parvovirus infection. *Biologicals* **2005**, *33*, 261–267. [CrossRef]

46. Decaro, N.; Buonavoglia, C. Canine parvovirus post-vaccination shedding: Interference with diagnostic assays and correlation with host immune status. *Vet. J.* **2017**, *221*, 23–24. [CrossRef]

Appendix II

Feline Calicivirus Virulent Systemic Disease: Clinical Epidemiology, Analysis of Viral Isolates and In Vitro Efficacy of Novel Antivirals in Australian Outbreaks

Matteo Bordicchia [1], Tulio Machado Fumian [2,3], Kate Van Brussel [1,4], Alice G. Russo [2], Maura Carrai [5], Shi-Jia Le [6], Patricia A. Pesavento [7], Edward C. Holmes [4], Vito Martella [8], Peter White [2], Julia A. Beatty [1,5], Mang Shi [6,†] and Vanessa R. Barrs [1,5,*,†]

[1] Faculty of Science, Sydney School of Veterinary Science, The University of Sydney, Sydney, NSW 2006, Australia; matteo.bordicchia@sydney.edu.au (M.B.); kate.vanbrussel@sydney.edu.au (K.V.B.); julia.beatty@cityu.edu.hk (J.A.B.)

[2] Faculty of Science, School of Biotechnology and Biomolecular Sciences, University of New South Wales, Sydney, NSW 2052, Australia; tuliomf@ioc.fiocruz.br (T.M.F.); a.russo@nsw.edu.au (A.G.R.); p.white@unsw.edu.au (P.W.)

[3] Laboratory of Comparative and Environmental Virology, Oswaldo Cruz Institute, Oswaldo Cruz Foundation, Fiocruz 4365, Brazil

[4] Marie Bashir Institute for Infectious Diseases and Biosecurity, School of Life and Environmental Sciences and School of Medical Sciences, University of Sydney, Sydney, NSW 2006, Australia; edward.holmes@sydney.edu.au

[5] Department of Veterinary Clinical Sciences, Jockey Club College of Veterinary Medicine and Life Sciences, Centre for Companion Animal Health, City University of Hong Kong, Kowloon Tong, Hong Kong 999077, China; mcarrai@cityu.edu.hk

[6] School of Medicine, Sun Yat-sen University Guangzhou East Campus, Panyu, Guangzhou 510080, China; leshij@mail2.sysu.edu.cn (S.-J.L.); shim23@mail.sysu.edu.cn (M.S.)

[7] Department of Pathology, Microbiology and Immunology, UC Davis School of Veterinary Medicine, 1044 Haring Hall, 1 Shields Avenue, Davis, CA 95616, USA; papesavento@ucdavis.edu

[8] Department of Veterinary Medicine, University of Aldo Moro of Bari, 70010 Valenzano, Italy; vito.martella@uniba.it

* Correspondence: vanessa.barrs@cityu.edu.hk

† These authors contributed equally to the manuscript.

Abstract: Feline calicivirus (FCV) causes upper respiratory tract disease (URTD) and sporadic outbreaks of virulent systemic disease (FCV-VSD). The basis for the increased pathogenicity of FCV-VSD viruses is incompletely understood, and antivirals for FCV-VSD have yet to be developed. We investigated the clinicoepidemiology and viral features of three FCV-VSD outbreaks in Australia and evaluated the in vitro efficacy of nitazoxanide (NTZ), 2′-C-methylcytidine (2CMC) and NITD-008 against FCV-VSD viruses. Overall mortality among 23 cases of FCV-VSD was 39%. Metagenomic sequencing identified five genetically distinct FCV lineages within the three outbreaks, all seemingly evolving in situ in Australia. Notably, no mutations that clearly distinguished FCV-URTD from FCV-VSD phenotypes were identified. One FCV-URTD strain likely originated from a recombination event. Analysis of seven amino-acid residues from the hypervariable E region of the capsid in the cultured viruses did not support the contention that properties of these residues can reliably differentiate between the two pathotypes. On plaque reduction assays, dose–response inhibition of FCV-VSD was obtained with all antivirals at low micromolar concentrations; NTZ EC_{50}, 0.4–0.6 μM, TI = 21; 2CMC EC_{50}, 2.7–5.3 μM, TI > 18; NITD-008, 0.5 to 0.9 μM, TI > 111. Investigation of these antivirals for the treatment of FCV-VSD is warranted.

Keywords: Caliciviridae; *Vesivirus*; nitazoxanide; 2′-C-methylcytidine; NITD-008

1. Introduction

Feline calicivirus (FCV) is a single-stranded, positive-sense, non-enveloped RNA virus in the genus *Vesivirus*, family Caliciviridae. The 7.5 kb FCV genome contains three overlapping open reading frames (ORFs) that encode non-structural proteins (ORF 1), the VP1 major capsid protein (ORF 2) and the VP2 minor capsid protein (ORF 3). The 5′ end of the genome is linked to the viral protein genome (VPg) and the 3′ end is polyadenylated [1–4]. Genetic variants of FCV are generated constantly through polymerase "errors" and recombination events. FCV is highly contagious and a common cause of acute upper respiratory tract disease (URTD) in cats, characterised by fever, oculonasal discharge, sneezing and oral ulceration. Polyarthritis and mucocutaneous ulcers are less common features [5]. The virus is spread directly and by contact with contaminated fomites. Young cats and kittens in multicat environments are most susceptible to FCV-URTD, but most recover with supportive care. Vaccination against FCV, which is routine, prevents or limits disease.

FCV also causes clinically distinct outbreaks of virulent systemic disease (FCV-VSD), especially in adults, with mortality rates of up to 79% [6–13]. FCV-VSD is characterised by systemic vasculitis and severe epithelial necrosis resulting in oedema of the head and limbs, multifocal ulceration of the skin and footpads, jaundice and pneumonia. Concurrent FCV-URTD is usually present [7,8,12]. As vaccination does not fully protect against FCV-VSD, there is interest in developing antivirals for use in the face of outbreaks. Three antiviral drugs, including two nucleoside analogues (2′-C-methylcytidine and NITD-008) and a thiazolide anti-infective agent (nitazoxanide), have been shown to have efficacy against the FCV-F9 prototype vaccine strain, but they have not yet been tested against viruses isolated from FCV-VSD outbreaks [14,15].

Attempts to define distinguishing molecular signatures of the highly pathogenic viruses isolated from cases of FCV-VSD have thus far been unsuccessful [10,11,16]. However, in a recent study, it was proposed that the majority of FCV-URTD and FCV-VSD viruses, or pathotypes, could be distinguished based on the physical and chemical properties of seven key amino acids in the hypervariable E region of VP1 (residues 426–521) involved in receptor binding and cell entry [17]. Specifically, a multiple correspondence analysis (MCA) suggested that these properties related to residues 438 (non-polar with an aliphatic chain), residue 440 (not small), residue 448 (polar with positive charge), residue 452 (not small), residue 455 (not negative), residue 465 (polar) and residue 492 (small) [17]. Whether this method is reliable for differentiation of FCV-VSD pathotypes requires further testing using a larger number of isolates.

Between 2015 and 2018, three separate nosocomial outbreaks of suspected FCV-VSD were reported in New South Wales (NSW), Queensland (QLD) and the Australian Capital Territory (ACT), in Australia. To the best of our knowledge, FCV-VSD has not been reported previously in the southern hemisphere. Herein, we aimed to provide a clinical and epidemiological description of the outbreaks, to investigate viral isolates for FCV-VSD pathotype-specific properties and to determine the in vitro efficacy of nitazoxanide (NTZ), 2′-C-methylcytidine (2CMC) and NITD-008 against FCV-VSD viruses. These antiviral agents were selected for testing against FCV-VSD strains based on the results of previous investigations [14,15]. In one study, from among 15 antiviral agents evaluated, NTZ and 2CMC were identified as potent inhibitors of replication of the F9 vaccine strain in vitro, with EC_{50} values in the low micromolar range [14]. Subsequently, NITD-008 was evaluated against three calicivirus model systems (FCV, murine norovirus and the human norovirus (Norwalk) replicon) and found to be a potent inhibitor of replication of all three caliciviruses in vitro, with low toxicity and EC_{50} values of <1 μM [15].

2. Materials and Methods

2.1. Case Data and Definitions

Outbreaks of FCV-VSD were reported at a single first-opinion veterinary hospital in Sydney, NSW, in 2015 (Outbreak 1); Ipswich, QLD, in 2017 (Outbreak 2) and Canberra, ACT, in 2018 (Outbreak 3). Data obtained from medical records of patients presenting with signs

of FCV-VSD and/or FCV-URTD included age, breed, sex, neuter status, FCV vaccination history, clinical signs, duration of illness, treatments prescribed and outcome. Disease phenotype was assigned as either (a) FCV-URTD defined as the presence of ≥ 2 of the following clinical signs: fever (rectal temperature > 39.3 °C), ocular or nasal discharge, conjunctivitis, oral or mucocutaneous ulcers or lameness, or (b) FCV-VSD defined as ≥ 1 signs of FCV-URTD and ≥ 1 of the following: limb or facial oedema, jaundice, skin ulceration or death [5]. Vaccination status was classified as complete (documented completion of a primary FCV vaccination course and, where a year or more had elapsed, revaccination at least once within the preceding three years), incomplete (cats <16 weeks of age that had received one or more vaccinations against FCV or cats that had not been revaccinated for >1 year after the primary vaccination course), unvaccinated (never vaccinated) or unknown vaccination status.

2.2. Sample Collection

Tissue samples were available from two cases that died during Outbreak 1. Cadavers of these cats were stored at −20 °C before transport to our laboratory for sample collection. Samples of liver, lung, lymph node and ulcerated skin were collected and stored at −80 °C until processing for viral culture. Oropharyngeal and conjunctival swabs were collected from cats showing clinical signs associated with the different pathotypes from Outbreak 2 (*n* = 9) and Outbreak 3 (*n* = 5). In addition, swabs were collected from a cat (QLD_13 KL) showing URTD signs during Outbreak 2 from a nearby veterinary hospital. Swabs were also collected from an asymptomatic cat (ACT_3) that had presented for a routine dental procedure during Outbreak 3. Swab tips were placed in 0.5 mL of viral transport medium (Dulbecco's modified Eagle's medium, with 1000 mg L^{-1} glucose, L-glutamine and sodium bicarbonate + 10% foetal bovine serum) and shipped at 4 °C for viral culture.

2.3. Virus Isolation

FCV was isolated from swab and tissue specimens on confluent Crandell–Rees feline kidney (CRFK) cells at 37 °C in 5% CO_2 in Dulbecco's modified Eagle's medium, with 1000 mg L^{-1} glucose, L-glutamine and sodium bicarbonate + 10% foetal bovine serum + streptomycin 5000 U/mL and amphotericin B 25 µg/mL [9]. One mock infected monolayer was incubated in parallel with each batch of samples and was considered negative if CPEs were absent after 5 days. Samples were considered positive for FCV if they developed characteristic cytopathic effects (CPEs) within 12–72 h post infection. Viruses were harvested, stored and processed separately to avoid cross-contamination.

2.4. Histopathology and Immunohistochemistry (IHC)

One case from Outbreak 2 that succumbed with clinical signs of FCV-VSD was submitted for post-mortem examination, including histopathology. Formalin-fixed paraffin-embedded liver tissue was immunohistochemically stained using the monoclonal anti-FCV clone S1–8 provided by Customs Monoclonals Intl., Sacramento, CA, USA, as previously described [13].

2.5. RNA Extraction RT-PCR

To confirm isolation of FCV, RNA was extracted from positive cultures using the RNAeasy Mini Kit (Qiagen, Hilden, Germany), according to the manufacturer's guidelines. Reverse transcription was performed using 200 ng random hexamers (SuperScript® III One-Step RT-PCR System, Thermo Fisher Scientific Inc., MA, USA). FCV capsid amplification by PCR was carried out as described [18]. Reverse transcription was carried out at 52 °C for 10 min, followed by initial denaturation at 95 °C for 5 min, then 35 cycles of denaturation at 95 °C for 1 min, annealing at 56–57 °C for 15 s, extension at 72 °C for 10 s, and a final extension at 72 °C for 5 min. The identity of PCR products migrating at the expected size on gel electrophoresis was confirmed by Sanger sequencing (Macrogen sGenome Centre, Seoul, Korea). Next-generation sequencing (NGS) libraries were prepared from viral cultures of

selected positive cases from each outbreak after RNA extraction, using the TruSeq RNA library preparation kit (Illumina, San Diego, CA, USA), and cytoplasmic ribosomal RNA was depleted using a Ribo-Zero Gold rRNA removal kit (Human/Mouse/Rat) (Illumina, USA). RNA sequencing of 100 bp paired-end libraries was performed on an Illumina NovaSeq 6000 platform.

2.6. Bioinformatic and Phylogenetic Analyses

The resulting sequencing reads were assembled, followed by the identification of full-length FCV genomes. The reads were assembled using Megahit [19], and the assembled sequences were annotated using diamond Blastx against the entire non-redundant (nr) database on GenBank. Contigs associated with FCV genomes were then identified, and complete virus genomes were obtained after mapping virus reads against the virus contigs. The assembled genomes were then compared with (i) complete or near-complete FCV genomes as well as (ii) partial VP1 gene sequences downloaded from GenBank, which were more representative of FCV diversity. Both datasets contained previously identified virulent strains of FCV. Phylogenetic trees were estimated based on both datasets using the maximum-likelihood algorithm implemented in the PhyML (version 3.0) [20], employing a general-time reversible (GTR) substitution model and subtree pruning and regrafting (SPR) branch-swapping algorithm. Support for the phylogeny was evaluated using an approximate likelihood ratio test (aLRT) with the Shimodaira–Hasegawa-like procedure.

The inferred amino-acid (aa) sequences of the capsid protein of Australian FCV viruses were aligned with reference FCV strains from cats with VSD or URTD as well as with enteric strains of FCV from cats with diarrhoea [21]. The specific physical and chemical properties of the seven residues previously identified as linked to the VSD pathotype were assigned binary outcomes (0 = no, 1 = yes) and compared for aa 438 (polar, aliphatic), aa 440 (small), aa 448 (polar, charged, small, positive), aa 452 (small), aa 455 (negative, charged), aa 465 (hydrophobic, polar) and aa 492 (small) [17]. Multiple correspondence analysis based on the Burt matrix of these 13 categorical variables was performed in XLSTAT 2020 (Addinsoft Pty. Ltd., Paris, France) in a blind analysis where pathotype (VSD vs. non-VSD) was not included as a variable.

2.7. Recombination Analysis

To identify possible recombination events among these sequences, we collected 56 FCV full-length genomes including the Australian outbreak viruses and genomes available on GenBank. Sequences were aligned using MAFFT v 7.0 [22] and then analysed for recombination events using the SimPlot program 3.5.1 [23] with a 1000 bp window size and 10 bp step size. In SimPlot analyses, Australian strains were used as a query and compared against representative viral genomes and outgroup viral genome sequences. Recombination breakpoints were identified based on observation of a cross-over of similarity against two different strains. Parental strains for each potential recombinant were confirmed by reconstructing phylogenies based on each non-recombinant region separated by breakpoints.

2.8. Evaluation of Antivirals in Plaque-Reduction Assays

The *in vitro* efficacy of the antivirals nitazoxanide (NTZ; Sapphire Bioscience, NSW, Australia), 2′-C-methylcytidine (2CMC; Sigma-Aldrich, St. Louis, MO, USA) and NITD-008 (In Vitro Technologies, VIC, Australia) against two FCV viruses isolated from cases of severe FCV-VSD, and the F9 vaccine strain, was evaluated using plaque-reduction assays, as previously described [14]. Briefly, NTZ, 2CMC and NITD-008 were dissolved in 100% dimethyl sulphoxide (DMSO) and the stock solutions (10 mM) were aliquoted and stored at $-20\,^{\circ}$C. CRFK monolayers (8×10^5 cells/well) in 6-well plates were inoculated with 80 plaque forming units (pfu) of FCV for 1 h at 37 $^{\circ}$C, followed by the addition of semisolid agarose overlays containing different concentrations of each antiviral in triplicate. After 24 h incubation, cells were fixed and stained with crystal violet, and plaque numbers

were determined for each treatment well. DMSO vehicle control was defined as having maximal viral infectivity. At least two independent experiments were performed for each treatment, with results presented as the mean with standard error of the mean (SEM). The therapeutic index was calculated from the half-maximal efficacy concentration (EC_{50}) and half-maximal cytotoxic concentration in CRFK cells (CC_{50}). The EC_{50} and CC_{50} were assessed as previously described [14]. The therapeutic index was then calculated ($TI = CC_{50}/EC_{50}$).

3. Results

3.1. Clinical and Epidemiological Descriptions of Outbreaks

In total, 23 cases of FCV-VSD were identified, including seven cases from Outbreak 1 (NSW_3 to NSW_9; Table 1), 12 from Outbreak 2 (QLD_1 to QLD_12; Table 2) and four from Outbreak 3 (ACT_4 to ACT_6 and ACT_9; Table 3). Patients ranged in age from 5 weeks to 8 years (median 12 months). In all, 22 of the 23 cases had been presented to the veterinary hospital involved in the outbreak for surgical procedures or consultations within the previous 14 days (*n* = 17) or were household contacts of such (*n* = 5; QLD_8, QLD_11, ACT_4, ACT_7, ACT_9; Tables 2 and 3). In one case, the source of exposure was not identified (NSW_6, Table 1). The median time from exposure to the onset of clinical signs was 7 days (range 2 to 14 days). FCV vaccination status was known in 21 cases and was complete in 19 and incomplete in one, while one cat was unvaccinated. The overall mortality rate was 9/23 (39%) and was highest in Outbreak 1, 6/7 (86%), intermediate in Outbreak 2 (3/12, 25%) and zero in Outbreak 3 (0/4, 0%). Hospitalised patients were treated with supportive treatment, including intravenous fluids and analgesia. The duration of the outbreaks was 4 to 6 weeks with no spread beyond the hospital identified in each outbreak.

Index cases were identified in Outbreaks 1 and 3. Outbreak 1 occurred after two unrelated rescue cats (NSW_1 and NSW_2) were hospitalised with signs of FCV-URTD, including lameness (Table 1). Outbreak 3 occurred after a cat with signs of FCV-URTD, including lameness, was admitted to hospital shortly after being adopted from a shelter (ACT_1, Table 3). Its littermate, also had signs of FCV-URTD (ACT_2, Table 3). No index case was identified for Outbreak 2, but the hospital at the centre of the outbreak was noted to service a large on-site animal shelter.

3.2. Histology and Immunohistochemistry

A post-mortem examination was performed on case QLD_4 from Outbreak 2. Diagnostic oropharyngeal swabs submitted antemortem to a commercial laboratory tested positive for FCV on qPCR, and negative for FHV-1. At post-mortem, diffuse oedema of the head, including the conjunctivae, and generalised subcutaneous oedema of the body were noted. Low-volume serosanguinous pleural (60 mL), abdominal (8 mL) and pericardial (2 mL) effusions were present, and the tissues of the mesentery were icteric. On histopathology, a fibrinonecrotising interstitial pneumonia, diffuse piecemeal hepatic necrosis and palpebral epidermal necrosis with suppurative adnexal dermatitis were described. No bacteria were isolated on aerobic and anaerobic culture of the effusion. FCV antigen was not detected on immunohistochemistry of sections of liver.

3.3. Virus Isolation and Genome Assembly

Liver and lung samples (*n* = 5) from both cases sampled in Outbreak 1 were culture positive for FCV, showing CPEs within 24 h and testing positive on RT-PCR assays for FCV (Table 1). From Outbreaks 2 and 3, 8/9 and 5/5 cases, respectively, were positive for FCV with CPEs detected within 36 to 72 h (Tables 2 and 3). RNA extracts from 15 virus cultures were submitted for WGS (Tables 1–3) and whole FCV genomes were assembled (Tables 1–3).

Table 1. Case details of cases of suspected FCV-VSD in Outbreak 1 in New South Wales (NSW) in 2015 and the suspected cases of origin (NSW_1 and NSW_2), disease phenotype, time until first appearance of cytopathic effects (CPEs) in viral culture, duration of illness and outcome.

Case	Date in 2015	Breed, Sex	Age	Origin	Vacc. Status	Exposure History and Clinical Signs	Disease Phenotype	CPEs	Duration of Illness	Outcome
NSW_1 Index case	15/11	DSH F	1.5 m	MCH	Unvacc.	Index case URT signs, lameness.	URTD	N/A	2 d	R
NSW_2 Index case	15/11	DSH F	1.5 m	MCH	Unvacc.	Index case URT signs, lameness.	URTD	N/A	4 d	R
NSW_3	02/12	DSH F	4 m	SCH	Unknown	Pyrexia, lethargy, bilateral forelimb oedema, jaundice. Onset of CS 2 days after a surgical procedure (hindlimb amputation).	VSD	N/A	4 d	D
NSW_4	06/12	DSH M	1.25 m	SCH	Unvacc.	Pyrexia, lethargy, facial and forelimb oedema. Onset of CS 7 days after a surgical procedure (abscess drainage).	VSD	N/A	5 d	D
NSW_5 [1,2,3]	07/12	DSH FN	6 y	SCH	Incomp.	Pyrexia, multiple limb oedema, jaundice. Onset of CS 4 days after a surgical procedure (abscess drainage).	VSD	24 h	7 d	D
NSW_6	09/12	DSH MN	1 y	SCH	Complete	Pyrexia, forelimb oedema. Onset of CS 4 days after a surgical procedure (abscess drainage).	VSD	N/A	9 d	R
NSW_7	14/12	DSH M	2 y	MCH	Complete	Pyrexia, facial and forelimb oedema, oral ulcers.	VSD	N/A	2 d	E
NSW_8	14/12	DSH FN	3 y	SCH	Complete	Pyrexia, facial oedema. Onset of CS 5 days after a surgical procedure (jaw fracture repair).	VSD	N/A	1 d	E
NSW_9 [1,2]	18/12	DSH F	1.5 m	MCH	Unknown	Pyrexia, facial oedema. Onset of CS 4 days after a surgical procedure (for intestinal intussusception).	VSD	24 h	1 d	E

[1] Samples collected for viral culture. [2] Whole-genome sequencing performed. [3] Isolate NSW_5_V1 was tested against 3 antiviral agents in vitro (Figure 4). CS, clinical signs; d, days; D, died; DSH, domestic shorthair; E, euthanised; F, female; FN, female neutered; Incomp., incomplete; m, months; M, male; MN, male neutered; MCH, multicat household; N/A, not applicable; R, recovered; SCH, single-cat household; Unvacc., unvaccinated; URTD, upper respiratory tract disease; Vacc., vaccinated; VSD, virulent systemic disease; y, years.

Table 2. Case details of cases of suspected FCV-VSD in Outbreak 2 in Queensland (QLD) in 2017 and the suspected cases of origin (NSW_1 and NSW_2), disease phenotype, time until first appearance of cytopathic effects (CPEs) in viral culture, duration of illness and outcome.

Case	Date in 2017	Breed, Sex	Age	Origin	Vacc. Status	Exposure History and Clinical Signs (CS)	Disease Phenotype	CPEs	Duration of Illness	Outcome
QLD_1	28/08	DSH FN	3 y	MCH	Complete	Acute respiratory effort, jaundice. Onset of CS 5 days after a surgical procedure (neutering).	VSD	N/A	2 d	D
QLD_2	30/08	DSH SCH	1 y	SCH	Complete	URT signs, facial oedema, oral ulcers. Onset of CS 5 days after a surgical procedure (neutering).	VSD	N/A	9 d	R
QLD_3	06/09	DSH MN	4 y	SCH	Complete	Pyrexia, jaundice, facial/limb oedema. Onset of CS 7 days after a surgical procedure (abscess drainage).	VSD	N/A	13 d	R
QLD_4	25/9	DSH FN	10 m	SCH	Complete	Pyrexia, facial/limb oedema, jaundice, dyspnoea. Onset of CS 4 days after a surgical procedure (neutering).	VSD	N/A	6 d	E
QLD_5 [*,1,2]	05/10	DSH MN	1 y	MCH	Complete	Pyrexia, facial/limb oedema, jaundice, oral/skin ulcers. Onset of CS 9 days after a surgical procedure (limb amputation).	VSD	48 h	6 d	R
QLD_6 [**,1,2]	06/10	DSH FN	1 y	MCH	Complete	Lameness, limb oedema, oral ulcers, elevated bilirubin. Onset of CS 7 days after a surgical procedure (neutering).	VSD	48 h	6 d	R
QLD_7 [**,1]	09/10	DSH FN	1 y	MCH	Complete	Pyrexia, inappetence, limb oedema, elevated bilirubin. Onset of CS 10 days after a surgical procedure (neutering).	VSD	72 h	10 d	R
QLD_8 [*,1,2]	09/10	DSH MN	2 y	MCH	Complete	Pyrexia, inappetence, facia/limb oedema, oral ulcers, nasal discharge, sneezing. Household contact of QLD_5.	VSD	48 h	7 d	R
QLD_9 [***,1,2,3]	09/10	DSH FN	1 y	MCH	Complete	Pyrexia, anorexia, limb oedema, nasal discharge, dyspnoea, jaundice. Onset of CS 11 days after a surgical procedure (neutering).	VSD	36 h	8 d	R
QLD_10 [***,1,2]	09/10	DSH FN	1 y	MCH	Complete	Pyrexia, nasal discharge, facial/limb oedema. Onset of CS 11 days after a surgical procedure (neutering).	VSD	36 h	6 d	R

270

Table 2. *Cont.*

Case	Date in 2017	Breed, Sex	Age	Origin	Vacc. Status	Exposure History and Clinical Signs (CS)	Disease Phenotype	CPEs	Duration of Illness	Outcome
QLD_11 ***,1	09/10	DSH FN	3 y	MCH	Complete	Pyrexia, facial/limb oedema, jaundice, nasal discharge, hypothermia. Household contact of QLD_9 and QLD_10.	VSD	72 h	6 d	E
QLD_12 1,2,3	03/10	DSH FN	6 y	MCH	Complete	Pyrexia, anorexia, limb oedema, elevated bilirubin. Onset of CS 5 days after treatment for brown snake envenomation.	VSD	36 h	4 d	R
QLD_13 1,2	15/10	Unkn.	N/A	MCH	Unkn.	Adult stray cat from a colony, oral ulcers.	URTD	N/A	Unkn.	Unkn.

* Same household; ** same household; *** same household. [1] Samples collected for viral culture. [2] Whole-genome sequencing performed. [3] Isolates QLD_9 and QLD-12 were tested against 3 antiviral agents in vitro (Figure 4). CS, clinical signs; D, died; DSH, domestic shorthair; E euthanised; F, female; FN, female neutered; Incomp., incomplete; m, months; M, male; MN, male neutered; MCH, multicat household; N/A, not applicable; R, recovered; SCH, single-cat household; Unkn., unknown; Unvacc., unvaccinated; URTD, upper respiratory tract disease; Vacc., vaccinated; VSD, virulent systemic disease; y, years.

Table 3. Case details of cases of suspected FCV-VSD in Outbreak 3 in the Australian Capital Territory (ACT) in 2018 and the suspected case of origin, disease phenotype, time until first appearance of cytopathic effects (CPEs) in viral culture, duration of illness and outcome.

Case	Date in 2018	Breed, Sex	Age	Origin	Vacc. Status	Exposure History and Clinical Signs (CS)	Disease Phenotype	CPEs	Duration of Illness	Outcome
ACT_1 **,1,2 Index case	22/01	DSH FN	4 m	MCH	Incomp.	Fever, inappetence, lameness, polyarthropathy. Adopted from a shelter.	URTD	36 h	14 d	R
ACT_2 **,1,2 Index case	22/01	DSH MN	4 m	MCH	Incomp.	Fever, lethargy, sneezing. Adopted from a shelter.	URTD	36 h	14 d	R
ACT_3 ****,1,2	23/01	DSH M	10 y	MCH	Unvacc.	No CS. Adopted from a rescue society. Presented on 23/01 for a dental procedure.	Asympt.	60 h	N/A	N/A
ACT_4 ****	30/01	DSH FN	5 y	MCH	Complete	Fever, pain on abdominal palpation, limb oedema, myopathy, creatine kinase 20,206 U/L (RR < 261); AST 487 U/L, (RR < 60), myoglobinuria. Indoor cat co-housed with ACT_3. Onset of CS 7 days after ACT_3 had a dental procedure.	VSD	N/A	9 d	R
ACT_5	02/02	DSH MN	8 y	MCH	Complete	Fever, inappetence, hypersalivation, jaundice, lumbar muscle pain, facial/limb oedema, ulcerated nasal planum. Onset of CS 4 days after a dental procedure.	VSD	N/A	21 d	R

Table 3. *Cont.*

Case	Date in 2018	Breed, Sex	Age	Origin	Vacc. Status	Exposure History and Clinical Signs (CS)	Disease Phenotype	CPEs	Duration of Illness	Outcome
ACT_6 ***	07/02	DSH FN	5 y	MCH	Complete	Vomiting, fever, painful kidneys on abdominal palpation, marked facial and limb oedema (all limbs), subcutaneous oedema of flanks, oral ulcers, swollen nose. Onset of CS 14 days after dental check-up.	VSD	N/A	10 d	R
ACT_7 *,1,2	08/02	Maine Coon MN	10 m	MCH	Complete	Fever, inappetence, oral ulcers. Onset of CS 8 days after ACT_8 had a dental procedure.	URTD	48 h	7 d	R
ACT_8 *	08/02	DSH MN	15 y	MCH	Unknown	Fever, inappetence, nasal planum ulcers. Onset of CS 8 days after being admitted to the hospital for a dental procedure.	URTD		12 d	R
ACT_9 ***,1,2	14/02	Ragdoll cross MN	4 y	MCH	Comp.	Fever, inappetence, lethargy, facial/limb oedema, swollen nose. Indoor cat co-housed with ACT-6.	VSD	36 h	7 d	R

* From same household; ** from same household; *** from same household. **** from same household [1] Samples collected for viral culture. [2] Whole-genome sequencing performed. Comp., complete; CS, clinical signs; D, died; DSH, domestic shorthair; E, euthanised; F, female; FN, female neutered; Incomp., incomplete; M, male; MN, male neutered; MCH, multicat household; N/A, not applicable; R, recovered; SCH, single-cat household; Unvacc., unvaccinated; URTD, upper respiratory tract disease; Vacc., vaccinated; VSD, virulent systemic disease; wks, weeks; y, years.

3.4. Metagenomic, Amino-Acid and Recombination Analyses

From the 14 RNA library preparations, RNA sequencing produced median read counts per library after filtering of 126,025,385 (range 83,299,626 to 145,687,464) (Table S1). The median number of contigs per library was 32,127 (range 1860 to 891,879), and the median number of reads mapped per library was 3,213,060 (range 152,719 to 220,862,249). Fifteen whole FCV genomes were assembled from this data (GenBank accession numbers MW880757–MW880771, Figure 1, Table S1).

Phylogenetic analysis of the whole FCV genomes generated revealed that the three outbreaks were caused by five independent lineages (Figure 1). Outbreak 1 was associated with the co-circulation of two viruses of phylogenetically distinct lineages with a nucleotide identity of 80.25% (V1, in NSW_5 and NSW_9; V2 in NSW_5 and NSW_9). In Outbreak 2, FCV-VSD viruses were highly conserved genetically, with a nt identity of >99.84%. A virus isolated from a cat with URTD (QLD_13) from a different facility to that where Outbreak 2 was reported was more closely related to the Outbreak 2 viruses (98.85% nt identity) than to other Australian FCV viruses (Figure 1). In Outbreak 3, one FCV-VSD case (ACT_9) and two FCV-URTD cases (ACT_1 and 7) were identified that shared >99.73% nt genomic identity. Interestingly, a virus (strain ACT_3) cultured from an asymptomatic cat co-housed with an FCV-VSD case was most closely related to the outbreak virus (98.69% nt identity, Figure 1). Nevertheless, an FCV-URTD virus (strain ACT_2) from a cat co-housed with the index case (ACT_1, Table 3) and recently adopted from a shelter was from a different lineage than the FCV-VSD viruses from Outbreak 3 (67.16% nt identity). Instead, it clustered with strains NSW_5 and 9 from Outbreak 1, but with only a distant relationship (82.67% nt identity).

Collectively, viruses identified from the three outbreaks formed a monophyletic cluster (i.e., shared a common ancestor) that was distinguished from previously described viruses based on the full-genome phylogeny (Figure 1). However, the phylogeny based on the VP1 gene alone suggested two separate clusters: (i) one was associated with Outbreak 2 virus sequences alone and distantly grouped with viruses from China, Germany and Australia, and (ii) a second cluster was associated with the remainder of the outbreaks studied here as well as an Australian virus strain (182cvs5A) identified from a cat with URTD in 1980. Of note, we did not observe any clustering of viruses from cats with different clinical presentations (VSD, URTD) or from asymptomatic cats in the phylogeny. Indeed, it was striking that even among highly identical sequences (>98.65% nucleotide identity), namely ACT_1, ACT_3, ACT_7 and ACT_9, different presentations (URTD, VSD, asymptomatic) were observed. These results suggest that there is no clear association between disease severity and virus genetic background, although this needs to be assessed with more data.

On residue mapping of the hypervariable region E of FCVs from Outbreak 1, one sequence type (NSW5_V1 and NSW9_V1) exhibited the proposed VSD-like pattern [17], whilst the other sequence type (NSW5_V2 and NSW5_V2) showed an intermediate configuration between the proposed pattern described for VSD and respiratory pathotypes (Table 4 and Figure 2). The FCV sequences from Outbreak 2 (QLD) had a residue pattern described by Brunet et al. [17] to be characteristic of the respiratory pathotype, while viruses from Outbreak 3 (ACT) had an intermediate configuration between the pattern described for VSD and respiratory pathotypes (Table 4, grey-shaded cells, and Figure 2).
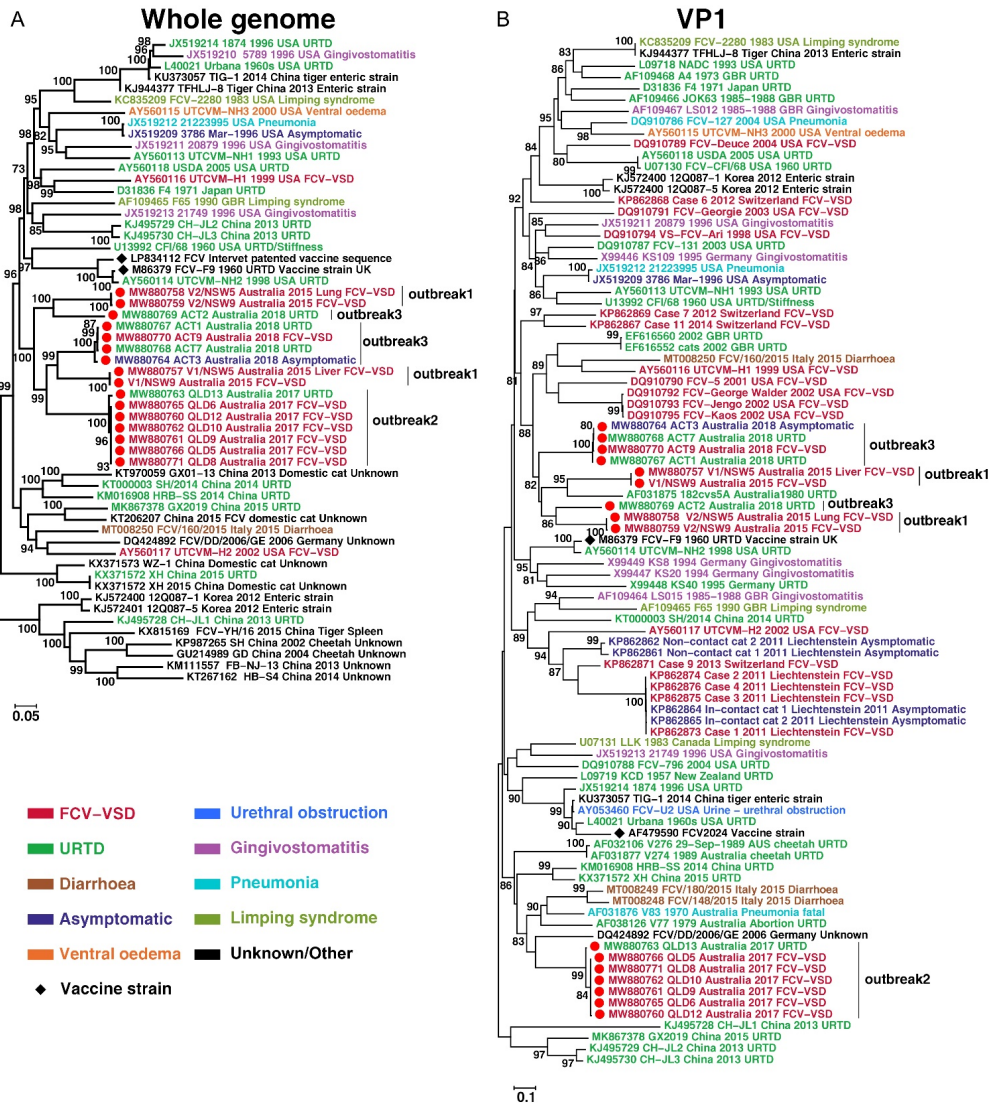
Figure 1. Evolutionary history of viruses discovered in this study. Maximum-likelihood trees were reconstructed based on (**A**) Whole-genome and (**B**) partial VP1 gene alignments, which included virus sequences obtained in this study (marked with solid red circles) as well as those obtained from the GenBank. The trees were mid-point rooted and bootstrap values of ≥70% are marked on the tree. Each sequence name contains the accession number, strain name, geographic location, host and isolation year, if available. Disease phenotype is colour coded.
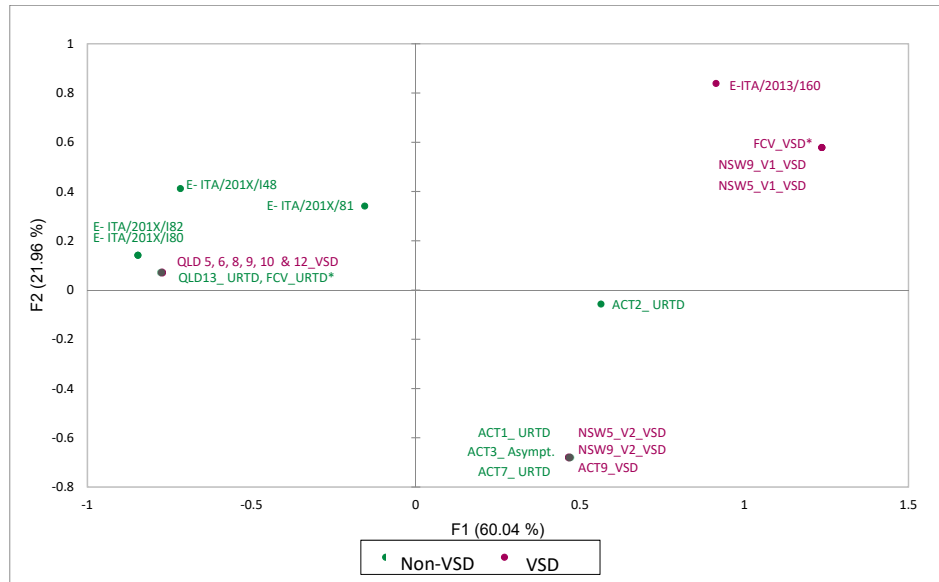
Figure 2. Multiple correspondence analysis (MCA) graph depicting the results of MCA of 13 physical and chemical categorical variables of 7 amino-acid residues of the hypervariable E region of VSD and non-VSD FCV strains from Table 4. * Most common amino-acid configuration of FCV_VSD and FCV_URTD reference strains (see Table 4); E-ITA, enteric FCV strains (see Table 4).

The Australian strains identified in this study also contained multiple signals for recombination, although no close parental strains were identified. Based on similarity plots and phylogenetic analyses, the strongest recombination signal was observed in strain "ACT_2": in 1–3989 bp of the genome alignment it clustered with two viruses from Outbreak 1 (V2/NSW_5 and 9), whereas for the rest of the genome it was with the other two viruses from Outbreak 1 (V1/NSW5 and 9) group (Figure 3). Other groups such as the one containing Outbreak 2 strains (QLD_5–6, 9–10 and 12–13) were also subject to alternative grouping in the phylogenetic analyses, although no close parental strains could be identified (Figure 3).

3.5. Antiviral Compound Efficacy

The EC_{50} values obtained for NTZ, 2CMC and NITD-008 tested against three FCV-VSD viruses from two of the outbreaks (NSW5_V1, QLD_9, QLD_12; Tables 2 and 3), and from the F9 vaccine virus varied from 0.4 to 0.6 μM (0.1 to 0.2 μg/mL), 2.6 to 5.3 μM and 0.5 to 0.9 μM, respectively (Figure 4). NTZ showed a half-maximal cytotoxic concentration (CC_{50}) value of 12.7 μM, whilst 2CMC and NITD-008 demonstrated CC_{50} values of >100 μM [14,15]. Therefore, using the higher EC_{50} values obtained for each compound, the therapeutic index (TI = CC50/EC50) values determined for NTZ, 2CMC and NITD-008 were 21, >18 and >111, respectively (Figure 4).

Table 4. Amino-acid residues from the E region of feline caliciviruses including regions with high variability 426–460 (N-HV portion) and 490–523 (C-HV portion), separated by a less-variable region (aa 461–489) (Brunet et al., 2019).

Strain	Amino-Acid Residues and Physico-Chemical Properties Associated with VSD Pathotype						
	438 Hydrophobic, Aliphatic ILV	**440** Non-Small EFHKIL MQRWY	**448** Polar, Positive Charge HKR	**452** Non-Small EFHKIL MQRWY	**455** Non-Negative All Except DE	**465** Polar DEHKN QRSTWI	**492** Small ADGNP STV
FCV-VSD	V_9T_7 (9)	$Q_6G_4E_4SK$ (11)	$K_7A_2E_27$ (7)	$E_{11}D_6$ (11)	$T_6D_3M_2I_2NES$ (12)	$S_{14}G_3$ (14)	$V_{16}R$ (16)
FCV-URTD	$T_{37}V_2I$	$G_{22}S_6Q_4R_2A_2END$	$A_{30}P_4G_3K_3$	$D_{36}E_3N$	$D_{28}T_5S_3G_2VR$	$G_{26}S_{14}$	$V_{17}L_8I_6R_5K_2$
E-ITA/2013/160	V	Q	R	E	T	G	V
E-FCV ITA others	T_3V_{11}	G_2SR	A_4	D_4	D_3E	G_3S	L_3V_2
E-ITA/201X/81	V	S	A	D	E	S	V
E-ITA/201X/I48	T	R	A	D	D	G	L
E-ITA/201X/I80	T	G	A	D	D	G	L
E-ITA/201X/I82	T	G	A	D	D	G	L
ACT7_URTD	T	G	**K**	**E**	D	**S**	**V**
ACT9_VSD	T	G	**K**	**E**	D	**S**	**V**
ACT1_URTD	T	G	**K**	**E**	D	**S**	**V**
ACT3_Asympt.	T	G	**K**	**E**	D	**S**	**V**
ACT2_URTD	T	G	**R**	**E**	**N**	**S**	I
QLD13_URTD	T	G	A	D	D	G	**V**
QLD8_VSD	T	G	A	D	D	G	**V**
QLD 5_VSD	T	G	A	D	D	G	**V**
QLD6_VSD	T	G	A	D	D	G	**V**
QLD9_VSD	T	G	A	D	D	G	**V**
QLD10_VSD	T	G	A	D	D	G	**V**
QLD12_VSD	T	G	A	D	D	G	**V**
NSW5_V1_VSD	**V**	**Q**	**K**	**E**	**I**	**S**	**V**
NSW9_V1_VSD	**V**	**Q**	**K**	**E**	**I**	**S**	**V**
NSW5_V2_VSD	T	S	**K**	**E**	D	**S**	**V**
NSW9_V2_VSD	T	S	**K**	**E**	D	**S**	**V**

A (blue): hydrophobic small; V (blue): hydrophobic aliphatic small; I (blue): hydrophobic aliphatic; M (blue): hydrophobic. T (green): hydrophobic polar small; S (green): polar small; Q (green): polar. D (pink): polar small charge -ve; E (pink): polar charge -ve. K (red): hydrophobic polar charge +ve; R (red): polar charge +ve. G: hydrophobic small. VSD, virulent strains; R, respiratory strains; E-ITA, enteric strains from cats with diarrhoea. Grey-shaded cells in the table with bolded font correspond to amino-acids of strains in this study with the predicted properties of VSD strains according to Brunet et al., 2019 [17].
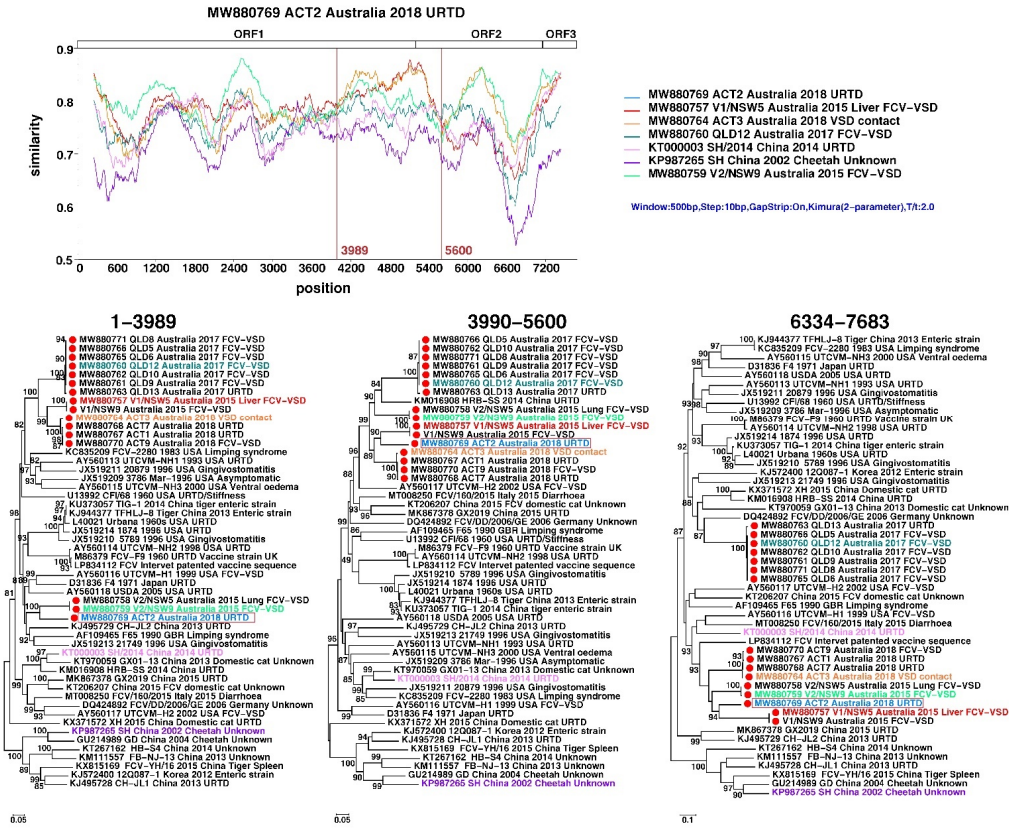
Figure 3. Recombination analyses of Australian FCV strains identified in this study. The top panel shows similarity comparisons of ACT2 against representative FCV strains across the entire genome using a sliding window (window size: 500 bp, step size: 10 bp). The potential recombination breakpoints are shown as red vertical lines. The bottom panel shows phylogenetic trees based on each non-recombinant region separated by recombination breakpoints. The strain names are labelled with different colours to mark the representative strains used in SimPlot analyses, including the parental groups for the recombinants.
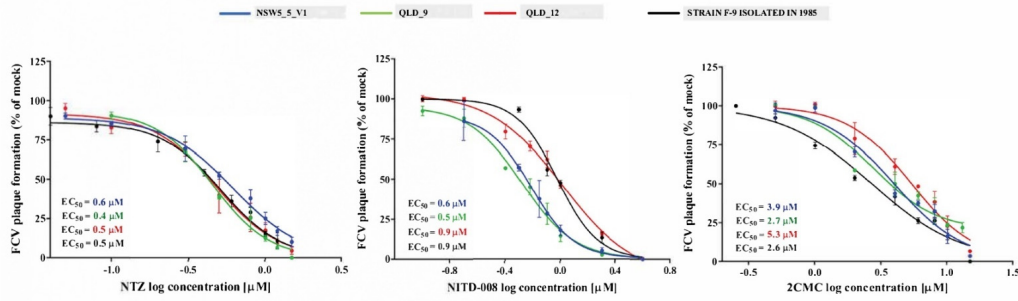
Figure 4. The antiviral activity of nitazoxanide (NTZ), NITD-008 and 2′-C-methylcytidine (2CMC) against four FCV strains in cell culture. The EC_{50} values of the three compounds against each of FCV strain were calculated by fitting the dose–response curves from a plaque reduction assay. Triplicate values from at least two independent experiments are presented, and the mean ± SEM are shown.

4. Discussion

This study documents the first epizootics of virulent systemic disease caused by FCV in Australia, although the association of FCVs with non-epizootic, atypical signs such as sudden death [24,25], jaundice [26] or severe ulcerative swelling of the footpads [27] was first described in Australia more than 20 years before FCV-VSD was reported in the U.S. [6]. Many features of the FCV-VSD outbreaks reported here resemble those reported in the U.S. [6,7,13,28], Europe [8,29] and the UK [30], including their nosocomial nature, the spectrum of clinical signs, outbreak duration of 4 to 6 weeks, absence of community transmission outside the affected hospital and, with 76% of affected cats being completely vaccinated, a non-protective effect of vaccination [6,8,28]. We also found no association between vaccination status and mortality. In Outbreak 1 in NSW, the only outbreak that involved unvaccinated cats, the proportion of unvaccinated or incompletely vaccinated cats that died was the same as that for vaccinated cats. Overall, the median time from exposure to the onset of clinical signs was longer (7 days) than in previous reports (4 to 4.5 days) [28,29]. However, the range was similar (from 1 to 14 days), supporting a minimum of 14 days quarantine for cats exposed during an outbreak.

The epidemiological and phylogenetic results of our study provide further evidence that any virus mutations responsible for the VSD phenotype arise de novo within multicat environments, in which persistent FCV infections are common and multiple FCV strains are circulating [7,28,30,31]. The strongest support comes from Outbreak 1, where the veterinary hospital routinely accepted unvaccinated rescued kittens and cats for rehoming that were subsequently housed together, with frequent mixing of kittens from different litters. The index cases, two unrelated 6-week-old kittens (NSW_1 and 2, Table 1) that developed an acute febrile illness and lameness one week before the FCV-VSD outbreak had been in the hospital from 2 weeks of age. Two other 6-week-old kittens that succumbed to FCV-VSD had been born in the hospital.

Notably, the viruses in each of the outbreaks were genetically distinct, did not cluster phylogenetically with other FCV-VSD viruses from previous outbreaks (Figure 1) and had no defining identifiable genomic mutations. This suggests extended in situ evolution in Australia of the viruses responsible for these outbreaks. Our study also confirmed the presence of high genetic diversity among FCV-VSD outbreak strains, which were present in multiple different clades, as has been previously described in other locations [28,31,32]. In general, only viruses sharing immediate temporal or spatial links, clustered together.

Analysis of amino acids from the hypervariable E region of the capsid in the cultured viruses did not support the hypothesis that the properties of the seven specific residues can reliably differentiate respiratory from virulent FCV pathotypes [17]. Indeed, the properties

expected to be predictive of a virulent pathotype were present in all seven residues from only two viruses isolated from liver tissue of two FCV-VSD cases in Outbreak 1. A second FCV-virus, isolated from the lungs of the same cats, had these predicted properties in four of the seven residues. It is not possible to determine whether one or both strains were responsible for the observed FCV-VSD phenotype. We cannot exclude the possibility of cross-contamination during sample collection at post-mortem.

In contrast, even though the clinical presentation in Outbreak 2 was typical of FCV-VSD with all cases exhibiting head or limb oedema, or jaundice, viruses from these cats had properties predictive of the virulent pathotype in only one of the seven residues. All viruses sequenced from cats in Outbreak 2 with the virulent pathotype were highly conserved, representing a unique FCV strain causing the outbreak. In Outbreak 3, near identical viruses (99.9% nucleotide identity) were isolated from four cats from different households with phenotypes ranging from asymptomatic, to URTD to VSD. The predicted properties for the virulent pathotype were present in four of the seven hypervariable E region amino-acid residue positions. We also analysed several FCV strains isolated from several cats with diarrhoea, of which one had the predicted properties for the virulent pathotype in all seven residues, whilst the others clustered more closely with the typical FCV-URTD pathotype and Outbreak 2 virulent and non-virulent strains on the MCA (Figure 2).

Whilst highly contagious, FCV strains responsible for VSD do not cause clinical disease in all cats, as was seen here in Outbreak 2, and in a previously reported outbreak in the U.S. [7]. Many factors can influence disease phenotype including route of exposure and dose of the infecting virus, as well as age, vaccination and immune status of the host [5]. In addition, there is a spectrum of virulence among FCV strains, rather than two clearly delineated groups of FCV-URTD and FCV-VSD as demonstrated by the identification of non-epizootic forms of FCV-infection from Switzerland, Lichtenstein, the UK and Italy with clinical disease resembling VSD [9,33,34]. Previous investigations to determine a role for co-pathogens are limited to transmission electron microscopy, where only virions with a morphology consistent with FCV were identified [13], or specific PCRs testing for feline parvovirus (FPV), feline herpesvirus-1, feline immunodeficiency virus and feline leukaemia virus [11]. In Italy, three cats from three separate FCV-VSD outbreaks were all co-infected with FPV [11], leading to speculation that FPV-associated immunosuppression may have facilitated systemic spread of low-virulence FCVs or the emergence of virulent FCVs. Concurrent immunosuppression could explain the finding of an FCV-URTD pathotype in Outbreak 2, despite strong evidence of an FCV-VSD phenotype. Future investigations to clarify the potential role of co-pathogens in FCV-VSD are warranted. Other factors implicated in the pathogenesis of VSD include host factors, the presence of viraemia [35], higher viral tissue loads [8] and broader tissue tropism of the virulent pathotype compared to the respiratory pathotype [6,8,9,28,30,33].

FCV was isolated from tissues of cats with FCV-VSD from Outbreak 1 and from oropharyngeal/conjunctival swabs collected prospectively from cats in Outbreaks 2 and 3. Since none of the swab-sampled cats died, it was not possible to culture virus from their tissues. The seven viruses isolated from cats in Outbreak 2 with severe clinical signs characteristic of VSD were identical or near identical and were considered representative of the VSD phenotype.

There is limited information regarding of the efficacy and safety of antiviral compounds against FCV-VSD strains. Accordingly, we investigated the in vitro efficacy of three antiviral compounds (NTZ, 2CMC, NITD-008) against representative strains of FCV-VSD. One isolate (NSW_5_V1) was in a different phylogenetic cluster to the other two (QLD_9 and 12), The NSW isolate had the hypervariable E region residue properties attributed to FCV-VSD pathotypes in the study of Brunet et al. [17], while the QLD isolates had residue properties typical of the FCV-URTD pathotype. These three antiviral molecules showed dose–response inhibition against the replication of FCV-VSD strains at low micromolar concentrations. Nucleoside analogues, 2CMC and NITD-008, inhibit the viral RNA-dependent RNA polymerase. Although the in vitro therapeutic index of 2CMC in

our study suggests it would be the safest of the three for treatment of FCV-VSD, clinical development of its 3′-valyl ester oral prodrug valopicitabine was halted in people because of adverse gastrointestinal effects [36]. Similarly, although NITD008 has exhibited in vitro efficacy against human and animal caliciviruses, adverse effects including weight loss, lethargy, nausea and diarrhoea occurred in dogs administered the drug intravenously for 2 weeks [37]. Nitazoxanide (NTZ) is a nitrothiazole benzamide compound approved by the U.S. Food and Drug Administration (FDA) for oral treatment of protozoal infections [38]. Its antiviral activity was discovered serendipitously during treatment of cryptosporidiosis (a parasitic disease) in patients with HIV-AIDS [39]. Since then, NTZ and its active circulating metabolite, tizoxanide, have been shown to have antiviral activity against a broad range of DNA and RNA viruses including hepatitis B, hepatitis C and influenza A virus [40]. By uncoupling oxidative phosphorylation, NTZ and tizoxanide inhibit mitochondrial activity, decreasing cellular ATP and thus inhibiting viral replication. NTZ also targets key viral proteins such as the haemagglutinin of influenza A virus and suppresses the secretion of proinflammatory cytokines [40]. It has both in vitro and in vivo efficacy in cats experimentally infected with FCV-URTD strains, and was well tolerated at dose rates from 5 to 20 mg/kg/day orally [41]. Higher dose rates (75 mg/kg/day) in cats cause vomiting and diarrhoea [42]. Based on our data, NTZ could be considered as a treatment option for FCV-VSD given its in vitro efficacy against the prototype vaccine F9 strain isolated in 1958 and contemporaneous isolates of FCV-VSD. Although the therapeutic index for NTZ (TI = 21) calculated in our study suggests it is selective, randomised controlled study in cats should be performed to further evaluate efficacy and safety in vivo.

5. Conclusions

FCV-VSD is a clinical diagnosis that can occur in cats worldwide. The trigger(s) for this severe disease syndrome remains (remain) elusive. Evaluation of the safety and efficacy of nitazoxanide as a specific treatment option for FCV-VSD is warranted.

Author Contributions: Conceptualisation, V.R.B., E.C.H., P.W., J.A.B. and M.B.; methodology, V.R.B., M.B., T.M.F., K.V.B., A.G.R., M.C., S.-J.L. and P.A.P.; software, M.S.; formal analysis, V.M., M.B., T.M.F., A.G.R. and M.S.; data curation, M.B., M.S. and V.R.B.; writing—original draft preparation, M.B.; writing—review and editing, T.M.F., K.V.B., A.G.R., M.C., S.-J.L., P.A.P., E.C.H., V.M., P.W., J.A.B. and M.S.; visualisation, M.S.; supervision, V.R.B., J.A.B., P.W., M.S. and E.C.H.; project administration, V.R.B. and M.B.; funding acquisition, J.A.B. and V.R.B. All authors have read and agreed to the published version of the manuscript.

Institutional Review Board Statement: The study was conducted according to the guidelines of the Declaration of Helsinki, and approved by the Animal Ethics Committee) of The University of Sydney (2016/1002; 17.05.2016).

Informed Consent Statement: Not applicable.

Data Availability Statement: The sequence data analysed in this project are publicly available on the BioProject database (Submission ID SUBID PRJNA768617 at https://www.ncbi.nlm.nih.gov/bioproject/768617, accessed on 12 August 2021).

Conflicts of Interest: The authors declare no conflict of interest. The funders had no role in the design of the study; in the collection, analyses, or interpretation of data; in the writing of the manuscript; or in the decision to publish the results.

References

1. Herbert, T.; Brierley, I.; Brown, T. Identification of a protein linked to the genomic and subgenomic mRNAs of feline calicivirus and its role in translation. *J. Gen. Virol.* **1997**, *78*, 1033–1040. [CrossRef]
2. Neill, J.D.; Mengeling, W.L. Further characterization of the virus-specific RNAs in feline calicivirus infected cells. *Virus Res.* **1988**, *11*, 59–72. [CrossRef]
3. Schaffer, F.; Ehresmann, D.; Fretz, M.; Soergel, M. A protein, VPg, covalently linked to 36S calicivirus RNA. *J. Gen. Virol.* **1980**, *47*, 215–220. [CrossRef]
4. Mitra, T.; Sosnovtsev, S.V.; Green, K.Y. Mutagenesis of tyrosine 24 in the VPg protein is lethal for feline calicivirus. *J. Virol.* **2004**, *78*, 4931–4935. [CrossRef]
5. Pesavento, P.A.; Chang, K.-O.; Parker, J.S. Molecular virology of feline calicivirus. *Vet. Clin. N. Am. Small Anim. Pract.* **2008**, *38*, 775–786. [CrossRef] [PubMed]
6. Pedersen, N.C.; Elliott, J.B.; Glasgow, A.; Poland, A.; Keel, K. An isolated epizootic of hemorrhagic-like fever in cats caused by a novel and highly virulent strain of feline calicivirus. *Vet. Microbiol.* **2000**, *73*, 281–300. [CrossRef]
7. Schorr-Evans, E.; Poland, A.; Johnson, W.; Pedersen, N.C. An epizootic of highly virulent feline calicivirus disease in a hospital setting in New England. *J. Feline Med. Surg.* **2003**, *5*, 217–226. [CrossRef]
8. Reynolds, B.S.; Poulet, H.; Pingret, J.L.; Jas, D.; Brunet, S.; Lemeter, C.; Etievant, M.; Boucraut-Baralon, C. A nosocomial outbreak of feline calicivirus associated virulent systemic disease in France. *J. Feline Med. Surg.* **2009**, *11*, 633–644. [CrossRef]
9. Battilani, M.; Vaccari, F.; Carelle, M.S.; Morandi, F.; Benazzi, C.; Kipar, A.; Dondi, F.; Scagliarini, A. Virulent feline calicivirus disease in a shelter in Italy: A case description. *Res. Vet. Sci.* **2013**, *95*, 283–290. [CrossRef]
10. Prikhodko, V.G.; Sandoval-Jaime, C.; Abente, E.J.; Bok, K.; Parra, G.I.; Rogozin, I.B.; Ostlund, E.N.; Green, K.Y.; Sosnovtsev, S.V. Genetic characterization of feline calicivirus strains associated with varying disease manifestations during an outbreak season in Missouri (1995–1996). *Virus Genes* **2014**, *48*, 96–110. [CrossRef]
11. Caringella, F.; Elia, G.; Decaro, N.; Martella, V.; Lanave, G.; Varello, K.; Catella, C.; Diakoudi, G.; Carelli, G.; Colaianni, M.L. Feline calicivirus infection in cats with virulent systemic disease, Italy. *Res. Vet. Sci.* **2019**, *124*, 46–51. [CrossRef]
12. Radford, A.D.; Coyne, K.P.; Dawson, S.; Porter, C.J.; Gaskell, R.M. Feline calicivirus. *Vet. Res.* **2007**, *38*, 319–335. [CrossRef]
13. Pesavento, P.A.; MacLachlan, N.J.; Dillard-Telm, L.; Grant, C.K.; Hurley, K.F. Pathologic, immunohistochemical, and electron microscopic findings in naturally occurring virulent systemic feline calicivirus infection in cats. *Vet. Pathol.* **2004**, *41*, 257–263. [CrossRef] [PubMed]
14. Fumian, T.M.; Tuipulotu, D.E.; Netzler, N.E.; Lun, J.H.; Russo, A.G.; Yan, G.J.; White, P.A. Potential therapeutic agents for feline calicivirus infection. *Viruses* **2018**, *10*, 433. [CrossRef] [PubMed]
15. Enosi Tuipulotu, D.; Fumian, T.M.; Netzler, N.E.; Mackenzie, J.M.; White, P.A. The adenosine analogue NITD008 has potent antiviral activity against human and animal caliciviruses. *Viruses* **2019**, *11*, 496. [CrossRef] [PubMed]
16. Foley, J.; Hurley, K.; Pesavento, P.A.; Poland, A.; Pedersen, N.C. Virulent systemic feline calicivirus infection: Local cytokine modulation and contribution of viral mutants. *J. Feline Med. Surg.* **2006**, *8*, 55–61. [CrossRef]
17. Brunet, S. Multiple Correspondence Analysis on amino acids properties within the variable region of the capsid protein shows differences between classical and virulent systemic Feline Calicivirus strains. *Viruses* **2019**, *11*, 1090. [CrossRef] [PubMed]
18. Coyne, K.P.; Gaskell, R.M.; Dawson, S.; Porter, C.J.; Radford, A.D. Evolutionary mechanisms of persistence and diversification of a calicivirus within endemically infected natural host populations. *J. Virol.* **2007**, *81*, 1961–1971. [CrossRef] [PubMed]
19. Li, D.; Liu, C.M.; Luo, R.; Sadakane, K.; Lam, T.W. MEGAHIT: An ultra-fast single-node solution for large and complex metagenomics assembly via succinct de Bruijn graph. *Bioinformatics* **2015**, *31*, 1674–1676. [CrossRef] [PubMed]
20. Guindon, S.; Dufayard, J.F.; Lefort, V.; Anisimova, M.; Hordijk, W.; Gascuel, O. New Algorithms and Methods to Estimate Maximum-Likelihood Phylogenies: Assessing the Performance of PhyML 3.0. *Syst. Biol.* **2010**, *59*, 307–321. [CrossRef]
21. Di Martino, B.; Lanave, G.; Di Profio, F.; Melegari, I.; Marsilio, F.; Camero, M.; Catella, C.; Capozza, P.; Bányai, K.; Barrs, V.R.; et al. Identification of feline calicivirus in cats with enteritis. *Transbound Emerg. Dis.* **2020**, *67*, 2579–2588. [CrossRef] [PubMed]
22. Katoh, K.; Standley, D.M. MAFFT multiple sequence alignment software version 7: Improvements in performance and usability. *Mol. Biol. Evol.* **2013**, *30*, 772–780. [CrossRef] [PubMed]
23. Lole, K.S.; Bollinger, R.C.; Paranjape, R.S.; Gadkari, D.; Kulkarni, S.S.; Novak, N.G.; Ingersoll, R.; Sheppard, H.W.; Ray, S.C. Full-length human immunodeficiency virus type 1 genomes from subtype C-infected seroconverters in India, with evidence of intersubtype recombination. *J. Virol.* **1999**, *73*, 152–160. [CrossRef] [PubMed]
24. Love, D.N.; Baker, K.D. Sudden death in kittens associated with a feline picornavirus. *Aust. Vet. J.* **1972**, *48*, 643. [CrossRef] [PubMed]
25. Love, D.N.; Zuber, R.M. Feline calicivirus associated with pyrexia, profound anorexia and oral and perianal ulceration in a cat. *Aust. Vet. Pract.* **1987**, *17*, 136–137.
26. Ellis, T.M. Jaundice in a Siamese cat with in utero feline calicivirus infection. *Aust. Vet. J.* **1981**, *57*, 383–385. [CrossRef]
27. Cooper, L.M.; Sabine, M. Paw and mouth disease in a cat. *Aust. Vet. J.* **1972**, *48*, 644. [CrossRef]
28. Hurley, K.F.; Pesavento, P.A.; Pedersen, N.C.; Poland, A.M.; Wilson, E.; Foley, J.E. An outbreak of virulent systemic feline calicivirus disease. *J. Am. Vet. Med. Assoc.* **2004**, *224*, 241–249. [CrossRef]
29. Deschamps, J.Y.; Topie, E.; Roux, F. Nosocomial feline calicivirus-associated virulent systemic disease in a veterinary emergency and critical care unit in France. *JFMS Open Rep.* **2015**, *1*, 2055116915621581. [CrossRef]

30. Coyne, K.; Jones, B.; Kipar, A.; Chantrey, J.; Porter, C.; Barber, P.; Dawson, S.; Gaskell, R.; Radford, A. Lethal outbreak of disease associated with feline calicivirus infection in cats. *Vet. Rec.* **2006**, *158*, 544–550. [CrossRef]

31. Ossiboff, R. Feline caliciviruses (FCVs) isolated from cats with virulent systemic disease possess in vitro phenotypes distinct from those of other FCV isolates. *J. Gen. Virol.* **2007**, *88*, 506–517. [CrossRef]

32. Coyne, K.P.; Dawson, S.; Radford, A.D.; Cripps, P.J.; Porter, C.J.; McCracken, C.M.; Gaskell, R.M. Long-Term analysis of feline calicivirus prevalence and viral shedding patterns in naturally infected colonies of domestic cats. *Vet. Microbiol.* **2006**, *118*, 12–25. [CrossRef]

33. Willi, B.; Spiri, A.M.; Meli, M.L.; Samman, A.; Hoffmann, K.; Sydler, T.; Cattori, V.; Graf, F.; Diserens, K.A.; Padrutt, I.; et al. Molecular characterization and virus neutralization patterns of severe, non-epizootic forms of feline calicivirus infections resembling virulent systemic disease in cats in Switzerland and in Liechtenstein. *Vet. Microbiol.* **2016**, *182*, 202–212. [CrossRef]

34. Meyer, A.; Kershaw, O.; Klopfleisch, R. Feline calicivirus-associated virulent systemic disease: Not necessarily a local epizootic problem. *Vet. Rec.* **2011**, *168*, 589. [CrossRef]

35. Brunet, S.; Jas, D.; David, F.; Bublot, M.; Poulet, H. Feline calicivirus: Vaccinations against virulent strains. In Proceedings of the Conference of the European Society of Veterinary Virology 2005: Comparative and Emerging Virus Infections of Dogs and Cats, Liverpool, UK, 20–22 June 2005.

36. Rocha-Pereira, J.; Jochmans, D.; Dallmeier, K.; Leyssen, P.; Cunha, R.; Costa, I.; Nascimento, M.; Neyts, J. Inhibition of norovirus replication by the nucleoside analogue 2′-C-methylcytidine. *Biochem. Biophys. Res. Commun.* **2012**, *427*, 796–800. [CrossRef]

37. Yin, Z.; Chen, Y.-L.; Schul, W.; Wang, Q.-Y.; Gu, F.; Duraiswamy, J.; Kondreddi, R.R.; Niyomrattanakit, P.; Lakshminarayana, S.B.; Goh, A. An adenosine nucleoside inhibitor of dengue virus. *Proc. Natl. Acad. Sci. USA* **2009**, *106*, 20435–20439. [CrossRef] [PubMed]

38. Hussar, D.A. New drugs of 2003. *J. Am. Pharm. Assoc.* **2004**, *44*, 168–210. [CrossRef] [PubMed]

39. Rossignol, J.F. Nitazoxanide in the treatment of acquired immune deficiency syndrome-related cryptosporidiosis: Results of the United States compassionate use program in 365 patients. *Aliment. Pharmacol. Ther.* **2006**, *24*, 887–894. [CrossRef]

40. Stachulski, A.V.; Rossignol, J.F.; Pate, S.; Taujanskas, J.; Robertson, C.M.; Aerts, R.; Pascal, E.; Piacentini, S.; Frazia, S.; Santoro, M.G.; et al. Synthesis, antiviral activity, preliminary pharmacokinetics and structural parameters of thiazolide amine salts. *Future Med. Chem.* **2021**. [CrossRef] [PubMed]

41. Cui, Z.; Li, D.; Xie, Y.; Wang, K.; Zhang, Y.; Li, G.; Zhang, Q.; Chen, X.; Teng, Y.; Zhao, S. Nitazoxanide protects cats from feline calicivirus infection and acts synergistically with mizoribine in vitro. *Antivir. Res.* **2020**, *182*, 104827. [CrossRef] [PubMed]

42. Gookin, J.L.; Levy, M.G.; Law, J.M.; Papich, M.G.; Poore, M.F.; Breitschwerdt, E.B. Experimental infection of cats with Tritrichomonas foetus. *Am. J. Vet. Res.* **2001**, *62*, 1690–1697. [CrossRef] [PubMed]

Appendix III

Canine parvovirus is shed infrequently by cats without diarrhoea in multi-cat environments

Maura Carrai [a,b], Nicola Decaro [c], Kate Van Brussel [a], Paola Dall'Ara [d], Costantina Desario [c], Marco Fracasso [c], Jan Šlapeta [a], Elena Colombo [d], Stefano Bo [e], Julia A. Beatty [a,b], Joanne Meers [f], Vanessa R. Barrs [a,b,*]

[a] *Sydney School of Veterinary Science, Faculty of Science, The University of Sydney, New South Wales 2006, Australia*
[b] *Jockey Club College of Veterinary Medicine & Life Sciences, City University of Hong Kong, Kowloon Tong, Hong Kong Special Administrative Region, China*
[c] *Department of Veterinary Medicine, University of Bari, Valenzano, Italy*
[d] *Department of Veterinary Medicine, University of Milan, Lodi, Italy*
[e] *Ambulatorio Veterinario Associato, Via Fratelli Calandra, 2, 10123 Torino, Italy*
[f] *University of Queensland, School of Veterinary Science, Gatton, Queensland 4343, Australia*

A R T I C L E   I N F O

A B S T R A C T

Whether subclinical shedding of canine parvovirus (CPV) by cats might contribute to the epidemiology of canine CPV infections, particularly in facilities housing both cats and dogs, requires clarification. Conflicting results are reported to date. Using conventional PCR (cPCR) to amplify the VP2 gene, shedding of the CPV variants (CPV-2a, 2b, 2c) by healthy cats in multi-cat environments was reportedly common in Europe but rare in Australia. The aim of this study was to determine whether low-level faecal CPV shedding occurs in multi-cat environments in Australia and Italy using a TaqMan real-time PCR to detect *Carnivore protoparvovirus 1* (CPV and feline parvovirus, FPV) DNA, and minor-groove binder probe real-time PCR assay to differentiate FPV and CPV types and to characterize CPV variants. In total, 741 non-diarrhoeic faecal samples from shelters in Australia (n = 263) and from shelters or cat colonies in Italy (n = 478) were tested. Overall, *Carnivore protoparvovirus 1* DNA was detected in 49 of 741 (6.61 %) samples. Differentiation was possible for 31 positive samples. FPV was most common among positive samples (28/31, 90.3 %). CPV was detected in 4/31 samples (12.9 %) including CPV-2a in one sample, CPV-2b in another and co-infections of FPV/CPV-2b and CPV-2a/CPV-2b in the remaining two samples. A high rate of subclinical FPV infection was detected in one shelter during an outbreak of feline panleukopenia, during which 21 of 22 asymptomatic cats (95.5 %) sampled were shedding FPV. Faecal shedding of CPV by cats in multi-cat environments is uncommon suggesting that domestic cats are not significant reservoirs of CPV.

1. Introduction

Parvoviruses are small, icosahedral, nonenveloped, single-stranded DNA viruses capable of prolonged environmental survival. The species *Carnivore protoparvovirus 1* in the Family *Parvoviridae* includes canine parvovirus (CPV) and feline parvovirus (FPV), which share over 99 % nucleotide identity (Parrish, 1999). Canine parvovirus type 2 (CPV-2) emerged from a FPV-like virus in the 1970s and caused a global pandemic in dogs, characterized by severe enteritis, myocarditis and immunosuppression (Parrish et al., 1988; Decaro and Buonavoglia, 2012). CPV-2 was non-infectious to cats until an antigenic variant, CPV-2a, evolved in the early 1980s. Indeed, CPV-2a had acquired the ability to bind the the viral receptor, the feline transferrin receptor (Tfr) through four mutations in the viral capsid protein VP2 (L87 M, I101 T, A300 G, D305Y) (Allison et al., 2014; Hueffer et al., 2003). Three antigenic variants CPV-2a, -2b and -2c are now circulating, which differ

* Corresponding author at: Jockey Club College of Veterinary Medicine and Life Sciences, City University of Hong Kong, Hong Kong Special Administrative Region, China.
E-mail addresses: mcarrai@cityu.edu.hk (M. Carrai), nicola.decaro@uniba.it (N. Decaro), kvan5385@uni.sydney.edu.au (K. Van Brussel), paola.dallara@unimi.it (P. Dall'Ara), costantina.desario@uniba.it (C. Desario), marco.fracasso@uniba.it (M. Fracasso), jan.slapeta@sydney.edu.au (J. Šlapeta), elena.colombo17@studenti.unimi.it (E. Colombo), stefano@veterinariassoiati.it (S. Bo), julia.beatty@cityu.edu.hk (J.A. Beatty), j.meers@uq.edu.au (J. Meers), vanessa.barrs@cityu.edu.hk (V.R. Barrs).

from each other at residue 426 of VP2. SNPs at genome positions 4062 and 4064 (positions 1276–1278 of the VP2 sequence) encode for either Asn, Asp or Glu in CPV -2a, -2b and -2c, respectively (Buonavoglia et al., 2001; Decaro et al., 2006; Parrish et al., 1991, 1988; Shackelton et al., 2005; Truyen et al., 1996)

FPV is the etiological agent of feline panleukopenia (FPL), a highly contagious and often fatal disease of cats characterized by severe enteritis and immunosuppression. CPV can also cause FPL, but only in around 5% of cases (Barrs, 2019; Truyen et al., 2009).

Healthy cats can be subclinically infected with FPV and CPV, shedding virus in non-diarrhoeic stools. An investigation carried out in shelters housing both cats and dogs in the United Kingdom, found a third of apparently healthy cats were shedding CPV-2a or -2b in faeces for up to 6 weeks (Clegg et al., 2012). CPV DNA in faeces was detected by conventional PCR (cPCR) targeting the VP2 region, and virus culture was successful for all PCR positive samples.VP2 nucleotide sequences in CPV shed by cats were identical to those detected previously in dogs with CPV-enteritis in the UK in 50 % of samples tested (Clegg et al., 2011). The implication of these findings is that cats may represent a significant source of environmental contamination by CPV that could cause fatal disease in non-immune dogs. Prior to the Clegg (2012) study, biosecurity protocols in shelters or hospital isolation units housing both cats and dogs had generally not considered this possibility. In contrast, a subsequent study carried out at mixed cat and dog shelters in Australia using cPCR found no evidence of CPV faecal shedding by healthy cats (Byrne et al., 2018). These divergent findings highlight the need to better understand the potential impact of CPV shedding by healthy cats on environmental contamination.

The aims of this study were to determine the prevalence and viral loads of FPV and CPV shed in the faeces of cats without diarrhoea in two different countries, Australia and Italy, using quantitative PCR (qPCR).

2. Materials and methods

2.1. Samples

Faecal samples were collected from enclosures of mixed cat and dog shelters housing apparently healthy cats without diarrhoea or from healthy free ranging colony cats, and frozen at −20 °C or −80 °C until processing. Samples from colony cats were collected from litter trays during hospitalization for neutering. At all shelters sampled, enclosures and litter trays were cleaned at least once per day.

2.2. Group 1 Australia

In Australia, non-diarrhoeic faecal samples were obtained from 3 mixed cat-dog shelters designated A1, in Sydney, New South Wales (NSW), and A2 and A3 in Brisbane, Queensland (QLD). The three shelters had a holding capacity of 100–180 dogs and 100–150 cats. In shelter A1 in Sydney, faecal samples were collected on 4 different days (A1−1 (Day 1) to A1−4 (Day 4)) between October 2015 and January 2016. The last sampling date (A1−4) occurred during an FPV outbreak at the shelter. Cats were mostly housed in groups of two to six and were all unvaccinated, while dogs were vaccinated against CPV on admission with two doses of an inactivated canine parvovirus vaccine 7 days apart (Parvac, Zoetis Australia, Silverwater Australia). The time between shelter admission and faecal sampling was variable for shelter A1. In Brisbane, samples were collected from both shelters (A2 and A3) within 24 h of admission on 4 days between October 2015 and February 2016 for shelter A2, and on 3 days between December 2015 and January 2016 for Shelter A3. All cats were vaccinated on admission with an attenuated trivalent core vaccination (Companion F3, MSD Animal Health Australia). Most cats were housed individually. Samples from shelters A2 and A3 and 78/185 samples from A1 were residual samples from a previous investigation which detected no CPV in faeces using cPCR (Byrne et al., 2018).

2.3. Group 2 Italy

In Italy, faecal samples were collected from mixed cat-dog shelters and from cat colonies in five regions designated B1 (Lombardy, 3 shelters and colony cats), B2 (Friuli-Venezia Giulia, 1 shelter), B3 (Piedmont, 3 shelters and 1 colony), B4 (Apulia, 1 colony) and B5 (Sicily, 1 shelter and 1 colony), between 2016 and 2020 inclusive. Vaccination status was recorded where known.

2.4. Template preparation - DNA extraction

DNA was extracted from faecal samples either using the QIAamp DNA Stool Mini Kit (Qiagen, Germany) according to the manufacturer's instructions or using boiling and homogenization as described previously (Decaro et al., 2006). Before extraction, an exogenous DNA internal control (Cal Orange 560 – Bioline) was added to each sample. DNA extracted using boiling and homogenization was diluted 1:10 in TE buffer (Tris−HCl and EDTA, pH = 8) to abolish interference from PCR inhibitors (Decaro et al., 2006, 2005).

2.5. Quantitative PCR assay (qPCR) for detection of Carnivore protoparvovirus 1

A quantitative PCR assay (qPCR), based on the TaqMan chemistry, to detect *Carnivore protoparvovirus 1* was performed on all DNA extracts from faecal specimens, as previously described (Decaro et al., 2005). Assay primers and probe are listed in Table 1. Quantitative PCR was carried out in a 25 µL reaction containing 12.5 µL of IQ Supermix (Bio-Rad Laboratories Srl), 600 nM of primers CPV-For and CPV-Rev, 200 nM of probe CPV-Pb, and 10 µL of template. For quantification of viral titre, each sample was tested in triplicate, and the mean no. of viral copies per reaction (per 10 µL of DNA template) was determined for positive samples. This value was then converted to viral copies/mg of faeces, based on the weight of faeces used in the DNA extraction of each sample. Samples were tested in triplicate and viral titres were reported in copies/mg of faeces. Signal derived from the internal control confirmed the presence of amplifiable DNA. Results were accepted with a cycle threshold (Ct) value ≤ 32.5 for the internal control (Cal Orange 560), and an $R^2 ≥ 0.970$ for the standard curve. The thermal cycle protocol consisted of a first activation step of Taq DNA polymerase at 95 °C for 10 min, followed by 40 cycles of denaturation at 95 °C for 15 s, primer annealing at 52 °C for 30 s, and extension at 60 °C for 1 min. All reactions were conducted in an a CFX Connect™ Real Time PCR Detection System (Bio-Rad Laboratories Pty., Ltd.), and the data were analyzed with software CFX Maestro.

2.6. Minor groove binding (MGB) probe assay for discrimination between FPV and CPV and identification of CPV variants

For samples in which *Carnivore protoparvovirus 1* DNA was detected on qPCR, real-time PCR assays using MGB probes were used to discriminate FPV from CPV, and if CPV was detected, to discriminate between CPV-2a-, 2b- and 2c- variants as previously described (Table 1) (Decaro et al., 2008; Decaro et al., 2006). The DNA probes in these assays have conjugated MGB ligands and form hyper-stabilized duplexes with complementary DNA. Minor modifications to these published protocols were as follows. The reactions were carried out in a total volume of 25 µL containing 10 µL of template, 12.5 µL of IQ Supermix (Bio-Rad Laboratories Srl) which includes dNTPs, 6 mM MgCl2 and 50 U/mL hot-start iTaq™ DNA polymerase, 900 nM of primers CPVa/b-For and CPVa/b-Rev (type 2a/2b assay) or CPVb/c-For and CPVb/c-Rev (type 2b/2c assay), 200 nM of probes CPVa-Pb and CPVb1-Pb (type 2a/2b assay) or CPVb2-Pb and CPVc-Pb (type 2b/2c assay). The thermal cycle protocol used was: activation of iTaq DNA polymerase at 95 C for 10 min and 45 cycles consisting of denaturation at 95 C for 30 s and primer annealing–extension at 60 C for 1 min. All samples were tested in duplicate.

2

Table 1
Sequence, position and specificity of oligonucleotides used in the study.

Assay	Primer/Probe	Sequence 5′ - 3′	Polarity	Amplicon size (bp)	Nucleotide Position
TaqMan[a]	CPV-For	AAACAGGAATTAACTATACTAATATATTTA	+	93	4102–4131 [d]
	CPV-Rev	AAATTTGACCATTTGGATAAACT	–		4172–4194 [d]
	CPV-Pb	FAM—TGGTCCTTTAACTGCATTAAATAATGTACC—TAMRA	+		4139–4168 [d]
FPV/CPV MGB[b]	FPV/CPV-For	ACAAGATAAAAGACGTGGTGTAACTCAA	+	83	3713–3760
	FPV/CPV-Rev	CAACCTCAGCTGGTCTCATAATAGT	–		3771–3795
	FPV-Pb	VIC–ATGGGAAATACAGACTATAT–MGB	+		3741–3760
	CPV-Pb	FAM–ATGGGAAATACAAACTATAT–MGB	+		3741–3760
Type 2a/2b MGB[c]	CPVa/b-For	AGGAAGATATCCAGAAGGAGATTGGA	+	93	1719–1744[e,f]
	CPVa/b-Rev	CCAATTGGATCTGTTGGTAGCAATACA	–		1785–1811[e,f]
	CPVa-Pb	VIC—CTTCCTGTAACAAATGATA—MGB	+		1765–1783 [e]
	CPVb1-Pb	FAM—CTTCCTGTAACAGATGATA—MGB	+		1765–1783 [f]
Type 2b/2c MGB[c]	CPVb/c-For	GAAGATATCCAGAAGGAGATTGGATTCA	+	150	1721 – 1748 [f]
	CPVb/c-Rev	ATGCAGTTAAAGGACCCATAAGTATTAAATATATTAGTATAGTTAATTC	–		1155–1182 [g]1823 –1870 [f]
	CPVb2-Pb	FAM—CCTGTAACAGATGATAAT—MGB	+		1768–1785 [f]
	CPVc-Pb	VIC—CCTGTAACAGAAGATAAT—MGB	+		1202–1219 [g]

[a] Decaro et al. (2005).
[b] Decaro et al. (2008).
[c] Decaro et al. (2006).
[d] Oligonucleotide positions are referable to the sequences of FPLV strain FPV-b (accession no. M24004) and of CPV-2 strain CPV-b (accession no. M38245).
[e] Oligonucleotide positions are referable to CPV-2a strain CPV-15 (accession no. M24003).
[f] Oligonucleotide positions are referable to CPV-2b strain CPV-39 (accession no. M74849).
[g] Oligonucleotide positions are referable to CPV-2c strain 56/00 (accession no. AY380577).

3. Results

In Australia, 263 feline faecal samples were collected from mixed cat-dog shelters including 185 from shelter A1 (A1−1: n = 46, A1−2: n = 83, A1−3: n = 34 A1−4: n = 22), 52 from shelter A2 and 26 from shelter A3. Signalment data were available for a subset of 136 Australian cats; all were domestic crossbreds with a median age of 1 year (range 1 month – 6 years), 57 % were male and 43 % were female. In Italy, 478 feline faecal samples were collected from mixed cat-dog shelters (55 %) and free roaming colony cats (45 %). Signalment data were available for a subset of 88 cats; all were domestic crossbreds with a median age of 3 years (range 1 month – 15 years), 53 % were male and 47 % were female.

Overall, *Carnivore protoparvovirus 1* DNA was detected in 49/741 (6.61 %) faecal samples from Australia and Italy (Tables 2 and 3), with 28/263 (10.65 %) and 21/478 (4.39 %) samples testing positive, respectively. Discrimination between FPV and CPV was possible in 31 positive samples in which DNA of 33 *Carnivore protoparvovirus* 1 viruses was detected (Tables 3 and 4); FPV DNA was detected in 28/31 (90.3 %) and CPV in 4/31 (12.9 %)samples including CPV-2a in one sample, CPV-2b in another and co-infections of FPV/CPV-2b and CPV-2a/CPV-2b in

the remaining two samples. Twenty one of 22 asymptomatic cats at shelter A1 in Sydney Australia, sampled during the time of an outbreak of feline panleukopenia FPV were found to be shedding FPV (Group A1−4, Table 2). FPV was shed in higher amounts overall (median 5.90×10^4 copies FPV DNA/mg faeces; range (1.91×10^0-1.34×10^{10}) than CPV (median 3.80×10^0 copies CPV DNA/mg faeces; range 1.99×10^0-2.04×10^4). For the 18 samples in which the virus could not be typed, the median viral titre was 2.85×10^1 copies/mg faeces (range 1.20×10^1 - 4.63×10^2). CPV-2a alone was detected in one cat from Italy, CPV-2b alone was detected in one cat from Australia, and coinfections with CPV-2a and CPV-2b, or CPV-2b and FPV were detected in one cat each from Australia (Tables 3 and 4).

4. Discussion

We found that shedding of CPV by cats without diarrhoea in multi-cat environments in two different countries, Australia and Italy, was uncommon. In a previous study, we failed to detect CPV faecal shedding by cats in mixed cat and dog shelters in Australia using a cPCR targeting a 583 bp region of the VP2 gene to detect *Carnivore protoparvovirus 1* but could not exclude the possibility of low-level CPV shedding occurring

Table 2
Prevalence and viral titre of canine parvovirus (CPV) and feline parvovirus (FPV) detected in faeces of cats without diarrhoea housed in shelters or free-roaming in colonies in Australia and Italy.

Group	Region	Type of MCE	Positive samples/ Total	Positive %	*Carnivore Protoparvovirus 1* variants detected[*] CPV No.	CPV Median Viral Titre/mg faeces	FPV No.	FPV Median Viral Titre/mg faeces	Unknown No.	Unknown Median Viral Titre/mg faeces
A1	NSW	S	26/185	14.1	2	$2.30 \times 10^\circ$	24	5.82×10^4	1	–
A3	QLD	S	2/52	3.9	2	1.48×10^1	1	1.35×10^4	0	–
B1	Lombardy	C, S	0/101	0	0	–	0	–	0	–
B2	Friuli -Venezia Giulia	S	1/10	10	0	–	0	–	1	4.63×10^2
B3	Piedmont	C, S	10/92	10.9	0	–	3	1.69×10^5	7	2.3×10^1
B4	Apulia	C	3/10	30	1	2.04×10^4	0	–	2	1.65×10^1
B5	Sicily	C, S	7/265	2.6	0	–	0	–	7	3.4×10^1
Totals			49/741	6.61	5		28		18	

MCEmulti-cat environment; Ccolony; Sshelter.
[*] total number of *Carnivore Protoparvovirus 1* variants detected is higher than the number of positive samples because of the presence of co-infections in two samples.

3

Table 3

Carnivore protoparvovirus 1 variants and viral titers detected in individual faecal samples from shelter-housed cats without diarrhoea in Australia.

Sample	Region	Group	*Carnivore protoparvovirus* 1 copies/mg faeces	Variants detected
D1S1	NSW	A1-2	3.21×10^2	FPV
JL3S2	NSW	A1-2	9.86×10^1	FPV
LL2S6	NSW	A1-2	5.36×10^3	FPV, CPV-2b
ML2S2	NSW	A1-2	4.18×10^3	CPV-2b
C8L1S4	NSW	A1-2	3.11×10^1	unknown
AL1S1	NSW	A1-4	6.77×10^3	FPV
AL1S1	NSW	A1-4	6.23×10^3	FPV
AL2S1	NSW	A1-4	5.82×10^4	FPV
AL2S2	NSW	A1-4	5.69×10^4	FPV
AL3S1	NSW	A1-4	3.12×10^4	FPV
BL1S1	NSW	A1-4	3.33×10^3	FPV
C12	NSW	A1-4	5.73×10^2	FPV
C13	NSW	A1-4	1.34×10^{10}	FPV
C16	NSW	A1-4	3.39×10^6	FPV
C19	NSW	A1-4	7.23×10^6	FPV
C21	NSW	A1-4	8.05×10^5	FPV
C25	NSW	A1-4	3.17×10^7	FPV
C7S1	NSW	A1-4	1.02×10^7	FPV
C9	NSW	A1-4	4.87×10^4	FPV
DL1S1	NSW	A1-4	7.71×10^4	FPV
GL1S1	NSW	A1-4	8.57×10^8	FPV
KL1S1	NSW	A1-4	1.06×10^6	FPV
KL2S1	NSW	A1-4	1.57×10^6	FPV
L2S1	NSW	A1-4	4.73×10^6	FPV
LL1S1	NSW	A1-4	1.64×10^4	FPV
C15	NSW	A1-4	1.20×10^5	FPV
16/63	QLD	A3	$7.24 \times 10^\circ$	CPV-2a, CPV-2b
16/103	QLD	A3	5.25×10^5	FPV
Median		All	1.2×10^5	–

NSWNew South Wales; QLD Queensland.

([Byrne et al., 2018](#)). The TaqMan qPCR used in this study has been shown previously to have a detection limit of around 1 log higher than that of gel-based cPCR ([Decaro et al., 2005](#)). Indeed, samples testing positive in this study had tested negative previously using cPCR ([Byrne et al., 2018](#)). Specifically, we found a high level of subclinical FPV shedding among cats in Shelter A1, where 21/22 samples collected on the same day tested positive for FPV DNA by qPCR, compared to only 4/21 identified as positive using cPCR ([Byrne et al., 2018](#)). These faecal

samples were collected two months after an FPL outbreak had been reported at the shelter. Since individual follow-up was not available for the sampled cats, whether they remained subclinically infected, or some subsequently developed FPL is not known. However, subclinical FPV infections are common among some cat populations as reflected by high seroprevalence levels in healthy animals, indicating previous exposure ([Barrs, 2019](#)). In a separate investigation, the seroprevalence of FPV among healthy shelter-housed cats in two Australian cities, Sydney and Perth, was reported to be 96 % ([Jenkins et al., 2020](#)).

Recently, faecal shedding of parvoviruses was serially monitored in 40 healthy owned cats from Germany, 1, 2, 3 and 4 weeks after vaccination with an attenuated FPV vaccine ([Bergmann et al., 2019](#)). Twelve cats (30 %) were found to be shedding parvoviral DNA at any time during the study. Variant typing was possible in eight of these, with four cats shedding FPV field virus, three shedding FPV vaccine virus and one cat shedding CPV. The finding of a higher prevalence of asymptomatic shedding of field strains of FPV than vaccine virus was unexpected but re-enforces that subclinical FPV infections in cats are common.

Of the four cats detected to be shedding CPV, three were shelter-housed and one was free roaming from a colony. Faeces were collected within 24 h of admission from one of the shelter-housed cats, suggesting it was infected with CPV before arriving at the shelter. For the other three positive cats it was not possible to ascertain the likely onset of infection. Two of the four CPV-shedding cats were infected with CPV-2a, consistent with infection by a field strain of virus. The two cats shedding CPV-2b could have been infected with a field or vaccine strain of virus, since live attenuated CPV-2b vaccines are available in Australia, where the cats were from. In the investigation by [Clegg et al. (2012)](#), data from their longitudinal sampling, which was performed weekly for 8 weeks, suggested that most of the positive cats were infected before admission to the shelter, although there were some instances where transmission may have occurred within the shelter.

CPV titres in the positive cats in this study were low compared to those reported previously in cats with FPL and measured using the same qPCR assay and conditions ([Decaro et al., 2010](#)). Although we did not attempt virus culture of positive samples, the low viral titres in these cats support their subclinical infection status and a low potential risk of transmission. However, since the potential for intra- and inter-species transmission of CPV by cats is not negligible, appropriate biosecurity measures in shelters are essential.

The low prevalence of CPV shedding by domestic cats reported here,

Table 4

Carnivore protoparvovirus 1 variants and viral titers detected in individual faecal samples from shelter-housed cats without diarrhoea and free-roaming colony cats in Italy.

Sample	Region	Group	*Carnivore protoparvovirus* 1 copies/mg faeces	Variants detected	Vaccination status, Domicile
518/19−6a	Friuli -Venezia Giulia	B2	4.63×10^2	unknown	Unvaccinated, Shelter
426/19−5	Piedmont	B3	1.69×10^5	FPV	Vaccinated, Shelter
426/19−11	Piedmont	B3	5.90×10^4	FPV	Unvaccinated, Shelter
471/19−2	Piedmont	B3	2.30×10^1	unknown	Unknown, Shelter
471/19−4	Piedmont	B3	1.30×10^1	unknown	Unknown, Shelter
471/19−5	Piedmont	B3	1.20×10^1	unknown	Unknown, Shelter
471/19−11	Piedmont	B3	3.20×10^1	unknown	Unknown, Shelter
472/19−1	Piedmont	B3	1.26×10^7	FPV	Unknown
507/19−2	Piedmont	B3	1.40×10^1	unknown	Unvaccinated, Shelter
507/19−5	Piedmont	B3	1.68×10^2	unknown	Vaccinated, Unknown
507/19−7	Piedmont	B3	1.80×10^4	unknown	Vaccinated, Unknown
473/19−1	Apulia	B4	2.04×10^4	CPV-2a	Unvaccinated, Colony
473/19−2	Apulia	B4	1.50×10^1	unknown	Unvaccinated, Colony
473/19−8	Apulia	B4	1.80×10^1	unknown	Unvaccinated, Colony
166/16−21	Sicily	B5	9.20×10^1	unknown	Unknown, Colony
166/16−25	Sicily	B5	4.70×10^1	unknown	Unknown, Colony
166/16−32	Sicily	B5	1.20×10^1	unknown	Unknown, Colony
166/16−35	Sicily	B5	2.50×10^1	unknown	Unknown, Colony
166/16−81	Sicily	B5	3.20×10^1	unknown	Unknown, Colony
166/16−83	Sicily	B5	3.40×10^1	unknown	Unknown, Colony
357/16−1004	Sicily	B5	6.90×10^1	unknown	Unknown, Colony
		Median	All	3.2×10^1	–

contrasts the situation in wild felids, where there is evidence that CPV is displacing FPV in sylvatic cycles. Among wild carnivore hosts susceptible to both FPV and CPV infection that were sampled in North America, 58/61 viruses (95.1 %) were of CPV origin (Allison et al., 2014). In a recent molecular survey conducted in wild carnivores in Italy, 34 out of 257 sampled animals were found positive for *Carnivore protoparvovirus 1* DNA (Ndiana et al., 2020). FPV was detected in red foxes (*Vulpes vulpes*) (2.8 %, 7/252) and Eurasian badgers (*Meles meles*) (10 %, 1/10), while CPV was evident in wolves (54.3 %, 19/35), Eurasian badgers (60 %, 6/10) and one beech marten (*Martes foina*) (100 %, 1/1), with more than one parvovirus type detected in some animals. CPV and FPV strains were also detected in 5/7 (71.4 %) carcasses of Eurasian otters (*Lutra lutra*) found dead from road accidents (Viscardi et al., 2019).

It is possible that the prevalence of CPV-shedding by cats tested in this study was slightly underestimated due to mis-matching of nucleotides of some variants with the primer sequences, which were designed based on CPV-2 prototype strains (Decaro et al., 2005), although single nucleotide mismatches do not always affect correct primer annealing. Most of the positive samples from Italy were from cats that were unvaccinated or of unknown vaccination status. Detailed vaccination history was not available; thus, it is not known whether parvoviral DNA detected in the vaccinated cats was from field or vaccine strains. In this study there was a higher proportion of positive samples from Italy compared to Australia for which the parvovirus type could not be identified using the MGB assays, reflecting the lower median titres of *Carnivore protoparvovirus 1* detected among Italian samples (3.2×10^1 copies/mg of faeces) compared to Australian samples 1.2×10^5 copies/mg of faeces). This could also reflect the different DNA extraction techniques used. For the Australian samples each 10 μL of DNA template was extracted using a commercial kit and was derived from 22 mg of faeces, whereas for the Italian samples each 10 μL of DNA template was extracted using the boiling/homogenization method and was derived from 1 mg of faeces.

We identified co-infections with CPV-2a/CPV-2b, and CPV-2b/FPV in one cat each from New South Wales and Queensland. Parvovirus co-infections have occasionally been reported in cats with feline panleukopenia (FPL), or in latently infected cats where *Carnivore protoparvovirus 1* DNA has been amplified by PCR utilizing peripheral blood monocytes (Balboni et al., 2018; Battilani et al., 2011). In one cat with FPL from Italy, a co-infection of FPV and CPV-2a was detected after PCR of faecal DNA, cloning and Sanger sequencing (Battilani et al., 2011). A virus intermediate between FPV and CPV-2a was also found in the same cat, although no potential recombination events were identified. In another study from Italy, an FPV and CPV-2c co-infection was identified in a latently infected cat with chronic kidney disease, using the same methodological approach on DNA extracted from the buffy-coat fraction of whole blood (Balboni et al., 2018).

Carnivore protoparvovirus 1 variant virus co-infections have rarely been described in dogs (Battilani et al., 2007; Pérez et al., 2014). In 2008, one pup from Portugal was found to be co-infected by CPV-2b and CPV-2c, which were detected as single infections in its littermates (Vieira et al., 2008). In one study of CPVs from 40 dogs in Uruguay with clinical disease, two co-infections were identified, one with CPV-2a/CPV-2a and another with CPV-2a and a recombinant CPV-2a/CPV-2c strain (Pérez et al., 2014). However, analysis of whole genome CPV sequences obtained from clinical samples from 28 naturally infected dogs using next generation sequencing showed that intra-host viral diversity was low, with only eight subconsensus single nucleotide variants (SNVs) above 0.5 % (Voorhees et al., 2019). The same investigators found low intra-host CPV diversity among other CPV or FPV infected host species including several raccoon dogs, a blue fox and a red wolf.

5. Conclusions

Domestic cats without diarrhoea in multi-cat environments shed CPV

infrequently and are unlikely to represent a significant reservoir of CPV. However, since cats can be infected with CPV and develop clinical disease, mixed species isolation wards in veterinary hospitals should apply appropriate biosecurity measures to prevent cross-species transmission. The presence of CPV/FPV and CPV variant co-infections, although infrequent, shows the potential for viral recombination and new variant formation.

Declaration of Competing Interest

The authors declare that they have no known competing financial interests or personal relationships that could have appeared to influence the work reported in this paper.

References

Allison, A.B., Kohler, D.J., Ortega, A., Hoover, E.A., Grove, D.M., Holmes, E.C., Parrish, C.R., 2014. Host-specific parvovirus evolution in nature is recapitulated by in vitro adaptation to different carnivore species. PLoS Pathog. 10, e1004475.

Balboni, A., Bassi, F., De Arcangeli, S., Zobba, R., Dedola, C., Alberti, A., Battilani, M., 2018. Molecular analysis of carnivore Protoparvovirus detected in white blood cells of naturally infected cats. BMC Vet. Res. 14, 41.

Barrs, V.R., 2019. Feline panleukopenia: a re-emergent disease. Vet. Clin. North Am. Small Anim. Pract. 49, 651–670.

Battilani, M., Gallina, L., Vaccari, F., Morganti, L., 2007. Co-infection with multiple variants of canine parvovirus type 2 (CPV-2). Vet. Res. Commun. 31 (Suppl. 1), 209–212.

Battilani, M., Balboni, A., Ustulin, M., Giunti, M., Scagliarini, A., Prosperi, S., 2011. Genetic complexity and multiple infections with more Parvovirus species in naturally infected cats. Vet. Res. 42, 43.

Bergmann, M., Schwertler, S., Speck, S., Truyen, U., Reese, S., Hartmann, K., 2019. Shedding of parvovirus deoxyribonucleic acid following modified live panleucopenia virus vaccination in healthy cats. Vet. Rec. 185, 83. https://doi.org/10.1136/vr.104661.

Buonavoglia, C., Martella, V., Pratelli, A., Tempesta, M., Cavalli, A., Buonavoglia, D., Bozzo, G., Elia, G., Decaro, N., Carmichael, L., 2001. Evidence for evolution of canine parvovirus type 2 in Italy. J. Gen. Virol. 82, 3021–3025.

Byrne, P., Beatty, J.A., Slapeta, J., Corley, S.W., Lyons, R.E., McMichael, L., Kyaw-Tanner, M.T., Dung, P.T., Decaro, N., Meers, J., Barrs, V.R., 2018. Shelter-housed cats show no evidence of faecal shedding of canine parvovirus DNA. Vet. J. 239, 54–58.

Clegg, S.R., Coyne, K.P., Dawson, S., Spibey, N., Gaskell, R.M., Radford, A.D., 2012. Canine parvovirus in asymptomatic feline carriers. Vet. Microbiol. 157, 78–85.

Decaro, N., Buonavoglia, C., 2012. Canine parvovirus–a review of epidemiological and diagnostic aspects, with emphasis on type 2c. Vet. Microbiol. 155, 1–12.

Decaro, N., Elia, G., Martella, V., Desario, C., Campolo, M., Trani, L.D., Tarsitano, E., Tempesta, M., Buonavoglia, C., 2005. A real-time PCR assay for rapid detection and quantitation of canine parvovirus type 2 in the feces of dogs. Vet. Microbiol. 105, 19–28.

Decaro, N., Elia, G., Martella, V., Campolo, M., Desario, C., Camero, M., Cirone, F., Lorusso, E., Lucente, M.S., Narcisi, D., Scalia, P., Buonavoglia, C., 2006. Characterisation of the canine parvovirus type 2 variants using minor groove binder probe technology. J. Virol. Methods 133, 92–99.

Decaro, N., Desario, C., Lucente, M.S., Amorisco, F., Campolo, M., Elia, G., Cavalli, A., Martella, V., Buonavoglia, C., 2008. Specific identification of feline panleukopenia virus and its rapid differentiation from canine parvoviruses using minor groove binder probes. J. Virol. Methods 147, 67–71.

Decaro, N., Buonavoglia, D., Desario, C., Amorisco, F., Colaianni, M.L., Parisi, A., Terio, V., Lucente, M.S., Martella, V., Buonavoglia, C., 2010. Charactersiation of canine parvovirus strains isolated from cats with feline panleukopenia. Res. Vet. Sci. 89, 275–278.

Hueffer, K., Parker, J.S., Weichert, W.S., Geisel, R.E., Sgro, J.Y., Parrish, C.R., 2003. The natural host range shift and subsequent evolution of canine parvovirus resulted from virus-specific binding to the canine transferrin receptor. J. Virol. 77, 1718–1726.

Jenkins, E., Davis, C., Carrai, M., Ward, M.P., O'Keeffe, S., van Boeijen, M., Beveridge, L., Desario, C., Buonavoglia, C., Beatty, J.A., Decaro, N., Barrs, V.R., 2020. Feline parvovirus seroprevalence is high in domestic cats from disease outbreak and non-outbreak regions in Australia. Viruses 12, 320.

Clegg, S.R., Coyne, K.P., Parker, J., Dawson, S., Godsall, S.A., Pinchbeck, G., Cripps, P.J., Gaskell, R.M., Radford, A.D., 2011. Molecular epidemiology and phylogeny reveal

complex spatial dynamics in areas where canine parvovirus is endemic. J. Virol. 85, 7892–7899.

Ndiana, L.A., Lanave, G., Desario, C., Berjaoui, S., Alfano, F., Puglia, I., Fusco, G., Colaianni, M.L., Vincifori, G., Camarda, A., Parisi, A., Sgroi, G., Elia, G., Veneziano, V., Buonavoglia, C., Decaro, N., 2020. Circulation of diverse protoparvoviruses in wild carnivores, Italy. Transbound. Emerg. Dis. https://doi.org/10.1111/tbed.13917. Online ahead of print.

Parrish, C.R., 1999. Host range relationships and the evolution of canine parvovirus. Vet. Microbiol. 69, 29–40.

Parrish, C.R., Have, P., Foreyt, W.J., Evermann, J.F., Senda, M., Carmichael, L.E., 1988. The global spread and replacement of canine parvovirus strains. J. Gen. Virol. 69, 1111–1116.

Parrish, C.R., Aquadro, C.F., Strassheim, M.L., Evermann, J.F., Sgro, J.Y., Mohammed, H. O., 1991. Rapid antigenic-type replacement and DNA sequence evolution of canine parvovirus. J. Virol. 65, 6544–6552.

Pérez, R., Calleros, L., Marandino, A., Sarute, N., Iraola, G., Grecco, S., Blanc, H., Vignuzzi, M., Isakov, O., Shomron, N., Carrau, L., Hernández, M., Francia, L., Sosa, K., Tomás, G., Panzera, Y., 2014. Phylogenetic and genome-wide deep-sequencing analyses of canine parvovirus reveal co-infection with field variants and emergence of a recent recombinant strain. PLoS One 9, e111779.

Shackelton, L.A., Parrish, C.R., Truyen, U., Holmes, E.C., 2005. High rate of viral evolution associated with the emergence of carnivore parvovirus. Proc. Natl. Acad. Sci. U. S. A. 102, 379–384.

Truyen, U., Evermann, J.F., Vieler, E., Parrish, C.R., 1996. Evolution of canine parvovirus involved loss and gain of feline host range. Virology 215, 186–189.

Truyen, U., Addie, D., Belak, S., Boucraut-Baralon, C., Egberink, H., Frymus, T., Gruffydd-Jones, T., Hartmann, K., Hosie, M.J., Lloret, A., Lutz, H., Marsilio, F., Pennisi, M.G., Radford, A.D., Thiry, E., Horzinek, M.C., 2009. Feline panleukopenia. ABCD guidelines on prevention and management. J. Feline Med. Surg. 11, 538–546.

Vieira, J.M., Silva, E., Desario, C., Decaro, N., Carvalheira, J., Buonavoglia, C., Thompson, G., 2008. Natural co-infection with 2 parvovirus variants in dog. Emerg. Infect. Dis. 14, 678–679.

Viscardi, M., Santoro, M., Clausi, M.T., Cozzolino, L., Decaro, N., Colaianni, M.L., Fusco, G., 2019. Molecular detection and characterization of carnivore parvoviruses in free-ranging Eurasian otters (*Lutra lutra*) in southern Italy. Transbound. Emerg. Dis. 66, 1864–1872.

Voorhees, I.E.H., Lee, H., Allison, A.B., Lopez-Astacio, R., Goodman, L.B., Oyesola, O.O., Omobowale, O., Fagbohun, O., Dubovi, E.J., Hafenstein, S.L., Holmes, E.C., Parrish, C.R., 2019. Limited intrahost diversity and background evolution accompany 40 years of canine parvovirus host adaptation and spread. J. Virol. 94, e01162–19.

6

Appendix IV

Article

Low Intrahost and Interhost Genetic Diversity of *Carnivore Protoparvovirus 1* in Domestic Cats during a Feline Panleukopenia Outbreak

Xiuwan Wang [1,2,†], Maura Carrai [3,4,†], Kate Van Brussel [5,6], Shuo Feng [1,2], Julia A. Beatty [3,4,5], Mang Shi [7], Edward C. Holmes [6], Jun Li [1,2,4] and Vanessa R. Barrs [3,4,5,*]

[1] City University of Hong Kong Shenzhen Research Institute, Shenzhen 518057, China; xiuwan.wang@my.cityu.edu.hk (X.W.); shuofeng8-c@my.cityu.edu.hk (S.F.); jun.li@cityu.edu.hk (J.L.)
[2] Department of Infectious Diseases and Public Health, Jockey Club College of Veterinary Medicine and Life Sciences, City University of Hong Kong, Hong Kong, China
[3] Department of Veterinary Clinical Sciences, Jockey Club College of Veterinary Medicine and Life Sciences, City University of Hong Kong, Hong Kong, China; mcarrai@cityu.edu.hk (M.C.); julia.beatty@cityu.edu.hk (J.A.B.)
[4] Centre for Animal Health and Welfare, City University of Hong Kong, Hong Kong, China
[5] School of Veterinary Science, Faculty of Science, University of Sydney, Sydney, NSW 2006, Australia; kate.vanbrussel@sydney.edu.au
[6] School of Life and Environmental Sciences and School of Medical Sciences, Sydney Institute for Infectious Diseases, University of Sydney, Sydney, NSW 2006, Australia; edward.holmes@sydney.edu.au
[7] School of Medicine, Sun Yat-sen University, Guangzhou 510275, China; shim23@mail.sysu.edu.cn
* Correspondence: vanessa.barrs@cityu.edu.hk
† These authors contributed equally to this work.

Abstract: Feline panleukopenia (FPL), a highly contagious and frequently fatal disease of cats, is caused by Feline parvovirus (FPV) and Canine parvovirus (CPV). We characterised the diversity of these *Carnivore protoparvovirus 1* variants in 18 faecal samples collected from domestic cats with FPL during an outbreak, using targeted parvoviral DNA metagenomics to a mean depth of >10,000 × coverage per site. All samples comprised FPV alone. Compared with the reference FPV genome, isolated in 1967, 44 mutations were detected. Ten of these were nonsynonymous, including 9 in nonstructural genes and one in VP1/VP2 (Val232Ile), which was the only one to exhibit interhost diversity, being present in five sequences. There were five other polymorphic nucleotide positions, all with synonymous mutations. Intrahost diversity at all polymorphic positions was low, with subconsensus variant frequencies (SVF) of <1% except for two positions (2108 and 3208) in two samples with SVF of 1.1–1.3%. Intrahost nucleotide diversity was measured across the whole genome (0.7–1.5%) and for each gene and was highest in the NS2 gene of four samples (1.2–1.9%). Overall, intrahost viral genetic diversity was limited and most mutations observed were synonymous, indicative of a low background mutation rate and strong selective constraints.

Keywords: feline panleukopenia; feline parvovirus; metagenomics; diversity; intrahost

1. Introduction

Feline panleukopenia (FPL) is a highly contagious and often fatal disease of cats caused by Feline parvovirus (FPV), a small nonenveloped single-stranded DNA virus in the species *Carnivore protoparvovirus 1* (genus *Protoparvovirus*, family *Parvoviridae*) that has circulated among felid hosts for approximately 100 years [1]. FPL is characterised by severe acute enteritis and sepsis [2]. In Australia, FPL re-emerged as a major cause of mortality in shelter-housed cats between 2014 and 2018, in association with low vaccination rates [3,4]. Canine parvovirus (CPV) is a closely related variant of *Carnivore protoparvovirus 1* that emerged in domestic dogs in the mid-to-late 1970s and subsequently acquired the feline host range. CPV has been reported to cause FPL in cats [5–8].

When it first emerged, CPV was unable to bind the feline transferrin receptor (fTfR), which is required to initiate viral infection of the host [9]. Four mutations in the VP2 of CPV (L87M, I101T, A300G, and D305Y) in an antigenic variant (termed CPV-2a) that evolved around 1980 enabled CPV to infect and replicate in cats [10,11]. All currently circulating CPVs, including CPV-2b (VP2 N426D) [12] and CPV-2c (VP2 D426E) [13], can infect cats and cause FPL, as evidenced by naturally occurring and experimental infections [5–8].

Mixed infections of FPV and CPV have been occasionally detected in both healthy and diseased cats using conventional VP2 PCR and sequencing. Such coinfections have been suggested to be a source of complexity and diversity of parvoviral genetic variation [14–17]. The rapid development of next-generation sequencing (NGS) has facilitated research in viral diversity through amplicon sequencing [18–20]. Here, we applied a metagenomics method combining NGS with targeted hybridisation probes to capture parvoviral DNA present in faecal samples from cats with FPL, obtained during the re-emergent Australian FPL outbreak [3]. Our aims were to determine whether CPV coinfections were present in FPV-infected cats with FPL and to reveal the extent and pattern of intra- and interhost *Carnivore protoparvovirus 1* genetic diversity.

2. Materials and Methods

2.1. Sample Collection

Eighteen faecal samples collected from cats with FPL from multiple shelters in 2016–2017 during a re-emergent epizootic of FPL in Sydney, New South Wales, Australia, were included in the study (Supplementary Materials Table S1). The presence of *Carnivore Protoparvovirus 1*, specifically FPV, had been confirmed by PCR of the partial capsid VP-2 gene and Sanger sequencing [3].

2.2. DNA Extraction, Baiting and Sequencing

Viral nucleic acids (RNA and DNA) were extracted using the QIAamp Viral RNA Mini Kit (Qiagen, Hilden, Germany) after enrichment according to a published protocol [21] with minor modifications [22] and split into two aliquots. One aliquot was used for RNA sequencing in another study [23]. For the other aliquot, viral genomic DNA was subjected to whole genome amplification using the Whole Genome Amplification Kit (WGA2) (Sigma-Aldrich, St. Louis, MO, USA) and purified using the GenElute PCR Clean-Up Kit (Sigma-Aldrich, St. Louis, MO, USA). Amplified DNA was quantified by Qubit 2.0 fluorometer. DNA libraries were created using the Nextera XT Library Preparation Kit (Illumina, San Diego, CA, USA) with no size selection and enriched for *Carnivore protoparvovirus 1* using customised, hybridisation-based target capture kits (myBaits, Arbor Biosciences, Ann Arbor, MI, USA). A total of 12,417 biotinylated RNA probe baits were designed with 80 bp with 3 × tiling, based on all *Carnivore protoparvovirus 1* sequences downloaded from NCBI GenBank targeting the VP2 gene. The enrichment method followed the manufacturer's instructions with minor modifications, including a pre-treatment phase to deplete any remaining streptavidin in the DNA libraries. One set of capture reactions was performed using a hybridisation temperature of 62 °C for 16 h. All PCR amplifications were carried out using KAPA Hi HotStart Mix (Kapa Biosystems, Cape Town, South Africa) with the "reamp" primers IS5_reamp.P5AATGATACGGCGACCACCGA and S6_reamp.P7CAAGCAGAAGACGGCATACGA [24], followed by purification with the GenElute PCR Clean-up kit (Sigma-Aldrich, St. Louis, MO, USA). The enriched target DNA of two libraries with low DNA concentrations was sequenced at the AGRF (Melbourne, Australia) using an Illumina NextSeq500 platform with NextSeq500 sequencing-300 cycles System midi-Output Kit (Illumina, San Diego, CA, USA). The remaining 16 samples were sequenced on the same platform using the NextSeq500 System High-Output Kit (Illumina, San Diego, CA, USA) with a final output of 32.5–39 Gb and 100–120 Gb, respectively.

2.3. Detection and Characterisation of FPV and CPV

We mapped all raw reads to the cat reference genome (Felis catus 9.0 assembly, Gen-Bank Assembly ID GCA_000181335.4) using BWA version 0.7.17 [25] and removed those with more than 95% mapping coverage. We then further processed the raw reads for quality control with the following procedures [26,27] (available at https://github.com/TingtZHENG/metagenomics/blob/master/scripts/fqc.pl (accessed on 1 June 2022)): (i) remove Illumina primers, adaptors, and linker sequences; (ii) remove paired-ends reads with 25 bp consecutively exact match from both ends to eliminate PCR duplicates; (iii) remove terminal regions with continuous Phred-based quality of less than 20. Reads were then mapped to the reference FPV sequence (FPV-3, GenBank accession no. EU659111.1) using BWA version 0.7.17 [25]. Reads with over 90% mapping coverage were then extracted. Sequencing depth and error rate across the entire genome were also determined.

We similarly mapped all the extracted reads against the FPV-3 reference genome using BWA version 0.7.17 [25]. Next, we converted BWA sam output to the bam format with SAMtools version 1.9 [28]. Based on the bam results for each sample, variant calling was performed by BCFtools version 1.9 [28]. First, BCFtools mpileup was used to generate Variant Call Format (VCF) files from bam results. Subsequently, the BCFtools call was utilised with a smaller mutation rate (0.01%) to obtain stricter calls for single nucleotide variants (SNV). Only SNVs with a QUAL (Phred-scaled probability) > 20 were retained. The residues at 26 amino acid positions (Supplementary Materials File S1) in the VP2 gene were used to characterise SNVs as FPV or CPV [29–31].

2.4. Evolutionary Analysis

The Metagenomic Intraspecies Diversity Analysis System (MIDAS) [32] was used to identify the majority consensus sequence for each sample. Using the FPV reference genome (FPV-3.us.67; GenBank accession no. EU659111), MIDAS used Bowtie2 [33] to globally align reads against the genome database. Mapped reads were used to determine the consensus sequences.

A separate study was conducted to characterise the faecal viromes of 17 of the same 18 faecal samples we analysed using metatranscriptomics without virion enrichment or baits [23]. The metatranscriptomics parvoviral data set was used to compare the accuracy and sensitivity of our ability to detect parvoviruses and SNPs in these 18 samples (Supplementary Materials File S3). In comparison with the FPV reference genome, we investigated the distribution of mutations for each sample in this metatranscriptomics parvoviral data set and our 18 consensus sequences using MUSCLE [34] in the MEGAX version 10.1.8 analytical package [35].

We used phylogenetic analysis to reveal the evolutionary relationships between the FPV sequences obtained in this study and the reference sequences at the full-genome and individual gene levels. A total of 33 whole-genome FPV sequences (Supplementary Materials Table S2) were downloaded from GenBank after excluding highly identical or identical sequences from the same geographic region and year. In addition, we chose four CPV sequences to represent CPV-2, CPV-2a, CPV-2b, and CPV-2c. Prior to phylogenetic analysis, all 55 sequences (37 sequences from NCBI and 18 sequences from this study) were screened for recombination using the Recombination Detection Program 4 (RDP4) [36], employing the RDP, GENECOV, and Bootscan programs and requiring a *p*-value of ≥0.05 and a consensus recombination score > 0.6.

Evolutionary relationships were determined by aligning the full genome, NS1 (58 sequences from NCBI) and VP2 (62 sequences from NCBI) nucleotide sequences (Supplementary Materials Table S2) retrieved from NCBI GenBank with MAFFT version 7 employing the E-INS-I algorithm [37]. Phylogenetic trees were inferred using the maximum likelihood approach in IQ-TREE [38] and the ModelFinder program [39] to the best-fit model of nucleotide substitution. Nodal support was accessed using the SH-like approximate likelihood ratio test and ultrafast bootstrap approximation (SH-aLRT/UFBoot) and 1000 replicates [40].

2.5. Nucleotide Diversity Analysis

We used MIDAS [31] to estimate the most abundant minor variant frequency and then calculated intrahost sample nucleotide diversity (pi diversity, π) for each site. In addition, average nucleotide diversity was calculated at the individual gene and full-genome levels.

3. Results

3.1. Overview

A total of 18 sequencing libraries were generated for the analysis of intra- and interhost feline parvovirus diversity. Read files generated by the sequencer provided near-complete genome coverage, covering all major open reading frames. We calculated confidence intervals for the mean of the sequencing depth, obtaining over 10,000 × coverage per site (Figure 1A) after the application of the quality control for raw reads. A short region (site 2470–2620, length: 150 nucleotides (nt)) flanked by a poly(A)- and G-rich sequence region near the beginning of the VP2 gene showed a lower sequencing depth (Figure 1A) and higher error rate (Figure 1B) when compared with other regions. We considered this short region and two regions at the beginning (site 1–10) and end (site 4260–4269) as three low coverage regions (LCRs) because of insufficient sequencing. Although LCRs did not influence calling the consensus sequences, they did affect the accuracy and sensitivity of variant frequency estimations. Thus, LCRs were excluded when determining intrahost diversity. In the following analyses, genome nucleotide numbering begins at the first position of the NS1/NS2 gene coding region, and amino acid numbering starts at the first methionine for each respective gene.
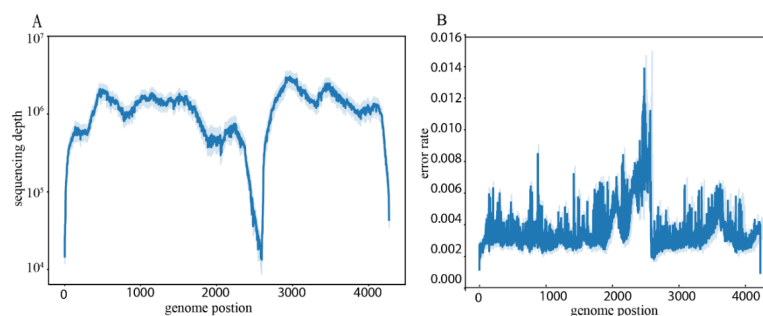
Figure 1. Overall description of the sequencing information in this study (mean lines with confidence interval bands). Dark blue represents the mean line, and light blue areas represent confidence intervals. (**A**) Sequencing depth along the genome coordinate. (**B**) Sequencing error rate along the genome coordinate.

3.2. Characterization of Carnivore Protoparvovirus 1 and Mutation Analysis

Using BCF tools, the number of SNVs detected for each sample in comparison to the reference genome ranged from 39 to 41 (Supplementary Materials File S2). All SNVs had a high Phred-scaled probability (130–218). All 18 samples had 39 identical SNVs compared with the reference FPV genome (EU659111). In addition, five other nucleotide positions were associated with SNVs in some samples. None of the SNVs detected in any sample were CPV-related single nucleotide polymorphism (SNP) markers. Thus, there was no evidence of CPV coinfection in any of the 18 samples. An FPV consensus sequence was determined for each sample (GenBank accession numbers MZ742166—MZ742180, Supplementary Materials Table S1) and compared with the FPV reference genome, spanning both the NS and VP coding regions (length: 4269 bp, hereafter referred to as the full genome). A total of 44 nucleotide positions (with LCR regions removed) were found to have mutations among the 18 FPV consensus sequences. All 44 positions shared the same mutations for

each sample in the metatranscriptomics parvoviral data set as the 18 consensus sequences generated here (Supplementary Materials Figure S1 and File S3).

3.3. Interhost FPV Diversity

Of the 10 nonsynonymous mutations identified compared with the FPV reference strain (Supplementary Materials Figure S1 and Table S3), only one—Val232Ile—exhibited interhost diversity among the 18 FPV sequences, being present in five sequences (Figure 2). In addition, five other polymorphic nucleotide positions were identified, all of which were synonymous substitutions (Figure 2).
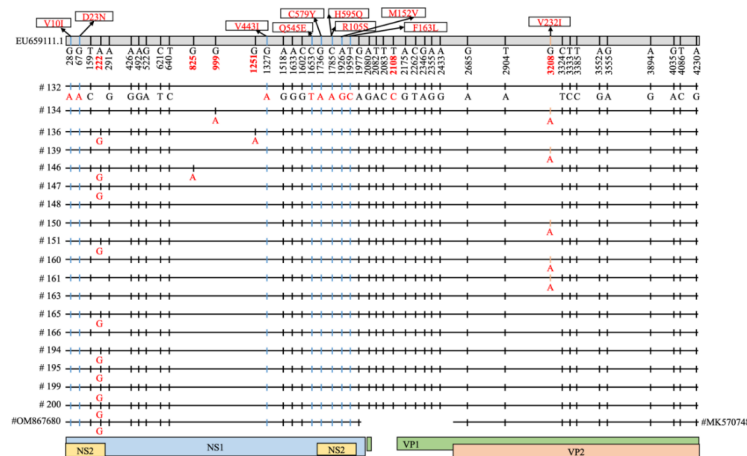
Figure 2. Mutations in the 18 FPV consensus sequences in this study and closely related VP2 (#MK570748) and NS1 (#OM867680) gene sequences in comparison with the FPV reference genome (EU659111). The nucleotide position is indicated in the bar at the top of the figure, together with changes in amino acid sequence, and the character state of individual nucleotides is indicated below for each consensus sequence. Synonymous mutations are indicated by black vertical bars, and nonsynonymous mutations are indicated by blue or orange vertical bars, corresponding to the relevant gene segment indicated at the bottom of the figure. Nucleotides of other sequences that are the same as for sample #132 are indicated by a vertical bar. A total of 10 nonsynonymous mutations (9 nucleotide positions were involved) were identified (NS1/NS2: Val10Ile, Asp23Asn; NS1: Val443Ile, Gln545Glu, Cys579Tyr, His595Gln; NS2: Arg105Ser, Met152Val, Phe163Leu; VP1/VP2: Val232Ile). The six nucleotide diversity positions (222, 825, 999, 1251, 2108, and 3208) are indicated by red font on the genome bar at the top of the figure.

3.4. Evolutionary Analysis

We scanned all 55 whole-genome sequences of FPV (37 from GenBank and 18 consensus sequences in this study) with RDP4 and detected no recombinant genomes. The FPV sequences from this study formed a distinct clade in the full genome, NS1 and VP2 phylogenies, supported by strong support values in the full genome and NS1 trees, although the positioning of the sequences within the clade has little resolution (Figure 3). Australian FPV sequences obtained by our research group for a previous study are most closely related to those presented here, as is particularly clear in the VP2 phylogeny [3].
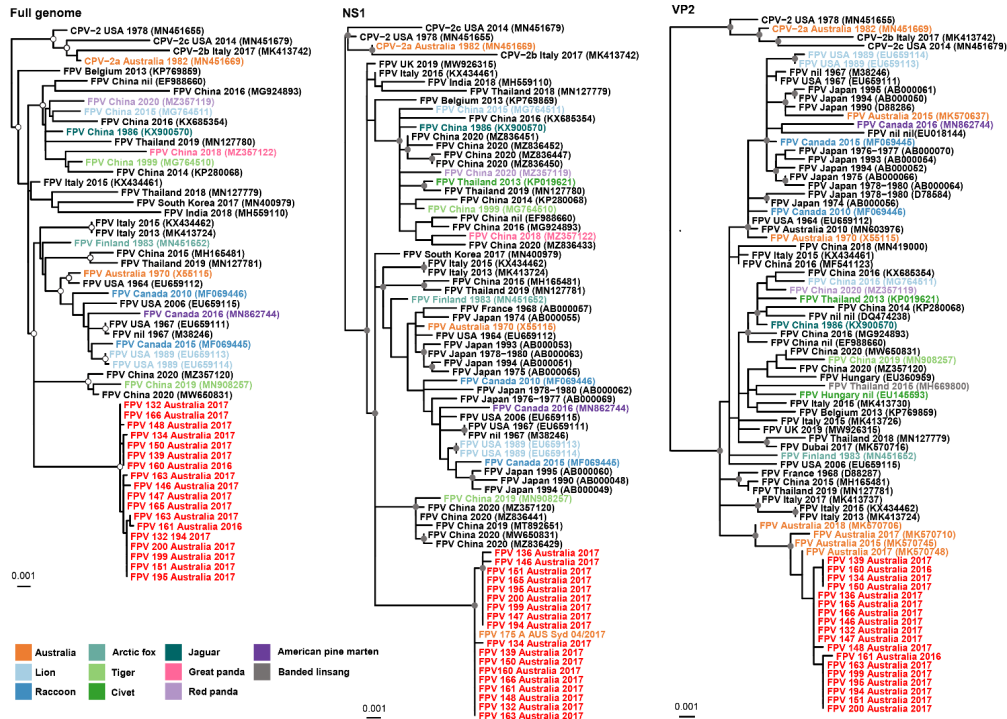
Figure 3. Phylogenetic relationships of the 18 FPV sequences described in this study and those retrieved from NCBI GenBank. All maximum likelihood trees are midpoint rooted for clarity, and sequences described in this study are highlighted in red and other Australian sequences in orange. Nodal support greater than 80% SH-aLRT and 95% UFBoot are represented by a grey circle. Sequences are designated in the phylogenetic trees by virus type (FPV or CPV), followed by the country year of isolation, and finally, accession number. The NS1 sequences for the Australian strains MK570748, MK570637, MK570710, and MK570706 are unavailable and therefore missing from both the full genome and NS1 phylogenies.

3.5. Intrahost Analyses

We next measured the subconsensus variant frequency (SVF) in each sequence, itself reflecting the most abundant minor variant frequency for each site. A low SVF implies that the major variant is conserved. Of the six polymorphic nucleotide positions identified among the 18 FPV sequences, all had low SVF (<1%) except for two positions in two samples, which had SVF > 1%, varied from 1.1% to 1.3% (Figure 4).

Nucleotide diversity, defined as the average number of nucleotide differences between the same regions in a sample (population) (i.e., π or pi diversity), was used to measure the degree of polymorphism in a sample. For each sample, we quantified π along the FPV genome (excluding the LCRs) and for each gene (Supplementary Materials Figure S2). The whole genome within-sample π diversity varied between 0.7% and 1.5%. A pi diversity of >1% was observed in four samples (#134, #139, #148, and #160). The highest pi diversity (1.9%) was observed in the NS2 gene for sample #148 (Figure 5, Supplementary Materials Table S4).
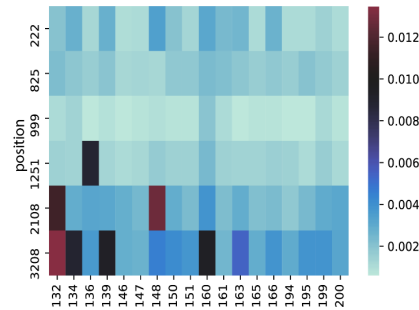
Figure 4. Heatmap of the subconsensus variant frequencies (SVF) in six diversity positions. SVF are displayed as colours ranging from blue to dark red. SVF was <1% in six positions in all samples, except for two positions in two samples (2108: #132 (SVF = 1.1%), #148 (SVF = 1.3%); 3208: #132 (SVF = 1.3%)).
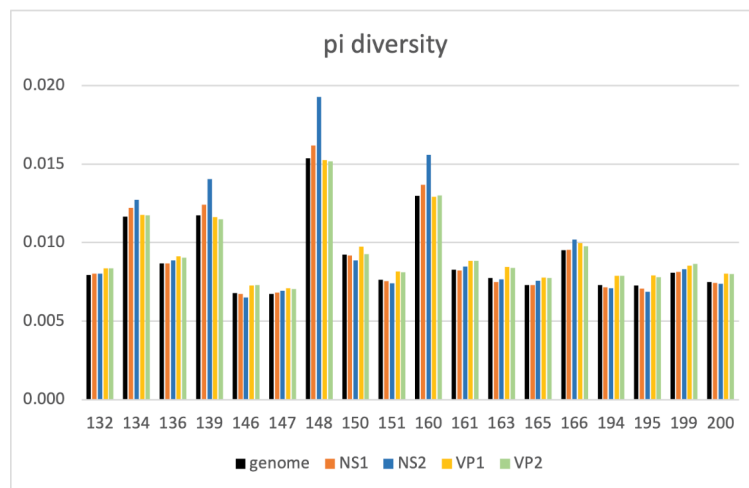
Figure 5. Nucleotide diversity (π) across the whole genome and per gene (NS1, NS2, VP1, and VP2). The whole genome within-sample π diversity varied between 0.7% and 1.5%. Four samples (#134, #139, #148, and #160) had a pi diversity >1%.

4. Discussion

There are few studies on the intrahost and interhost diversity of FPV. Here, using a fine-scale metagenomics approach, we identified 44 mutations (10 nonsynonymous) in Australian FPV strains collected in 2016/2017 compared with the reference strain (FPV-3) isolated in 1967. By contrast, an earlier study examined NS1 clones (7 to 40) and VP2 clones (5 to 40) from six strains of FPV in various feline tissues collected over a 43-year period and found 33 mutations (six nonsynonymous) compared with FPV-4, isolated in 1963 [41]. The limited FPV genetic diversity observed at both the inter- and intra- host levels, largely comprising synonymous mutations, is strongly suggestive of a low background mutation rate and the presence of strong selective constraints against amino acid variation.

Most studies on *Carnivore protoparvovirus 1* evolution have focused on the VP2 gene because of its role in host range determination, whereas mutations in the NS genes have been investigated infrequently. Notably, we identified only one nonsynonymous mutation

in FPV genomes in this study in the VP2 coding region. This mutation (Val232Ile) has been detected previously on several occasions [3,42,43]. In contrast to previous work, 9 of the 10 nonsynonymous mutations detected here were in the NS coding region. Of the six nonsynonymous mutations in FPV strains analysed by Hoelzer et al. (2008), three were in NS1 and three were in the VP genes (2 in VP1, 1 in VP2).

Two NS1 gene mutations we detected are novel (Val10Ile and Cys579Tyr), while the other four have been detected previously (Asp23Asn, Val443Ile, Gln545Glu, and His595Gln). The three nonsynonymous mutations (Arg105Ser, Met152Val and Phe163Leu) we found in the NS2 gene have been detected previously in FPVs from Italy (Arg105Ser), Europe, and China (Met152Val), and the Phe163Leu substitution is common globally [44]. For CPV, although most naturally occurring mutations are synonymous and involve the VP2 gene, several have also arisen and become widespread in the NS genes, including the Met152Val substitution detected in our FPV genomes [30,31]. Parvoviral NS proteins interact with the cellular proteins of the host, so it is possible that selection pressures differ for cats compared with dogs, although the phenotypic effects of NS gene mutations in CPV and FPV are poorly understood.

For phylogenetic trees based on the whole genome, NS1 and VP2, strains were mainly clustered by country and year of isolation. The 18 FPV sequences we examined were clustered closely in a single clade (Figure 4) and were most closely related to Australian viruses from the same region over a similar time frame. Because there are more polymorphic positions in NS1 than in VP2, there was a bootstrap-supported subclade of FPVs in this study in the phylogenetic tree for NS1 but not for VP2. In the whole genome and NS1 phylogenies, the viruses most closely related to the Australian FPVs were from a tiger and domestic cats in 2019 and 2020 from China that fell in a clade with high bootstrap support. In the VP2 tree, apart from an Australian virus collected from a domestic cat in 2018, the most closely related viruses were from domestic cats in Italy.

Since cats are susceptible to both FPV and CPV and given the resilience of these viruses, which can withstand harsh environmental conditions for at least 12 months [2], individual cats could be coinfected with multiple *Carnivore protoparvovirus 1* strains, facilitating recombination. However, using targeted hybridised baits to capture parvovirus DNA, we found no evidence of FPV/CPV coinfections in the faeces of any cats with FPL sampled during an outbreak, although the sample size was small.

Although some evidence suggests that CPV is displacing FPV among wild carnivores [45,46], this is not the case among domestic cats, where no outbreaks of FPL have been attributed to CPV. Similarly, FPV/CPV coinfections appear to be sporadic, being detected in only a few cases by cloning and Sanger sequencing PCR products of strains with VP2 and NS1 chromatograms suggestive of mixed viral populations [14,15,17]. One cat with enteritis was coinfected with FPV, CPV-2a, and a parvovirus variant with intermediate characteristics between FPV and CPV-2a [15]. Similarly, we determined that faecal shedding of CPV is uncommon among asymptomatic shelter-housed cats [47].

Finally, the high genetic diversity in the NS2 gene of several samples in this study highlights the need for additional investigations to determine the frequency of diversity observed in this gene among a larger population of feline parvoviruses.

References

1. Cotmore, S.F.; Agbandje-McKenna, M.; Canuti, M.; Chiorini, J.A.; Eis-Hubinger, A.-M.; Hughes, J.; Mietzsch, M.; Modha, S.; Ogliastro, M.; Pénzes, J.J. ICTV virus taxonomy profile: Parvoviridae. *J. Gen. Virol.* **2019**, *100*, 367. [CrossRef] [PubMed]
2. Barrs, V.R. Feline Panleukopenia: A Re-emergent Disease. *Vet. Clin. N. Am. Small Anim. Pract.* **2019**, *49*, 651–670. [CrossRef] [PubMed]
3. Van Brussel, K.; Carrai, M.; Lin, C.; Kelman, M.; Setyo, L.; Aberdein, D.; Brailey, J.; Lawler, M.; Maher, S.; Plaganyi, I. Distinct lineages of feline parvovirus associated with epizootic outbreaks in Australia, New Zealand and the United Arab Emirates. *Viruses* **2019**, *11*, 1155. [CrossRef] [PubMed]
4. Jenkins, E.; Davis, C.; Carrai, M.; Ward, M.P.; O'Keeffe, S.; van Boeijen, M.; Beveridge, L.; Desario, C.; Buonavoglia, C.; Beatty, J.A. Feline parvovirus seroprevalence is high in domestic cats from disease outbreak and non-outbreak regions in Australia. *Viruses* **2020**, *12*, 320. [CrossRef] [PubMed]
5. Mochizuki, M.; Horiuchi, M.; Hiragi, H.; San Gabriel, M.C.; Yasuda, N.; Uno, T. Isolation of canine parvovirus from a cat manifesting clinical signs of feline panleukopenia. *J. Clin. Microbiol.* **1996**, *34*, 2101–2105. [CrossRef] [PubMed]
6. Ikeda, Y.; Nakamura, K.; Miyazawa, T.; Tohya, Y.; Takahashi, E.; Mochizuki, M. Feline host range of canine parvovirus: Recent emergence of new antigenic types in cats. *Emerg. Infect. Dis.* **2002**, *8*, 341. [CrossRef]
7. Gamoh, K.; Shimazaki, Y.; Makie, H.; Senda, M.; Itoh, O.; Inoue, Y. The pathogenicity of canine parvovirus type-2b, FP84 strain isolated from a domestic cat, in domestic cats. *J. Vet. Med. Sci.* **2003**, *65*, 1027–1029. [CrossRef]
8. Decaro, N.; Desario, C.; Amorisco, F.; Losurdo, M.; Colaianni, M.L.; Greco, M.F.; Buonavoglia, C. Canine parvovirus type 2c infection in a kitten associated with intracranial abscess and convulsions. *J. Feline Med. Surg.* **2011**, *13*, 231–236. [CrossRef]
9. Hueffer, K.; Govindasamy, L.; Agbandje-McKenna, M.; Parrish, C.R. Combinations of two capsid regions controlling canine host range determine canine transferrin receptor binding by canine and feline parvoviruses. *J. Virol.* **2003**, *77*, 10099–10105. [CrossRef]
10. Parrish, C.R.; Have, P.; Foreyt, W.J.; Evermann, J.F.; Senda, M.; Carmichael, L.E. The global spread and replacement of canine parvovirus strains. *J. Gen. Virol.* **1988**, *69*, 1111–1116. [CrossRef]
11. Parrish, C.R.; O'Connell, P.H.; Evermann, J.F.; Carmichael, L.E. Natural variation of canine parvovirus. *Science* **1985**, *230*, 1046–1048. [CrossRef] [PubMed]
12. Parrish, C.R.; Aquadro, C.F.; Strassheim, M.; Evermann, J.; Sgro, J.; Mohammed, H. Rapid antigenic-type replacement and DNA sequence evolution of canine parvovirus. *J. Virol.* **1991**, *65*, 6544–6552. [CrossRef]
13. Buonavoglia, C.; Martella, V.; Pratelli, A.; Tempesta, M.; Cavalli, A.; Buonavoglia, D.; Bozzo, G.; Elia, G.; Decaro, N.; Carmichael, L. Evidence for evolution of canine parvovirus type 2 in Italy. *J. Gen. Virol.* **2001**, *82*, 3021–3025. [CrossRef] [PubMed]
14. Balboni, A.; Bassi, F.; De Arcangeli, S.; Zobba, R.; Dedola, C.; Alberti, A.; Battilani, M. Molecular analysis of Carnivore Protoparvovirus detected in white blood cells of naturally infected cats. *BMC Vet. Res.* **2018**, *14*, 41. [CrossRef] [PubMed]
15. Battilani, M.; Balboni, A.; Ustulin, M.; Giunti, M.; Scagliarini, A.; Prosperi, S. Genetic complexity and multiple infections with more Parvovirus species in naturally infected cats. *Vet. Res.* **2011**, *42*, 43. [CrossRef] [PubMed]
16. Battilani, M.; Gallina, L.; Vaccari, F.; Morganti, L. Co-infection with multiple variants of canine parvovirus type 2 (CPV-2). *Vet. Res. Commun.* **2007**, *31*, 209–212. [CrossRef] [PubMed]

17. Battilani, M.; Balboni, A.; Giunti, M.; Prosperi, S. Co-infection with feline and canine parvovirus in a cat. *Vet. Ital.* **2013**, *49*, 127–129.
18. Tang, P.; Chiu, C. Metagenomics for the discovery of novel human viruses. *Future Microbiol.* **2010**, *5*, 177–189. [CrossRef]
19. Chiu, C.Y. Viral pathogen discovery. *Curr. Opin. Microbiol.* **2013**, *16*, 468–478. [CrossRef]
20. Pallen, M. Diagnostic metagenomics: Potential applications to bacterial, viral and parasitic infections. *Parasitology* **2014**, *141*, 1856–1862. [CrossRef]
21. Conceição-Neto, N.; Zeller, M.; Lefrère, H.; De Bruyn, P.; Beller, L.; Deboutte, W.; Yinda, C.K.; Lavigne, R.; Maes, P.; Van Ranst, M. Modular approach to customise sample preparation procedures for viral metagenomics: A reproducible protocol for virome analysis. *Sci. Rep.* **2015**, *5*, 16532. [CrossRef] [PubMed]
22. Chong, R.; Shi, M.; Grueber, C.E.; Holmes, E.C.; Hogg, C.J.; Belov, K.; Barrs, V.R. Fecal viral diversity of captive and wild Tasmanian devils characterized using virion-enriched metagenomics and metatranscriptomics. *J. Virol.* **2019**, *93*, e00205–e00219. [CrossRef]
23. Van Brussel, K.; Wang, X.; Shi, M.; Carrai, M.; Feng, S.; Li, J.; Holmes, E.; Beatty, J.; Barrs, V.R. The enteric virome of cats with feline panleukopenia differs in abundance and diversity from healthy cats. *Transbound. Emerg. Dis.* 2022. [CrossRef]
24. Meyer, M.; Kircher, M. Illumina sequencing library preparation for highly multiplexed target capture and sequencing. *Cold Spring Harb. Protoc.* **2010**, *2010*, pdb.prot5448. [CrossRef] [PubMed]
25. Li, H.; Durbin, R. Fast and accurate short read alignment with Burrows–Wheeler transform. *Bioinformatics* **2009**, *25*, 1754–1760. [CrossRef]
26. Li, J.; Rettedal, E.A.; Van Der Helm, E.; Ellabaan, M.; Panagiotou, G.; Sommer, M.O. Antibiotic treatment drives the diversification of the human gut resistome. *Genom. Proteom. Bioinform.* **2019**, *17*, 39–51. [CrossRef]
27. Zheng, T.; Li, J.; Ni, Y.; Kang, K.; Misiakou, M.-A.; Imamovic, L.; Chow, B.K.; Rode, A.A.; Bytzer, P.; Sommer, M. Mining, analyzing, and integrating viral signals from metagenomic data. *Microbiome* **2019**, *7*, 42. [CrossRef]
28. Li, H.; Handsaker, B.; Wysoker, A.; Fennell, T.; Ruan, J.; Homer, N.; Marth, G.; Abecasis, G.; Durbin, R. The sequence alignment/map format and SAMtools. *Bioinformatics* **2009**, *25*, 2078–2079. [CrossRef]
29. Kwan, E.; Carrai, M.; Lanave, G.; Hill, J.; Parry, K.; Kelman, M.; Meers, J.; Decaro, N.; Beatty, J.A.; Martella, V. Analysis of canine parvoviruses circulating in Australia reveals predominance of variant 2b and identifies feline parvovirus-like mutations in the capsid proteins. *Transbound. Emerg. Dis.* **2021**, *68*, 656–666. [CrossRef]
30. Ogbu, K.I.; Mira, F.; Purpari, G.; Nwosuh, C.; Loria, G.R.; Schirò, G.; Chiaramonte, G.; Tion, M.T.; Di Bella, S.; Ventriglia, G. Nearly full-length genome characterization of canine parvovirus strains circulating in Nigeria. *Transbound. Emerg. Dis.* **2020**, *67*, 635–647. [CrossRef]
31. Voorhees, I.E.; Lee, H.; Allison, A.B.; Lopez-Astacio, R.; Goodman, L.B.; Oyesola, O.O.; Omobowale, O.; Fagbohun, O.; Dubovi, E.J.; Hafenstein, S.L. Limited intrahost diversity and background evolution accompany 40 years of canine parvovirus host adaptation and spread. *J. Virol.* **2019**, *94*, e01162-19. [CrossRef] [PubMed]
32. Nayfach, S.; Rodriguez-Mueller, B.; Garud, N.; Pollard, K.S. An integrated metagenomics pipeline for strain profiling reveals novel patterns of bacterial transmission and biogeography. *Genome Res.* **2016**, *26*, 1612–1625. [CrossRef] [PubMed]
33. Langmead, B.; Salzberg, S.L. Fast gapped-read alignment with Bowtie 2. *Nat. Methods* **2012**, *9*, 357. [CrossRef] [PubMed]
34. Edgar, R.C. MUSCLE: Multiple sequence alignment with high accuracy and high throughput. *Nucleic Acids Res.* **2004**, *32*, 1792–1797. [CrossRef]
35. Kumar, S.; Stecher, G.; Li, M.; Knyaz, C.; Tamura, K. MEGA X: Molecular Evolutionary Genetics Analysis across Computing Platforms. *Mol. Biol. Evol.* **2018**, *35*, 1547–1549. [CrossRef]
36. Martin, D.P.; Murrell, B.; Golden, M.; Khoosal, A.; Muhire, B. RDP4: Detection and analysis of recombination patterns in virus genomes. *Virus Evol.* **2015**, *1*, vev003. [CrossRef]
37. Katoh, K.; Standley, D.M. MAFFT multiple sequence alignment software version 7: Improvements in performance and usability. *Mol. Biol. Evol.* **2013**, *30*, 772–780. [CrossRef]
38. Nguyen, L.-T.; Schmidt, H.A.; Von Haeseler, A.; Minh, B.Q. IQ-TREE: A fast and effective stochastic algorithm for estimating maximum-likelihood phylogenies. *Mol. Biol. Evol.* **2015**, *32*, 268–274. [CrossRef]
39. Kalyaanamoorthy, S.; Minh, B.Q.; Wong, T.K.; Von Haeseler, A.; Jermiin, L.S. ModelFinder: Fast model selection for accurate phylogenetic estimates. *Nat. Methods* **2017**, *14*, 587–589. [CrossRef]
40. Hoang, D.T.; Chernomor, O.; Von Haeseler, A.; Minh, B.Q.; Vinh, L.S. UFBoot2: Improving the ultrafast bootstrap approximation. *Mol. Biol. Evol.* **2018**, *35*, 518–522. [CrossRef]
41. Hoelzer, K.; Shackelton, L.A.; Holmes, E.C.; Parrish, C.R. Within-host genetic diversity of endemic and emerging parvoviruses of dogs and cats. *J. Virol.* **2008**, *82*, 11096–11105. [CrossRef] [PubMed]
42. Hoang, M.; Wu, C.-N.; Lin, C.-F.; Nguyen, H.T.T.; Chiou, M.-T.; Lin, C.-N. Genetic characterization of feline panleukopenia virus from dogs in Vietnam reveals a unique Thr101 mutation in VP2. *PeerJ* **2020**, *8*, e9752. [CrossRef] [PubMed]
43. Chowdhury, Q.M.K.; Alam, S.; Chowdhury, M.S.R.; Hasan, M.; Uddin, M.B.; Hossain, M.M.; Islam, M.R.; Rahman, M.M.; Rahman, M.M. First molecular characterization and phylogenetic analysis of the VP2 gene of feline panleukopenia virus in Bangladesh. *Arch. Virol.* **2021**, *166*, 2273–2278. [CrossRef] [PubMed]
44. Mira, F.; Canuti, M.; Purpari, G.; Cannella, V.; Di Bella, S.; Occhiogrosso, L.; Schirò, G.; Chiaramonte, G.; Barreca, S.; Pisano, P. Molecular characterization and evolutionary analyses of Carnivore protoparvovirus 1 NS1 gene. *Viruses* **2019**, *11*, 308. [CrossRef]

45. Allison, A.B.; Kohler, D.J.; Ortega, A.; Hoover, E.A.; Grove, D.M.; Holmes, E.C.; Parrish, C.R. Host-specific parvovirus evolution in nature is recapitulated by in vitro adaptation to different carnivore species. *PLoS Pathog.* **2014**, *10*, e1004475. [CrossRef]
46. Chang, A.-M.; Chen, C.-C. Molecular characteristics of Carnivore protoparvovirus 1 with high sequence similarity between wild and domestic carnivores in Taiwan. *Pathogens* **2021**, *10*, 671. [CrossRef]
47. Carrai, M.; Decaro, N.; Van Brussel, K.; Dall'Ara, P.; Desario, C.; Fracasso, M.; Šlapeta, J.; Colombo, E.; Bo, S.; Beatty, J.A. Canine parvovirus is shed infrequently by cats without diarrhoea in multi-cat environments. *Vet. Microbiol.* **2021**, *261*, 109204. [CrossRef]